PROPERTIES EVALUATION OF ELECTROSPUN ALGINATE-BASED NANOFIBROUS MEMBRANES FOR FILTRATION APPLICATIONS

by

Teboho Clement Mokhena (M.Sc.)

Submitted in accordance with the requirements for the degree:

Philosophiae Doctor (Ph.D.) in Polymer Science

Department of Chemistry

Faculty of Natural and Agricultural Sciences

at the

University of the Free State (Qwaqwa Campus)

Supervisors: Dr. N.V. Jacobs and Prof. A.S. Luyt

December 2016

DECLARATION

I, the undersigned, hereby declare that the research in this thesis is my original work, which has not been partly or fully submitted to any other university/faculty in order to obtain a degree.

_____

T.C. Mokhena

DEDICATION

This work is dedicated to my late parents, Letsatsi Ramateka Mokhena, Maboteng Agnes Nondlala and the entire Mokhena family. To my late sisters (Mapule Mokhena and Maletsatsi Mokhena) and my brother Lesuping Mokhena and sister Hlouwe Mokhena. Ho bohle baha Malaka, Nondlala le baha Mmipi. Se keitse haelale makwala re none bakgatla ba batle Maananong, Matebele, Batloung le Bataung.

ABSTRACT

This study entails the electrospinning of a sodium alginate (SA) natural polymer with the aid of an electrospinnable synthetic polymer, polyethylene oxide (PEO), in order to develop nanofibrous-based membranes for wastewater treatment. The two most abundant natural polymers (i.e. cellulose and chitosan) were also incorporated in order to improve the selectivity and antifouling of the membrane. In order to improve the antibacterial activity of the membrane, chitosan was used to synthesize silver nanoparticles (AgNPs). The membranes were characterized under different conditions, depending on their intended wastewater treatment application. The electrospinnability of the alginate/PEO blend was dependent on the storage time, with 10 days being the minimum duration to obtain smooth defect-free nanofibres. The adsorption capacity of the electrospun alginate nanofibres was studied under different concentrations, pH, and temperature using copper (Cu^{2+}) as a model heavy metal. The maximum adsorption was approximately 15.6 mg g^{-1} at 25 °C and a pH of 4, and it maintained a reasonable metal adsorption over 5 recycling intervals. The adsorption capacity for chromium of the membrane based on the electrospun alginate nanofibres coated with cellulose nanowhiskers was 78 mg g^{-1} at a pH of 11. Complete removal of nanoparticles and a high retention of oil/water (>98%) was obtained. This was as a result of the pore size, the functional groups, and the inherited hydrophilic character of the membrane. In the case of the antibacterial alginate electrospun nanofibre membranes, the fibres were coated with silver nanoparticles and the susceptibility of gram negative and gram positive bacteria was also investigated using diffusion and kinetic methods. Spherical silver nanoparticles were obtained after 12 hours of heating at 95 °C using chitosan as a capping and reducing agent. The composite membrane was potent to gram negative and gram positive bacteria due to the presence of the AgNPs. The complexation between alginate and chitosan illustrated the possibility of the controlled release of AgNPs into wastewater streams. Further analyses were carried out on the silver nanoparticles containing chitosan as selective barrier in a three-tier membrane. The electrospun nanofibres (middle layer) was double-crosslinked by using calcium and glutaraldehyde in order to reduce the swelling behaviour of the alginate in an aqueous medium. The membrane displayed a larger than 98% rejection of nanoparticles (10-35 nm) and a larger than 93% retention of oil emulsions retention. It was found that the presence of AgNPs in the barrier layer did not affect the membrane performance.

Table of contents

ABBREVIATIONS

3D	three dimensional
AgNPs	silver nanoparticles
Alg	electrospun alginate nanofibres
BSA	bovine serum albumin
C	concentration
CA	cellulose acetate
CaA	electrospun calcium alginate
CaA-AgNPs	glutaraldehyde crosslinked electrospun alginate coated with chitosan-containing AgNPs
CaA-CS	glutaraldehyde crosslinked electrospun alginate coated with chitosan
Ca-CNs	electrospun calcium alginate reinforced with cellulose nanowhiskers
CMC	carbomethyl chitin
CMCs	carboxymethyl cellulose sodium salt
CoPc	cobalt tetraaminophthalocyanine
CV	crystal violet
D	diameter
DCM	dichloromethane
DD	deacetylation degree
DMAc	N,N-dimethylacetamide
DMF	N,N-dimethylformamide
DNA	deoxyribonucleic acid
DOSE	dual-opposite-spinneret electrospinning
EA	ethylenediamine
EC	ethyl cellulose
EDC	N-(3-dimethylaminopropyl)-N’-ethylcarbodiimide hydrochloride
EDS/EDX	energy-dispersive X-ray spectroscopy
EDTA	ethylenediaminetetraacetic acid
ENM	electrospun nanofibrous membrane
Ga-CaA	glutaraldehyde crosslinked electrospun alginate
GAG	glycosaminoglycan
GJF	gas jet nanofibre
HA	hyaluronic acid
HAp	hydroxyapatite

HFIP/HFP	1.1.1.3.3.3-hexaflouro-2-propanol
HPMC	hydroxypropyl methyl cellulose
HTACC	N-(2-hydroxlpropyl-3-trimethyl ammonium chitosan chloride)
ID	internal dimeter of the syringe
LOD	lowest detection value
MeOH	methanol
MF	microfiltration
M_w	molecular weight
MWNT	multiwalled carbon nanotube
NHS	N-hydroxysuccinimide
NMMO	N-methylmorpholine-N-oxide
NP	nanoparticles
P(CLLA)	poly(L-lactide-co-caprolactome)
P(LLA-CL)	poly(L-lactide-co-caprolactone)
PAA	polyacrylic acid
PAAm	poly(acrylamide)
PAN	poly(acrylonitrile)
PBS	phosphate buffered saline
PCL	polycaprolactone
PCLDLLA	poly(ε-caprolectome-co-D-L-lactide)
PEC_10min	alginate nanofibres immersed in chitosan-containing AgNPs for 10 minutes
PEC_15min	alginate nanofibres immersed in chitosan-containing AgNPs for 15 minutes
PEC_5min	alginate nanofibres immersed in chitosan-containing AgNPs for 5 minutes
PEG	poly(ethylene glycol)
PEGDA	poly(ethylene glycol) diacrylate
PEI	polyethyleneimine
PEO	poly(ethylene oxide)
PES	poly(ether sulphone)
PET	poly(ethylene terephthalate)
PF	paraformaldehyde
PGA	poly(glycolic acid)
PIP	piperazine
PLA	commercial ultrafiltration membrane (PLAC07610)

PLA	poly(lactic acid)
PMAA	poly(methacrylic acid)
PS	polystyrene
PU	polyurethane
PVA	poly(vinyl alcohol)
PVAm	polyvinylamine
PVDF	poly(vinylidene flouride)
PVP	poly(vinyl pyrrolidone)
QB_zCSN	N-benzyl-N,N-dimethyl chitosan iodide
QCh	quaternized chitosan
RJS	rotary-jet spinning
RNA	ribonucleic acid
SEM	scanning electron microscopy
SF	silk fibroin
SNE	standard electrospinning
SO_3H	sulphonate groups
SWNT	single walled carbon nanotube
TCD	tip-to-collector distance
TCP	tip-to-collector distance
TEM	transmission electron microscopy
TEMPO	2,2,6,6-tetramethylpiperidiooxy
TFA	trifluoroacetic acid
TFC	thin film composite membrane
T_g	glass transition temperature
TGA	thermogravimetric analysis
T_m	melting temperature
TMP	trans-membrane pressure
TNFC	thin film composite membrane
TPU	thermoplastic polyurethane
UF	ultrafiltration
WK	wool keratose
XPS	X-ray photoelectron spectroscopy

LIST OF TABLES

LIST OF FIGURES

Chapter 1

Introduction

1.1 General background

The disparity between the current population growth and water availability/supply necessitates novel strategies to either reduce wastewater discharge or decontaminate the available water resources without generating harmful by-products [1-3]. Apparently, there are more than 1.2 billion people that do not have access to fresh usable water as a result of new pollutants introduced by the undesirable activities of man [4]. These include waste dumping, industrialization, and introduction of alien plants. There have been many efforts to remove these pollutants from contaminated water by using different technologies such as pressure-driven membrane separation, ion exchange, adsorption and a combination of these processes. Among these technologies, adsorption and pressure-driven membrane-separation (reverse osmosis (RO), nanofiltration (NF), ultrafiltration (UF), and microfiltration (MF)) processes have received a lot of interest due to their reliability, efficiency and ease of operation [3,5,6].

A great deal of literature demonstrate that there are two valuable properties that have to be met by the adsorbent: i) large surface area and ii) the presence of functional groups in the membrane [4,7-13]. The first property depends mostly on the structure and shape of the material used, while the second property depends on the type of material used [4,9,12-14]. A wide variety of materials, such as activated carbon and red mud, have been studied as possible adsorbents of different heavy metals [15-17]. These materials are expensive and add to the current environmental crisis. This has resulted in a shift to natural polymers as a result of their unique properties such recyclability, renewability, abundant availability and low cost. Moreover, they have functional groups that can be modified to enhance the adsorption capacity of the adsorbents [4,11]. In the case of the structure of the material, there has been growing interest to utilize one of the new nanotechnology products, i.e. electrospun nanofibres [4,18]. These fibres have diameters ranging from a few micrometres to a few nanometres. This results in valuable distinctive properties, such as large specific surface areas, and open and interconnected pore structures that add a new dimension to separation and adsorption membranes. The large specific surface area and ease of functionalization of

electrospun nanofibres can result in a high adsorption efficiency, selectivity, equilibrium time, regeneration, and stability [4,18].

Similar to the latter, the pressure-driven membrane-separation has two significant properties which include high selectivity and high filtration productivity (flux) while operating at relatively low energy consumption [19,20]. However, there is a trade-off between these properties which has spurred a lot of interest culminating in novel strategies to modify and/or improve the conventional membrane. In order to improve or/and balance (flux, reduction of the membrane resistance and high selectivity) the properties of the membrane, thin film composite membranes (TFC) were coated onto the developed support membrane. Film composite membranes (TFC) consist of two or more layers: (i) top ultrathin selective barrier layer, (ii) middle porous support layer, and (iii) additional mechanical support layer made from non-woven fabric. More research have been dedicated to improve selective barrier layer (i) and middle layer (ii) in order to enhance the membrane selectivity without hampering membrane flux [19-25]. Although the supporting layer (iii) does not partake in filtration, it is often included in order to provide the mechanical integrity and alleviate the material handling issues. Despite their advantages such as improved water flux and pollutants removal, these membranes are prone to fouling, non-selective and operate at high energy rate due to their asymmetric structure and broad pore structure, since they are often produced by phase immersion method [25]. It was recently demonstrated that these limitations can be overcome by the inclusion of the electrospun nanofibres into the TFC membrane as a middle layer [21,26-28]. It was reported that the overall flux was enhanced several folds than the commercial available membranes with similar rejection ration (> 90%) [21,23]. In addition, it was also demonstrated that the introduction of the natural polymers as the selective barrier layer enhanced the antifouling property of the membrane [24,29]. This was as a result the hydrophilic nature of these natural polymers.

Despite the advantages provided by electrospun fibres and natural polymers, there is still a lot of work that has to be done with regard to the spinnability of the natural polymers. There are several problems associated with the spinnability of the natural polymers [30]. Some of the primary key factors associated with the spinning process include high conductivity and gelation at fairly low concentration below chain entanglements [31,32]. Even though a great deal of work was primarily concerned about their preparation by using appropriate solvents targeting specific fields of interest, such as tissue engineering and drug-delivery, the progress

recorded has brought the success to their application in wastewater treatment [4, 7]. One of the suitable solutions includes the use of electrospinnable synthetic polymers as carrier polymers to facilitate their spinnability followed by the removal of these carrier polymers [7,33,34].

Alginate is a linear polysaccharide composed of guluronate (G) and mannuronate (M) acid residues [35,36], and it is extracted from seaweeds. The acid residues may vary in sequence and proportions depending on the growth conditions, harvesting time and depth of the oceanic zones. These groups may be sequentially arranged as repeating units (MM or GG), or alternating (MG). Alginate is well-known by its gelation when interacting with divalent cations [35,37]. The metal interacts ionically with the acid residue in order to form a network structure known as the 'egg box' model. This property has been explored to produce different structures such as beads, hydrogels, 3D scaffolds and microfibres for various applications, but especially for wastewater treatment [36-40]. Alginate is one of the most difficult natural polymers to electrospin [34]. This is associated with its limited solubility, high viscosity and conductivity. Several authors managed to electrospin it with the aid of electrospinnable synthetic polymers (e.g. poly(ethylene oxide) (PEO) or poly(vinyl alcohol) (PVA)) [34,39,41,42]. Some reported that it can be electrospun in the presence of a cosolvent such as glycol [43]. It was found that the addition of the electrospinnable synthetic polymers or cosolvent reduces the viscosity and conductivity and in this manner facilitates its spinnability. This is the result of the strong interaction between the alginate and synthetic polymers through hydrogen bonding. Alginate also has a strong interaction with other polyelectrolytic polymers to form a polyelectrolytic complex [44,45]. This property has been explored to encapsulate different substances in order to control their release. Due to the capability of alginate to interact with metal ions and complexate with other polyelectrolytic polymers, electrospun alginate was chosen in this study as the core structure of the membranes produced.

Cellulose is the most available natural polymer on earth with more than 10^{11} tonnes produced per year, and it can be obtained from plants and animals. It serves as structural support in the complex structural cell wall. It has been established by most studies that the cellulose content may vary depending on the source [3,46,47]. Recent reports revealed that cellulose nanowhiskers can be used as a selective barrier layer in thin film composite (TFC) membrane in order to enhance the flux and the selectivity of the membrane [3,26,46,48]. Cellulose

nanowhiskers were also found to improve the mechanical properties of the membrane [24,48,49]. The coating of electrospun alginate with cellulose can also improve the selectivity and mechanical strength of the membrane [46,49].

Chitosan is a linear copolymer composed of β-(1,4)-2-acetamido-2-deoxy-β-D-glucopyranose and 2-amino-2-deoxy-β-D-glucopyronose [50]. Chitosan is obtained from the deacetylation of the second most available natural polymer on earth, namely chitin. Chitin can be extracted from crabs, shrimps and plants [50]. The deacetylation degree of chitin determines the polymer molecular weight and the degree of NH_2 functionalization along the polymer chains. Different methods such as alkali treatment and enzymatic treatment in the presence of a chitin deacetylase have been used to produce chitosan. The presence of these NH_2 groups plays an important role in the properties such as metal adsorptivity, and antimicrobial, antifungal of chitosan, and the interaction with other polyelectrolytic polymers such hyaluronic acid (HA), collagen and alginate [7,8,51-54]. The chelation of metal ions was explored to synthesize different nanoparticles such as silver and gold nanoparticles [52,54-56]. In this case, chitosan was used as a capping and reducing agent at the same time. Additionally, several studies have reported on the use of chitosan as barrier layer in a TFC membrane [19,57]. Chitosan also enhanced the antifouling and membrane selectivity. The membrane displayed a higher flux rate than the commercial membranes while maintaining a high rejection efficiency [19]. Chitosan was, therefore, used in this study as a barrier layer in a TFC membrane, and as a stabilizing and reducing agent for the synthesis of silver nanoparticles.

1.2 Aims and objectives

This study deals with the electrospinning of a sodium alginate natural polymer in order to develop different membranes for wastewater treatment. The objectives are to i) investigate the heavy metal adsorption behaviour of the electrospun alginate, ii) demonstrate the filtration performance of electrospun alginate membranes coated with cellulose nanowhiskers as a selective barrier layer, iii) develop an antibacterial electrospun alginate membrane by impregnating it with silver nanoparticles using ionic complexation with chitosan, and iv) evaluate a thin film composite filtration membrane (TFC) composed of dual crosslinked electrospun-alginate nanofibres as a middle layer, chitosan/silver nanoparticles as a barrier selective layer and nonwoven PET fabric as a substrate.

1.3 Thesis organization

The outline of this thesis is as follows:

Chapter 1: Introduction

Chapter 2: A review on electrospun bio-based polymers for water treatment

Chapter 3: Electrospun alginate nanofibres as potential bio-sorption agent of heavy metals in water treatment

Chapter 4: Nanofibrous alginate membrane reinforced with cellulose nanowhiskers for water purification

Chapter 5: Electrospun alginate nanofibres impregnated with silver nanoparticles: Fabrication and property analysis

Chapter 6: Development of multifunctional nano/ultrafiltration membrane based on a chitosan thin film on alginate electrospun nanofibres

Chapter 7: Conclusions

1.4 References

[1] M.T.M. Pendergast, E.M.V. Hoek, A review of water treatment membrane nanotechnologies, Energy & Environmental Science, 4 (2011) 1946-1971.

[2] K. Yoon, B.S. Hsiao, B. Chu, Functional nanofibers for environmental applications, Journal of Materials Chemistry, 18 (2008) 5326-5334.

[3] H. Ma, C. Burger, B.S. Hsiao, B. Chu, Ultra-fine cellulose nanofibers: new nano-scale materials for water purification, Journal of Materials Chemistry, 21 (2011) 7507-7510.

[4] A.A. Taha, Y.-N. Wu, H. Wang, F. Li, Preparation and application of functionalized cellulose acetate/silica composite nanofibrous membrane via electrospinning for Cr(VI) ion removal from aqueous solution, Journal of Environmental Management, 112 (2012) 10-16.

[5] H. Ma, K. Yoon, L. Rong, Y. Mao, Z. Mo, D. Fang, Z. Hollander, J. Gaiteri, B.S. Hsiao, B. Chu, High-flux thin-film nanofibrous composite ultrafiltration membranes containing cellulose barrier layer, Journal of Materials Chemistry, 20 (2010) 4692-4704.

[6] R. Yang, K.B. Aubrecht, H. Ma, R. Wang, R.B. Grubbs, B.S. Hsiao, B. Chu, Thiol-modified cellulose nanofibrous composite membranes for chromium (VI) and lead (II) adsorption, Polymer, 55 (2014) 1167-1176.

[7] M. Aliabadi, M. Irani, J. Ismaeili, H. Piri, M.J. Parnian, Electrospun nanofiber membrane of PEO/chitosan for the adsorption of nickel, cadmium, lead and copper ions from aqueous solution, Chemical Engineering Journal, 220 (2013) 237-243.

[8] K. Desai, K. Kit, J. Li, P. Michael Davidson, S. Zivanovic, H. Meyer, Nanofibrous chitosan non-wovens for filtration applications, Polymer, 50 (2009) 3661-3669.

[9] L. Li, Y. Li, L. Cao, C. Yang, Enhanced chromium (VI) adsorption using nanosized chitosan fibers tailored by electrospinning, Carbohydrate Polymers, 125 (2015) 206-213.

[10] F. Ji, C. Li, B. Tang, J. Xu, G. Lu, P. Liu, Preparation of cellulose acetate/zeolite composite fiber and its adsorption behavior for heavy metal ions in aqueous solution, Chemical Engineering Journal, 209 (2012) 325-333.

[11] Y.-N. Wu, B. Zhang, F. Li, W. Zhu, D. Xu, P. Hannam, G. Li, Electrospun fibrous mats as a skeleton for fabricating hierarchically structured materials as sorbents for Cu^{2+}, Journal of Materials Chemistry, 22 (2012) 5089-5097.

[12] M. Aliabadi, M. Irani, J. Ismaeili, S. Najafzadeh, Design and evaluation of chitosan/hydroxyapatite composite nanofiber membrane for the removal of heavy metal ions from aqueous solution, Journal of the Taiwan Institute of Chemical Engineers, 45 (2014) 518-526.

[13] H.R. Pant, H.J. Kim, M.K. Joshi, B. Pant, C.H. Park, J.I. Kim, K. Hui, C.S. Kim, One-step fabrication of multifunctional composite polyurethane spider-web-like nanofibrous membrane for water purification, Journal of Hazardous Materials, 264 (2014) 25-33.

[14] S. Haider, S.-Y. Park, Preparation of the electrospun chitosan nanofibers and their applications to the adsorption of Cu(II) and Pb(II) ions from an aqueous solution, Journal of Membrane Science, 328 (2009) 90-96.

[15] J. Pradhan, S.N. Das, R.S. Thakur, Adsorption of hexavalent chromium from aqueous solution by using activated red mud, Journal of Colloid and Interface Science, 217 (1999) 137-141.

[16] S. Babel, T.A. Kurniawan, Low-cost adsorbents for heavy metals uptake from contaminated water: a review, Journal of Hazardous Materials, 97 (2003) 219-243.

[17] T.A. Kurniawan, G.Y. Chan, W.-H. Lo, S. Babel, Comparisons of low-cost adsorbents for treating wastewaters laden with heavy metals, Science of the Total Environment, 366 (2006) 409-426.

[18] P.K. Neghlani, M. Rafizadeh, F.A. Taromi, Preparation of aminated-polyacrylonitrile nanofiber membranes for the adsorption of metal ions: comparison with microfibers, Journal of Hazardous Materials, 186 (2011) 182-189.

[19] K. Yoon, K. Kim, X. Wang, D. Fang, B.S. Hsiao, B. Chu, High flux ultrafiltration membranes based on electrospun nanofibrous PAN scaffolds and chitosan coating, Polymer, 47 (2006) 2434-2441.

[20] X. Wang, D. Fang, K. Yoon, B.S. Hsiao, B. Chu, High performance ultrafiltration composite membranes based on poly(vinyl alcohol) hydrogel coating on crosslinked nanofibrous poly(vinyl alcohol) scaffold, Journal of Membrane Science 278 (2006) 261-268.

[21] S. Kaur, S. Sundarrajan, D. Rana, T. Matsuura, S. Ramakrishna, Influence of electrospun fiber size on the separation efficiency of thin film nanofiltration composite membrane, Journal of Membrane Science, 392-393 (2012) 101-111.

[22] R. Wang, Y. Liu, B. Li, B.S. Hsiao, B. Chu, Electrospun nanofibrous membranes for high flux microfiltration, Journal of Membrane Science, 392-393 (2012) 167-174.

[23] Z. Tang, J. Wei, L. Yung, B. Ji, H. Ma, C. Qiu, K. Yoon, F. Wan, D. Fang, B.S. Hsiao, B. Chu, UV-cured poly (vinyl alcohol) ultrafiltration nanofibrous membrane based on electrospun nanofiber scaffolds, Journal of Membrane Science, 328 (2009) 1-5.

[24] L.A. Goetz, B. Jalvo, R. Rosal, A.P. Mathew, Superhydrophilic anti-fouling electrospun cellulose acetate membranes coated with chitin nanocrystals for water filtration, Journal of Membrane Science, 510 (2016) 238-248.

[25] B. Khorshidi, T. Thundat, B.A. Fleck, M. Sadrzadeh, A novel approach toward fabrication of high performance thin film composite polyamide membranes, Scientific reports, 6 (2016) 1-10.

[26] M. Li, Z. Wu, M. Luo, W. Wang, K. Chang, K. Liu, Q. Liu, M. Xia, D. Wang, Highly hydrophilic and anti-fouling cellulose thin film composite membrane based on the hierarchical poly(vinyl alcohol-co-ethylene) nanofiber substrate, Cellulose, 22 (2015) 2717-2727.

[27] S. Kaur, S. Sundarrajan, D. Rana, R. Sridhar, R. Gopal, T. Matsuura, S. Ramakrishna, Review: The characterization of electrospun nanofibrous liquid filtration membranes, Journal of Materials Science, 49 (2014) 6143-6159.

[28] X. Wang, X. Chen, K. Yoon, D. Fang, B.S. Hsiao, B. Chu, High flux filtration medium based on nanofibrous substrate with hydrophilic nanocomposite coating, Environmental Science & Technology, 39 (2005) 7684-7691.

[29] H. Ma, C. Burger, B.S. Hsiao, B. Chu, Ultrafine polysaccharide nanofibrous membranes for water purification, Biomacromolecules, 12 (2011) 970-976.

[30] D. Fang, Y. Liu, S. Jiang, J. Nie, G. Ma, Effect of intermolecular interaction on electrospinning of sodium alginate, Carbohydrate Polymers, 85 (2011) 276-279.

[31] I.C. Um, D. Fang, B.S. Hsiao, A. Okamoto, B. Chu, Electro-spinning and electro-blowing of hyaluronic acid, Biomacromolecules, 5 (2004) 1428-1436.

[32] X. Wang, I.C. Um, D. Fang, A. Okamoto, B.S. Hsiao, B. Chu, Formation of water-resistant hyaluronic acid nanofibers by blowing-assisted electro-spinning and non-toxic post treatments, Polymer, 46 (2005) 4853-4867.

[33] C.D. Saquing, C. Tang, B. Monian, C.A. Bonino, J.L. Manasco, E. Alsberg, S.A. Khan, Alginate-polyethylene oxide blend nanofibers and the role of the carrier polymer in electrospinning, Industrial & Engineering Chemistry Research, 52 (2013) 8692-8704.

[34] H. Nie, A. He, W. Wu, J. Zheng, S. Xu, J. Li, C.C. Han, Effect of poly(ethylene oxide) with different molecular weights on the electrospinnability of sodium alginate, Polymer, 50 (2009) 4926-4934.

[35] N. Bhattarai, M. Zhang, Controlled synthesis and structural stability of alginate-based nanofibers, Nanotechnology, 18, (2007) 455601.

[36] K. Zhao, X. Zhang, J. Wei, J. Li, X. Zhou, D. Liu, Z. Liu, J. Li, Calcium alginate hydrogel filtration membrane with excellent anti-fouling property and controlled separation performance, Journal of Membrane Science, 492 (2015) 536-546.

[37] S. Papageorgiou, F. Katsaros, E. Kouvelos, N. Kanellopoulos, Prediction of binary adsorption isotherms of Cu^{2+}, Cd^{2+} and Pb^{2+} on calcium alginate beads from single adsorption data, Journal of Hazardous Materials, 162 (2009) 1347-1354.

[38] T. Gotoh, K. Matsushima, K.-I. Kikuchi, Preparation of alginate-chitosan hybrid gel beads and adsorption of divalent metal ions, Chemosphere, 55 (2004) 135-140.

[39] D. Song, S.-J. Park, H.W. Kang, S.B. Park, J.-I. Han, Recovery of lithium(I), strontium(II), and lanthanum(III) using Ca-alginate beads, Journal of Chemical & Engineering Data, 58 (2013) 2455-2464.

[40] X. Zhang, B. Lin, K. Zhao, J. Wei, J. Guo, W. Cui, S. Jiang, D. Liu, J. Li, A free-standing calcium alginate/polyacrylamide hydrogel nanofiltration membrane with high

anti-fouling performance: Preparation and characterization, Desalination, 365 (2015) 234-241.

[41] J.-W. Lu, Y.-L. Zhu, Z.-X. Guo, P. Hu, J. Yu, Electrospinning of sodium alginate with poly(ethylene oxide), Polymer, 47 (2006) 8026-8031.

[42] K. Shalumon, K. Anulekha, S.V. Nair, S. Nair, K. Chennazhi, R. Jayakumar, Sodium alginate/poly(vinyl alcohol)/nano ZnO composite nanofibers for antibacterial wound dressings, International Journal of Biological Macromolecules, 49 (2011) 247-254.

[43] H. Nie, A. He, J. Zheng, S. Xu, J. Li, C.C. Han, Effects of chain conformation and entanglement on the electrospinning of pure alginate, Biomacromolecules, 9 (2008) 1362-1365.

[44] G. Lawrie, I. Keen, B. Drew, A. Chandler-Temple, L. Rintoul, P. Fredericks, L. Grøndahl, Interactions between alginate and chitosan biopolymers characterized using FTIR and XPS, Biomacromolecules, 8 (2007) 2533-2541.

[45] S.I. Jeong, M.D. Krebs, C.A. Bonino, J.E. Samorezov, S.A. Khan, E. Alsberg, Electrospun chitosan-alginate nanofibers with in situ polyelectrolyte complexation for use as tissue engineering scaffolds, Tissue Engineering Part A, 17 (2011) 59-70.

[46] X. Cao, M. Huang, B. Ding, J. Yu, G. Sun, Robust polyacrylonitrile nanofibrous membrane reinforced with jute cellulose nanowhiskers for water purification, Desalination, 316 (2013) 120-126.

[47] A. Mtibe, L.Z. Linganiso, A.P. Mathew, K. Oksman, M.J. John, R.D. Anandjiwala, A comparative study on properties of micro and nanopapers produced from cellulose and cellulose nanofibres, Carbohydrate Polymers, 118 (2015) 1-8.

[48] Z. Wang, H. Ma, B.S. Hsiao, B. Chu, Nanofibrous ultrafiltration membranes containing cross-linked poly(ethylene glycol) and cellulose nanofiber composite barrier layer, Polymer, 55 (2014) 366-372.

[49] H. Ma, C. Burger, B.S. Hsiao, B. Chu, Nanofibrous microfiltration membrane based on cellulose nanowhiskers, Biomacromolecules, 13 (2012) 180-186.

[50] K. Sun, Z. Li, Preparations, properties and applications of chitosan based nanofibers fabricated by electrospinning, eXPRESS Polymer Letters, 5 (2011) 342-361.

[51] Z. Chen, X. Mo, F. Qing, Electrospinning of collagen-chitosan complex, Materials Letters, 61 (2007) 3490-3494.

[52] X. Zhuang, B. Cheng, W. Kang, X. Xu, Electrospun chitosan/gelatin nanofibers containing silver nanoparticles, Carbohydrate Polymers, 82 (2010) 524-527.

[53] C. Tapia, Z. Escobar, E. Costa, J. Sapag-Hagar, F. Valenzuela, C. Basualto, M.N. Gai, M. Yazdani-Pedram, Comparative studies on polyelectrolyte complexes and mixtures of chitosan-alginate and chitosan-carrageenan as prolonged diltiazem clorhydrate release systems, European Journal of Pharmaceutics and Biopharmaceutics, 57 (2004) 65-75.

[54] C. Sun, R. Qu, H. Chen, C. Ji, C. Wang, Y. Sun, B. Wang, Degradation behavior of chitosan chains in the 'green' synthesis of gold nanoparticles, Carbohydrate Research, 343 (2008) 2595-2599.

[55] A. Regiel, S. Irusta, A. Kyzioł, M. Arruebo, J. Santamaria, Preparation and characterization of chitosan-silver nanocomposite films and their antibacterial activity against *Staphylococcus aureus*, Nanotechnology, 24 (2012) 015101.

[56] S. Kumar-Krishnan, E. Prokhorov, M. Hernández-Iturriaga, J.D. Mota-Morales, M. Vázquez-Lepe, Y. Kovalenko, I.C. Sanchez, G. Luna-Bárcenas, Chitosan/silver nanocomposites: Synergistic antibacterial action of silver nanoparticles and silver ions, European Polymer Journal, 67 (2015) 242-251.

[57] D.A. Musale, A. Kumar, Effects of surface crosslinking on sieving characteristics of chitosan/poly(acrylonitrile) composite nanofiltration membranes, Separation and Purification Technology, 21 (2000) 27-37.

Chapter 2

A review on electrospun bio-based polymers for water treatment

This chapter has been published as:
T.C. Mokhena, V. Jacobs, A.S. Luyt, A review on electrospun bio-based polymers for water treatment, eXPRESS Polymer Letters 9 (2015) 839-880.

Abstract
Over the past decades, electrospinning of biopolymers down to nanoscale garnered much interest to address most of the millennia issues related to water treatment. The fabrication of these nanostructured membranes has added a new dimension to the current nanotechnologies where a wide range of materials can be processed to their nanosize level. Electrospinning is a simple and versatile technique employed to fabricate unique nanostructured membranes with fascinating properties for a wide spectrum of applications such as filtration and others. These nanostructured membranes, fabricated by electrospinning, are of a paramount importance because of their advanced inherited properties such as large surface-to-volume ratio, as well as tuneable porosity, stability, and high permeability. The extensive research conducted on these materials extended the success of electrospinning not only to bio-based polymer nanofibres, but to their hybrids and their derivatives. The technique also created avenues for advanced and massive production of nanofibres. This paper reviews the recent developments in electrospinning technique. Electrospinning of biopolymers, their blends and functionalization using metals/metal oxides, and the potential applications of electrospun nanofibrous membranes in water filtration are discussed.

Keywords: Nanomaterials; Electrospinning; Nanofibre materials; Biopolymers; Biocomposites

2.1 Introduction

The high exponential growth of the world population especially in developing countries, water scarcity, and man undesirable practices have spurred efforts to develop innovative technologies to produce high quality water at relatively low cost and energy [1,2]. Urbanization, industrial activities, waste dumping, and alien plants are common practices

contributing to the current environmental crisis [3,4]. For example, the mining industries, although serving as one of the driving forces of many countries' economy, dump billions of tons of hazardous materials into the environment. The emissions of such pollutants into the air and water are seriously considered as primary factors to the common respiratory, neural and intestinal diseases. A safe and healthy environment is a priority that needs immediate intervention in developing and developed countries [5,6]. These challenges call upon novel and effective technologies to address the current environmental issues, either by protecting the environment and current water sources or by producing high quality water from available sources (oceans and wastewater) without harmful by-products [5,6].

During the past decades, the production of nanofibres has gained a lot of interest and attention in the development of innovative materials with properties that are suitable to address the challenges related to water treatment. Nanofibres are a new class of nanomaterials with inherited properties such as the large surface-to-area ratio, high porosity, flexibility, stability, and permeability. Several routes have been employed to fabricate these nanostructured products from different materials such as drawing, templates synthesis, phase separation, self-assembly, electrospinning etc. [8-10]. Amongst them, electrospinning technique has received considerable interest due to its simplicity, efficiency and versatility in producing nanofibres [8-10].

In the electrospinning process, an electric field is introduced to the solution (or melt) in order to produce extremely long fibres with diameters down to a few nanometers. Almost all soluble materials can be electrospun into nanofibres. These include synthetic and natural polymers, polymer alloys and polymers loaded with chromophores, nanoparticles, or active agents, as well as metals and ceramics [8]. This technique has gained considerable interest in the past two decades, not only because of its simplicity, but also due to its feasibility to produce consistent long nanofibres with desirable properties which cannot be fabricated through other techniques. The resulting nanostructured materials with an extremely large surface to volume ratio, and engineered porosity, malleability, stability and functionality, have been applied in a wide variety of fields [8,10].

Research has escalated in electrospinning of biopolymers, their hybrids and derivatives, for various applications because of their unique properties such as renewability, biodegradability and their abundant availability [7,11]. Generally, biopolymers are defined as polymeric biomolecules generated by living organisms. They are categorized according to the monomeric units that build up the complex polymeric structure, namely polynucleids

(ribonucleic acid (RNA) and deoxyribonucleic acid (DNA)), polypeptides (proteins), and polysaccharides (cellulose, and chitosan). The electrospinnability of most biopolymers is still a challenge because of numerous factors [11-15]. These include their rigid structure, high conductivity, high surface tension, and their gelation at fairly low concentrations. Several routes have been proposed to improve their electrospinnability such as the use of copolymers [16] and the modification of the processing device [13,15].

A number of biopolymers, such as DNA [17], silk [18], chitosan [19], collagen [20], fibrinogen [21], gelatin [22], hyaluronic [13,15], cellulose [23], and alginate [24] were successfully electrospun into nanofibres for their application in various fields such as filtration, biomedical and tissue engineering. Only few of them were, however, applied in air and water treatment [25-27]. The readily water solubility of these biopolymers and biodegradation are common factors that disrupt the success of electrospun bio-based nanofibrous membranes, especially in water filtration. The addition of nanoparticles [28,29], functionalization and the use of co-polymers [30] to enhance stability and biocidal activity have been the major subject of research in electrospun nanofibrous membranes (ENM).

Even though there have been some successes in the electrospinning of a broad spectrum of materials since its invention a century ago, the throughput of nanofibres is still a limiting factor to the industrial production for commercial purposes. However, there are several modifications on the classical laboratory electrospinning setup and new technological innovations to increase the production rate of the electrospun nanofibres. These technologies include bubble electrospinning [31], multi-jet [32] and bowl electrospinning [33].

In this review, we discuss the fabrication of electrospun biobased nanofibres, their hybrids and derivatives using electrospinning technique. The factors that influence the properties of the electrospun nanofibres, and their functionalization using various methods, to enhance their performance in water and wastewater treatment, are discussed. We also look at other innovative technologies to modify classic electrospinning and to improve the properties and production of electrospun nanofibres.

2.2. Electrospinning process

2.2.1 Historical background on electrospinning

Electrospinning was initially not considered a viable technique because of difficulties with drying and collection of the nanofibres during its execution. However, it gained scientific and commercial publicity in the past two decades. Raleigh in 1897, was the first to discover electrospinning and a thorough study on electrospraying was done by Zeleny in 1914 [34,35]. Cooley [36] was one of the scientists that patented the electrospinning technique about 100 years ago. However, the electrospinning technique gained enormous interest later in the early 1990s, thanks to the Reneker group. The group studied the mechanisms involved during electrospinning which spurred a huge interest in the nanotechnology arena because of the size of the resulting nanofibres. In Germany (in the early 1930s and the 1940s), Formhals published a series of patents based on the process and apparatus to execute this simple and versatile technique [37-39]. Later in the 1960s, Taylor studied the initiation of the jet from the drop on the apex of the needle when an electric field was applied. The conical shape formed because of the electric forces surmounting the solution surface tension was later named after him, "*Taylor cone*" [10,40]. By that time, the technique was called '*electrostatic spinning*'. The considerable interest in the electrospinning technique in the 1990s resulted in the new name '*electrospinning'* [40,41]. The name '*electrospinning*' was then accepted and it is now widely used in the literature as a description of this viable technique to produce ultrathin fibres from a polymer solution or melt through application of electrical forces. The success of this technique is evidenced by the number of publications each year by universities, research institutes, and some commercial enterprises, who are involved in the application of electrospun nanofibres (Donalson company Inc., Espin technologies Inc., and Elmarco etc.) [31].

2.2.2 Fundamentals of electrospinning

Almost all soluble materials can be electrospun into nanofibres, with diameters ranging from several micrometres down to tens of nanometres. More than 200 polymers have been successfully electrospun into long ultrathin fibres for a wide variety of applications, mostly from polymer solutions [40,42]. A classical setup of the electrospinning technique is shown in Figure 2.1. It consists of a spinneret with a metallic needle, a syringe pump, a high voltage

power supply, and a grounded collector [8,40,43]. Horizontal and vertical setups are commonly adapted configurations, but in some cases upward electrospinning was also utilized [44].

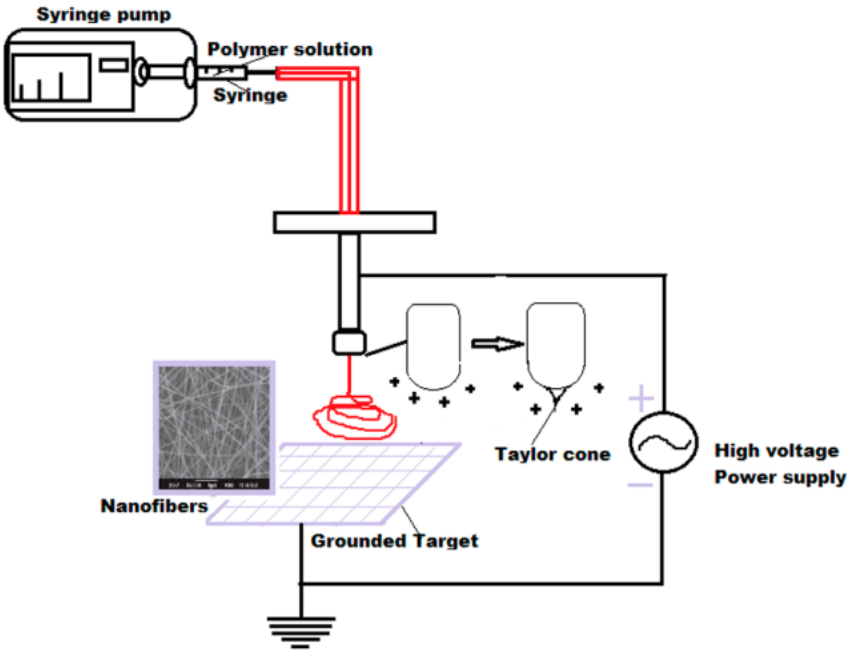

Figure 2.1 Schematic representation of electrospinning apparatus.

Basically, the sol-gel, blend, composite, or polymer solution/melt is loaded in the syringe and it is driven to the needle tip by a syringe pump, forming a hemispherical droplet at the tip. A voltage (5-40 kV) is applied to the solution on the needle which causes the drop to stretch into a conical shape (known as Taylor cone) [45]. Depending on the viscosity of the solution (which must be sufficient enough to withstand stretching and whipping in order to avoid any varicose breakup, which forms nanoparticles) an electrified jet is formed and moves towards to an oppositely charged collector. During this trip, the solvent evaporates and the jet solidifies to form nonwoven webs on the collector. The jet is only stable from the tip of the needle, whereafter instability starts. Interestingly, this technique offers the processor a platform to control the resulting morphology and structure of the nanofibres through changing of solution properties and physical parameters. Many well-organized papers describe in detail the effect of these parameters [8,34,43,45]. Furthermore, the solvent and co-solvent play a significant effect in determining the resulting morphology and structure. The resulting nanofibres have high porosity, large surface to volume ratio, and good mechanical properties, which open doors for a wide variety of applications (Figure 2.2) [8,46].

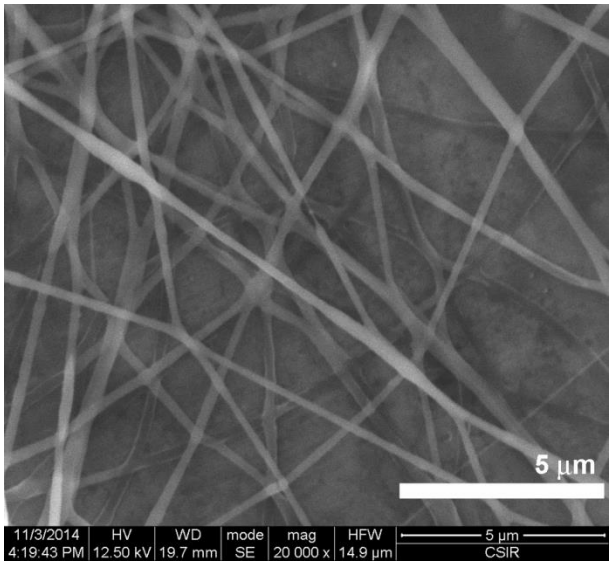

Figure 2.2 SEM micrograph of alginate nanofibres

2.3 Factors affecting the electrospinning process

Although electrospinning is a simple and straightforward technique, there are several parameters (solution properties, processing parameters, and ambient conditions), that are important which must be considered since they significantly affect the quality of the resulting nanofibrous membranes. The solution properties include conductivity, concentration, surface tension, and molecular weight; the processing parameters include voltage, tip-to-collector distance, collector shape, diameter of the needle and feeding rate; the ambient conditions such as humidity and temperature of the surroundings are also important.

2.3.1 Solution parameters

Despite the fact that all these parameters have a significant effect on the resulting product, the solution properties serves as a more decisive parameter. The solution concentration and/or viscosity have to be sufficient enough to prevent the varicose breakup of the jet in order to allow a continuous stream in the spinning solution. Both are directly dependent on the polymer molecular weight which defines the entanglement of the chains to withstand the Coulombic stretching force to prevents the jet breakage into droplets by surface tension [47-50]. Optimal concentration and/or viscosity are required since too high concentration/viscosity may result in large diameter and clogging of the capillary [47-50]. Nevertheless, gelation (highly viscous) at fairly low concentrations (below entanglement

concentration) disrupts the electrospinnability of the biopolymers, resulting in the collection of droplets. Moreover, most of these polymers are inherently polyelectrolytic (e.g. alginate and chitosan) which increases the solution conductivity. This also contributes to the difficulties in electrospinning of natural polymers from their aqueous solutions [47,51]. Several modifications have been done to improve their spinnability. The use of copolymers such as poly(vinyl alcohol) (PVA) and polyethylene oxide (PEO) was found to be suitable for the reduction of conductivity of the natural polymeric spinning solutions [47,52-54]. On the other hand, some solvents may be added either to increase [55,56] or decrease the electric properties of the spinning solution [12,19]. The most commonly used solvents in electrospinning are shown in Table 2.1.

Table 2.1 Properties of solvents and liquids used in electrospinning

Solvent	Density / g cm^{-3}	Viscosity / cP	Boiling point / °C	Dipole moment / D	Dielectric constant	Surface tension/ mN m^{-1}
Acetic acid	1.05	1.12	118.0	1.68	6.15	26.9
Acetone	1.39	0.32	78.0	2.88	27.0	21.4
Chloroform	1.50	0.53	61.6	1.15	4.80	26.5
Dichloromethane	1.33	0.41	40.0	1.60	8.93	28.1
Dimethylacetamide	0.94	1.96	165.0	3.72	37.8	36.7
Dimethylformamide	0.99	0.80	153.0	36.70	38.3	37.1
Dimethyl sulfoxide	1.10	2.00	189.0	3.90	46.7	43.0
Ethylene glycol	1.11	16.13	197.0	2.20	37.7	47.0
Formamide	1.13	3.30	211.0	3.37	110.	59.1
Formic acid	1.22	1.57	101.0	1.41	57.9	37.6
Glycerol	1.26	950	290.0	2.62	42.5	64.0
Hexafluoro isopropanol	1.60	1.02	58.2	1.85	16.7	16.1
Methanol	0.79	0.54	65.0	1.70	33.0	22.7
Tetrahydrofuran	0.89	0.46	66.0	1.75	7.52	26.4
Triflouroethanol	1.38	1.24	74.0	2.52	8.55	43.3
Water	1.00	1.00	100.0	-	21.0	25.2

Solvents with good volatility, moderate vapour pressure, moderate boiling point, good conductivity and good cohesion with the polymer are important in the electrospinning process [12,56-61]. The solubility of the polymer, however, does not guarantee the solution spinnability [12]. For example, partial solubility in a solvent can result in smooth bead-free nanofibres. Some reports have suggested that a single solvent system could result in beaded nanofibres, whereas the addition of partially soluble solvent could improve the nanofibre morphology [57,59,61].

2.3.2 Setup parameters

Essentially, the electrospinning process begins directly at the point at which electrostatic forces overcome the solution surface tension and viscoelastic forces. Typically, a critical voltage is required to eject the charged jet from the drop at the nozzle (Taylor cone) [15,62]. For instance as the concentration, or similarly, the viscosity increases, higher electrical forces are required to overcome the surface tension and the viscoelastic forces necessary for fibre stretching. The size of the droplet at the tip of the nozzle depends on the feeding rate as well as the needle shape and diameter [13,62-64]. Therefore, these factors influence the forces acting on the drop which contribute to the jet initiation and stretching. An optimal distance is required to give the electrified jet sufficient time for nanofibre dryness [65-67]. At longer tip-to-collector distance (TCD), the fibre will have sufficient time to solidify before reaching the collector, but if the distance is too long, either beaded fibres or no fibres are collected [65]. Similarly, when the distance is too short, it reduces the flight distance and solvent evaporation, and increases electric field, which results in beads.

One of the essential aspects in electrospinning is the type of collector used. These collectors act as a conductive substrate to collect the charged fibres. Aluminium foil [61] is usually used to collect the nanofibres. However, due to the difficulty to transfer the nanofibres from this collector [13,15], other collectors such as liquid baths [68], metal plates [69], grids [70], parallel or gridded bars [71,72], rotating disks [73], and rotating drums [74] were investigated as possible collectors. Different collectors used in electrospun nanofibres were recently reviewed [46]. The collectors specifically used in electrospun biopolymers as well as the optimal conditions are summarized in Table 2.2. The collectors are often used to engineer and design the structure and morphology of the fibres. For example, Matthews *et al*. [75] observed that collagen nanofibres, collected at lower speeds, were random filaments, whereas collection at high speeds resulted in the deposition of the nanofibres along the rotation axis**.**

Table 2.2 The optimal conditions of electrospun biopolymer nanofibres

Type of collector	Polymer system	Solvent system	Conditions	Morphology	Diameters	Reference
Aluminium foil	Cellulose (DP = 210)	NMMO/water	9 wt%, 15-20 kV, 15 cm, 0.05 $ml.min^{-1}$	Film	-	[70]
	Alginate (37 kDA)/PEO (600 kDA)	Distilled water	Alginate-PEO-Pluronic (10.0:0.8:1.5 wt%), 12 cm, 0.5 $ml.hr^{-1}$, 30% relative humidity (RH)	Three dimensional (3D) nanofibrous structure	237 ± 33 nm	[71]
	Carbomethyl cellulose (CMC)/ PEO (1:1 ratio)	1:1 water:ethanol	8%, 20 cm, 35 kV	Uniform	200-250 nm	[5]
	Hydroxypropyl methyl cellulose (HPMC) (with 29.2% methoxy and 8.8% hydroxypropyxy)	1:1 water:ethanol	2.14%, 20 cm, 35 kV	Uniform	128 nm	[5]
	Cellulose (DP=1140)	LiCl/DMAc	3 wt%, 15-20 kV, 15 cm, 0.05 $ml.min^{-1}$	Film		[70]
	Chitosan (106 kDA)	90% Acetic acid	7%, 3 $kV.cm^{-1}$, 20 $\mu l.min^{-1}$	Uniform	180 nm	[61]
	Chitosan	90% Acetic acid	5 wt% (hydrolyzed in	Uniform	50-250 nm	[72]

			50% NaOH at 95ºC for 48 hours), 16 cm, 17 kV, 8×10^{-2} $mg.h^{-1}$, ID = 0.7 mm			
		80% Acetic acid	7 wt%	Uniform	250 ±76 nm	
		70% Acetic acid	7.5 wt%		284 ± 94 nm	
	Chitosan (DD = 85%)/agarose	TFA/DCM (7/3v/v)	7% (50% of agarose), 15kV, 12 cm, 0.5 $ml.hr^{-1}$	Cylindrical	0.14 ± 0.09 μm	[73]
	Chitosan (8-20 kDA)/PLA (5kDA)	TFA	17.4 wt%(1:20 chitosan:PLA)	Uniform	-	[74]
	Carboxymethyl chitosan (89 kDa, 0.36 DS)/PVA (124-186 kDa, 87-89% hydrolysed)	Water	8% mixture of 60/40 (CMCS/PVA) with 0.5 Triton X100, 10-15 kV, 17-20 cm		135 nm	[75]
	Hexanoyl chitosan	Chloroform	14 wt%, viscosity = 956 mPas, 1 $kV.cm^{-1}$	Ribbon-like	3.93 μm	[76]
	Quaternized chitosan(QCh)/PVP	Distilled water	20 wt%(QCh)/ PVP (4:1), 2.2 $kV.cm^{-1}$, viscosity = 25550 cP,	cylindrical	1.53 ± 0.48 μm	[77]
	PEG-N,O-chitosan(DS=1.50)	75/25 v/v (THF/DMF)	15% with 0.5 wt% Triton X100, 10-15 kV, 17-20 cm	Uniform	162 nm	[78]
	Gelatin	Distilled water	At 37ºC,14 cm, 13 kV	Beaded	295 nm	[79]

				cylindrical		
	Gelatin	Formic acid	8 wt%, 7.5 cm, 1 kV.cm^{-1}	smooth	79 ± 14 nm	[60]
	Hyaluronic acid (HA)	Acidic water	40 kV, 9.5 cm, 40 µl.min^{-1}			
	Thiolated HA (158 kDA)/PEO (900 kDA)	Dulbecco's modified eagle's medium	HA-DTPH (2.5%, w/v)/ PEO (2.5%, w/v), 20 µl.min^{-1}, 10 cm, 18kV	3D nanofibrous structure	90 ± 15 nm	[80]
Rotating mandrel	N-carboxyethyl chitosan/PEO/ $AgNO_3$	Formic acid	37 kV, 14 cm, 800 rpm, 1.1 ml.hr^{-1}	Self-bundled/ yarn	460 ±87 nm and 200 ± 40 nm	[81]
	Collagen (calf skin type 1)	HFIP	0.083 g.ml^{-1}, 25 kV, 125 mm, 5.0 ml.hr^{-1}	3D	100 ± 40 nm	[69]
	Ethyl cellulose	TFA	10 wt%, 20 kV, 5 cm, 0.01 ml.min^{-1}	Uniform	100 nm	[82]
	Cellulose Acetate (CA)(40 kDA)	DMAc/acetone(1/2)	10%, 15 cm, 20 kV	Uniform	420 nm	[23]
Liquid bath	Cellulose	1-butyl-3-methylimidazolium chloride	10% cellulose, 15 cm ethanol bath, 15-20 kV, 0.03-0.05 ml.min^{-1}	Highly-branched	8.65 ±7.70 µm	[8]
	Alginate (3500 cps)	Glycol/water (2/1)	2 w/v%, 28 kV, 12 cm, copper mesh in 10 wt%	Uniform	200 nm	[6]

			of $CaCl_2$ in ethanol, 105 $\mu L.min^{-1}$			
Rotating collector immersed in liquid bath	Cellulose (DP=210)	NMMO/water	9 wt%,15-20 kV, 15 cm, 0.01 $ml.min^{-1}$, 1.2 rpm, water bath	Uniform	300 nm and	[70]
	Cellulose (DP=1140)	NMMO/water	2.5 wt%,15-20 kV, 15 cm, 0.01 $ml.min^{-1}$, 1.2 rpm, water bath	Uniform	250-750nm	[70]

2.3.3 Ambient conditions

Ambient conditions, temperature and humidity, can also affect the morphology and diameter of nanofibres [77]. It was deduced that the increase in temperature reduces the viscosity of the solution and enhances the solvent evaporation, which results in thinner nanofibres [89]. Depending on the system under investigation, two antagonistic effects are observed: (1) reduction in fibre diameters, and (2) increase in diameter which may result in the fusion of the nanofibres [90]. Tripatanasuwan *et al*. [91] reported that an increase in relative humidity resulted in smaller diameters of nanofibres. They stated that at low relative humidity the rate of solvent evaporation increased, with the opposite effect at high humidity. Furthermore, the humidity can generate pores of different sizes and depths depending on the molecular weight of the polymer [92].

2.4 Recent advances in electrospinning techniques

During the past years research on various advancements and modifications on standard needle electrospinning (SNE) with the aim to scale up nanofibres production, to enhance the stability of the electrospinning technique, and to engineer patterns and desired morphologies of the resulting nanofibres for various applications, have escalated. The production rate has been one of the inhibiting factors for the commercial implementation and industrial viability of electrospinning processing technique. In SNE, the mass production rate ranges between 0.01 and 0.1 g h^{-1}, where the nanofibre source is a single jet arising from a single needle apex through which the polymer solutions is ejected. Various innovative ways to produce electrospun nanofibres with enhanced functionalities were developed. These advances, namely multi-needle and needleless electrospinning, gas-jet electroblowing spinning, and co-axial electrospinning (Table 2.3) are described in the following sections**.** However, most of these technological advances are mostly applied in synthetic polymers as deliberated in Table 2.3.

Table 2.3 The novel advances on standard laboratory electrospinning

Technique	Polymer concentration / wt%	Average diameter / nm and voltage / kV	Throughput / g h^{-1}	Reference
Bowl	6 (PEO) and 12 (PCL)	268 ± 25 at 16 and 344 ± 97 at 30	7.0	[31]
Bubble	10 (PVA)	111-48.6 at 10-30	-	[33]
Conical wire coil	9 (PVA)	275 ± 113 at 50	2.8	[93, 94]
Gas jet	8 (PVA)	220 at 25	1.1	[95]
Multi-jet	15 (PVA)	230000	0.66-0.72	[96]
Nanospider	15 (PU)	193 at 81.2	96.6 [a]	[97]
Porous tubular	20 (nylon-6)	170.6 ±75.0 at 20	5.0	[98]
Splashing	9 (PEO)	368 ± 45.37 at 60	3.0	[99]

[a] Units g h^{-1} m^{-1}

2.4.1 Multi-needle electrospinning

An increase in the number of nozzles is the most convenient way to increase the production rate of the nanofibres [100,101]. However, there are some drawbacks associated with multi-needle electrospinning, such as complicated design and large operating space, and repulsion between the nanofibres that causes the uneven deposition of the nanofibres [102]. Furthermore, the clogging of needles discourages the industrial viability of multijet spinning. In the industry needles would require regular cleaning, which would result in complex processes and too much labour. Therefore, several modifications have been suggested to overcome the nanofibre repulsions without compromising the production rate. For example, Kim and Park [103] electrospun alginate/PEO nanofibres using multi-nozzle electrospinning with an extra auxiliary electrode in order to alleviate the repulsion between the jets. PEO (2 wt%)/alginate (2 wt%) doped with lecithin (0.7 wt%) as surfactant produced smooth nanofibres by using SNE. The same composition was used for a comparison between nanofibres produced with and without auxiliary electrodes in multi-nozzle spinning. The

auxiliary supported multi-nozzle showed a higher production rate and smoother nanofibres with diameters of 174 ± 62 nm when compared to the unsupported spun nanofibres that had diameters of 246 ± 62 nm. A wide variety of multijet electrospinning heads, namely series, elliptic, concentric, line, rectangular and matrix can be employed to produce nanofibres [96]. Biodegradable blend of cellulose acetate and PVA was prepared by varying the ratio of the jets from 1:3 to 3:1. The average diameters of the fibres increased (220 to 290 nm) with a decrease in the number ratio of PVA/CA from 3:1 to 1:3. The tensile strength and the modulus increased from 7.0 to 9.4 MPa and 18.1 to 34.0 MPa respectively with an increasing the number ratio of the jets of PVA/CA from 1:3 to 3:1 [26].

2.4.2 Needleless electrospinning

2.4.2.1 Confined needleless electrospinning

One of the promising processes for the scaling-up of nanofibre production is the needleless electrospinning. This technique avoids the issues of clogging and cleaning of the needles and the complexity of the multi-axial spinning setup. The needleless process is divided into two categories depending on the feeding system *viz*: confined feeding and unconfined feeding. The difference between the confined and unconfined needleless electrospinning is the fact that in confined electrospinning the electrospun fluid is enclosed in a reservoir such as an insulating tube [98,104,105] or any other material in which the polymer is protruded, whereas in unconfined systems there is no reservoir for the spinning solution and the droplets are projected naturally from the surface of the solution.

The replacement of needles in multi-jet spinning is the most convenient way to resolve the complexity and difficulties without compromising the mass throughput [92,99]. In this route the polymer fills a porous hollow tube [93,104]. The drilled holes on the surface of the tube can be made in different configurations. The positive electrode is immersed into the solution and by using a minimal pressure the polymer solution is driven through the holes. The production rate is 3-250 times that of the standard electrospinning (SNE), while the nanofibre diameters may range from 300 nm to several hundreds of microns. Dosunmu *et al.* [98] used a porous polyethylene tube with pore sizes 10-100 μm as reservoir for a 20 wt% nylon 6 spinning solution. The polymer solution was pushed with air pressure to form multiple jets on the porous surface. The jets protruding from the tube surface were collected on a surrounding

vertically placed grounded co-axial wire mesh. The resulting nanofibres have equivalent mean diameters to those produced by SNE, with a much broader distribution. Moreover, different polymers can be electrospun *via* this method and the porous tube can be made from different materials such as ceramic.

Rotary-jet spinning (RJS) is composed of a rotating motor, a reservoir and a stationary or rotating collector [106]. The polymer solution is loaded into a punched reservoir, either continuously or once in one measurement or production. The perforated reservoir has two side wall orifices which rotate vertically to the surrounding collector. As a result of the centrifugal forces on the solution, the polymer jets are forced out of the reservoir through the punched side wall, and subsequent jet extension and dryness yield three dimensions nanofibres. The advantages include the use of low voltages, the production of three dimensional (3D) morphologies, controlled porosity, independence of solution conductivity, and larger mass production than SNE. Various polymer solutions (poly(lactic acid) (PLA) in chloroform, polyethylene oxide (PEO) in water, poly(acrylic acid) (PAA) in water, gelatin in acetic acid were successfully electrospun to three dimensional nanofibres by Badrossamay *et al.* [106]. They indicated that with the control over the spinning solution concentration and rotating speed the morphology of the nanofibres can be tuned.

2.4.2.2 Unconfined needleless electrospinning

Unconfined needleless electrospinning is the electrospinning of solutions naturally from a liquid surface. Yarin and Zussman [107] prepared nanofibres by a needleless method by using ferromagnetic liquid sub-layer below the polymer solution. It was established that the nanofibres can also be produced without the ferromagnetic sub-layer, but at a considerable higher voltage. The disadvantage of this method is that the number of jets and their location cannot be controlled since the jets protrude naturally from the liquid surface. Nevertheless, they produced nanofibres with diameters ranging from 200 to 800 nm.

Another technique involves the use of charged cylindrical rotators dipped in the spinning solution [108,109]. This is the only technique that was applied industrially since research on the enhancement of the production rate started, and it is known as nanospider^{TM} [97]. The technique involves a polymer solution in a container and a cylindrically charged metal rotating at a certain speed. The charged rotating metal is partially immersed in the solution.

When the solution is electrified by the voltage supplied to the cylindrical rotators, the multiple polymer jets are launched from the circumference of the cylindrical rotators to the grounded collector. Nanofibres with average diameters of between 50 and 200 nm are produced at a rate of 2.53 g h^{-1}, when compared to the conventional electrospinning technique with a rate of 0.01-0.1 g h^{-1}. Various shapes of the rotating nozzles, such as disk and spiral coils, can be used to generate narrow distribution nanofibres with a higher mass production than the SNE. A rotating spiral coil made of metal wire was used by Wang *et al*. [94] to eject the jets from the surface of each spiral wire. Depending on the concentration and applied voltage, ultrafine nanofibres were produced. Nanofibres with narrower distribution were generated with mass production rate increasing with voltage from 2.94 g h^{-1} to 9.42 g h^{-1} for 45 kV and 60 kV, respectively. The disadvantage of these nozzle processes is the uneven electric field distribution on the spiral wire. Niu *et al*. [110] compared a rotating disk and cylinder in order to envisage the effect of the shape on the resulting nanofibre production. They indicated that the disk nozzle requires a lower voltage in order to initiate the fibre production than the cylinder nozzle, with finer nanofibre than those from the cylinder at similar conditions. The mass production was equivalent to the rotating disk and cylinder techniques, but higher than that of SNE.

Yet, another approach is when the polymer solution drips from the reservoir onto a rotating cylinder and this known as splashing electrospinning. In this case, the reservoir is held horizontal to a charged cylinder rotating at a certain speed. With a controlled speed, gap distance, and solution parameters the nanofibre structure can be tuned with enhanced production (24-45 times) compared to SNE [99] (Table 2.3). The influence of the processing and solution properties on the resulting nanofibres *via* splashing was studied by Tang *et al*. [111]. Increased concentration was found to increase the mean diameter of the fibre, whereas an increase in the voltage decreased the diameter. A decrease in mean diameter was reported with an increase in both the rotating speed and gap distance. They found that by using statistical analysis (analysis of variance (ANOVA)), the optimal conditions for fine nanofibres with narrower distribution (PEO in water) were as follows: concentration (6.94 wt%), voltage (12.38 kV), gap distance (3.5 cm), and rotational speed (0.76 rpm). In addition, nanofibres with mean diameters ranging from 100 to 400 nm, were obtained.

In the bowl-edge unconfined process, the primary interaction between the electric field and the polymer solution caused fluid perturbations within the bath reservoir filled with polymer

solution [31,41]. These fluid perturbations were responsible for the Raleigh-Taylor instabilities formed by gravitational forces in the polymer solution. The polymer solutions, due to the instabilities, produced jets protruding from the edge of the bowl which are similar to the jets ejected from the SNE. The bowl has a thin-lipped edged structure where the droplets are ejected to the concentric collector. At the beginning, a high voltage is supplied and then the voltage to initiate the jet formation is reduced to a lower operational value. Stable nanofibres are formed on the collector with high quality nanofibres similar to the optimal nanofibres from SNE, and 40 times faster production.

Bubble electrospinning is primarily based on the bubbles on the surfaces of polymer solutions [28]. These bubbles serve as the droplets in which the Taylor cone is formed. The gas tube and metal electrode are inserted in the solution to produce the bubbles. When the gas is blown into the solution, the bubbles are formed (in a spherical shape) on the surface of the solution, and when voltage is applied the bubble shape changes into a conical shape. When the voltage is above a critical value, multiple jets are ejected from the bursting bubble to the collector, while new bubbles are formed and broken again – the process repeats itself until the solution is depleted.

Another process necessitates that drops of a polymer solution dripped onto a standard spin coater followed by rotation of the chuck [112]. The fibres are produced by the instability of the spin-coated liquid that results from the competition of the centrifugal force and the Laplace force induced by the surface curvature. By adjusting the solution parameters (concentration, spinning speed, surface tension) and solvent evaporation rate, different polymers can be processed to their nanofibres. Dabirian *et al*. [113] modified the centrifugal spinning method by enclosing a nozzle in order to avoid the influence of the surrounding air on the dryness of the protruding polymer solution. They also applied a voltage which was not applied in the centrifugal spinning proposed by Weitz *et al*. [112]. They obtained uniform aligned nanofibres with an average diameter of 440 ± 11.3 nm. The mechanical properties of the resulting nanofibres were significantly improved when compared to those of the electrospun nanofibres from SNE.

Yet another proposed electrospinning process necessitates the use of one or more plates held at a certain angle with respect to the horizontal and vertical oriented collector [114]. The reservoir on top of the plates drops the polymer solution onto the metal plate (which serves as

a spinneret), and because of the angle (~40°) and gravitational force the solution slowly flows until it reaches the edge of the plate. At this point, the solution forms a drop that changes its shape to Taylor cone as a result of the electric field at the edge of the plate. More plates were used, given a '*waterfall geometry*'. However, the plates resulted in an irregular spinning due to the electric field difference and the polymer solution on each of the plates. The *waterfall geometry* process displayed lower production rate than the SNE and single edge-plate geometry. The advantage of the single plate method lies in its simplicity and ease of operation with a large number of jets ejected from the plate edge. The disadvantage is the inhomogeneous electric field distribution in the solution, which contributes to the nanofibre structures.

Another needleless setup involves concurrently provoking numerous jets from a sufficiently large liquid surface [115]. The electrospinning is carried out on the free liquid surface with a stainless steel cleft with a certain width. Numerous jets are generated on the surface of the conductive liquid when sufficient voltage is applied. Mathematical equations were proposed and found to be well applicable to SNE and to most of the theories based on this processing technique. The hypothesis from different parameters and dimensionless analysis created a comprehensive description which affords the opportunity for the development of the liquid surface technique.

Nanofibres were also synthesized from conical wire coils as a spinneret [94]. The technique involves a copper wire-coil nozzle with a conical shape with a certain distance between the wires connected to the voltage supply. This technique falls in between the confined and unconfined, because the dripping solution is inside the cone held upside-down, while the reservoir is not enclosed since the droplets are ejected from the solution flowing through the space (gaps) between the wires. The flowing solution is exposed to a high voltage (40-70 kV) in order to produce the jets which travel towards the collector where the nanofibres are collected.

2.4.3 Gas-jet electrospinning

One of the recent advances includes new designs of the needle to fabricate the desired morphology and patterns for various applications. It necessitates a gas jet device connected to the needle and it is known as the gas-jet electrospinning technique [13,15,116-118]. In this

technique the needle of the spinning solution is encircled by the tube of the gas jet. Lin et al. [116] studied the effect of ID and gas flow rate while keeping the other parameters fixed. They found that a smaller ID led to smaller average diameters, while the average diameter decreased monotonically as the gas flow rate increased. It was suggested that the blown gas imposes an additional drawing action on the polymer jet. Other groups used hot stream air-blowing to control the solution properties, solvent dryness and to impose additional stretching to the jet [13,15]. The blown air is heated by passing through heating elements offering control over the rate and temperature of the blown air. The tip-to-collector distance is considerably shorter than for the conventional electrospinning with very high voltages (~40 kV). The method offers an opportunity to increase the processing window boundaries. Ultrahigh molecular weight polymers, and polymers that are difficult or impossible to electrospin from their aqueous solutions, can easily be electrospun through a gas jet process [13,15,86]. However, the throughput is still equivalent to that of SNE, while the diameters of the nanofibres range between 500 and 1000 nm. The disadvantage of this process is the difficulty of solvent recovery. An increase in the throughput will also require an increase in the number of the needles as well as large gas volumes [118].

Another gas jet process necessitates the exploitation of the protruding jet by applying compressed air to further stretch the jet [119,120]. This process is known as gas jet nanofibre (GJF). The GJF consists of a syringe pump, modified nozzle, jet compressed gas (often air), and a collector. Several parameters, such as air jet pressure, feeding rate, and tip-to-collector distance, can be adjusted to engineer the nanofibres morphology. The mass production rate ranges between 0.9 and 8.6 g h^{-1} depending on the polymer properties, solution parameters and processing parameters. However, bi-component and core-shell morphologies can easily be fabricated. Benavides *et al*. [120] produced nanofibres with average diameters of 280, 186 and 425 nm from 6% v/v PEO, 6% v/v poly(vinyl pyrrolidone) (PVP) and poly (vinyl acetate) (PVAc) respectively by using a 276 kPa pressure of compressed air jet with a feeding rate of 0.8 ml min^{-1}. They demonstrated the fact that the nanofibre diameter can be reduced by increasing the air pressure. They also indicated that core-shell by co-axial syringe and side-by-side morphologies from immiscible polymers can easily be prepared.

2.4.4 Nozzle configurations for multi-component nanofibres

2.4.4.1 Co-electrospinning

The modifications of the standard electrospinning devices created a new avenue to combine one or more components with ease of functionalization. One of the simplest ways to fabricate one or more polymeric components is through the use of two or more needles containing different solutions (double electrospinning). This can be done by spinning both solutions, fed from different reservoirs, in a programmed manner such that both solutions reach the collector at the same time [121]. Another way involves the deposition of the nanofibres in a sequential manner, where one polymer solution is first deposited followed by the other [122]. In these methods the syringes filled with different polymers are placed opposite each other with the collector between them, and perpendicular to the principal axis of the collector. The ejected jets are collected using the same collector (mandrel). Nanofibrous membranes containing chitosan and alginate were produced *via* the dual-jet system reported by Hu and Yu [123]. The PEO/chitosan and PEO/alginate were fed from two different nozzles and the jetting difference was 15 seconds [123]. X-ray photon-electron spectroscopy (XPS) confirmed the compositions of the two biopolymers, and fluorescent microscopy micrographs showed that these polymers were evenly dispersed onto each other. A hybrid of chitin and silk fibroin (SF) were also electrospun simultaneously from their solutions fed from two syringes on opposite sides facing a rotating target [124]. Chitin/SF (75/25, 50/50, 25/75) hybrids were prepared from chitin (5 wt% in 1.1.1.3.3.3-hexaflouro-2-propanol (HFIP)) and SF (7 wt% in HFIP) and they were fed to two syringes in opposite directions. The resulting bimodal type of distribution consisted of thinner chitin nanofibres and thicker SF nanofibres with each component dominant depending on their concentration in the composition.

Similarly, the two polymer solutions in the syringes can be placed in opposite sides of the collector. The voltage applied to the syringes result in the ejection of the jets which come into contact (merge into single nanofibres) while moving towards the collector (Figure 2.3) [125]. Duan *et al*. [126] simultaneously electrospun poly(lactide-co-glycolide) (PLGA) and chitosan/poly(vinyl alcohol) (PVA) from different syringes and mixed them on the collector (drum). The solutions from the two syringes connected to a high voltage (15 kV) were fed by a double-way syringe pump at a feeding rate of 0.2 ml h^{-1} onto a grounded drum (tip-to-collector distance (TCP) = 10 cm). The composite nanofibres with an average diameter of 275

± 175 nm consisted of smooth nanofibres with large diameters and beaded nanofibres. Ji *et al*. [86] crosslinked hyaluronic acid (HA) hydrogel nanofibres by a primary syringe (2.5 % w/v/ 2.5 % w/v HA/PEO) connected to a T-shaped three-way steel adapter, and the secondary syringe (9.0% w/v PEGDA) connected by Teflon tubing. A voltage of 18 kV was applied with a TCP of 10 cm. The primary syringe feeding rate was 20 μL min^{-1} and the secondary syringe feeding rate was maintained at 5 μL min^{-1} in order to yield a final 3.3'-dithiobis(propanoic dihydrazide)-modified HA (HA-DTPH) concentration of 2.0 % (w/v) in the mixture. Ultrafine nanofibres with diameters of 90 ± 15 nm were obtained. The fibrous structure was maintained after dissolution of PEO in water, but the average diameter increased to 110 ± 28 nm.

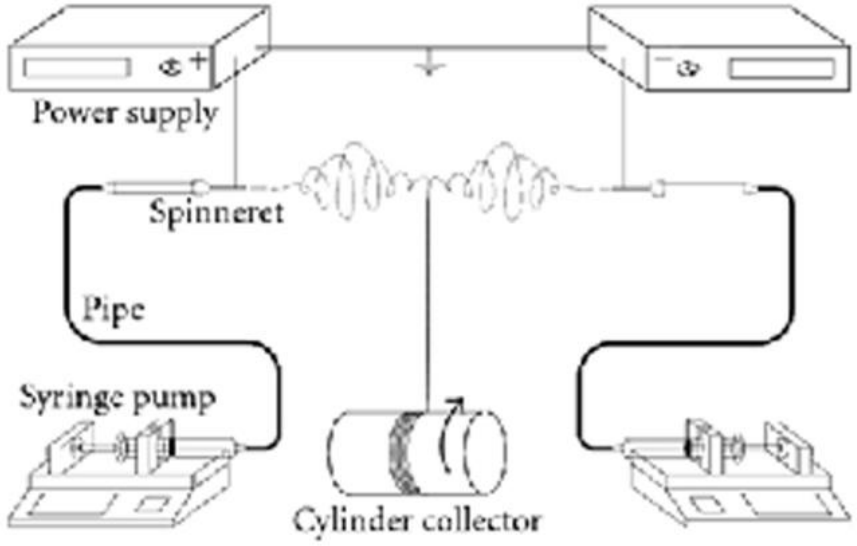

Figure 2.3 Schematic representation of other side-by-side electrospinning (Reprinted with permission from *Xu et al.* [125] Copyright © 2012 Fu Xu *et al*.).

The most convenient manner to electrospin two polymers is through blending the two or more polymers in a suitable solvent [127]. In this case, the selection of the polymers and the solvent are important due to the fact that the interactions between the polymers must not cause phase separation during electrospinning. Nonetheless, the proposition to use a single nozzle with two polymer solutions lying in a side-by-side fashion and coming into contact at the tip of the needle and flowing towards the counter electrode overcame the complications of blending the polymers [127]. This technique is known as side-by-side dual spinneret (Figure 2.4) [128]. These authors synthesized bicomponent nanofibres made up of two small fibres bound together and respectively containing titanium dioxide (TiO_2) and tin dioxide (SnO_2). This was

confirmed by SEM-EDS results, which showed that TiO_2 and SnO_2 were on different surfaces of the fibre.

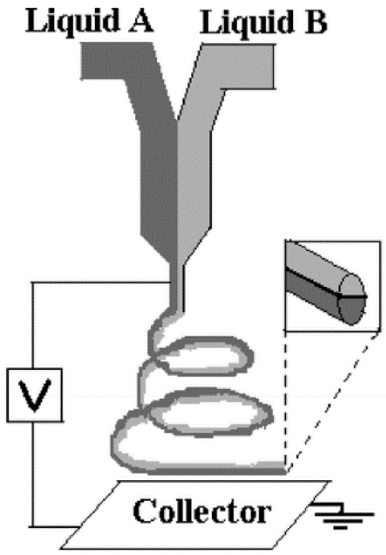

Figure 2.4 Schematic diagram of side-by-side dual spinneret (Reprinted with the permission from Liu *et al.* [128]. Copyright (2007) American Chemical Society).

2.4.4.2 Co-axial electrospinning

Other designs include co-axial electrospinning where hollow or core-shell fibres can be produced with easy functionalization (Figure 2.5). Various materials such as polymers, oligomers, nanoparticles, metal salts, proteins, oils, and enzymes immobilized into the core can be produced to achieve integrated multifunctional materials [1,129-132]. Coaxial electrospinning offers an avenue to prepare nanofibres from the materials which are difficult or impossible to be electrospun into nanofibres using conventional electrospinning processes [129,132]. It can be used in various applications where the stability and control release of small molecules are of significance [133-136]. With appropriate choice of solvent and components a variety of functionalised hollow structures can be fabricated from blend to composite materials [134]. A core-shell of collagen-r-poly(ε-caprolactone) was prepared by this technique [136]. The inner and outer solutions were poly(ε-caprolactone) (PCL)/ triflouroethanol (TFE) (100 mg ml^{-1}) and collagen/TFE (72 mg ml^{-1}), respectively. TEM revealed a core-shell structure with a dark PCL component inside with a diameter 385 ± 82 nm, and a lighter collagen shell with a thickness of 64 ± 26 nm. The variation of the concentration of the solutions for the inner and outer layers influences the overall diameters of the nanofibres, the thickness of the shell and the diameter of the core. Gulfam *et al*. [137]

produced porous co-shell structured nanofibres by utilizing a collecting water bath. They varied the concentration of PCL (outer shell) in order to evaluate its effect on the overall diameter of the resulting nanofibres. The overall diameters of the gelatin-PCL core-shell nanofibres gradually increased with an increase in PCL concentration from 105 ± 31 nm at 4% PCL to 210 ± 49 nm at 12% PCL.

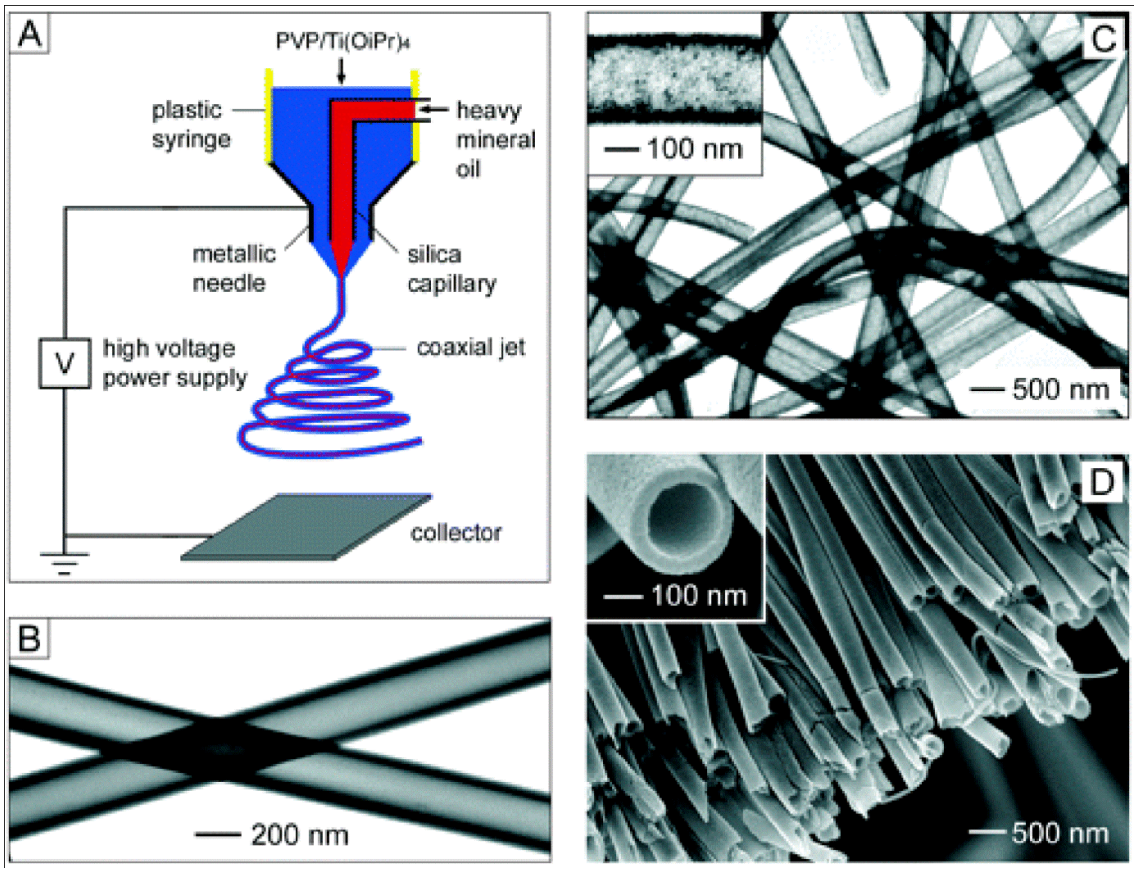

Figure 2.5 Schematic representations for co-axial electrospinning (A). It consists of a spinneret with two coaxial capillaries in which the polymer solution, mineral oil and functional group are ejected simultaneously to fabricate functionalized hollow fibres. TEM image of two as-spun hollow fibres (B). TEM image of TiO_2 (anatase) hollow fibres (C). SEM image of a uniaxially aligned array of anatase hollow fibres (D). (**Reprinted with the permission from Li and Xia. [134]. Copyright (2004) American Chemical Society).**

2.4.4.3 Tri-axial electrospinning

Additional to the conventional co-axial electrospinning, various researchers have developed a novel tri-axial electrospinning technique [130,138,139]. The method uses a nozzle with three concentric needles and three solutions are delivered by different pumps to meet at the tip of

the nozzle. Liu *et al*. [140] produced multi-layered biodegradable nanofibres made of gelatin as core and sheath and PCL as middle layer by triaxial electrospinning (Figure 2.6). The gelatin shell (17 wt%) and core (10 wt%) solutions in 80/20 w/w TFE/deionized water and the middle layer PCL (11 wt%) solution in TFE were fed from the triaxial concentric nozzle at 1.0, 0.15, and 0.4 ml h^{-1}, respectively. The confocal fluorescence microscopy (with the aid of dyes) and FIB-SEM images confirmed the presence of the gelatin/PCL/gelatin layers. The thickness of the sheath was 130 nm, that of the intermediate layer 240 nm, and that of the core layer 230 nm. Even miscible and immiscible polymer solutions, that were impossible to electrospin with traditional co-axial electrospinning, can be fabricated by introduction of the solvent between the two solutions and a reasonable flow rate [130,140]. The incorporated multilayers can perform different functions and incorporate functional groups to target specific applications of the nanofibres.

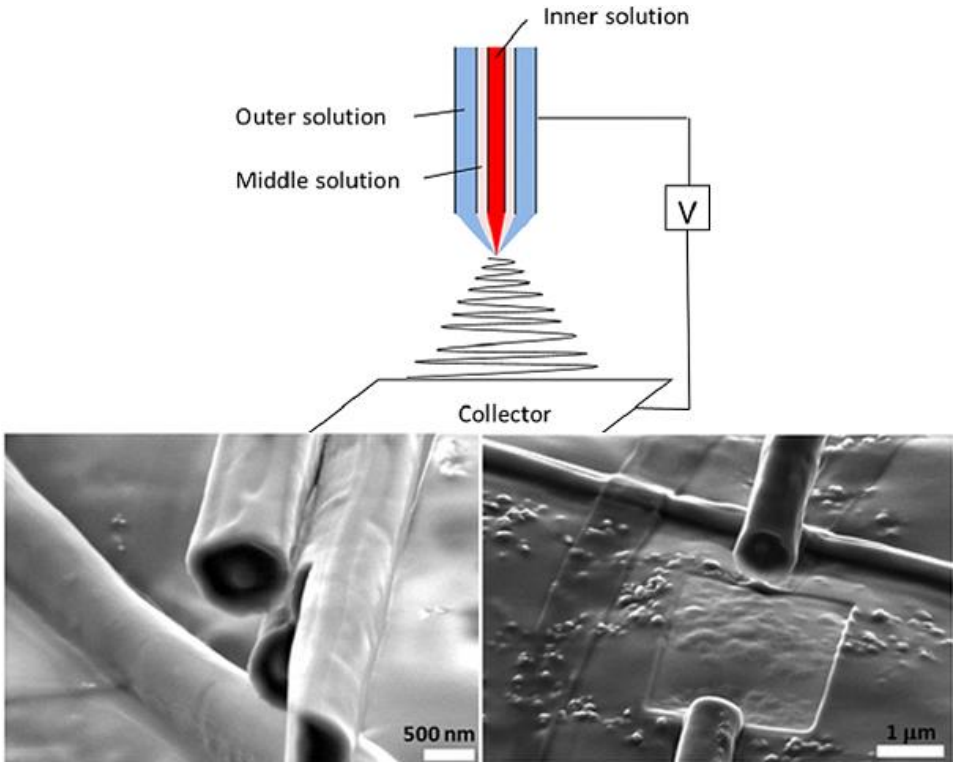

Figure 2.6 Schematic presentation of triaxial and FIB-FESEM images of triaxial electrospun nanofibres. (Reprinted with permission from Liu *et al*. [140]. Copyright (2013) American Chemical Society)

2.5 Electrospinning of biopolymers

A wide array of biopolymers have been electrospun into ultrafine fibres with some difficulty due to the rigid structure and lack of solubility in common solvents. The functional groups,

biocompatibility, biodegradability and non-toxicity of biopolymers are unique properties that afford their applications in various fields. The major disadvantage of some biopolymers in water treatment is their solubility and biodegradation in an aqueous medium, giving synthetic polymers the edge to be the most applied in water filtration and treatment. As already mentioned earlier, different metal oxides were incorporated into the polymers to enhance their biocidal efficacy and the mechanical strength of the electrospun membranes. Most of these biopolymers bear unique functional groups that can be explored in wastewater treatment in order to adsorb various heavy metals *via* different mechanisms such as chelation, electrostatic attraction and ion-exchange. They have abundant availability, biocompatibility, large surface-to-area ratio, high porosity, and malleable mechanical properties and structure, with some unique and interesting potential applications (Table 2.4).

2.5.1 Cellulose

Cellulose is the most abundant natural polymer on earth and it is derived from a wide variety of cellulose-containing sources such as plants, animals and bacteria [26,141]. It is composed of a linear chain of β(1-4) linked D-glucose units as shown in Figure 2.7. Cellulose has interesting properties such as biocompatibility, biodegradability, and recyclability. Electrospinning of pure cellulose, from its aqueous solutions, like most biopolymers poses many challenges, where some modifications of the electrospinning setup/devices are needed [11,14]. For example, Frenot *et al*. [11] found that the collected fibre stood straight up on the collector when plastic and aluminium covered plates are used as collectors. However, the use of a rotating drum/copper or liquid bath collector in a suitable humidity resulted in smooth bead-free fibres [76,142,143]. Cellulose cannot melt and it is insoluble in water and most of the common organic solvents because of the dense hydrogen network which limits its applications and processability. Only a few solvents such as paraformaldehyde (PF)/N.N-dimethylformamide (DMF), lithium chloride (LiCl)/N.N-dimethylacetamide (DMAc), N-methylmorpholine-N-oxide (NMMO), urea/sodium hydroxide (NaOH) and ionic liquids can dissolve cellulose [23,76].

The possibility to functionalize cellulose *via* the hydroxyl side groups on the backbone offers the opportunity to electrospin it in a derivative-form followed by its regeneration *via* deacetylation or hydrolysis treatments.

Table 2.4 The potential applications of electrospun biopolymer membranes in water treatment

Biopolymer	Desirable properties	Current application	Potential future applications
Cellulose and derivatives	Easy functionalization, hydroxyl groups, and functional groups from derivatives	Drug delivery, food, tissue scaffolds, personal care, detergent, paper making, textile, mining flotation, Pharmaceuticals, personal care, cigarette filters	Bioadsorbent, metal and impurities separation, ultralfitration, microfiltration and bioadsorbent, trace metal detection
Cellulose nanowhiskers	High specific area, easy functionalization, high crystallinity, high modulus	Polymer reinforcement	Selective layer in ultrafiltration and nanofiltration membranes, microfiltration, reinforcement
Chitin and derivatives	Easy functionalization, availability of amino groups and other functional groups from derivatives	Drug delivery, environmental engineering, tissue scaffolds, food wraps, flocculants in water, biocidal membranes, tissue scaffolds	Anti-biofouling membranes, membrane coating, flocculation agent
Chitin nanowhiskers	High specific area, easy functionalization, high crystallinity, high modulus	Polymer reinforcement	Barrier layer in TNFC, reinforcement
Alginate	Carboxyl groups and hydroxyl groups	Food texturing, tissue scaffolds	Metal chelation, anti-biofouling membrane, heavy metal detectors
Collagen	Unique triple-helical structure	Food, tissue scaffolds, cosmetics	Metal chelation
Gelatin	Thermoreversible viscosity, independent of pH	Cosmetics, food industry, pharmaceutical, coatings	Membrane coating, controlled release and encapsulation of disinfection agents
Hyaluronic and derivatives	Easy functionalization	Dermal fillers, tissue scaffolds	Metal chelation
Aloe vera	Different functional groups	Antibacterial creams, lotions, ointment, tissue scaffolds	Immobilizer of bacteria, enzymes and other biological molecules

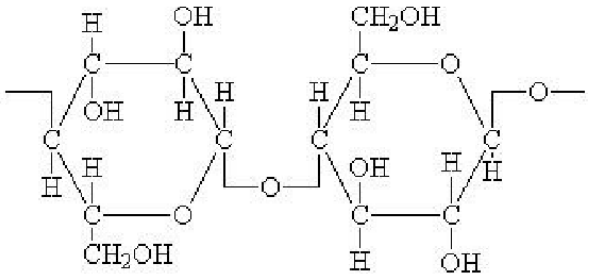

Figure 2.7 Structure of cellulose

Cellulose derivatives through –OH (hydroxyl group) functionalization include cellulose acetate, hydroxyl propyl cellulose, hydroxyl propyl methyl cellulose, and methyl cellulose [11]. These derivatives are soluble in most of the common organic solvents and they can be converted to pure cellulose *via* hydrolysis and deacetylation. Stephen *et al*. [142] functionalized cellulose nanofibrous membrane with oxolane-2,5-dione in order to enhance their heavy metal adsorption efficiency. They first electrospun cellulose acetate, followed by deacetylation of the resulting nanofibres membrane by using sodium hydroxide (0.3M NaOH) to generate pure cellulose. The nanofibrous membrane displayed a large surface area of 13.7 $m^2\ g^{-1}$ compared to raw cellulose fibres membrane with a surface area of only 3.2 $m^2\ g^{-1}$. The adsorption capacity for lead (Pb) and cadmium (Cd) were respectively 1.0 and 2.9 mmol g^{-1}. The regeneration of the mats was done through nitric acid (HNO_3) treatment, and the regenerated mats performed quite well.

2.5.1.1 Cellulose nanowhiskers

Cellulose nanowhiskers can be extracted from their abundant source (cellulose) by mechanical and chemical means [141,144]. The high aspect ratio, high crystallinity, easy functionalization, and large surface areas make the nanowhiskers the next generation of wastewater treatment nanomaterials. Several researchers incorporated various whiskers in different polymers such as poly(2-hydroxy ethyl methacrylate) [145], PVA [146], and PEO [147] in order to improve the mechanical properties of the resulting electrospun nanofibres. These researchers found that higher modulus and stiffer nanowhiskers improved the mechanical properties of the electrospun nanofibres despite the observed agglomeration of the whiskers [147].

Oxidized jute cellulose whiskers with diameters ranging between 3 and 10 nm were coated onto polyacrylonitrile (PAN) nanofibres membrane (mean diameter ~173 nm) either once (single layer) or twice (double layer) by using a glass rod [148]. This method afforded the formation of pore sizes ranging between 5 and 65 nm. The membrane was tested under ultrafiltration (UF) and nanofiltration (NF) conditions, in which the rejection of both nanosilica (in the case of UF) and oil and water (in the case of NF) was above 99%. The mechanical properties of the resulting electrospun nanofibrous membrane (ENM) were improved by the presence of the whiskers, with the tensile strength increasing from 4 to 10 MPa (for a single coating of the whiskers onto the ENM) and 14 MPa (for double coating).

Cellulose nanowhiskers and nanofibres have also been thoroughly studied by the Chu and Hsiao group in water treatment and filtration applications [149-152]. The cellulose nanowhiskers were either employed as barrier layer of thin-film nanofibrous composite membranes (TFNC) (Figure 2.8), or they were infused into the electrospun membrane, depending on the intended filtration application (microfiltration (MF) or UF).

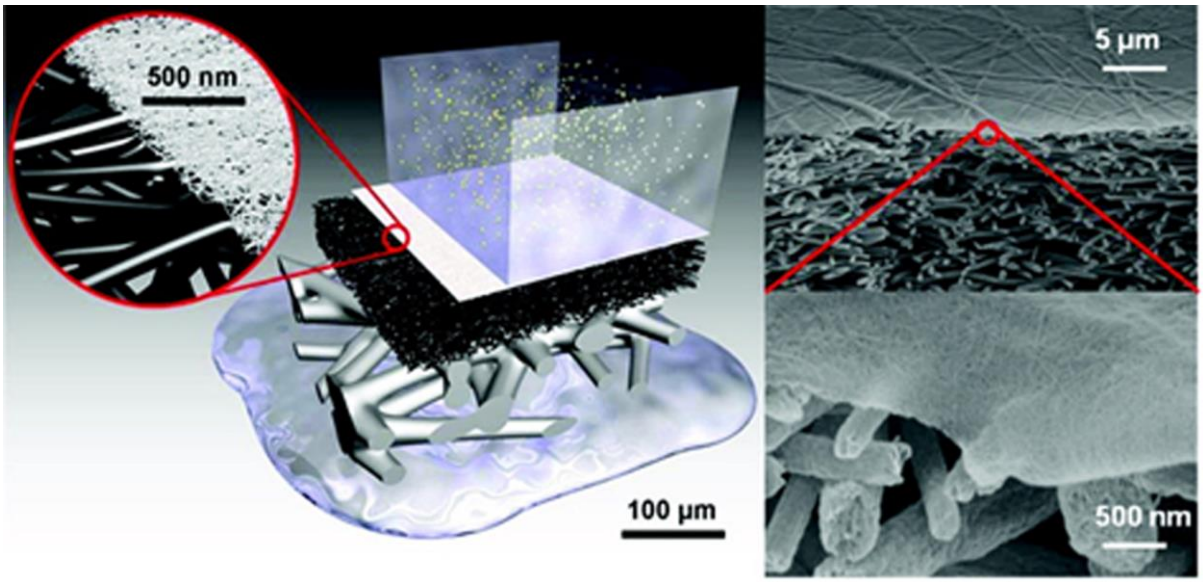

Figure 2.8 (Left) A schematic representation of a thin-film nanofibre composite membrane (TNFC) with three layers: selective/barrier layer, mid-layer of electrospun nanofibres, and nonwoven supporting mat (poly(ethylene terephthalate) (PET)). (Right) Cross-sectional SEM views of the barrier layer and electrospun nanofibres in a typical TNFC membrane. (Reprinted with permission from *Ma et al.* [150]. Copyright (2012) American Chemical Society).

Cellulose nanowhiskers were prepared through a [2.2.6.6-tetramethylpiperidinooxy (TEMPO)/sodium bromide (NaBr)/sodium hypochlorite (NaClO)] oxidation method. The length of the cellulose nanowhiskers ranged between 200 and 400 nm and the diameters between 5 and 10 nm. In the case of MF, the infusion of the whiskers resulted in a reduction of the mean pore size with a narrower distribution than the electrospun PAN nanofibrous membrane. In comparison with the commercial membrane GS0.22 made of nitrocellulose and acetyl cellulose ester, the water flux of the cellulose nanowhisker-based membrane was better because of the difference in porosity (>80 % versus 52 %) [144]. The mechanical properties were improved with the Young's modulus and tensile strength values of 375 ± 15 and 14.3± 0.4 MPa, respectively, when compared to the unmodified membrane (226 ± 20 and 8.5 ± 0.3 MPa) which was still higher than the commercial membrane with a tensile strength of 5.6 ± 0.3 MPa. The adsorption of crystal violet (CV) dye was better in the case of the cellulose nanowhiskers-based membrane than in GS0.22 (Figure 2.9a). The adsorption was two times higher at 10 mg L^{-1} of CV dye with a high rate of adsorption because of the hydrophilicity and large surface area. The adsorption data fitted the Langmuir isotherm showing a monolayer adsorption characteristic (Figure 2.9b). The adsorption capacity was 16 times higher for the cellulose nanowhiskers-based membrane. The cellulose nanowhiskers as a thin barrier layer in TNFC displayed a superior performance when compared to the commercial known membranes [144]. The hydrophilicity, large surface area to volume ratio and the surface charges of the cellulose nanowhiskers played a significant role in improving the rejection and flux of the membrane.

2.5.1.2 Cellulose derivatives

Cellulose acetate

Among the cellulose derivatives, cellulose acetate (CA) is the most studied derivative due to its potential to regenerate pure cellulose via deacetylation [23,152]. Cellulose acetate is synthesized by acetylation of the hydroxyl groups on cellulose with an average of 2-4 degree of substitution per glucose units (Figure 2.10). The CA has enjoyed its success in membrane filtration for more than seven decades now [149,153,154]. It has been widely used as a selective layer in nanofiltration and ultrafiltration. With its unique functional groups that can be modified, it is rated as one of the good metal adsorbents [149,150]. The functionalization of CA with -COOH, $-SO_3H$ and NH_2 offers an opportunity for the application of CA in heavy

metal complexation [151,152]. Some nanofillers can be added to a cellulose acetate membrane in order to enhance the metal adsorption capacity [149].

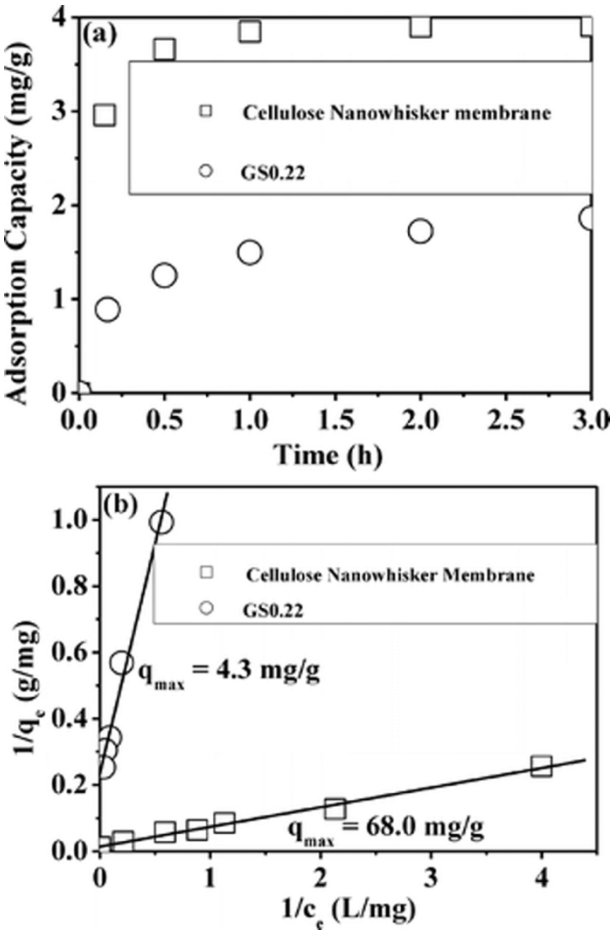

Figure 2.9 (a) Adsorption capacity of cellulose nanowhiskers-based nanofibrous MF membrane and GS0.22 against time; (b) respective Langmuir adsorption isotherms for the two membranes (Reprinted with permission from *Ma et al.* [144]. Copyright (2012) American Society).

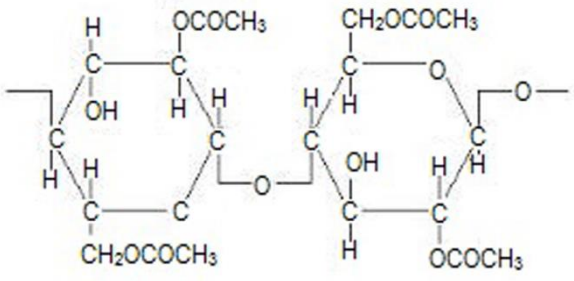

Figure 2.10 Structure of cellulose acetate

Zhou *et al.* [153] prepared cellulose acetate nanofibrous membranes from various solvents (dichloromethane, formic acid, acetic acid, and triflouroacetic acid). Only trifluoroacetic acid afforded the production of smooth nanofibres with diameters ranging between 100 and 300 nm. This membrane displayed a porosity and surface area of respectively 87% and 2.02×10^7 m^{-1} with high water permeability and hydrolytic stability. Tungprapa *et al*. [61] studied the influence of various solvents and their mixtures on the electrospinning of CA. Using a single solvent like chloroform, N,N-dimethylformamide (DMF), dichloromethane (DCM), methanol (MeOH), formic acid, or pyridine, it was not possible to fabricate smooth nanofibres. Only discrete beads were formed, and acetone produced short beaded nanofibres. CA (5 % w/v) in a mixture of chloroform-MeOH and DCM-MeOH produced beaded and smooth fibres, especially at 4:1 (v/v). The average diameters were 0.79-1.09 μm and 0.67-1.06 μm respectively for the binary mixtures of chloroform-MeOH and DCM-MeOH. Smooth fibres were formed at solvent mixture concentrations of a 16 % (w/v) solution of CA in 1:1, 2:1 and 3:1 acetone- N,N-dimethylacetamide (DMAc), 14-20 % (w/v) solution of CA in 2:1 acetone-DMAc, and 8-12 % (w/v) solutions of CA in 4:1 (v/v) DCM-MeOH. The diameters ranged between 0.14-0.37 μm and 0.48-1.58 μm for fibres prepared from acetone-DMAc and DCM-MeOH, respectively.

Chen *et al*. [160] functionalized cellulose acetate nanofibrous membrane with chlorhexidine for their biocidal efficacy. In order to facilitate the electrospinnability in N,N-dimethylformamide (DMF), high molecular weight PEO was added. The electrospun nanofibrous membrane was crosslinked by using titanium triethanolamine in isopropanol. The biocidal efficiency against *E. coli* and *S. epidermisidis* increased with the concentration of chlorohexidine. The membrane displayed biocidal efficiency above 99%. Moreover, different drugs can be incorporated in cellulose acetate as carrier [69,161,162]. Suwatong *et al*. [162] incorporated curcumin in cellulose acetate nanofibres in order to investigate its releasing character. The cellulose acetate nanofibres retained their structure and morphology after the addition of curcumin. A 95% release without toxicity was established. This property can be explored in incorporating different functions/biocides for controlled release in water treatment. For example, Ma and Ramakrishna [163], covalently bond protein A/G onto the oxidized CA membrane to bind IgG molecules and a capturing capacity of 18 μg/mg was reported. Similarly, Chen *et al*. [164] functionalized hydrolysed CA with cobalt tetraaminophthalocyanine (CoPc) for the adsorption of reactive red X-3B dye and more than 95% of the dye was eliminated within 3 hours.

Other cellulose derivatives

Four different carboxymethyl cellulose sodium salts (CMC) were electrospun by Frenot *et al*. [11]. CMCs with different molecular weight and degree of substitution were electrospun in the presence of PEO as copolymer, dissolved in a water and ethanol mixture at a ratio of 1:1. The nanofibres displayed similar homogeneous structures with mean diameters of 200-250 nm, regardless of the molecular weight and degree of substitution. In the same study, two hydroxypropyl methyl cellulose (HMPC) samples with equal M_w, and with varying contents of methoxy and hydroxypropoxy groups, were compared. Mean diameters of 127 and 128 nm were obtained for the two HMPCs, regardless of the functional group contents, but at different spinnable concentrations. Lim *et al*. [88] studied the effect of different parameters (concentration, voltage, flow rate and tip-to-collector distance) on the electrospinning of ethyl cellulose (EC). At a low concentration (6 wt%) a mixture of smooth and beaded-fibre structures was observed, which disappeared as the concentration was increased to 8 wt% of the EC and above. The mean diameter of the nanofibres gradually increased with flow rate, whereas an increase in voltage reduced the mean diameter of the nanofibres.

2.5.2 Chitin

Chitin is the second most abundant natural polymer on earth after cellulose. It appears as ordered crystalline structure of microfibrils in the exoskeleton of arthropods, and the cell walls of fungi and yeast [165]. Chitin, the mucopolysaccharides that is made up of ß-(1-4)-N-acetyl-D-glucosamine units linked by 1-4 glycosidic bonds, acts as mechanical strength and supporting structure in crustaceans, insects, etc. (Figure 2.11) [51,166,167]. Chitin with desirable properties such as good biocompatibility, biodegradability and ubiquitous availability has been used in various fields such as cosmetic, biomedical and in food additives [165].

Very few studies have dealt with the electrospinning of chitin from its aqueous solution, because of its poor solubility [168,169]. In these studies, the solubility of chitin was enhanced by Co^{60} gamma ray irradiation. Chitin nanofibres with diameters ranging between 50 nm and several microns were electrospun in 1.1.1.3.3.3-hexaflouro-2-propanol (HFIP), with diameters depending on the electrospinning technique parameters such as concentration [167-169]. Min *et al*. [168] irradiated chitin (200 kGy) and obtain an average molecular weight of 91000 to

enhance its dissolution in HFIP. They produced chitin nanofibres with a broad fibre diameter distribution (40 to 640 nm) and most of them were less than 100 nm.

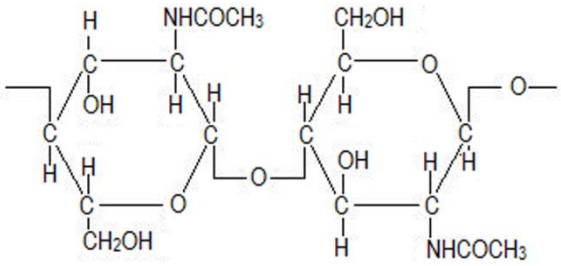

Figure 2.11 Structure of chitin

2.5.2.1 Chitin nanowhiskers

Nanocomposites of PVA and chitin whiskers were reported for the first time by Junkasem *et al*. [170]. Nanowhiskers with the lengths in the range 231-969 nm and widths of 12 to 65 nm were produced. Nanocomposite nanofibres (prepared from water) with diameters ranging between 175 and 214 nm, depending on the concentration of the chitin whiskers, were obtained. The thermomechanical properties of PVA were enhanced by the presence of the chitin whiskers [171]. Naseri *et al*. [172] reinforced a blend of chitosan and PEO with chitin nanowhiskers. The Young's modulus and tensile strength were significantly increased from 0.4 to 4.3 GPa and from 4.6 to 34.9 MPa, respectively. An antibacterial TNFC membrane was developed by including chitin nanowhiskers as barrier layer onto electrospun PAN nanofibres (as a mid-layer on top of a PET nonwoven support) [144]. The flux permeation was 217.0 L m^{-2} h^{-1} (which was 8-10 times higher than that of commercial PAN10) for two days at 30 psi with a rejection above 99.7%.

2.5.2.2 Chitin with synthetic/biopolymers

A nanofibre blend of poly(glycolic acid) (PGA) and chitin was prepared by Park *et al*. [173]. The nanofibres had a broad diameter distribution in the range of 50-350 nm, with most of the nanofibres having an average diameter of 150 nm. Chitin/silk blend nanofibres were prepared by several researchers using HFIP as a solvent [124,173]. The nanofibres had diameters ranging between 340 to 920 nm depending on the content of silk in the composite material.

Irradiation and mild deacetylation (8% DD) of chitin was also adopted to reduce its molecular weight and improve its solubility.

2.5.2.3 Chitin derivatives

Dibutyryl chitin

One of the readily soluble chitin derivatives in most common organic solvents (acetone, ethanol) is dibutyryl chitin. It is synthesized from butyric anhydride and perchloric acid. Blasińsk *et al*. [174] electrospun an ester derivative of chitosan, dibutyrylchitin (DBC), from ethanol. 9 wt/v of DBC at 25 kV were the optimal conditions to establish bead-free nanofibres with a transverse dimension of 0.3 μm. DBC and a cellulose acetate hybrid were electrospun in a 1:1 ratio of acetone and acetic acid [175]. The mixture of CA/DBC at a concentration of 5% from 100/0 to 0/100 ratio compositions produced bead-free nanofibres with diamaters ranging between 30 and 350 nm. Pant *et al.* [176] synthesized chitin butyrate from a mixture of butyric acid, trifluoro acetic anhydride and phosphoric acid, followed by the addition of ethyl alcohol and filtration. The resulting solution was washed repeatedly with diethyl ether and water, followed by drying for 3 days in a hood and then in a 60 °C oven for 6 hours. The resulting butyric chitosan was electrospun with nylon-6 in formic acid/acetic acid to give spider-web-like nanofibres with an average diameter of 15 nm at a low butyric chitosan content (90/10 nylon-6/butyric chitosan).

Carboxymethyl chitin

In order to circumvent the solubility issues of chitin and chitosan, some of their derivatives have been electrospun into nanofibres either from their aqueous solutions or by blending with other polymers. This not only to improved their spinnability, but also alleviated the use of a toxic solvent utilized in the electrospinning chitin and chitosan. Carbomethyl chitin (CMC) is one of the chitin derivatives that are readily soluble in water. However, the electrospinning of CMC from its aqueous solution results in spherical drops [177]. Nevertheless, ultrafine nanofibres from a CMC/PVA blend at a 20:80 ratio (CMC (7%):PVA (8%)) was reported. Sohofi *et al*. [178] were the first group of scientists to fabricate CMC electrospun nanofibres from its aqueous solutions by using binary solvents. The 6 wt% CMC (with degree of substitution of 0.65) was electrospun in a 30/70 dichloromethane/trifluoroacetic acid mixture

to ultrafine nanofibres with an average diameter of 260 ± 42 nm. Although the carbomethylated chitosan showed a potential in metal adsorption [179], nanofiltration [180], and microfiltration [181] processes, however, little has been done on electrospun CMC in wastewater treatment.

Chitosan

Chitosan results from the deacetylation of chitin under alkaline conditions, or from enzymatic hydrolysis in the presence of chitin deacetylase. It is an aminopolysacchride with unique properties and functionalities for a wide spectrum of applications from biomedical to industrial areas. Chitosan is a copolymer made up of 2-acetamido-2-deoxy-β-D-glucopyranose and 2-amino-2-deoxy-β-glycopyranose linked together through (1-4)-β-glycosidic bonds (Figure 2.12). Similar to alginates, different forms of chitin and chitosan such as gels, membranes, beads, microparticles, nanoparticles and nanofibres have been produced for various applications [51,166]. Chitosan is well-known for its unique antimicrobial activity and metal adsorption [182,183]. These result from the protonation of NH_2^- groups on its backbone. It is capable of chelating ions from aqueous media and inhibiting the growth of a broad spectrum of fungi, yeasts and bacteria. The cations along the chitosan repeating units can be varied through deacetylation. A high degree of deacetylation results in a large number of cations on the backbone of the chitosan. Chitosan is soluble in most acids, which protonate it into a polyelectrolyte.

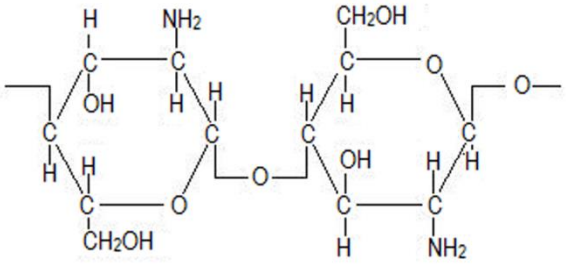

Figure 2.12 Structure of chitosan

Different solvents such as dilute hydrochloric acid, acetic acid, formic acid and triflouroacetic acid (TFA) were tested to envisage the electrospinnability of chitosan [184]. Only with TFA as solvent chitosan nanofibres were successfully established [184]. It was indicated that the TFA either forms amino groups on chitosan, which results in the destruction of the rigid interaction between the chitosan molecules, or that the high volatility of TFA caused rapid

solidification of the electrified jet. More homogeneous nanofibres were obtained by addition of dichloromethane, due to its high volatility. Geng *et al*. [67] successfully electrospun chitosan from concentrated acetic acid. 30% of acetic acid in water resulted in a combination of droplets and thinner nanofibres with an average diameter of ~40 nm, whereas at 90% acid concentration the diameter of the nanofibres increased to ~130 nm without beads.

Chitosan with synthetic polymers

Over the past decades, electrospun chitosan hybrids have been fabricated by using various synthetic polymers such as polyvinyl alcohol (PVA) [126,185], poly(lactide-co-glycolide) (PLGA) [126], polyethylene oxide (PEO) [186], polyvinyl pyrrolidone (PVP) [83], poly(lactic acid) (PLA) [80], and poly(ethylene terephthalate) (PET) [187]. Interestingly, the synthetic polymer did not only improve the electrospinnability of chitosan, but significantly enhanced the biocompatibility, antibacterial, mechanical strength and other properties of the hybrid nanofibres. These broadened the applicability of the chitosan-based nanofibres in a broad spectrum of applications. PEO is a biocompatible synthetic polymer favourable for biomedical and tissue engineering. Su *et al*. [186] prepared chitosan/PEO blends doped with monovalent (Na^{+}), divalent (Ca^{2+}) and trivalent (Fe^{3+}) metal chlorides to enhance the homogeneity of the resulting nanofibres. They found that these metal chlorides promoted the fibrous morphology of the chitosan/PEO blends, thereby opening doors for the use of these nanofibres in various applications such as wound dressing, bone regeneration, etc.

Chitosan with other biopolymers

The electrospun nanofibres of chitosan and other natural polymer blends were studied by several researchers [188,189]. Torres-Giner *et al*. [188] prepared a bioblend of chitosan and zein for biocidal applications. Low zein content (1 wt%) in the bioblend resulted in ribbon-like nanofibres with an average diameter of 320.9 ± 92.3 nm. An increase in the percentage of chitosan in the blend yielded beaded-fibres with smaller average diameters between 161.7 ± 39.6 and 128.5 ± 26.2 nm. The electrospun bioblend inhibited bacterial growth. Bioblend electrospun nanofibrous membrane of chitosan and a type I collagen were fabricated with the aid of PEO, followed by crosslinking with glutaraldehyde [190]. The ultrafine fibres had average diameters of 134 ± 42 nm before crosslinking and 98 ± 76 nm after crosslinking. The difficulty of electrospinning CS/collagen, due to its high conductivity/charge density, was

improved by the addition of PEO. Young modulus improved from 0.29 ± 0.04 to 0.65 ± 0.02 MPa by crosslinking. Maeda *et al*. [191] electrospun chitosan with the aid of PEO, followed by coating with hyaluronic acid. The composite was made by dissolving PEO in water and coating with hyaluronic acid, and it was stable in water with an improved swelling ratio due to the increased hydrophilicity as a result of the presence of hyaluronic acid. PVA/CS was electrospun onto a PVDF micro-filter, followed by crosslinking with glutaraldehyde [192]. The membrane was immersed in glutaraldehyde (5 mM) and an HCl (0.01 N) solution for six hours, and the membrane shrinked by ~5%. Dead-end filtration was utilized to evaluate the metal adsorption capacity of the membrane. A 5% adsorption capacity was reported.

Chitosan derivatives

Quaternized chitosan (QCh) nanofibrous membrane for antibacterial activity were electrospun by Ignatova *et al*. [83,193,194] using poly(vinyl pyrrolidone), polyvinyl alcohol, and poly(lactic acid). The addition of these synthetic polymers significantly improved the electrospinnability of quaternized chitosan. The composite nonwoven mats showed good antibacterial activity against Gram negative and Gram positive bacteria. Kangwansupamonkon *et al*. [195] prepared chitosan/PEO mats followed by functionalization to form N-(2-hydroxyl) propyl-3-trimethyl ammonium chitosan chloride (HTACC) and N-benzyl-N,N-dimethyl chitosan iodide (QBzCS) membranes. They prepared the nanofibres from a blend of chitosan and PEO (6.7:0.3 % w/v) in a mixture of trifluoroacetic acid/dichloromethane (70/30 v/v) followed by functionalization. They obtained ultrafine nanofibres with average diameters of 272 ± 56 nm. The membranes displayed good antibacterial efficiency against both *S. aureus* and *E. coli*. Ultrathin nanofibres of N-[(2-hydroxy-3-trimethlammonium) propyl] chitosan chloride (HTTC) through blending with PVA was reported by Alipour *et al*. [196]. The HTTC was synthesized from a reaction between chitosan and glycidyl-trimethylammonium chloride. The water soluble derivative, HTTC, was electrospun through blending with PVA to give nanofibres with 200-600 nm diameters. Good antibacterial efficiency was reported for these membranes.

Chitosan can be modified by various acyl chlorides (dodecyl, hexanoyl, decanoyl, and lauronyl) in the presence of mixed pyridine and chloroform as solvents [197]. These modifications are usually adapted to improve the solubility of the chitosan. Hexanoyl-chitosan from chitosan modification by hexanoyl chloride in chloroform was electrospun by Naemark

et al. [82]. The ribbon-like fibres with an average diameter of 3.93 ± 1.82 μm at a concentration of 14 % w/v were obtained. This was due to the rapid evaporation of the chloroform from the electrified jet. Peesan, Rujiravanit, & Supaphol, [198] fabricated a blend of hexanoyl chitosan/polylactide using chloroform, dichloromethane and tetrahydrofuran as solvents. The smooth bead-free nanofibres were obtained at 50 wt% of chitosan in the blends using chloroform as spinning solvent. Cooper *et al*. [27] electrospun lactic acid-modified chitosan by using TFA as solvent and MC as co-solvent. The nanofibres were stabilized by using thermal treatment to convert the lactate to lactamide. The resulting nanofibres showed good nanofibrous integrity, even after exposure to a bovine serum albumin (BSA) medium for 72 hours.

Different molecular weights (40-405 kDa) and degrees of substitution (DS) (0.25-1.19) carbomethyl chitosan (CMCS) were synthesized *via* chitosan alkalization, followed by carbomethylation with monochloroacetic acid [81]. Despite the difference in DS and M_w, and with the incorporation of Triton X-100 (to reduce both solution surface tension and conductivity) into the aqueous CMCS solution, the spinning solution still led to drops (6-20% concentration). The blending of the CMCS with hydrosoluble synthetic polymers (PVA, polyacrylic acid (PAA), polyacrylamide (PAAm) and PEO) enhanced the spinnability of CMCS into smooth nanofibres, but it depended on the polymer used. PEO (100 kDa) with 30 % CMCS gave merged non-cylindrical nanofibres mostly with 300 nm diameter, while PAAm at 1/10 w/w of 5000 kDa/10 kDa (18 wt%) resulted into a similar structure as the PEO/CMCS blend. A 10 wt% binary aqueous mixture with equal mass PAA (450 kDa), produced straight cylindrical nanofibres with elongated beads (100 nm diameter). A mixture of PAAm and PAA resulted in higher CMCS content (50%), but with a large number of beads. In the case of a PVA binary solution with a concentration of 8.5 wt% (CMCS 405 kDa), nanofibres with average diameters ranging between 210 and 170 nm were obtained on increasing the CMCS content from 20% to 50%. The PVA/CMCS system is therefore feasible to produce bead-free nanofibres. The stability of the PVA/CMCS in water was further enhanced by heat treatment at 140 °C for 30 minutes.

Another interesting approach to overcome the problem of solubility of chitosan is PEGylation. Du and Hsieh [84] synthesized PEG-N-chitosan and PEG-*N,O*-chitosan *via* the reductive amination and acylation of the chitosan. A small DS value of 0.2 for the solubility of the derivatives in water was reported. For the PEG-*N,O*-chitosan a DS value of 1.5 was

sufficient for its solubility in $CHCl_3$, DMF, DMSO and THF. Regardless of the degree of substitution of PEG (DS) and the derivative of chitosan, only droplets were collected due to a lack of chain entanglements. All the aqueous solutions of PEG-N-chitosan (from reductive amination) resulted in spraying (drops), regardless of the DS of PEG. Smooth nanofibres with diameters ranging between 40 and 306 nm (average 162) were obtained by increasing the concentration of the PEG-*N,O*-chitosan with the aid of a surfactant (0.5 % Triton X-100^{TM}) and a co-solvent (75/25 v/v THF/DMF).

2.5.3 Alginate

Alginate is a well-known polyelectrolyte binary copolymer derived from seaweeds/algae [199-202]. It contributes to the flexibility and strength of the seaweeds against adverse water forces. It is usually found in the cell wall matrix and intercellular material (mucilage). Alginate is a linear polysaccharide made up of D-mannuronic (M) and L-guluronic (G) units linked together by 1-4 glycosidic bond (Figure 2.13). These units appear in varying sequences and ratios, M/G, along the polymer chain depending on the source or specie, the growth conditions, season and depth at which it is extracted. The variation of M and G along the alginate chain determines its physical properties and reactivity. The molecular conformation and functional groups (especially carbonate ions) have been found to play a significant role in the heavy metal affinity of the alginates [202]. Alginate can gel at room temperature in the presence of polyvalent or divalent metal ions. This phenomenon has been exploited to prepare different morphologies and structures for certain applications. Beads [203], films [204,205], hydrogels [206], as well as porous membranes and nanofibres [200] were fabricated for different applications such as wound dressings and metal adsorption. There has been significant interest in the use of alginate in biomedical applications because of its antimicrobial efficiency and structural resemblance to glycosamineglycan (GAG) (one of the significant components of natural extracellular matrices (EMCs) found in mammalian tissues). Furthermore, the good cellular compatibility, non-toxicity, biodegradability, and availability of alginate opened doors for its exploitation in various applications such as metals recovery [202,203].

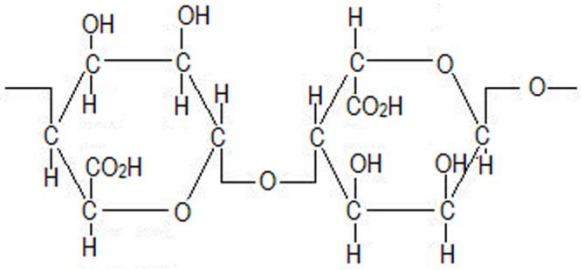

Figure 2.13 Structure of alginate

Until now the electrospinnability (in this case electrospinnability is used to describe bead-free smooth nanofibres) of sodium alginate is still impossible. In most studies carrier polymers are generally used to improve this. Alginate is readily soluble in water. However, it is still controversial on why it is not possible to electrospin alginate on its own. It has been postulated that a high conductivity, lack of entanglements, and gelation of the alginate solution at low concentration (below the concentration for the formation of entanglements) are responsible for this. The rigidity of the chains, worm-like molecular structure and high surface tension also contribute to this. Nevertheless, Nie *et al*. [12] managed to prepare pure alginate nanofibres using glycol as a solvent. They found that the glycol altered the chain conformation of the alginate and improved chain entanglements (viscosity and elasticity). Glycol decreased the surface tension and conductivity which contributed to the electrospinnability of pure alginate. Bonino *et al*. [207] tried to electrospin pure alginate using water as a solvent, which resulted in large droplets on the collector, that were reduced by a surfactant. The production of alginate nanofibres from its aqueous solution was also reported by Fang *et al*. [24]. Calcium ions improved the intermolecular interaction which enhanced its electrospinnability from water. 1 wt% Ca^{2+} was sufficient to ensure continuous electrospinning and the production of long nanofibres. The hydrolysis degradation of alginate in water *via* glycosidic hydrolysis after 15 days (reducing alginate solution viscosity) was exploited to electrospin alginate solution (4 wt%) with the aid of a Triton X-100 surfactant and dimethyl formamide (DMF) as a cosolvent [208].

2.5.3.1 Alginate with synthetic polymers

One of the convenient ways to enhance the electrospinnability of biopolymers consists of choosing a compatible copolymer to co-spin with. Polyethylene oxide (PEO) is a biocompatible and biodegradable synthetic polymer. It is non-ionic and hydrosoluble.

Alginate is also hydrosoluble and therefore offers the opportunity to co-spin the two without difficulties [54]. The two interact with each other through hydrogen bonding which reduces the viscosity of the alginate solution. Cylindrical nanofibres from alginate/PEO with a mean diameter of ~75 nm were prepared by Bhattarai *et al*. [52]. Recently, Saquing *et al*. [54] reported that higher molecular weight PEO is required to increase the concentration of alginate in the PEO/alginate blend. They indicated that the PEO-PEO interaction is responsible for the electrospinnability of alginate. Co-axial electrospinning of alginate (core) and PEO (shell) was recently reported. PEO was easily extracted by dissolving the nanofibres in water containing calcium chloride to crosslink the alginate [129]. They successfully incorporated 85 wt% of alginate in the blend with the aid of the surfactant. Another hydrosoluble synthetic polymer, with good mechanical properties, thermal stability, chemical stability and biocompatibility, is poly(vinyl alcohol) (PVA). A number of researchers utilized this polymer as copolymer for alginate electrospinning [208-210]. Similar to PEO, the flexible PVA interacts with the alginate *via* hydrogen bonding, thus improving the electrospinnability of the rigid alginate [208]. Different morphologies of PVA/alginate were reported by Lee *et al*. [210]. At low alginate concentrations, ultrafine nanofibres were produced, and when the concentration was increased, electrospinning led to bigger beads with smaller average distances between the beads.

The solubility of alginate has been one difficulty facing its applicability in various fields. In order to improve the stability of the electrospun alginate, various crosslinking agents were investigated [211]. The electrospun nanofibrous membrane retained their fibrous structure after incubation for 7 days in aqueous medium (simulated body fluid (SBF)). The morphology of the electrospun alginate/PEO blend as vitamin carrier was directly dependent on the viscosity of the alginate [212]. Higher viscosity alginate favoured beaded nanofibres with smaller average diameters, when compared to low viscosity alginate-based nanofibres that were bead-free with larger diameters. The most significant part of using PEO as copolymer, beside the fact of enhancing the electrospinnability, is the opportunity to extract PEO from the nanofibres by incubation in water [53]. In this case the alginate is crosslinked through ionic bonds followed by leaching the PEO. A natural surfactant such as lecithin has been used to impart uniformity to the nanofibres [213]. The surfactant readily renders the opportunity to increase the alginate content in the blend without losing the uniformity of the nanofibres.

2.5.3.2 Alginate with other biopolymers

A blend of gelatin/sodium alginate produced smooth nanofibres in heated water (45 °C) [22]. A blend of chitosan and alginate was also electrospun with the aid of PEO as copolymer [214]. Since chitosan is a cationic copolymer and alginate is an anionic copolymer, they form a polyionic complex that does not need further crosslinking. Due to the gelation of these polymers, side-by-side electrospinning technique was employed where the alginate and chitosan meet at the tip of the spinneret. The swelling of the nanofibres was reduced by the incorporation of chitosan which is not soluble in water. Core-sheath morphology of alginate and chitosan was achieved by spinning the alginate into a chitosan coagulation bath [133]. The average diameter of the nanofibres ranged between 600 and 900 nm coated with chitosan. This enhanced the stability of the alginate in saline solution.

2.5.4 Collagen

One of the most abundant proteins is collagen. Collagen is a kind of protein that gives strength, elasticity and structural support. The two most electrospun collagen types are collagen type I and type III [75,215]. Collagen is soluble in a water/ethanol mixture, HIFP [216], TFE [217] and acetic acid [218]. Most research based on collagen was aimed to develop collagen nanofibrous membrane from non-toxic solvents, since collagen is usually used in biomedical applications [219]. These authors established that collagen nanofibrous membrane electrospun from fluoroalcohols lost their natural inherited properties. Matthews *et al*. [75] fabricated aligned collagen nanofibres using 1,1,1,3,3,3 hexafluoro-2-propanol as solvent with a rotating drum collector. The nanofibres were randomly oriented at a mandrel rotating speed of less than 500 rpm, and an increase to 4500 rpm aligned the fibres along the rotation axis. Optimization of the collagen nanofibres was studied by Li *et al*. [218]. Through manipulation of the processing and solution parameters it was possible to produce smooth nanofibres with diameters below 100 nm, but at the expense of the fibre structure. A decrease in concentration from 5% gradually reduced the fibre diameter from ~500 nm to ~200 nm, and a further decrease in concentration led to fibres with diameters below 100 nm, but with significant formation of beads. It was concluded that the minimal concentration of collagen in 1,1,1,3,3,3 hexafluoro-2-propanol to produce smooth and uniform nanofibres is 5%.

2.5.4.1 Collagen with synthetic polymers

Another feasible approach to avoid the use of toxic solvents is to co-spin collagen with a spinnable polymer. Yogeshwar Chakrapani *et al.* [220] produced collagen nanofibrous membrane from a blend of PCL and collagen in acetic acid. The nanofabric network was made up of fibres with diameters ranging between 100 and 200 nm and having a porosity of about 60%. Dong *et al.* [20] prepared collagen nanofibres from phosphate-buffered saline (PBS) and ethanol in the presence of a salt (NaCl). They found out that 16 wt% of collagen was readily soluble when the salt was 5 wt% or more. Nanofibres with diameter ranging between 210 and 540 nm, depending on the salt concentration, were produced. A co-axial morphology of collagen (outer shell) and PCL (inner core) as structural support was produced by using both TFE and 1.1.1.3.3.3-hexaflouro-2-propanol (HFP). The co-axial structure was fabricated by using a co-axial nozzle or by coating the electrospun membrane by immersion into a collagen solution [217]. The co-axially electrospun nanofibres displayed a similar morphology as pure PCL nanofibres, with an average diameter of 385 ± 82 nm, and a coating thickness of 64 ± 26 nm. Another copolymer often used to enhance the spinnability of collagen without toxic solvents is poly(L-lactide-co-ε-caprolactone) [221]. Zhong *et al*. [222] prepared collagen-glycosaminoglycan scaffolds through electrospinning in a mixture of TFE and water, followed by glutaraldehyde vapour crosslinking. The biostability of the smooth nanofibres with a mean diameter of 260 nm was improved. Although much work has been done on collagen in clinical applications, not much has been done on the application of the collagen in water treatment [219,223]. However, Davis and Maffia [224] successfully prepared collagen from type 1 bovine for water treatment and sludge dewatering. The collagen showed good potential as a coagulant of colloidal solids.

2.5.5 Gelatin

Gelatin, similar to other naturally occurring polymers, is biocompatible, biodegradable and non-toxic [12]. It is derived from animal tissue such as skin, muscle and bone. Gelatin is subdivided into Type A and Type B, depending on the extraction and chemical treatment. Gelatin type A is obtained from the acidic pre-treatment of collagen, whereas Type B is from alkali pre-treatment. Glutamine and asparagine are converted into glutamic and aspartic acid during alkali pre-treatment, yielding a high carboxylic acid content in gelatin Type B. Gelatin has been processed into various forms for a wide spectrum of applications such as food

products, cosmetics and pharmaceuticals [225]. Although gelatin is readily soluble in water and polar solvents, the electrospinnability of gelatin is still a challenge. However, some reports indicated the possibility of electrospinning gelatin using solvents such as using 2.2.2-trifluoroethanol TFE [226], formic acid [66], and 1.1.1.3.3.3-hexaflouro-2-propanol (HIFP) [85]. Electrospinning gelatin in water can be done by applying heat above 37ºC [220].

The use of copolymers is another conducive route, not only to electrospin gelatin, but also to improve its mechanical integrity and chemical stability [85, 136]. Huang *et al.* [227] indicated that gelatin can be electrospun into smooth nanofibres with a diameter of 140 nm by using 2,2,2-trifluoroethanol (TFE) as a solvent. With a concentration of 7.5 wt% of gelatin, the modulus was 117 MPa and the ultimate tensile strength was 4.9 MPa. Similar to collagen, the gelation of gelatin and its solubility in water is the reason why it cannot be used in water treatment applications. The limitations of the application of gelatin are its weak mechanical strength and its ready solubility in water. The crosslinking of electrospun gelatin nanofibrous membrane is the most convenient way to improve the stability and mechanical strength [227].

2.5.6 Hyaluronic acid

Hyaluronic acid (HA), a natural polysaccharide, is often found in connective tissues in the body, such as the vitreous humour, the umbilical cord, and the joint fluid. It is a polyanionic acid made-up of N-acetyl-D-glucosamine and D-glucuronic repeating units as shown in Figure 2.14.

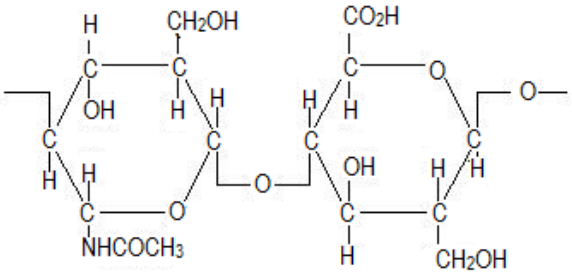

Figure 2.14 Structure of hyaluronic acid

Thanks to the recent advancements in electrospinning, pure hyaluronic has been successfully electrospun into nanofibrous membrane from its solution [13,15]. The electro-blowing of hyaluronic acid affords the preparation of its nanofibres with diameters ranging from 49 to 83 nm depending on the preparation and solution properties employed. HA mats with an average

fibre diameter of 39 ± 12 nm were produced from NH_4OH:DMF at a ratio 2:1 [228]. Many researchers studied the application of the hyaluronic acid in biomedical applications. The hyalorunic was immobilized on the surface of silica microspheres in order to fabricate a magnetic adsorbent. This shows the possibility to develop new adsorbents for wastewater treatment [229].

2.5.6.1 Hyaluronic acid with other biopolymers

Hyaluronic acid/chitosan electrospun bioblend nanofibres were prepared by Ma *et al.* [230] in a mixture of formic acid and water. Smooth fibres with smaller average diameters (83 nm) were obtained at high contents of hyaluronic acid (hyaluronic/chitosan at 9/1), while at low contents beaded-fibres (7/3) and drops (6/4) were formed.

2.5.6.2 Hyaluronic acid derivatives

A thiolated HA derivative, 3,3'-dithiobis(propanoic dihydrazide)-modified HA (HA-DTPH), was synthesized and electrospun into nanofibrous membrane by Ji *et al*. [86]. Dithiobis(propanoic dihydrazine) was synthesized and coupled to the carboxylic groups of HA *via* carbodiimide chemistry. The thiolated bond formed were reduced by using dithiothreitol to produce thiolated HA-DTPH. HA-DTPH (2 % w/v)/PEO (2 % w/v) resulting in uniform nanofibres with diameters ranging from 70 to 110 nm. The resulting fibres were crosslinked with PGEDA (9 w/v), followed by the dissolution of PEO in deionized water for 48 hours. After the extraction of PEO the fibre diameter distribution became much wider (with 85% of the fibre diameters ranging between 50 and 300 nm). The crosslinking of the nanofibres reduced the swelling ratio of the mats. Another group investigated a similar system, but they used dual-syringe reactive electrospinning with thiolated HA/PEO in contact with PEGDA before electrospinning to induce crosslinking [86].

2.5.7 Aloe vera

Aloe vera is one of the oldest herbal products used for medicinal purposes. It contains more than 200 nutrients which include amino acids, saliycilic acid, absorbic acid, enzymes and lots of minerals and vitamins [231,232]. It is largely made up of water with long chain polysaccharides of acetylated glucomannan and carbohydrates. So far there is no work based

on the electrospinning of aloe vera alone, but blends of synthetic and biopolymers were used to facilitate its electrospinnability. We included aloe vera as biopolymer because of its biocidal efficacy (towards different pathogenic organisms), and the possibility to functionalize electrospun mats in water filtration and treatment to reduce the biofouling of the electrospun membrane. Nonetheless, aloe vera enjoyed its success over a wide array of medical applications [233].

2.5.7.1 Aloe vera with synthetic/biopolymers

A hybrid of hydroxypropyl methylcellulose (HPMC), poly(vinyl alcohol) PVA, poly(vinyl pyrrolidone), iodine PVP and poly(ethylene glycol) (PEG) were doped with aloe vera to investigate the effect of aloe vera on the properties of the resulting nanofibrous membrane. Like any biopolymer, aloe vera influenced the solution properties such as viscosity and conductivity. The addition of aloe vera increased both the viscosity and conductivity of the spinning solution, and decreased the mean diameter of the ensuing nanofibres from 660 nm to 596 nm at 1% of aloe vera. SEM showed an interfuse with each other when the content of aloe vera increased in the composition. In another study the addition of aloe vera (at 6%) resulted in finer and more homogeneous nanofibres with mean diameters of 150 to 350 nm [232]. A similar study on the hybrid of biodegradable PCL and aloe vera to prepare a transdermal biomaterial showed homogeneity and small average diameters of the nanofibres in the presence of aloe vera (519 ± 28 versus 215 ± 63 nm at 10% aloe vera), and greatly improved mechanical properties and hydrophilicity [234].

2.6 Electrospun biopolymers with nanomaterials

In the past few years there has been an ever increasing interest in incorporating different nanoparticles in biopolymers for a broad range of applications [26,235]. Nanoparticles have a promising potential in wastewater/water treatment as biocidal agents, sensors, and adsorbents. If these nanoparticles are used alone for water/wastewater treatment there are some limitations such as their recovery and reuse, cost and their long-term effect on health and/or the environment. The biocidal activities of these nanoparticles are depicted in Table 2.5. A possible solution is to immobilize and control their release to overcome these complications/limitations [236,237]. Electrospinning these nanomaterials (with known

content) with biopolymers offers the possibility to retain their nanosize and their release into streams without any harmful by-products, thus reducing the overall cost.

2.6.1 Silver nanoparticles

Silver is well-known for centuries for its attractive antimicrobial, antiviral and fungicidal activities [236,238]. The metal enjoyed its success in a broad spectrum of consumer products, such as plastics, soaps, pastes, food and textiles. The antimicrobial and antifungal activity of silver nanoparticles (AgNP) makes it the most studied metal nanoparticle for different applications [234-236]. There are several ways by which ionic silver can be reduced into silver nanoparticles [26,238]. There is still a lot of controversy on the mechanism behind the antibacterial, fungicidal, and antiviral activities displayed by silver nanoparticles. Three mechanisms were postulated, namely i) attachment of the silver nanoparticles on the surface of the cell membrane and disturbing its permeability and respiration, ii) penetrating the cell and reacting with some compounds containing sulphur and phosphorus such as DNA and proteins, and iii) releasing silver ions which contributes to its activity towards pathogens [236]. These mechanisms depend on the distribution, shape and size of the silver nanoparticles.

Formic acid was used as solvent to prepare chitosan/PVA nanofibres with optimal conditions of 0.5 ml h^{-1} flow rate, 18 kV voltage and a TCD of 7.5 cm. Chitosan/PVA was doped with silver oxides and titanium oxides to significantly improve the antibacterial activity of the ensuing nanofibres [26]. The prepared nanofibres had mean diameters ranging between 270 and 360 nm. They were cultured to find their antibacterial activity against Gram negative and Gram positive bacteria. The antibacterial activity of $AgNO_3$-loaded composite nanofibres increased with an increase in $AgNO_3$ content with 99% bacteria eradicated for *S. aures* and 98 % for *Escherichia coli* at only 0.04 wt% of $AgNO_3$. TiO_2-loaded composite nanofibres showed a maximum of 90% bacteria for *S. aures* and 85% bacteria for *Escherichia coli* eradicated at concentrations above 0.03 wt% of TiO_2.

The diameter of the nanofibres also influenced the antibacterial activity, with smaller diameters showing better efficiency because of the large surface-to-volume ratio giving more contact with the bacteria. A similar blend of chitosan and PVA was doped with AgNPs [239]. A 12 wt% PVA solution containing $AgNO_3$ blended with a 6 wt% chitosan solution (15 wt%

in acetic acid) was electrospun, followed by either refluxing for 48 hours or annealing at 130ºC for 16 hours (to reduce Ag ions of the nanofibres). The intensities of surface plasmon resonance (SPR) of AgNPs increased in the presence of chitosan when compared to that of PVA and $AgNO_3$ only, indicating that chitosan can act as a stabilizer as well as a reducing agent for the formation of AgNPs. The spherical AgNPs on the surface of the electrospun nanofibrous membranes were fairly uniform and smaller in size when refluxed, while large particles were associated with diffusion and agglomeration of residual Ag ions and AgNPs formed in the solid during heating were formed when annealed. This resulted in a low killing efficiency of the annealed samples due to the surface area of the AgNPs coming into contact with the bacteria.

An *et al*. [240] prepared chitosan (CS)/polyethylene oxide (PEO) containing AgNPs nanofibres by means of *in situ* chemical reduction of Ag ions. The average diameter of the nanofibres decreased with an increase in AgNPs because of the increased charge density in the spinning solution, imparting stretching of the electrified jet under the electrical field. The cubic crystal AgNPs were fairly well dispersed in the CS/PEO ultrafine nanofibres with average diameter of less than 5 nm. The tensile modulus and tensile strength of the CS/PEO/AgNP nanofibres were better than that of the CS/PEO nanofibres. The CS/PEO/AgNP nanofibrous membrane exhibited higher antibacterial activity than the CS/PEO nanofibres towards *E. coli*. Silver nanoparticles were also incorporated into PVA/CS blends for their antibacterial activity [241]. The electrospinnability of the PVA/CS was enhanced by the AgNPs, and the size of the AgNPs varied between 2.4 to 10.7 nm depending on the CS concentration in the blends. A biopolymer blend of CS/gelatin containing AgNPs was successfully electrospun by Zhuang *et al*. [242]. The study indicates that the microcrystalline chitosan was used as a reducing agent and as a stabilizer to synthesize the AgNPs at room temperature. By using a noniogenic polymer (PEO), a natural polymer (N-carboxyethylchitosan), and silver nanoparticles, Penchev *et al*. [87] observed a complete killing of the bacteria (*Staphylococcus aureus*) within an hour of contact at high concentrations of silver nanoparticles, whereas at low concentrations the nanoparticles only inhibits bacterial growth. They used a one pot system to fabricate the nanofibre in which all the components were added into the spinning solution. Formic acid was again used as a reducing agent and as a solvent, and the sizes of the NPs were 4 ± 0.5 nm and 6 ± 1.5 nm respectively for 5 and 10 wt% of the $AgNO_3$. Son *et al*. [31] fabricated antimicrobial membrane by using cellulose acetate and $AgNO_3$ through slow and fast photoreductions. The

mats were tested against *Staphylococcus aureus, Escherilia coli, Klebsiella pneumonia*, and *Pseudomonas aeruginosa* by an attachment method. The mean diameter of the ultrafine nanofibres ranged between 680 and 610 nm for 0.05 and 0.5 wt% content of $AgNO_3$, respectively. Most of the nanoparticles had a mean diameter between 3 and 16 nm, whereas 15.4 nm resulted after rapid photoreduction. The killing efficiency for all the bacteria was 99.9% at very low concentration of 0.05 wt%. Lee *et al*. [243] produced electrospun chitosan nanofibres with chemically reduced AgNPs *via* electrospinning. The resulting spherical nanoparticles with sizes ranging between 10 and 11 nm (average diameter of 10 ± 2 nm) were evenly distributed in the chitosan nanofibres. The growth inhibition of *Pseudomonas aeruginosa* (gram negative) and *Staphylococcus aureus* (gram positive) increased with an increase in AgNPs in the composite materials.

2.6.2 Hydroxyapatite (HAp) nanoparticles

Celebi *et al.* [244] produced electrospun chitosan/PVA nanofibrous membrane containing silver ion-incorporated hydroxyapatite (HAp) nanoparticles. A mean diameter of ~70 nm of silver ions-incorporated HAp particles were obtained with good antibacterial efficiency against *Escherichia coli*. Hydroxyapatite (HAp)/chitosan was synthesized by co-precipitation synthesis followed by electrospinning of 10 wt% UHMPEO in aqueous solution with the solvent composed of acetic acid (HAc) and dimethyl sulphoxide (DMSO). The X-ray diffraction (XRD) patterns and selected area electron diffraction (SAED) spectra confirmed that the crystalline structure of HAp was retained in the nanofibres [217]. The electrospun nanocomposite nanofibrous membranes were very fine and homogeneous with diameters of 214 ± 25 nm with spindle-like HAp parallel to the nanofibres direction. A similar dispersion of HAp and structure were reported by using gelatin as matrix [245]. The mechanical properties were also improved in the presence of HAp.

2.6.3 Carbon nanotubes

Carbon nanotubes have excellent antimicrobial activity and mechanical strength. Similar to Ag nanoparticles, the mechanism of the carbon nanotubes against pathogenic organisms is still controversial [236]. The proposed mechanisms include physical membrane perturbation and oxidative stress. Their antimicrobial activity is also influenced by their distribution, diameter, length, and electronic structure. Most of the carbon nanotubes exhibit good

cytotoxicity towards pathogenic organisms, with single-walled carbon nanotubes reported to be the most efficient. Well-aligned single walled carbon nanotube (SWNT) along the fibre axis of the *bombyx mori* silk nanofibre were produced by Ayutsede *et al*. [246]. A very low concentration of SWNT (1 wt%) was enough to increase the crystallinity and mechanical properties. Multiwalled carbon nanotubes (MWNTs) were also incorporated in electrospun cellulose acetate (CA) nanofibres to investigate the effect of these nanoparticles on biopolymers [247]. The mean diameter of the nanofibres reduced from 267 nm for pure CA to 193 nm with MWNTs at only 0.55 wt%. The MWNTs impart significant water wetting, surface area (from 4.3 to 7.7 m g^{-1}), Young's modulus (doubled from 553 to 1144 MPa), tensile strength (from 21.9 to 40.7 MPa) and elongation at break (from 8.0 to 10.5%). A core-sheath structure of PVA/ CS-MWNT with outer and inner sheath-core nanofibres of 200 and 100 nm respectively was reported by Feng *et al*. [248]. The composite nanofibres showed fast transfer kinetics and good electrochemical properties. In one of their recent studies on electrospun silk fibroin (B. mori)/multiwalled carbon nanotubes they reported that MWNTs induced crystallization of silk and significantly improved the mechanical properties [249].

Table 2.5 Summary of common antibacterial nanomaterials and applications

Nanomaterial	Proposed antimicrobial mechanism	Potential water treatment applications
Silver (AgNP)	Release of Ag^+ ions, disruption of cell membrane and electron transport, DNA damage	Surface coatings, membranes, membrane reinforcement
Carbon nanotube (CNT)	Disruption of intracellular metabolic pathways, oxidative stress, physical membrane damage	Biofouling resistance membranes, carbon hollow fibres, membrane reinforcement
Hydroxyapatite (Hap)	Easy functionalization with different biocidal metal oxide	Membrane reinforcement
Zinc (ZnO)	Intracellular accumulation of nanoparticles, disruption of cell membrane, H_2O_2 production, release of Zn^+ ions	Surface coating, membranes, membrane reinforcement

2.6.4 Zinc nanoparticles

Zinc nanoparticles (ZnO) antibacterial activity is still not clear, but several mechanisms were proposed. It was suggested that the lethal effect of ZnO results from disruption of the cell membrane activity and induction of intercellular reactive oxygen species, such as H_2O_2, a strong oxidizing agent harmful to bacterial cells [236]. Zinc oxide was produced by mixing the precursor (zinc acetate) in 0.1 M sodium hydroxide in methanol [250]. The prepared ZnO was introduced in an alginate/PVA blend dissolved in distilled water. With a large contact area the composite exhibited high toxicity to both gram-negative and gram-positive bacteria. Taha *et al*. [156] functionalized a cellulose acetate/silica composite with NH_2 to enhance its affinity towards Cr(IV) ions. They used tetraethoxysilane (TEOS) as silica source, cellulose acetate as precursor and 3-ureidoptopyltriethoxysilane as a compatibilizer. They produced NH_2 functionalized nanofibres with a mean diameter of 100-500 nm and a porosity and surface area of 73% and 126.5 m^2 g^{-1}. Using static and dynamic experiments the membrane showed adsorption of 98%. ZnO nanoparticles were impregnated into the electrospun cellulose acetate nanofibre membrane by Anitha *et al*. [251]. The membrane displayed a superhydrophobic nature (water contact angle of 124º) and antibacterial property against well-known bacteria.

2.7 Applications of electrospun biopolymers in water treatment

Electrospun nanofibres afford the opportunity to be applied in various fields such as biosensors, and filtration because of their unique properties such as large surface area, engineered porosity, and physico-mechanical properties. The manipulation of the solution properties and technique advancement rendered the opportunity to produce the desired morphology and structure of the resulting nanofibres for specific applications.

2.7.1 Bioremediation

Heavy metals in wastewater is still a big problem, and a challenge to researchers to come up with reliable solutions without leaving by-products. Cellulose acetate has been functionalized to increase its adsorption efficiency which depends mostly on the functional groups found on the main chain. Poly(methacrylic acid) (PMAA) with additional carboxyl groups was used to functionalize cellulose acetate in order to increase the number of metal binding sites [252].

The efficiency was enhanced by the presence of PMAA on the cellulose acetate fibres, but the adsorption was more effective for the removal of mercury (Hg(II)) with an adsorption capacity of 4.8 mg g^{-1}. The efficiency may, however, depend on the metal ion type and the pH. The de-adsorption of the metals is possible with an appropriate solvent such as ethylenedinitrilotetraacetic acid (EDTA). Cellulose acetate/silica composites were tested for Cr(VI) adsorption [156]. In this case, the CA/SiO_2 was functionalized with NH_2 in order to enhance the adsorption of the resulting fibre membranes. The membranes displayed a good adsorption, and desorption after washing five times with an aqueous solution of sodium hydroxide (NaOH). The adsorption data of Cr(VI) fitted well with the Langmuir isotherm with an adsorption capacity of 19.5 mg g^{-1}.

Although various mechanisms were proposed to describe the metal ions adsorption of chitosan, the electrostatic attraction on the protonated amine groups is the accepted mechanism [253]. The heavy metal adsorption efficiency of an electrospun chitosan membrane was studied by several researchers [10,254]. It was found to depend on several aspects such as the degree of deacetylation [254], pH, fibre structure and morphology [181,254]. Desai *et al*. [254] studied the adsorption efficiency of PEO/chitosan nanofibres electrospun towards chromium by using simulated flow conditions at a pH of 7.3. The chromium solution (prepared from 5 mg l^{-1} K_2CrO_4) was passed ten consecutive times through the chitosan nanofibrous filter. The binding efficiency of the membrane decreased with an increase in nanofibre diameter (81-131 nm). However, the heavy metal adsorption efficiency increased with an increase in the degree of deacetylation. By using static conditions, the same group found that the metal adsorption depends on the molecular weight of chitosan, the degree of deacetylation, the percentage of chitosan in the blend, and the surface area to mass ratio. The molecular weight is related to the length of the chains and therefore to the number of cations on the backbone of the chitosan acting as active binding sites.

Haider and Park [10] neutralized the nanofibres with K_2CO_3 to obtain an -NH_2 group on the backbone of the chitosan membrane. This improved the stability of the electrospun membrane in water, with negligible weight reduction after 24 hours. The adsorption of the metals (Cu(II), 419.2 mg g^{-1} and Pb(II) 202.8 mg.g^{-1}) increased significantly for the first 15 min to 4 hours and levelled off after 8 hours, due to the unavailability of binding sites (amine, primary and secondary hydroxyl groups), large surface area, and inter- and intrafibrous pores in the

fibrous membrane. The Langmuir isotherm data showed that the equilibrium adsorption capacities for Cu(II) and Pb(II) were respectively 485.4 mg g^{-1} (2.85 mmol g^{-1}) and 263.2 mg g^{-1} (0.79 mmol g^{-1}). The difference between the values for the two metals was attributed to the differences in their atomic radii. It was suggested that the chitosan' adsorption followed a monolayer mechanism.

A nanofibrous membrane of pure silk fibroin (SF), and a blend of wool keratose and silk fibroin (WK/SF), were compared with pure silver wool and filter paper for their Cu(II) adsorption capacity [255]. The nanofibrous membranes displayed a significant Cu(II) adsorption capacity compared to silver wool and filter paper because of the large specific area which is ~50 times larger than those of filter paper and silver wool. The blend membrane showed a higher capacity than the SF membrane. The difference in Cu(II) adsorption capacity was related to the different chemical compositions (especially amino acids compositions). Both membranes displayed good desorption percentages. Desorption and re-adsorption was repeated six times, but the membrane kept 90% of its adsorption capacity. The Langmuir isotherm fits the experimental results better than the Freudlinch model. The Cu(II) adsorption followed a monolayer adsorption model.

Yang *et al*. [256] functionalized oxidized cellulose nanofibres embedded in an electrospun polyacrylonitrile (PAN) nanofibrous membrane with thiol groups to evaluate the metal adsorption capacity. Besides the increased stiffness due to the functionalization, the functionalized composite membrane displayed an adsorption of 76.5 ± 2.0 $Cr_2O_7^{2-}$ metal ions per gram of cellulose nanofibre at pH = 4.0, while the adsorption of Pb(II) was 133 ± 2.5 mg g^{-1} at pH = 5 in static conditions. The membrane also reached 80.0 mg g^{-1} of Pb(II) within 15 minutes, and 125 mg g^{-1} within 20 minutes. Under dynamic conditions the membrane showed 60 mg Cr(VI) g^{-1} (pH = 4) and 115 mg Pb(II) g^{-1} were adsorbed. Wang *et al*. [257] grafted cellulose nanowhiskers with amine groups using polyvinylamine (PVAm). The membrane displayed a maximum dynamic adsorption of 100 mg Cr(VI) (at pH = 4) and 260 mg Pb(II) (at a pH of 6) per gram of cellulose nanofibre.

2.7.2 Filtration membrane

Even though electrospun nanofibrous membranes were successful in air filtration, much work is still needed for water filtration. The breakthrough came when the electrospun nanofibres

were spun onto more rigid nonwoven polyesters in order to improve the handling issues and their mechanical properties [29]. Thin composite membrane (TNFC) can significantly enhance the rejection and flux permeation of the membranes, because of the nanofibres with high porosity and controllable pore size for specific filtration processes. TNFC membranes have been one of the growing subjects in water filtration, because of the performance displayed by these materials since the introduction of electrospun nanofibres as one of the sub-layers.

Several researchers found that coating of these TNFC with cellulose nanowhiskers imparts significant hydrophilicity and mechanical properties to the membrane [144, 149-152]. The thin top-layer coating enhanced the rejection and flux. Wang *et al*. [258] found that the interfacial polymerization of polyamide around the ultrafine cellulose nanofibres layer in TFNC showed a good rejection of MgCl and $MgSO_4$, depending on the adapted interfacial polymerization (i.e. IP, the organic phase on top of the aqueous phase, or IP-R, the aqueous phase on top of the organic phase). The IP based membrane showed a rejection of 67.6% at 1% of piperazine (PIP), while the IP-R showed a rejection of 91.6% of $MgSO_4$. However, both membranes displayed similar rejection percentages for $MgSO_4$ and MgCl at high PIP concentrations. The same group electrospun PAN onto PET and infused cellulose nanowhiskers (diameter 5 nm) for the microfiltration process [257]. The cellulose nanowhiskers were functionalized with different amines such as polyethyleneimine (PEI), ethylenediamine (EA), and polyvinylamine (PVAm) by using N-(3-Dimethylaminopropyl)-N'-ethylcarbodiimide hydrochloride (EDC) and N-Hydroxysuccinimide (NHS) as catalysts. The resulting cellulose-based membrane had a mean pore size of 0.38 μm with a maximum pore size of 0.78 μm, and the water permeation was about 1300 l m^{-2} h^{-1} psi^{-1}. All the membranes showed complete removal of the bacteria by size exclusion. The coating of chitosan on electrospun PAN enhanced the filtration efficiency and rejection both ultrafiltration and nanofiltration processes [259]. The membrane displayed a rejection of 99% due to the inherited hydrophilicity of chitosan.

2.7.3 Biocidal membrane

Biofouling is a major problem for most membranes, because it results in the accumulation and biological growth of pathogenic organisms, and the deterioration of the membrane performance. A variety of metal oxides have been added to electrospun biopolymer

nanofibres in order to impart biocidal activity to the resulting nanofibres. Most of the diseases in developing countries are caused by pathogenic organisms. There has been an escalation of research in the incorporation of silver nanoparticles in electrospun membrane in order to impart biocidal activity [156,239,240,243,244]. Even though there is still much controversy over the biocidal activity of silver nanoparticles, electrospun nanofibres displayed enhanced antibacterial efficiency when the membranes contained silver. ZnO particles were introduced in an alginate/PVA blend dissolved in distilled water, followed by electrospinning [250]. With high contact area the electrospun composite displayed good toxicity to negative and positive bacteria. ZnO nanoparticles were also incorporated in cellulose acetate membrane to enhance the antibacterial efficiency against *Staphylococcus aureus*, *E. coli*, and *Citrobacter freundii*. [251]. The impregnated ZnO nanoparticles significantly inhibited the growth of the bacteria and the inhibition zone diameters were 27 mm, 22 mm, and 14 mm for *Staphylococcus aureus*, *Escherichia coli*, and *Citrobacter freundii*, respectively. The functionalization of the electrospun membrane also enhanced the biocidal efficiency [83,193,195]. A quaternized chitosan membrane displayed inhibition of bacterial growth on the mat. Blending biopolymers with good antibacterial efficiency was also significantly reduced the biocidal activity of the resulting membrane [83].

2.7.4 Chemosensors

Chemosensors are detectors that selectively identify and recognize ions and molecules. A number of studies have been done on implantation of chemosensing agent onto solid matrices in order to improve the sensitivity, robustness, and lifetime of such matrices [260]. A variety of polymers and nanomaterials were used as supporting materials in solid-state sensors. The sensitivity detection and exposure of the chemosensors were found to be directly dependent on the structure of the supporting material [261].

The sensing agent embedded onto electrospun nanofibres (with large surface areas) improves the detection sensitivity and response time, and reduces the concentration detection value (lowest detection value (LOD)) compared to commonly used films. The presence and concentration of the heavy metals can therefore be traced and removed at fairly low concentrations. Several biobased nanofibres such as ethyl acetate, cellulose acetate and cellulose have been functionalized with different fluorescent compounds in order to detect Cu [260,261]; Cr [260], Fe [263] and Hg ions [261,264]. Due to the large surface areas of the

electrospun nanofibres, the sensitivity, selectivity, response time, and stability were enhanced. Kacmaz *et al*. [263] produced electrospun EC-doped with dye to detect Fe^{3+} ions. The membrane sensed Fe^{3+} ions over a concentration range of 10^{-12}-10^{-6} M (with an LOD of 0.07 pM), with a sensitivity response time of less than 30 s and sensor regeneration within 60 s.
Zdyrko *et al*. [265] developed a self-deployable colorimetric sensor by taking advantage of the super-absorbency of alginate, and functionalizing it with a heavy metal sensitive compound/dye. A blend of alginate and PEO electrospun onto rigid nonwoven (PET) absorbed metal ions from contaminated water.

2.8 Limitations of electrospun biopolymers in water treatment

Besides the hurdles based on the production scale-up of biopolymers, properties from the same source differ and the growth conditions influence the resulting properties. The harsh chemical treatment used to extract some biopolymers put an additional burden onto water and the environment. It is important to do a lot of research on genetically engineered organisms and novel designed productions in order to scale up the production of biopolymers with high purity/quality and having identical properties. Electrospun nanofibrous membranes have limited mechanical strength to withstand the pressures involved in water filtration, thus they are only applicable in membrane technologies where low pressures are involved (MF, UF and NF). Even though the work done on electrospun biopolymers shows potential to use eco-friendlier solvents, their application in water/wastewater treatment is still in its infancy. Most of these polymers are naturally prone to biodegradation and some are readily soluble in water, hence their lifetime is too short and they will need to be regularly replaced over time. This results in increasing the price of the membrane. The enhancement of the stability *via* either chemical or physical treatment without altering the unique valuable properties of the biobased membranes is important for their application in water/wastewater treatment. The dispersion of the nanomaterials in electrospun nanofibres (without agglomeration in order to retain their nanosize), and their exposure and release into the stream requires a lot of understanding. Most methods used to prepare the electrospun composite materials revolve around coating the mat (immersing the mat in a metal oxide solution) or adding the nanomaterial intoa spinning solution. Nanomaterials from these methods have different release rates and exposure to the water stream. In the near future, investigation of the controlled release and exposure of the nanomaterials is required in order to understand and control their disinfection efficiency.

2.9 Conclusions

In the past decades, electrospinning has been highly recognized as a new class of nanotechnology providing access to a range of nanomaterials with unique properties. Significant progress has been made on the fundamental understanding of the mechanism, and the modelling of the envisaged processes that govern fibre formation. This was proven by advanced developments necessary to engineer the desired nanostructured materials through electric field manipulation, solution properties and new designs. Control over their deposition, dimensions and assemblies created new avenues to generate desired configurations for specific applications. There is currently a big paradigm shift towards the industrialization and commercialization of the electrospun nanofibres. The new technical advances (fibre collections strategies, needle shapes, and high throughput production) proved to be successful in the synthesis of these fascinating nanostructured materials. A fair amount of work has been done on the electrospinning of biopolymers for a broad array of applications, especially in the biomedical field. Much of this work was based on the electrospinning of biopolymers with and without copolymers and using non-toxic solvents. Water filtration and wastewater treatment received little attention, despite the unique properties of biopolymers that are important in addressing environmental concerns. The biodegradation and mechanical strength of the electrospun mats are critical limitations in water filtration and wastewater treatment. In future, the mutual relation to protect and improve the strength of the electrospun biopolymers by blending, chemical and physical treatments, and the addition of metal oxides and their controlled release into water streams will revolutionize wastewater treatment and water filtration. Through further researches it will be possible to bridge the gap and enable the application of biopolymers in water filtration and treatment.

2.10 References

[1] M.T.M.Pendergast, E.M.V. Hoek, A review of water treatment membrane nanotechnologies, Energy & Enviromental Science, 4 (2011) 1946-1971

[2] Progress on sanitation and drinking water, 2013 update,"WHO and UNICEF

[3] S. Ahmad, P.N. Martens, F.J. Pateiro, M. Fuchsschwanz, Mine waste dumping and corresponding enviromental impacts at Chihn Bac waste dump in Vietnam, Securing the Future and 8th ICARD, Skellefttes, Sweden, (2009).

[4] J. Binns, P. Illgner, E. Nel, Water shortage, deforestation and development: South Africa's working for water programme, Land Degradation & Development, 12 (2001) 341-355.

[5] R. Balamurugan, S. Sundarrajan, S. Ramakrishna, Recent trends in nanofibrous membrane and their suitability for air and water filtrations, Membranes, 1 (2011) 232-248.

[6] S. Ramakrishna, K. Fujihara, W.-E. Teo, T. Yong, Z. Ma, R. Ramaseshan, Electrospun nanofibers: solving global issues, Materials Today, 9 (2006) 40-50.

[7] S. Haider, S.-Y. Park, Preparation of the electrospun chitosan nanofibers and their applications to the adsorption of Cu(II) and Pb(II) ions from an aqueous solution, Journal of Membrane Science, 328 (2009) 90-96.

[8] A. Greiner, J.H. Wendorff, Electrospinning: a fascinating method for the preparation of ultrathin fibers, Angewandte Chemie International Edition, 46 (2007) 5670-5703.

[9] A.L. Andrady, Science and technology of polymer nanofibers, John Wiley & Sons, Inc., Hoboken, New Jersey (2008).

[10] H. Cho, S.Y. Min, T.W. Lee, Electrospun organic nanofiber electronics and photonics, Macromolecular Materials and Engineering, 298 (2013) 475-486.

[11] A. Frenot, M.W. Henriksson, P. Walkenström, Electrospinning of cellulose-based nanofibers, Journal of Applied Polymer Science, 103 (2007) 1473-1482.

[12] H. Nie, A. He, J. Zheng, S. Xu, J. Li, C.C. Han, Effects of chain conformation and entanglement on the electrospinning of pure alginate, Biomacromolecules, 9 (2008) 1362-1365.

[13] I.C. Um, D. FanG, B.S. Hsiao, A. Okamoto, B. Chu, Electro-spinning and electro-blowing of hyaluronic acid, Biomacromolecules, 5 (2004) 1428-1436.

[14] G. Viswanathan, S. Murugesan, V. Pushparaj, O. Nalamasu, P.M. Ajayan, R.J. Linhardt, Preparation of biopolymer fibers by electrospinning from room temperature ionic liquids, Biomacromolecules, 7 (2006) 415-418.

[15] X. Wang, I.C. Um, D. Fang, A. Okamoto, B.S. Hsiao, B. Chu, Formation of water-resistant hyaluronic acid nanofibers by blowing-assisted electro-spinning and non-toxic post treatments, Polymer, 46 (2005) 4853-4867.

[16] S. Safi, M. Morshed, S. Hosseini Ravandi, M. Ghiaci, Study of electrospinning of sodium alginate, blended solutions of sodium alginate/poly (vinyl alcohol) and sodium alginate/poly (ethylene oxide), Journal of Applied Polymer Science, 104 (2007) 3245-3255.

[17] X. Fang, D. Reneker, DNA fibers by electrospinning, Journal of Macromolecular Science, Part B: Physics, 36 (1997) 169-173.

[18] C.J. Buchko, L.C. Chen, Y. Shen, D.C. Martin, Processing and microstructural characterization of porous biocompatible protein polymer thin films, Polymer, 40 (1999) 7397-7407.

[19] V. Jacobs, A. Patanaik, R.D. Anandjiwala, M. Maaza, Optimization of electrospinning parameters for chitosan nanofibres, Current Nanoscience, 7 (2011) 396-401.

[20] B. Dong, O. Arnoult, M.E. Smith, G.E. Wnek, Electrospinning of collagen nanofiber scaffolds from benign solvents, Macromolecular Rapid Communications, 30 (2009) 539-542.

[21] G.E. Wnek, M.E. Carr, D.G. Simpson, G.L. Bowlin, Electrospinning of nanofiber fibrinogen structures., Nano Letters, 3 (2003) 213-216.

[22] S. Moon, R.J. Farris, Electrospinning of heated gelatin-sodium alginate-water solutions, Polymer Engineering & Science, 49 (2009) 1616-1620.

[23] M.W. Frey, Electrospinning cellulose and cellulose derivatives, Polymer Reviews, 48 (2008) 378-391.

[24] D. Fang, Y. Liu, S. Jiang, J. Nie, G. Ma, Effect of intermolecular interaction on electrospinning of sodium alginate, Carbohydrate Polymers, 85 (2011) 276-279.

[25] R. Barhate, S. Ramakrishna, Nanofibrous filtering media: filtration problems and solutions from tiny materials, Journal of Membrane Science, 296 (2007) 1-8.

[26] R. Gopal, S. Kaur, Z. Ma, C. Chan, S. Ramakrishna, T. Matsuura, Electrospun nanofibrous filtration membrane, Journal of Membrane Science, 281 (2006) 581-586.

[27] A. Patanaik, V. Jacobs, R.D. Anandjiwala, Performance evaluation of electrospun nanofibrous membrane, Journal of Membrane Science, 352 (2010) 136-142.

[28] W.K. Son, J.H. Youk, T.S. Lee, W.H. Park, Preparation of antimicrobial ultrafine cellulose acetate fibers with silver nanoparticles, Macromolecular Rapid Communications, 25 (2004) 1632-1637.

[29] B. Son, B.Y. Yeom, S.H. Song, C.S. Lee, T.S. Hwang, Antibacterial electrospun chitosan/poly (vinyl alcohol) nanofibers containing silver nitrate and titanium dioxide, Journal of Applied Polymer Science, 111 (2009) 2892-2899.

[30] A. Cooper, R. Oldinski, H. Ma, J.D. Bryers, M. Zhang, Chitosan-based nanofibrous membranes for antibacterial filter applications, Carbohydrate Polymers, 92 (2013) 254-259.

[31] R. Yang, J. He, L. Xu, J. Yu, Bubble-electrospinning for fabricating nanofibers, Polymer, 50 (2009) 5846-5850.

[32] B. Ding, E. Kimura, T. Sato, S. Fujita, S. Shiratori, Fabrication of blend biodegradable nanofibrous nonwoven mats via multi-jet electrospinning, Polymer, 45 (2004) 1895-1902.

[33] N. Thoppey, J. Bochinski, L. Clarke, R. Gorga, Edge electrospinning for high throughput production of quality nanofibers, Nanotechnology, 22 (2011) 345301/1-345301/11.

[34] N. Bhardwaj, S.C. Kundu, Electrospinning: a fascinating fiber fabrication technique, Biotechnology Advances, 28 (2010) 325-347.

[35] J. Zeleny, The electrical discharge from liquid points, and a hydrostatic method of measuring the electric intensity at their surfaces, Physical Review, 3 (1914) 69.

[36] J.F. Cooley, Apparatus for electrically dispersing fluids, US692631A, USA (1902).

[37] A. Formhals, Process and apparatus for preparing artificial threads, 1975504, USA (1934).

[38] F. Anton, Method and apparatus for the production of fibers, 2,116,942, USA (1938).

[39] F. Anton, Artificial thread and method of producing same, 2,187,306, USA (1940).

[40] S. Ramakrishna, K. Fujihara, W.-E. Teo, T.-C..Lim, Z. Ma, An introduction to electrospinning and nanofibers, World Scientific, Singapore (2005).

[41] N.M. Thoppey, R.E. Gorga, J.R. Bochinski, L.I. Clarke, Effect of solution parameters on spontaneous jet formation and throughput in edge electrospinning from a fluid-filled bowl, Macromolecules, 45 (2012) 6527-6537.

[42] N. Masilela, P. Kleyi, Z. Tshentu, G. Priniotakis, P. Westbroek, T. Nyokong, Photodynamic inactivation of *Staphylococcus aureus* using low symmetrically substituted phthalocyanines supported on a polystyrene polymer fiber, Dyes and Pigments, 96 (2013) 500-508.

[43] Z.-M. Huang, Y.-Z. Zhang, M. Kotaki, S. Ramakrishna, A review on polymer nanofibers by electrospinning and their applications in nanocomposites, Composites Science and Technology, 63 (2003) 2223-2253.

[44] F. Abdel-Hady, A. Alzahrany, M. Hamed, Experimental validation of upward electrospinning process, ISRN Nanotechnology, 2011 (1022) 1-14.

[45] T. Subbiah, G. Bhat, R. Tock, S. Parameswaran, S. Ramkumar, Electrospinning of nanofibers, Journal of Applied Polymer Science, 96 (2005) 557-569.

[46] W.-E. Teo, R. Inai, S. Ramakrishna, Technological advances in electrospinning of nanofibers, Science and Technology of Advanced Materials, 12 (2011) 013002/1-031002/19.

[47] A. Haghi, M. Akbari, Trends in electrospinning of natural nanofibers, Physica Status Solidi (a), 204 (2007) 1830-1834.

[48] J. Deitzel, J. Kleinmeyer, D. Harris, T.N. Beck, The effect of processing variables on the morphology of electrospun nanofibers and textiles, Polymer, 42 (2001) 261-272.

[49] G. Eda, S. Shivkumar, Bead-to-fiber transition in electrospun polystyrene, Journal of Applied Polymer Science, 106 (2007) 475-587.

[50] K. Pawlowski, H. Belvin, D. Raney, J. Su, J. Harrison, E. Siochi, Electrospinning of a micro-air vehicle wing skin, Polymer, 44 (2003) 1309-1314.

[51] J.D. Schiffman, C.L. Schauer, A review: electrospinning of biopolymer nanofibers and their applications, Polymer Reviews, 48 (2008) 317-352.

[52] N. Bhattarai, Z. Li, D. Edmondson, M. Zhang, Alginate-based nanofibrous scaffolds: structural, mechanical, and biological properties, Advanced Materials, 18 (2006) 1463-1467.

[53] S.I. Jeong, M.D. Krebs, C.A. Bonino, S.A. Khan, E. Alsberg, Electrospun alginate nanofibers with controlled cell adhesion for tissue engineering, Macromolecular Bioscience, 10 (2010) 934-943.

[54] C.D. Saquing, C. Tang, B. Monian, C.A. Bonino, J.L. Manasco, E. Alsberg, Alginate-polyethylene oxide blend nanofibers and the role of the carrier polymer in electrospinning, Industrial & Engineering Chemistry Research, 52 (2013) 8692-8704.

[55] V. Jacobs, R.D. Anandjiwala, M. Maaza, The influence of electrospinning parameters on the structural morphology and diameter of electrospun nanofibers, Journal of Applied Polymer Science, 115 (2010) 3130-3136.

[56] K. Lee, H. Kim, M. Khil, Y. Ra, D. Lee, Characterization of nano-structured poly (ε-caprolactone) nonwoven mats via electrospinning, Polymer, 44 (2003) 1287-1294.

[57] N. Choktaweesap, K. Arayanarakul, D. Aht-Ong, C. Meechaisue, P. Supaphol, Electrospun gelatin fibers: effect of solvent system on morphology and fiber diameters, Polymer Journal, 39 (2007) 622-631.

[58] R. Fryczkowski, M. Gorczowska, B. Fryczkowska, J. Janicki, The effect of solvent on the properties of nanofibres obtained by electrospinning from a mixture of poly (3-hydroxybutyrate) and polyaniline, Synthetic Metals, 166 (2013) 14-21.

[59] T. Uyar, F. Besenbacher, Electrospinning of uniform polystyrene fibers: the effect of solvent conductivity, Polymer, 49 (2008) 5336-5343.

[60] Z. Sun, J.M. Deitzel, J. Knopf, X. Chen, J.W. Gillespie, The effect of solvent dielectric properties on the collection of oriented electrospun fibers, Journal of Applied Polymer Science, 125 (2012) 2585-2594.

[61] S. Tungprapa, T. Puangparn, M. Weerasombut, I. Jangchud, P. Fakum, S. Semongkhol, C. Meechaisue, P. Supaphol, Electrospun cellulose acetate fibers: effect of solvent system on morphology and fiber diameter, Cellulose, 14 (2007) 563-575.

[62] X. Yuan, Y. Zhang, C. Dong, J. Sheng, Morphology of ultrafine polysulfone fibers prepared by electrospinning, Polymer International, 53 (2004) 1704-1710.

[63] A. Aluigi, A. Varesano, A. Montarsolo, C. Vineis, F. Ferrero, Mazzuchetti, Electrospinning of keratin/poly (ethylene oxide) blend nanofibers, Journal of Applied Polymer Science, 104 (2007) 863-870.

[64] D.S. Katti, K.W. Robinson, F.K. Ko, C.T. Laurencin, Bioresorbable nanofiber-based systems for wound healing and drug delivery: optimization of fabrication parameters, Journal of Biomedical Materials Research Part B: Applied Biomaterials, 70 (2004) 286-296.

[65] K. Arayanarakul, N. Choktaweesap, D. Aht-ong, C. Meechaisue, P. Supaphol, Effects of poly (ethylene glycol), inorganic salt, sodium dodecyl sulfate, and solvent system on electrospinning of poly (ethylene oxide), Macromolecular Materials and Engineering, 291 (2006) 581-591.

[66] C.S. Ki, D.H. Baek, K.D. Gang, K.H. Lee, I.C. Um, Y.H. Park, Characterization of gelatin nanofiber prepared from gelatin-formic acid solution, Polymer, 46 (2005) 5094-5102.

[67] X. Geng, O.-H. Kwon, J. Jang, Electrospinning of chitosan dissolved in concentrated acetic acid solution, Biomaterials, 26 (2005) 5427-5432.

[68] C.S. Ki, J.W. Kim, J.H. Hyun, K.H. Lee, M. Hattori, D.K. Rah, Electrospun three-dimensional silk fibroin nanofibrous scaffold, Journal of Applied Polymer Science, 106 (2007) 3922-3998.

[69] S. Tungprapa, I. Jangchud, P. Supaphol, Release characteristics of four model drugs from drug-loaded electrospun cellulose acetate fiber mats, Polymer, 48 (2007) 5030-5041.

[70] P. Heikkilä, A. Harlin, Electrospinning of polyacrylonitrile (PAN) solution: effect of conductive additive and filler on the process, Express Polymer Letter, 3 (2009) 437-445.

[71] D. Li, Y. Wang, Y. Xia, Electrospinning of polymeric and ceramic nanofibers as uniaxially aligned arrays, Nano Letters, 3 (2003) 1167-1171.

[72] D. Li, Y. Wang, Y. Xia, Electrospinning nanofibers as uniaxially aligned arrays and layer-by-layer stacked films, Advanced Materials, 16 (2004) 361-366.

[73] A. Theron, E. Zussman, A. Yarin, Electrostatic field-assisted alignment of electrospun nanofibres, Nanotechnology, 12 (2001) 384-390.

[74] C. Errico, N. Detta, D. Puppi, A.M. Piras, F. Chiellini, E. Chiellini, Polymeric nanostructured items electrospun on a cylindrical template: a simple procedure for their removal, Polymer International, 60 (2011) 1162-1166.

[75] J.A. Matthews, G.E. Wnek, D.G. Simpson, G.L. Bowlin, Electrospinning of collagen nanofibers, Biomacromolecules, 3 (2002) 232-238.

[76] C.-W. Kim, D.-S. Kim, S.-Y. Kang, M. Marquez, Y.L. Joo, Structural studies of electrospun cellulose nanofibers, Polymer, 47 (2006) 5097-6107.

[77] C.A. Bonino, K. Efimenko, S.I. Jeong, M.D. Krebs, E. Alsberg, S.A. Khan, Three-dimensional electrospun alginate nanofiber mats via tailored charge repulsions. Small, 8 (2012) 1928-1936.

[78] H. Homayoni, S.A.H. Ravandi, M. Valizadeh, Electrospinning of chitosan nanofibers: processing optimization, Carbohydrate Polymers, 77 (2009) 656-661.

[79] S.-H. Teng, P. Wang, H.-E. Kim, Blend fibers of chitosan-agarose by electrospinning. Materials Letters, 63 (2009) 2510-2512.

[80] J. Xu, J. Zhang, W. Gao, H. Liang, H.Wang, J. Li, Preparation of chitosan/PLA blend micro/nanofibers by electrospinning, Materials Letters, 63 (2009) 658-660.

[81] J. Du, Y.-L. Hsieh, Nanofibrous membranes from aqueous electrospinning of carboxymethyl chitosan, Nanotechnology, 19, (2008) 125707/1-125707/9.

[82] A. Neamnark, R. Rujiravanit, P. Supaphol, Electrospinning of hexanoyl chitosan, Carbohydrate Polymers, 66 (2006) 298-305.

[83] M. Ignatova, N. Manolova, I. Rashkov, Novel antibacterial fibers of quaternized chitosan and poly (vinyl pyrrolidone) prepared by electrospinning, European Polymer Journal, 43 (2007) 1112-1122.

[84] J. Du, Y.-L. Hsieh, PEGylation of chitosan for improved solubility and fiber formation via electrospinning, Cellulose, 14 (2007) 543-552.

[85] M. Li, Y. GuoM, Y. Wei, A.G. MacDiarmid, P.I. Lelkes, Electrospinning polyaniline-contained gelatin nanofibers for tissue engineering applications, Biomaterials, 27 (2006) 2705-2715.

[86] Y. Ji, K. Ghosh, B. Li, S.J. Sokolov, R.A. Clark, M.H. Rafailovich, Dual-syringe reactive electrospinning of cross-linked hyaluronic acid hydrogel nanofibers for tissue engineering applications, Macromolecular Bioscience, 6 (2006) 811-817.

[87] H. Penchev, D. Paneva, N. Manolova, I. Rashkov, Hybrid nanofibrous yarns based on *N*-carboxyethylchitosan and silver nanoparticles with antibacterial activity prepared by self-bundling electrospinning, Carbohydrate Research, 345 (2010) 2374-2380.

[88] Y.-M. Lim, H.-J. Gwon, J.P. Jeun, Y.-C. Nho, Preparation of cellulose-based nanofibers using electrospinning, (2010).

[89] C. Wang, H-S.. Chien, C.-H. Hsu, Y.-C. Wang, C.-T. Wang, H.-A. Lu, Electrospinning of polyacrylonitrile solutions at elevated temperatures, Macromolecules, 40 (2007) 7973-7983.

[90] S. De Vrieze, T. Van Camp, A. Nelvig, B. Hagström, P. Westbroek, K. De Clerck, The effect of temperature and humidity on electrospinning. Journal of Materials Science, 44 (2009) 1357-1362.

[91] S. Tripatanasuwan, Z. Zhong, D.H. Reneker, Effect of evaporation and solidification of the charged jet in electrospinning of poly (ethylene oxide) aqueous solution, Polymer, 48 (2007) 5742-5746.

[92] C.L. Casper, J.S. Stephens, N.G. Tassi, D.B. Chase, J.F. Rabolt, Controlling surface morphology of electrospun polystyrene fibers: effect of humidity and molecular weight in the electrospinning process, Macromolecules, 37 (2004) 573-578.

[93] X. Wang, H. Niu, T. Lin, X. Wang, Needleless electrospinning of nanofibers with a conical wire coil, Polymer Engineering & Science, 49 (2009) 1582-1586.

[94] X. Wang, H. Niu, X. Wang, T. Lin, Needleless electrospinning of uniform nanofibers using spiral coil spinnerets, Journal of Nanomaterials, 2012 (2012) 3.

[95] W. Liu, Y. Yao, Y. Lin, B. Wang, Y. Luo, N. Li, Q. Zhang, Y. Wu, A. Niu, Electrospinning assisted by gas jet for preparing ultrafine poly (vinyl alcohol) fibres, Iran Polymer Journal, 18 (2009) 89-96.

[96] W. Tomaszewski, M. Szadkowski, Investigation of electrospinning with the use of a multi-jet electrospinning head, Fibres and Textiles in Eastern Europe, 13 (2005) 22.

[97] F. Cengiz, O. Jirsak, The effect of salt on the roller electrospinning of polyurethane nanofibers, Fibers and Polymers, 10 (2009) 177-184.

[98] O.O. Dosunmu, G.G. Chase, W. Kataphinan, D.H. Reneker, Electrospinning of polymer nanofibres from multiple jets on a porous tubular surface, Nanotechnology, 17, (2006) 1123-1127.

[99] D. Nurwaha, W. Han, X. Wang, Investigation of a new needleless electrospinning method for the production of nanofibers. Journal of Engineered Fabrics & Fibers (JEFF), 8 (2013) 42-49.

[100] S. Theron, A. Yarin, E. Zussman, E. Kroll, Multiple jets in electrospinning: experiment and modeling, Polymer, 46 (2005) 2889-2899.

[101] Y. Yamashita, F. Ko, H. Miyake, A. Higashiyama, Establishment of nanofiber preparation technique by electrospinning, The Society of Fiber Science and Technology, Japan ,64 (2008) 24-28.

[102] A. Varesano, R.A. Carletto, G. Mazzuchetti, Experimental investigations on the multi-jet electrospinning process, Journal of Materials Processing Technology, 209 (2009) 5178-5185.

[103] G. Kim, K.E. Park, Alginate-nanofibers fabricated by an electrohydrodynamic process, Polymer Engineering & Science, 49 (2009) 2242-2248.

[104] J. Varabhas, G. Chase, D. Reneker, Electrospun nanofibers from a porous hollow tube, Polymer, 49 (2008) 4226-4229.

[105] A. Kumar, M. Wei, C. Barry, J. Chen, J. Mead, Controlling fiber repulsion in multijet electrospinning for higher throughput, Macromolecular Materials and Engineering, 295 (2010) 701-708.

[106] M.R. Badrossamay, H.A. McIlwee, J.A. Goss, K.K. Parker, Nanofiber assembly by rotary jet-spinning, Nano letters, 10 (2010) 2257-2261.

[107] A. Yarin, E. Zussman, Upward needleless electrospinning of multiple nanofibers, Polymer, 45 (2004) 2977-2980.

[108] X. Huang, D. Wu, Y. Zhu, D. Sun, Needleless electrospinning of multiple nanofibers, in: Poceedings of the 7th IEEE International Conference on Nanotechnology. Hong Kong, China, (2007) 823-826.

[109] E. Kostakova, L. Meszaros, J. Gregr, Composite nanofibers produced by modified needleless electrospinning, Materials Letters, 63 (2009) 2419-2422.

[110] H. Niu, T. Lin, X. Wang, Needleless electrospinning. I. A comparison of cylinder and disk nozzles, Journal of Applied Polymer Science, 114 (2009) 3524-3230.

[111] S. Tang, Y. Zeng, X. Wang, Splashing needleless electrospinning of nanofibers, Polymer Engineering & Science, 50 (2010) 2252-2257.

[112] R. Weitz, L. Harnau, S. Rauschenbach, M. Burghard, K. Kern, Polymer nanofibers via nozzle-free centrifugal spinning. Nano Letters, 8 (2008) 1187-1191.

[113] F. Dabirian, S. Hosseini Ravandi, A. Pishevar, R. Abuzade, A comparative study of jet formation and nanofiber alignment in electrospinning and electrocentrifugal spinning systems, Journal of Electrostatics, 69 (2011) 540-546.

[114] N.M. Thoppey, J.R. Bochinski, L.I. Clarke, R.E. Gorga, Unconfined fluid electrospun into high quality nanofibers from a plate edge, Polymer, 51 (2010) 4928-4936.

[115] D. Lukas, A. Sarkar, P. Pokorny, Self-organization of jets in electrospinning from free liquid surface: a generalized approach, Journal of Applied Physics, 103 (2008) 084309.

[116] Y. Lin, Y. Yao, X. Yang, N. Wei, X. Li, P. Gong, R. Li, D. Wu, Preparation of poly (ether sulfone) nanofibers by gas-jet/electrospinning, Journal of Applied Polymer Science, 107 (2008) 909-917.

[117] B. Wang, Y. Yao, J. Peng, Y. Lin, W. Liu, Y. Luo, R. Xiang, R. Li, D. Wu, Preparation of poly (ester imide) ultrafine fibers by gas-jet/electrospinning, Journal of Applied Polymer Science, 114 (2009) 883-891.

[118] E. Zhmayev, D. Cho, Y.L. Joo, Nanofibers from gas-assisted polymer melt electrospinning, Polymer, 51 (2010) 4140-4144.

[119] R.E. Benavides, S.C. Jana, D.H. Reneker, Role of liquid jet stretching and bending instability in nanofiber formation by gas jet method, Macromolecules, 46 (2013) 6081-6090.

[120] R.E. Benavides, S.C. Jana, D.H. Reneker, Nanofibers from scalable gas jet process, ACS Macro Letters, 1 (2012) 1032-1036.

[121] W. Bonani, D. Maniglio, A. Motta, W. Tan, C. Migliaresi, Biohybrid nanofiber constructs with anisotropic biomechanical properties, Journal of Biomedical Materials Research Part B: Applied Biomaterials, 96 (2011) 276-286.

[122] W. Bonani, A. Motta, C. Migliaresi, W. Tan, Biomolecule gradient in micropatterned nanofibrous scaffold for spatiotemporal release, Langmuir, 28 (2012) 13675-13687.

[123] W.-W. Hu, H.-N. Yu, Coelectrospinning of chitosan/alginate fibers by dual-jet system for modulating material surfaces, Carbohydrate Polymers, 95 (2013) 716-727.

[124] C.R. Yoo, I.-S. Yeo, K.E. Park, J.H. Park, S.J. Lee, W.H. Park, B.-M. Min, Effect of chitin/silk fibroin nanofibrous bicomponent structures on interaction with human epidermal keratinocytes, International Journal of Biological Macromolecules, 42 (2008) 324-334.

[125] F. Xu, L. Li, X. Cui, Fabrication of aligned side-by-side TiO_2/SnO_2 nanofibers via dual-opposite-spinneret electrospinning, Journal of Nanomaterials, 2012 (2012) 1-5.

[126] B. Duan, X. Yuan, Y. Zhu, Y. Zhang, X. Li, Y. Zhang, K. Yao, A nanofibrous composite membrane of PLGA–chitosan/PVA prepared by electrospinning, European Polymer Journal, 42 (2006) 2013-2022.

[127] A.V. Bazilevsky, A.L. Yarin, C.M. Megaridis, Co-electrospinning of core-shell fibers using a single-nozzle technique, Langmuir, 23 (2007) 2311-2314.

[128] Z. Liu, D.D. Sun, P. Guo, J.O. Leckie, An efficient bicomponent TiO_2/SnO_2 nanofiber photocatalyst fabricated by electrospinning with a side-by-side dual spinneret method, Nano Letters, 7 (2007) 1081-1085.

[129] J.E. Díaz, A. Fernández-Nieves, A. Barrero, M. Márquez, I.G. Loscertales, Fabrication of structured micro and nanofibers by coaxial electrospinning, Journal of Physics: Conference, 127 (2008) 1-8.

[130] S. Jiang, G. Duan, E. Zussman, A. Greiner, S. Agarwal, Highly flexible and tough concentric triaxial polystyrene fibers, ACS Applied Materials & Interfaces, 6 (2014) 5918-5923.

[131] M. Pakravan, M.-C. Heuzey, A. Ajji, Core-shell structured PEO-chitosan nanofibers by coaxial electrospinning, Biomacromolecules, 13 (2012) 412-421.

[132] H.-W. Tong, X. Zhang, M. Wang, A new nanofiber fabrication technique based on coaxial electrospinning, Materials Letters, 66 (2012) 257-260.

[133] J.-J. Chang, Y.-H. Lee, M.-H. Wu, M.-C. Yang, C.-T. Chien, Preparation of electrospun alginate fibers with chitosan sheath, Carbohydrate Polymers, 8 (2012) 2357-2361.

[134] D. Li, Y. Xia, Direct fabrication of composite and ceramic hollow nanofibers by electrospinning, Nano Letters, 4 (2004) 933-938.

[135] S. Sakuldao, T. Yoovidhya, S. Wongsasulak, Coaxial electrospinning and sustained release properties of gelatin-cellulose acetate core-shell ultrafine fibres, ScienceAsia, 37 (2011) 335-343.

[136] Y. Zhang, Z.-M. Huang, X. Xu, C.T. Lim, S. Ramakrishna, Preparation of core-shell structured PCL-r-gelatin bi-component nanofibers by coaxial electrospinning, Chemistry of Materials, 16 (2004) 3406-3409.

[137] M. Gulfam, J.M. Lee, J.-E. Kim, D.W. Lim, E.K. Lee, B.G. Chung, Highly porous core-shell polymeric fiber network, Langmuir, 27 (2011) 10993-10999.

[138] H. Chen, N. Wang, J. Di, Y. Zhao, Y. Song, L. Jiang, Nanowire-in-microtube structured core/shell fibers via multifluidic coaxial electrospinning, Langmuir, 26, (2010) 11291-11296.

[139] W. Kim, S.S. Kim, Synthesis of biodegradable triple-layered capsules using a triaxial electrospray method, Polymer, 52 (2011) 3325-3336.

[140] W. Liu, C. Ni, D.B. Chase, J.F. Rabolt, Preparation of multilayer biodegradable nanofibers by triaxial electrospinning, ACS Macro Letters, 2 (2013) 466-468.

[141] T.C. Mokhena, A.S. Luyt, Investigation of polyethylene/sisal whiskers nanocomposites prepared under different conditions, Polymer Composites, 35 (2014) 2221-2233.

[142] M. Stephen, N. Catherine, M. Brenda, K. Andrew, P.Leslie, G. Corrine, Oxolane-2, 5-dione modified electrospun cellulose nanofibers for heavy metals adsorption, Journal of Hazardous Materials, 192 (2011) 922-927.

[143] S. Xu, J. Zhang, A. He, J. Li, H. Zhang, C.C. Han, Electrospinning of native cellulose from nonvolatile solvent system, Polymer, 49 (2008) 2911-2917.

[144] H. Ma, C. Burger, B.S. Hsiao, B. Chu, Nanofibrous microfiltration membrane based on cellulose nanowhiskers, Biomacromolecules, 13 (2011) 180-186.

[145] S.S. Rao, S.G. Jeyapal, S. Rajiv, Biodegradable electrospun nanocomposite fibers based on poly (2-hydroxy ethyl methacrylate) and bamboo cellulose, Composites Part B: Engineering, 60 (2014) 43-48.

[146] M.S. Peresin, Y. Habibi, A.-H. Vesterinen, O.J. Rojas, J.J. Pawlak, J.V. Seppälä, Effect of moisture on electrospun nanofiber composites of poly (vinyl alcohol) and cellulose nanocrystals, Biomacromolecules, 11 (2010) 2471-2477.

[147] W.I. Park, M. Kang, H.S. Kim, H.J. Jin, Electrospinning of poly (ethylene oxide) with bacterial cellulose whiskers, Macromolecular Symposia, 249-250 (2007) 289-294.

[148] X. Cao, M. Huang, B. Ding, J. Yu, G. Sun, Robust polyacrylonitrile nanofibrous membrane reinforced with jute cellulose nanowhiskers for water purification, Desalination, 316 (2013) 120-126.

[149] B. Chu, B.S. Hsiao, H. Ma, High flux high efficiency nanofiber membranes and methods of production thereof. 20110198282 A1, USA (2009).

[150] Ma H., Burger C., Hsiao B. S., Chu B.: Highly permeable polymer membranes containing directed channels for water purification. ACS Macro Letters, 1, 723-726 (2012).

[151] H. Ma, C. Burger, B.S. Hsiao, B. Chu, Ultrafine polysaccharide nanofibrous membranes for water purification, Biomacromolecules, 12 (2011) 970-976.

[152] A. Sato, R. Wang, H. Ma, B.S. Hsiao, B. Chu, Novel nanofibrous scaffolds for water filtration with bacteria and virus removal capability, Journal of Electron Microscopy, 60 (3) (2011) 201-209.

[153] Z. Ma, M. Kotaki, S. Ramakrishna, Electrospun cellulose nanofiber as affinity membrane, Journal of Membrane Science, 265 (2005) 115-123.

[154] I.G. Wenten, Recent development in membrane science and its industrial applications, Membrane Science Technology, 24 (2002) 1010-1024.

[155] F. Ji, C. Li, B. Tang, J. Xu, G. Lu, P. Liu, Preparation of cellulose acetate/zeolite composite fiber and its adsorption behavior for heavy metal ions in aqueous solution, Chemical Engineering Journal, 209 (2012) 325-333.

[156] A.A. Taha, Y.-N. Wu, H. Wang, F. Li, Preparation and application of functionalized cellulose acetate/silica composite nanofibrous membrane via electrospinning for Cr (VI) ion removal from aqueous solution, Journal of Environmental Management, 112 (2012) 10-16.

[157] A. Bodalo, J.-L. Gomez, E. Gomez, G. Leon, M. Tejera, Ammonium removal from aqueous solutions by reverse osmosis using cellulose acetate membranes, Desalination, 184 (2005) 149-155.

[158] R. Konwarh, N. Karak, M. Misra, Electrospun cellulose acetate nanofibers: the present status and gamut of biotechnological applications, Biotechnology Advances, 31 (2013) 421-437.

[159] W. Zhou, J. He, S. Cui, W. Gao, Studies of electrospun cellulose acetate nanofibrous membranes, The Open Materials Science Journal, 5 (2011) 51-55.

[160] L. Chen, L. Bromberg, T.A. Hatton, G.C. Rutledge, Electrospun cellulose acetate fibers containing chlorhexidine as a bactericide, Polymer, 49 (2008) 1266-1275.

[161] P. Taepaiboon, U. Rungsardthong, P. Supaphol, Vitamin-loaded electrospun cellulose acetate nanofiber mats as transdermal and dermal therapeutic agents of vitamin A acid and vitamin E, European Journal of Pharmaceutics and Biopharmaceutics, 67 (2007) 387-397.

[162] O. Suwantong, P. Opanasopit, U. Ruktanonchai, P. Supaphol, Electrospun cellulose acetate fiber mats containing curcumin and release characteristic of the herbal substance, Polymer, 48 (2007) 7546-7557.

[163] Z. Ma, S. Ramakrishna, Electrospun regenerated cellulose nanofiber affinity membrane functionalized with protein A/G for IgG purification, Journal of Membrane Science, 319 (2008) 23-28.

[164] S.-L. Chen, X.-J. Huang, Z.-K. Xu, Functionalization of cellulose nanofiber mats with phthalocyanine for decoloration of reactive dye wastewater, Cellulose, 18 (2011) 1295-1303.

[165] R.A. Muzzarelli, Chitins and chitosans as immunoadjuvants and non-allergenic drug carriers, Marine Drugs, 8 (2010) 292-312.

[166] R. Jayakumar, D. Menon, K. Manzoor, S. Nair, H. Tamura, Biomedical applications of chitin and chitosan based nanomaterials-a short review, Carbohydrate Polymers, 82 (2010) 227-232.

[167] K. Sun, Z. Li, Preparations, properties and applications of chitosan based nanofibers fabricated by electrospinning, Express Polymer Letters, 5 (4) (2011) 342-361.

[168] B.-M. Min, S.W. Lee, J.N. Lim, Y. You, T.S. Lee, P.H. Kang, W.H. Park, Chitin and chitosan nanofibers: electrospinning of chitin and deacetylation of chitin nanofibers, Polymer, 45 (2004) 7137-7142.

[169] H.K. Noh, S.W. Lee, J.-M. Kim, J.-E. Oh, K.-H. Kim, C.-P. Chung, S.-C. Choi, W.H. Park, B.-M. Min, Electrospinning of chitin nanofibers: degradation behavior and cellular response to normal human keratinocytes and fibroblasts, Biomaterials, 27 (2006) 3934-3944.

[170] J. Junkasem, R. Rujiravanit, P. Supaphol, Fabrication of α-chitin whisker-reinforced poly (vinyl alcohol) nanocomposite nanofibres by electrospinning, Nanotechnology, 17 (2006) 4519-4528.

[171] J. Junkasem, R. Rujiravanit, B.P. Grady, P. Supaphol, X-ray diffraction and dynamic mechanical analyses of α-chitin whisker-reinforced poly (vinyl alcohol) nanocomposite nanofibers., Polymer International, 59 (2010) 85-91.

[172] N. Naseri, C. Algan, V. Jacobs, M. John, K. Oksman, A.P. Mathew, Electrospun chitosan-based nanocomposite mats reinforced with chitin nanocrystals for wound dressing, Carbohydrate Polymers, 109 (2014) 7-15.

[173] K.E. Park, H.K. Kang, S.J. Lee, B.-M. Min, W.H. Park, Biomimetic nanofibrous scaffolds: preparation and characterization of PGA/chitin blend nanofibers, Biomacromolecules, 7 (2006) 635-643.

[174] A. Błasińska, I. Krucińska, M. Chrzanowski, Dibutyrylchitin nonwoven biomaterials manufactured using electrospinning method, Fibres & Textiles in Eastern Europe, 12 (48) (2004) 51-55.

[175] J. Du, Y.-L. Hsieh, Cellulose/chitosan hybrid nanofibers from electrospinning of their ester derivatives, Cellulose, 16 (2009) 247-260.

[176] H.R. Pant, H.J. Kim, L.R. Bhatt, M.K. Joshi, E.K. Kim, J.I. Kim, A. Abdal-hay, K. Hui, C.S. Kim, Chitin butyrate coated electrospun nylon-6 fibers for biomedical applications, Applied Surface Science, 285 (2013) 538-544.

[177] K. Shalumon, N. Binulal, N. Selvamurugan, S. Nair, D. Menon, T. Furuike, H. Tamura, R. Jayakumar, Electrospinning of carboxymethyl chitin/poly (vinyl alcohol) nanofibrous scaffolds for tissue engineering applications, Carbohydrate Polymers, 77 (2009) 863-869.

[178] N. Sohofi, H. Tavanai, M. Morshed, A. Abdolmaleki, Electrospinning of 100% carboxymethyl chitosan nanofibers, Journal of Engineered Fabrics & Fibers (JEFF), 1, (2014) 87-92.

[179] Y. Qin, H. Hu, A. Luo, Y. Wang, X. Huang, P. Song, Effect of carboxymethylation on the absorption and chelating properties of chitosan fibers, Journal of Applied Polymer Science, 99 (2006) 3110-3115.

[180] J. Miao, L. Li, G. Chen, C. Gao, S. Dong, Preparation of *N,O*-carboxymethyl chitosan composite nanofiltration membrane and its rejection performance for the fermentation effluent from a wine factory, Chinese Journal of Chemical Engineering, 16 (2008) 209-213.

[181] Z.-P. Zhao, Z. Wang, S.-C. Wang, Formation, charged characteristic and BSA adsorption behavior of carboxymethyl chitosan/PES composite MF membrane, Journal of Membrane Science, 217 (2003) 151-158.

[182] R.A. Muzzarelli, Potential of chitin/chitosan-bearing materials for uranium recovery: an interdisciplinary review, Carbohydrate Polymers, 84 (2011) 54-63.

[183] W. Wan Ngah, L. Teong, M. Hanafiah, Adsorption of dyes and heavy metal ions by chitosan composites: a review, Carbohydrate Polymers, 83 (2011) 1446-1456.

184] K. Ohkawa, D. Cha, H. Kim, A. Nishida, H. Yamamoto, Electrospinning of chitosan, Macromolecular Rapid Communications, 25 (2004) 1600-1605.

[185] Y.-T. Jia, J. Gong, X.-H. Gu, H.-Y. Kim, J. Dong, X.-Y. Shen, Fabrication and characterization of poly (vinyl alcohol)/chitosan blend nanofibers produced by electrospinning method, Carbohydrate Polymers, 67 (2007) 403-409.

[186] P. Su, C. Wang, X. Yang, X. Chen, C. Gao, X.-X. Feng, J.-Y. Chen, J. Ye, Z. Gou, Electrospinning of chitosan nanofibers: the favorable effect of metal ions, Carbohydrate Polymers, 84 (2011) 239-246.

[187] K.H. Jung, M.W. Huh, W. Meng, J. Yuan, S.H. Hyun, J.S. Bae, S.M. Hudson, I.K. Kang, Preparation and antibacterial activity of PET/chitosan nanofibrous mats using an electrospinning technique, Journal of Applied Polymer Science, 105 (2007) 2816-2823.

[188] S. Torres-Giner, M.J. Ocio, J.M. Lagaron, Novel antimicrobial ultrathin structures of zein/chitosan blends obtained by electrospinning, Carbohydrate Polymers, 77 (2009) 261-266.

[189] Z. Chen, X. Mo, F. Qing, Electrospinning of collagen-chitosan complex, Materials Letters, 61 (2007) 3490-3494.

[190] J.-P. Chen, G.-Y. Chang, J.-K. Chen, Electrospun collagen/chitosan nanofibrous membrane as wound dressing, Colloids and Surfaces A: Physicochemical and Engineering Aspects, 313 (2008) 183-188.

[191] N. Maeda, J. Miao, T. Simmons, J. Dordick, R. Linhardt, Composite polysaccharide fibers prepared by electrospinning and coating, Carbohydrate Polymers, 102 (2014) 950-955.

[192] C. Santos, C.J. Silva, Z. Büttel, R. Guimarães, S.B. Pereira, P. Tamagnini, A. Zille, Preparation and characterization of polysaccharides/PVA blend nanofibrous membranes by electrospinning method, Carbohydrate Polymers, 99 (2014) 584-592.

[193] M. Ignatova, K. Starbova, N. Markova, N. Manolova, I. Rashkov, Electrospun nano-fibre mats with antibacterial properties from quaternised chitosan and poly (vinyl alcohol), Carbohydrate Research, 341 (2006) 2098-2107.

[194] M. Ignatova, N. Manolova, N. Markova, I. Rashkov, Electrospun non-woven nanofibrous hybrid mats based on chitosan and PLA for wound-dressing applications, Macromolecular Bioscience, 9 (2009) 102-111.

[195] W. Kangwansupamonkon, W. Tiewtrakoonwat, P. Supaphol, S. Kiatkamjornwong, Surface modification of electrospun chitosan nanofibrous mats for antibacterial activity, Journal of Applied Polymer Science, 131 (2014) 1-9.

[196] S.M. Alipour, M. Nouri, J. Mokhtari, S.H. Bahrami, Electrospinning of poly (vinyl alcohol)-water-soluble quaternized chitosan derivative blend, Carbohydrate Research, 344 (2009) 2496-2501.

[197] Z. Zong, Y. Kimura, M. Takahashi, H. Yamane, Characterization of chemical and solid state structures of acylated chitosans, Polymer, 41 (2000) 899-906.

[198] M. Peesan, R. Rujiravanit, P. Supaphol, Electrospinning of hexanoyl chitosan/polylactide blends, Journal of Biomaterials Science, Polymer Edition, 17 (2006) 547-565.

[199] E. Alsberg, K. Anderson, A. Albeiruti, R. Franceschi, D. Mooney, Cell-interactive alginate hydrogels for bone tissue engineering, Journal of Dental Research, 80 (2001) 2025-2029.

[200] A. Dar, M. Shachar, J. Leor, S. Cohen, Optimization of cardiac cell seeding and distribution in 3D porous alginate scaffolds, Biotechnology and Bioengineering, 80 (2002) 305-312.

[201] T. Hashimoto, Y. Suzuki, M. Tanihara, Y. Kakimaru, K. Suzuki, Development of alginate wound dressings linked with hybrid peptides derived from laminin and elastin, Biomaterials, 25 (2004) 1407-1414.

[202] T.A. Davis, B. Volesky, A. Mucci, A review of the biochemistry of heavy metal biosorption by brown algae, Water Research, 37 (2003) 4311-4330.

[203] S. Papageorgiou, F. Katsaros, E. Kouvelos, N. Kanellopoulos, Prediction of binary adsorption isotherms of Cu^{2+}, Cd^{2+} and Pb^{2+} on calcium alginate beads from single adsorption data, Journal of Hazardous Materials, 162 (2009) 1347-1354.

[204] C. Xiao, Y. Lu, H. Liu, L. Zhang, Preparation and physical properties of blend films from sodium alginate and polyacrylamide solutions, Journal of Molecular Science Part A: Pure Appliaed Chemistry, 37 (2000) 1663-1675.

[205] T. Caykara, S. Demirci, M.S. Eroğlu, O. Güven, Poly (ethylene oxide) and its blends with sodium alginate, Polymer, 46 (2005) 10750-10757.

[206] H. Omidian, J.G. Rocca, K. Park, Elastic, superporous hydrogel hybrids of polyacrylamide and sodium alginate. Macromolecular Bioscience, 6 (2006) 703-710.

[207] C.A. Bonino, M.D. Krebs, C.D.Saquing, S.I. Jeong, K.L. Shearer, E. Alsberg, S.A. Khan, Electrospinning alginate-based nanofibers: from blends to crosslinked low molecular weight alginate-only systems, Carbohydrate Polymers, 85 (2011) 111-119.

[208] M.S. Islam, M. Ashaduzzaman, S.M. Masum, J.H. Yeum, Mechanical and electrical properties: electrospun alginate/carbon nanotube composite nanofiber, Dhaka University Journal of Science, 60 (2012) 125-128.

[209] K. Tarun, N. Gobi, Calcium alginate/PVA blended nano fibre matrix for wound dressing, Indian Journal of Fibre & Textile Research, 37 (2012) 127-132.

[210] Y.J. Lee, D.S. Shin, O.W. Kwon, W.H. Park, H.G. Choi, Y.R. Lee, S.S. Han, S.K. Noh, W.S. Lyoo, Preparation of atactic poly (vinyl alcohol)/sodium alginate blend nanowebs by electrospinning, Journal of Applied Polymer Science, 106 (2007) 1337-1342.

[211] N. Bhattarai, M. Zhang, Controlled synthesis and structural stability of alginate-based nanofibers, Nanotechnology, 18 (2007) 455601/1-455601/10.

[212] S. Alborzi, L.T. Lim, Y. Kakuda, Electrospinning of sodium alginate-pectin ultrafine fibers, Journal of Food Science, 75 (2010) C100-C107.

[213] S.A. Park, K.E. Park, W. Kim, Preparation of sodium alginate/poly (ethylene oxide) blend nanofibers with lecithin, Macromolecular Research, 18 (2010) 891-896.

[214] S.I. Jeong, M.D. Krebs, C.A. Bonino, J.E. Samorezov, S.A. Khan, E. Alsberg, Electrospun chitosan-alginate nanofibers with in situ polyelectrolyte complexation for use as tissue engineering scaffolds, Tissue Engineering Part A, 17 (2010) 59-70.

[215] L. Buttafoco, N. Kolkman, P. Engbers-Buijtenhuijs, A. Poot, P. Dijkstra, I. Vermes, J. Feijen, Electrospinning of collagen and elastin for tissue engineering applications. Biomaterials, 27 (2006) 724-734.

[216] T. Telemeco, C. Ayres, G. Bowlin, G. Wnek, E. Boland, N. Cohen, C. Baumgarten, J. Mathews, D. Simpson, Regulation of cellular infiltration into tissue engineering scaffolds composed of submicron diameter fibrils produced by electrospinning, Acta Biomaterialia, 1 (2005) 377-385.

[217] Y. Zhang, J. Venugopal, Z.-M. Huang, C. Lim, S. Ramakrishna, Characterization of the surface biocompatibility of the electrospun PCL-collagen nanofibers using fibroblasts, Biomacromolecules, 6 (2005) 2583-2589.

[218] M. Li, M.J. Mondrinos, M.R. Gandhi, F.K. Ko, A.S. Weiss, P.I. Lelkes, Electrospun protein fibers as matrices for tissue engineering, Biomaterials, 26 (2005) 5999-6008.

[219] D.I. Zeugolis, S.T. Khew, E.S. Yew, A.K. Ekaputra, Y.W. Tong, L.-Y.L. Yung, D.W. Hutmacher, C. Sheppard, M. Raghunath, Electro-spinning of pure collagen nano-fibres-just an expensive way to make gelatin? Biomaterials, 29 (2008) 2293-2305.

[220] V.Y. Chakrapani, A. Gnanamani, V. Giridev, M. Madhusoothanan, G. Sekaran, Electrospinning of type I collagen and PCL nanofibers using acetic acid, Journal of Applied Polymer Science, 125 (2012) 3221-3227.

[221] I.K. Kwon, T. Matsuda, Co-electrospun nanofiber fabrics of poly (L-lactide-co-ε-caprolactone) with type I collagen or heparin, Biomacromolecules, 6 (2005) 2096-2105.

[222] S. Zhong, W.E. Teo, X. Zhu, R. Beuerman, S. Ramakrishna, L.Y.L. Yung, Formation of collagen-glycosaminoglycan blended nanofibrous scaffolds and their biological properties. Biomacromolecules, 6 (2005) 2998-3004.

[223] M.G. Haugh, M.J. Jaasma, F.J. O'Brien, The effect of dehydrothermal treatment on the mechanical and structural properties of collagen-GAG scaffolds, Journal of Biomedical Materials Research Part A, 89 (2009) 363-369.

[224] J.F. Davis, G.J. Maffia, Collagen dispersions for liquid-solid separations in water treatment and sludge dewatering, Separations Technology, 5 (1995) 147-152.

[225] Y. Zhang, H. Ouyang, C.T. Lim, S. Ramakrishna, Z.M. Huang, Electrospinning of gelatin fibers and gelatin/PCL composite fibrous scaffolds, Journal of Biomedical Materials Research Part B: Applied Biomaterials, 72 (2005) 156-165.

[226] D.E. Elliott, F.J. Davis, G.R. Mitchell, R.H. Olley, Structure development in electrospun fibres of gelatin, Journal of Physics: Conference: Conference Series: IOP Publishing, (2009) 012021/1-012021/4.

[227] Z.-M. Huang, Y. Zhang, S. Ramakrishna, C. Lim, Electrospinning and mechanical characterization of gelatin nanofibers, Polymer, 45 (2004) 5361-5368.

[228] E.K. Brenner, J.D. Schiffman, E.A. Thompson, L.J. Toth, C.L. Schauer, Electrospinning of hyaluronic acid nanofibers from aqueous ammonium solutions, Carbohydrate Polymers, 87 (2012) 926-929.

[229] S. Lan, X. Wu, L. Li, M. Li, F. Guo, S. Gan, Synthesis and characterization of hyaluronic acid-supported magnetic microspheres for copper ions removal, Colloids and Surfaces A: Physicochemical and Engineering Aspects, 425 (2013) 42-50.

[230] G. Ma, Y. Liu, D. Fang, J. Chen, C. Peng, X. Fei, J. Nie, Hyaluronic acid/chitosan polyelectrolyte complexes nanofibers prepared by electrospinning, Materials Letters, 74 (2012) 78-80.

[231] İ. Uslu, A. Aytimur, Production and characterization of poly (vinyl alcohol)/poly (vinylpyrrolidone) iodine/poly (ethylene glycol) electrospun fibers with (hydroxypropyl) methyl cellulose and aloe vera as promising material for wound dressing, Journal of Applied Polymer Science, 124 (2012) 3520-3524.

[232] I. Uslu, S. Keskin, A. Gül, T.C. Karabulut, M.L. Aksu, Preparation and properties of electrospun poly (vinyl alcohol) blended hybrid polymer with aloe vera and HPMC as wound dressing, Hacettepe Journal of Biology Chemistry, 38 (2010) 19-25.

[233] A. Surjushe, R. Vasani, D. Saple, Aloe vera: a short review, Indian Journal of Dermatology, 53 (2008) 163-166.

[234] S. Suganya, J. Venugopal, S.A. Mary, S. Ramakrishna, B. Lakshmi, V.G. Dev, Aloe vera incorporated biomimetic nanofibrous scaffold: a regenerative approach for skin tissue engineering, Iranian Polymer Journal, 23 (2014) 237-248.

[235] A.M. Abdelgawad, S.M. Hudson, O.J. Rojas, Antimicrobial wound dressing nanofiber mats from multicomponent (chitosan/silver-NPs/polyvinyl alcohol) systems, Carbohydrate Polymers, 100 (2014) 166-178.

[236] Q. Li, S. Mahendra, D.Y. Lyon, L. Brunet, M.V. Liga, D. Li, P.J. Alvarez, Antimicrobial nanomaterials for water disinfection and microbial control: potential applications and implications, Water Research, 42 (2008) 4591-4602.

[237] X. Qu, P.J. Alvarez, Q. Li, Applications of nanotechnology in water and wastewater treatment, Water Research, 47 (2013) 3931-3946.

[238] Q.H. Tran, A.-T. Le, Silver nanoparticles: synthesis, properties, toxicology, applications and perspectives, Advances in Natural Sciences: Nanoscience and Nanotechnology, 4 (2013) 033001/1-033001/20.

[239] T.T.T. Nguyen, B. Tae, J.S. Park, Synthesis and characterization of nanofiber webs of chitosan/poly (vinyl alcohol) blends incorporated with silver nanoparticles, Journal of Materials Science, 46 (2011) 6528-6537.

[240] J. An, H. Zhang, J. Zhang, Y. Zhao, X. Yuan, Preparation and antibacterial activity of electrospun chitosan/poly (ethylene oxide) membranes containing silver nanoparticles, Colloid and Polymer Science, 287 (2009) 1425-1434.

[241] A.T. Hang, B. Tae, J.S. Park, Non-woven mats of poly (vinyl alcohol)/chitosan blends containing silver nanoparticles: fabrication and characterization, Carbohydrate Polymers, 82 (2010) 472-479.

[242] X. Zhuang, B. Cheng, W. Kang, X. Xu, Electrospun chitosan/gelatin nanofibers containing silver nanoparticles, Carbohydrate Polymers, 82 (2010) 524-527.

[243] S.J. Lee, D.N. Heo, J.-H. Moon, W.-K. Ko, J.B. Lee, M.S. Bae, S.W. Park, J.E. Kim, D.H. Lee, E.-C. Kim, Electrospun chitosan nanofibers with controlled levels of silver nanoparticles. Preparation, characterization and antibacterial activity, Carbohydrate Polymers, 111 (2014) 530-537.

[244] H. Celebi, M. Gurbuz, S. Koparal, A. Dogan, Development of antibacterial electrospun chitosan/poly (vinyl alcohol) nanofibers containing silver ion-incorporated HAP nanoparticles, Composite Interfaces, 20 (2013) 799-812.

[245] H.W. Kim, J.H. Song, H.E. Kim, Nanofiber generation of gelatin-hydroxyapatite biomimetics for guided tissue regeneration, Advanced Functional Materials, 15 (2005) 1988-1994.

[246] J. Ayutsede, M. Gandhi, S. Sukigara, H. Ye, C.-M. Hsu, Y. Gogotsi, F. Ko, Carbon nanotube reinforced Bombyx mori silk nanofibers by the electrospinning process, Biomacromolecules, 7 (2006) 208-214.

[247] P. Lu, Y.-L. Hsieh, Multiwalled carbon nanotube (MWCNT) reinforced cellulose fibers by electrospinning. ACS Applied Materials & Interfaces, 2, (2010) 2413-2420.

[248] W. Feng, Z. Wu, Y. Li, Y. Feng, X. Yuan, The fabrication and electrochemical properties of electrospun nanofibers of a multiwalled carbon nanotube grafted by chitosan, Nanotechnology, 19 (2008) 105707/1-105707/6.

[249] H. Pan, Y. Zhang, Y. Hang, H. Shao, X. Hu, Y. Xu, C. Feng, Significantly reinforced composite fibers electrospun from silk fibroin/carbon nanotube aqueous solutions, Biomacromolecules, 13 (2012) 2859-2867.

[250] K. Shalumon, K. Anulekha, S.V. Nair, S. Nair, K. Chennazhi, R. Jayakumar, Sodium alginate/poly (vinyl alcohol)/nano ZnO composite nanofibers for antibacterial wound dressings, International Journal of Biological Macromolecules, 49 (2011) 247-254.

[251] S. Anitha, B. Brabu, D.J. Thiruvadigal, C. Gopalakrishnan, T. Natarajan, Optical, bactericidal and water repellent properties of electrospun nano-composite membranes of cellulose acetate and ZnO, Carbohydrate Polymers, 87 (2012) 1065-1072.

[252] Y. Tian, M. Wu, R. Liu, Y. Li, D. Wang, J. Tan, R. Wu, Y. Huang, Electrospun membrane of cellulose acetate for heavy metal ion adsorption in water treatment, Carbohydrate Polymers, 83 (2011) 743-748.

[253] E. Guibal, Interactions of metal ions with chitosan-based sorbents: a review, Separation and Purification Technology, 38 (2004) 43-74.

[254] K. Desai, K. Kit, J. Li, P. Michael Davidson, S. Zivanovic, H. Meyer, Nanofibrous chitosan non-wovens for filtration applications, Polymer, 50 (2009) 3661-3669.

[255] C. Ki, E. Gang, I. Um, Y. Park, Nanofibrous membrane of wool keratose/silk fibroin blend for heavy metal ion adsorption, Journal of Membrane Science, 302 (2007) 20-26.

[256] R. Yang, K.B. Aubrecht, H. Ma, R. Wang, R.B. Grubbs, B.S. Hsiao, B. Chu, Thiol-modified cellulose nanofibrous composite membranes for chromium (VI) and lead (II) adsorption, Polymer, 55 (2014) 1167-1176.

[257] R. Wang, S. Guan, A. Sato, X. Wang, Z. Wang, R. Yang, B.S. Hsiao, B. Chu, Nanofibrous microfiltration membranes capable of removing bacteria, viruses and heavy metal ions, Journal of Membrane Science, 446 (2013) 376-382.

[258] X. Wang, T.-M. Yeh, Z. Wang, R. Yang, R. Wang, H. Ma, B.S. Hsiao, B. Chu, Nanofiltration membranes prepared by interfacial polymerization on thin-film nanofibrous composite scaffold, Polymer, 55 (2014) 1358-1366.

[259] K. Yoon, K. Kim, X. Wang, D. Fang, B.S. Hsiao, B. Chu, High flux ultrafiltration membranes based on electrospun nanofibrous PAN scaffolds and chitosan coating, Polymer, 47 (2006) 2434-2441.

[260] M. Wang, G. Meng, Q. Huang, Y. Qian, Electrospun 1, 4-DHAQ-doped cellulose nanofiber films for reusable fluorescence detection of trace Cu^{2+} and further for Cr^{3+}, Environmental Science & Technology, 46 (2011) 367-373.

[261] S. Kacmaz, K. Ertekin, A. Suslu, Y. Ergun, E. Celik, U. Cocen, Sub-nanomolar sensing of ionic mercury with polymeric electrospun nanofibers, Materials Chemistry and Physics, 133 (2012) 547-552.

[262] M.Z. Ongun, K. Ertekin, M. Gocmenturk, Y. Ergun, A. Suslu, Copper ion sensing with fluorescent electrospun nanofibers, Spectrochimica Acta Part A: Molecular and Biomolecular Spectroscopy, 90 (2012) 177-185.

[263] S. Kacmaz, K. Ertekin, M. Gocmenturk, A. Suslu, Y. Ergun, E. Celik, Selective sensing of Fe^{3+} at pico-molar level with ethyl cellulose based electrospun nanofibers, Reactive & Functional Polymers, 73 (2013) 674-682.

[264] M.Z. Ongun, K. Ertekin, C.G. Hizliates, O. Oter, Y. Ergun, E. Celik, Determination of Hg (II) at sub-nanomolar levels: a comparative study with nanofibrous materials and continuous thin films, Sensors and Actuators B: Chemical, 181 (2013) 244-250.

[265] B. Zdyrko, Nanofibrous materials as sensors for heavy metals.

Chapter 3

Electrospun alginate nanofibres as a potential bio-sorption agent of heavy metals in water treatment

This chapter has been submitted for publication as:
T.C. Mokhena, N.V Jacobs, A.S. Luyt, Electrospun alginate nanofibres as potential bio-sorption agent of heavy metals in water treatment, Journal of Membrane Science

Abstract

This paper reports on the potential of the electrospun alginate nanofibrous membranes to be used for the bio-sorption of heavy metals from aqueous solutions. Poly(ethylene oxide) (PEO) and its blends were electrospun at an applied voltage of 1-1.3 kV/cm and a solution flow rate of 0.8 mL hr^{-1}. The electrospinnability of the nanofibres blends were enhanced by storing the blend solutions in a controlled environmental chamber. The electrospun nanofibre membranes were washed with calcium chloride in order to remove PEO. Beadless nanofibres with average diameters of 114 nm and a surface area of 18.03 m^2 g^{-1} were obtained. Fourier transform infra-red (FTIR) spectroscopy and thermogravimetric analysis (TGA) confirmed the removal of PEO after washing with calcium chloride. The adsorption behaviour of the nanofibrous membranes was investigated using Cu ions as model metalloid at different concentrations (0-1000 mg L^{-1}), temperatures (25, 40, and 60°C) and pH values (2-6). The Langmuir isotherm better presented the equilibrium experimental data than the Freundlich model. The electrospun alginate membranes displayed maximum monolayer sorption capacity (Q_0) of 15.6 mg g^{-1} at a pH of 4.

Keywords: Electrospun alginate; Copper adsorption; Water treatment

3.1 Introduction

One of the major problems of this century is the environmental pollution resulting from industrial activities such as metal finishing, mining, electroplating, painting, dying, photography, surface treatment, and printed circuit board manufacture [1-4]. These activities

release large quantities of heavy metals into the environment, which poses a threat to the whole ecosystem (terrestrial and aquatic environments) [5]. The persistence of the metal ions in the ecosystem and their non-biodegradability necessitates suitable and cheaper alternative methods for their removal [1,4]. Various techniques including chemical precipitation, reverse osmosis, electro-dialysis, membrane separation and solvent extraction have been employed for this purpose [5,6]. These techniques are usually associated with high cost and energy, and some are time consuming [5].The adsorption method is considered as one of the most effective methods due to its simplicity, high efficiency, economic feasibility, easy recovery and reuse of the adsorbents [3].

There are two main mechanisms associated with the adsorption method, namely physisorption or chemisorption. In most cases, both of these mechanisms are involved during adsorption. The most important properties of any adsorbent are a large surface area and the availability of functional groups. A number of researchers have investigated nanofibre membranes as adsorbents of heavy metal ions from various sources [7-11]. Nanofibre membranes prepared by electrospinning are especially important due to their unique properties such as large surface area to volume ratio, high porosity, and malleability [4,12]. Haider and Park [13] prepared electrospun chitosan nanofibre membranes for the adsorption of copper (Cu(II)) and lead (Pb(II)). They reported that the data fitted the Langmuir model well, with a monolayer adsorption capacity for Cu(II) of 485.44 mg $g^{-1}$and for Pb(II) of 263.15 mg g^{-1}. According to the authors these values were 6-10 times higher than the values of chitosan microspheres reported in the literature.

A wide variety of low cost adsorbents such as algae, alginate, chitosan, fungi, peanut husks, and lignin were studied in order to evaluate their potentials as viable alternatives to the mostly used expensive adsorbents such as activated carbon [14]. Among these adsorbents, alginate received considerable interest due to its potential to gel when it comes in contact with metal ions. This property has been exploited to adsorb different metal ions form aqueous media [3,5,15,16]. Alginate is one of the most abundant polysaccharides, usually extracted from seaweeds (brown algae), and it is composed of mannuronate (M) and guluronate (G) acid residues. These residues may vary in sequence and M/G ratio along the polymer, depending on the species and the nature of growth.

To our knowledge, there is no study based on electrospun alginate nanofibres as metal adsorbent. The aim of this study was therefore to prepare calcium alginate nanofibre

membranes by electrospinning and to investigate its application as an adsorbent for the removal of copper, a model metalloid from aqueous solutions. The effect of contact time, initial metal concentration, and temperature were evaluated in order to find the optimal conditions for maximum metal adsorption capacity. The electrospinnability of alginate from its aqueous solution is still a problem, and poly(ethylene oxide) PEO was therefore used to facilitate its spinnability.

3.2 Experimental

3.2.1 Materials

Sodium alginate (SA) (Sigma, viscosity (25°C, 2 wt% aqueous solution) = 2000 cP, medium viscosity, Mw = 100 kDa), poly (ethylene oxide) (PEO) (Sigma, Mw = 2000kDa) and copper sulphate ($CuSO_4$) (Ibhayi Suppliers).

3.2.2 Preparation of PEO/alginate nanofibre membranes

Sodium alginate (SA) and PEO were separately dissolved in deionized water for 24 hours in order to ensure complete dissolution. The SA (3 wt%) and PEO (3 wt%) aqueous solutions were mixed at a 1:1 ratios and stirred for an additional 4 hours in order to ensure homogeneity. The alginate solution was aged in an environmental chamber (Binder GmBH) set at a temperature of 23 ± 2°C and a relative humidity of 60 ± 5% for 30 days. Aliquots of the alginate solution were removed at 5 day intervals and mixed with freshly prepared PEO solutions. The mixtures were stirred for 4 hours and then electrospun. Mixtures of freshly prepared alginate and PEO blend solutions were stored under the same conditions as the aged solutions. Aliquots were also removed at 5 day intervals and electrospun. The electrospinning solution flow rate was 0.8 mL hr^{-1}. A high voltage of 22 kV was applied to generate electric fields between the tip of the needle capillary and collector over a distance of 17 cm. The obtained bead-free nanofibres were further crosslinked using $CaCl_2$ solution at ambient conditions. The nanofibres were soaked in 80% ethanol for 5 min and rinsed with 2 wt% $CaCl_2$ solution in ethanol for 10 min. The nanofibres were incubated in an aqueous solution of $CaCl_2$ for an hour, and then immersed in deionized water for another hour. The $CaCl_2$ treated membranes were then rinsed with deionized water, followed by washing with absolute ethanol, and dried at room temperature. In subsequent sections of the paper these membranes are designated CaA.

3.2.3 Characterization

A Crison CM 35 conductivity meter and a Brookfield DV-II viscometer were used to measure the conductivity and viscosity of the SA and PEO/SA blend solutions.

The IR spectra of the electrospun nanofibres were obtained on a Perkin Elmer Spectrum 100 FTIR spectrometer equipped with an attenuated total reflection (ATR) accessory with a diamond/ZnSe crystal. The ATR-FTIR spectra were obtained at room temperature with the wavenumber ranging between 500 and 4000 cm^{-1}, using 16 scans and 4 cm^{-1} resolution.

The thermal stability of the nanofibre membranes was analysed with a Perkin Elmer TGA7 thermogravimetric analyzer. Samples with masses in the range of 10 to 20 mg were heated under a nitrogen flow of 20 mL min^{-1} from 30 to 600ºC at a heating rate of 10ºC min^{-1}, and the corresponding mass loss was recorded.

The morphologies of the electrospun nanofibres were determined by an FEI Quanta 200 scanning electron microscope (SEM). About 100 readings per sample were taken in order to determine the average fibre diameter. The specific surface area, as well as pore size and volume, were determined using the Brunauer-Emmett-Teller (BET) method.

3.2.4 Batch adsorption experiments

The copper (Cu) adsorption onto the electrospun alginate nanofibre membranes was studied under different contact times, concentrations, pH and temperatures. Tests solutions were prepared by dissolving $CuSO_4$ in deionized water. The electrospun alginate nanofibre membranes (~0.25 g) were placed in a 50 mL metal ion solutions of different concentrations ranging from 0 to 1000 mg L^{-1}. The concentrations of heavy metal ions in the adsorption medium were measured by using atomic absorption spectroscopy (Varian Spectra AAS 220Z). The amount of the adsorbed metal ions, Q_e (mg g^{-1}), was calculated by using Equation 1.

$$Q_e = \frac{(C_o - C_e)V}{m} \qquad (1)$$

where Q_e (mg g^{-1}) is the amount of metal adsorbed on the adsorbent at equilibrium, C_0 (mg L^{-1}) is the initial solution concentration, C_e (mg L^{-1}) is the final concentration of metalloid in the solution at equilibrium, m (g) is the mass of the adsorbent used and V (L) is the volume of the metalloid solution.

The removal percentage (%) of metal ion from aqueous solution at different initial concentrations was calculated using Equation 2.

$$R(\%) = \frac{C_0 - C_e}{C_0} \times 100 \qquad (2)$$

For the adsorption experiments, the electrospun alginate membrane (0.25 g) was placed in a stoppered conical flask (100 mL) kept in a continuously stirred silicon oil bath (150 rpm) at a fixed temperature (25, 40 or 60°C) for 3 hours.

The nanofibres were regenerated by washing with ethylenediaminetetraacetic acid (EDTA) and then rinsed with deionized water followed by drying in a vacuum oven at 60°C.

3.3 Results and discussion

3.3.1 Electrospun alginate nanofibre membranes

Although electrospinning has been proven to be a feasible and a simple technique to consistently produce long nanofibres from different polymers, its applicability to produce beadless nanofibres is determined by voltage, tip-to-collector distance, feeding rate, solution concentration and viscosity. Table 3.1 shows the properties of SA, PEO, a freshly prepared PEO/SA blend, and the blends aged under controlled environmental conditions. As expected, PEO, a non-ionic polymer, showed very low conductivity and a moderate viscosity when compared to pure alginate due to the absence of charged groups along the PEO chains. SA displayed both high conductivity and viscosity that can be ascribed to its inherent anionic polyelectrolytic character and the strong inter- and intramolecular forces [16]. Mixing of SA and PEO increased both the viscosity and conductivity by 4 and 22 folds, respectively. The solution viscosity of the aged PEO/SA blend decreased gradually with an increase in the number of storage days. This can be related to the aqueous hydrolysis of alginate which

causes the fractionation of the glycosidic bonds and results in a significant decrease in viscosity [17,18]. These glycosidic bonds serve as a strong intra- and intermolecular network between the alginate chains. The conductivity of the aged blend solutions slightly increased with storage time. This may be due to some dissociated ions from the alginate chains during storage which contributed to the overall conductivity of the solution.

Table 3.1 Properties of SA, PEO, and the freshly prepared and aged PEO/SA blends

Sample	Viscosity (cP)	Conductivity ($mScm^{-1}$)	Diameter (nm)	Morphology
PEO	1192 ± 50	0.10 ± 0.00	313 ± 86	Bead-free
SA	12382 ± 167	5.60 ± 0.01	-	Droplets
PEO/SA day 0	4905 ± 90	2.28 ± 0.01	-	Droplets
PEO/SA day 5	4525 ± 3	2.75 ± 0.03	83 ± 26	Beaded
PEO/SA day 10	3517 ± 0	2.77 ± 0.03	114 ± 49	Beaded
PEO/SA day 15	2516 ± 23	2.74 ± 0.04	112 ± 47	Bead-free
PEO/SA day 20	2111 ± 8	2.80 ± 0.04	132 ± 55	Bead-free
PEO/SA day 25	1117 ± 0	2.80 ± 0.08	171 ± 69	Beaded
PEO/SA day 30	1088 ± 8	3.10 ± 0.06	178 ± 75	Beaded

We also found out that the viscosity of the solutions played a major role in controlling the morphology of the resulting electrospun nanofibres. A freshly prepared blend of alginate and PEO (stirred for 4 hours followed by spinning) yielded droplets on the collector (Table 3.1). However, when the PEO/alginate blend solutions were stored for a certain period under controlled environmental conditions, the morphology of the fibres improved, especially after 10 days (Figure 3.1, Table 3.1). It is clear from Figure 3.1 that the electrospinnability was improved from an electrospraying phenomenon that produced droplets, to an electrospinning process that yielded beaded and bead-free nanofibres for the aged samples. Although there was no particular trend in the morphology of the stored electrospun nanofibres, bead-free nanofibres were obtained from day 15 to day 20 (Figures 3.1(c) and 3.1(d)), whereafter beaded nanofibres were obtained after longer ageing periods (Figures 3.1(e) and 3.1(f)). Bhattarai and Zhang [18] reported that 15 days was the optimum storage time (at ambient conditions) for a PEO/alginate blend in order to produce bead-free nanofibres. Although they related this phenomenon to a significant reduction in the viscosity of the solutions, which is

also reflected in Table 3.1, it seems as if there are several factors that could have influenced the solution properties during their storage. One possibility is the interaction between the alginate and PEO during their storage. It is possible that the longer the PEO/SA blends are aged, the bigger the chances for the formation of a large number of carboxylate groups due to the dissociation of sodium ions from the alginate, as justified by the slight increase in conductivity (Table 3.1). The resulting carboxylate and sodium ions interacted with the ether group of PEO, resulting in a better interaction between these components; however, this will depend on the number of the carboxylate and sodium ions in the system. In order to confirm the above-mentioned observations, a solution of alginate alone (0.025 wt%) was kept at room temperature without stirring, and a brown sediment was observed after 15 days which may have been due to the dissociated sodium ions from the alginate. In such cases, the sodium ions are normally responsible for the dissolution of alginate in water. After 30 days, the solution was saturated and no reaction took place to further dissolve the remainder of the sediment. Similarly, when the 50/50 w/w solution of SA and PEO (0.025 wt%) was kept at room temperature, there was no segregation in the solution for 30 days. This may be because of the interactions between PEO, sodium ions and carboxylate groups from the alginate, *via* the ether oxygen. This enhanced the interaction between the PEO and SA, which in turn improved the spinnability of the aged blend, independent of storage period and regardless of a decrease in the solution viscosity.

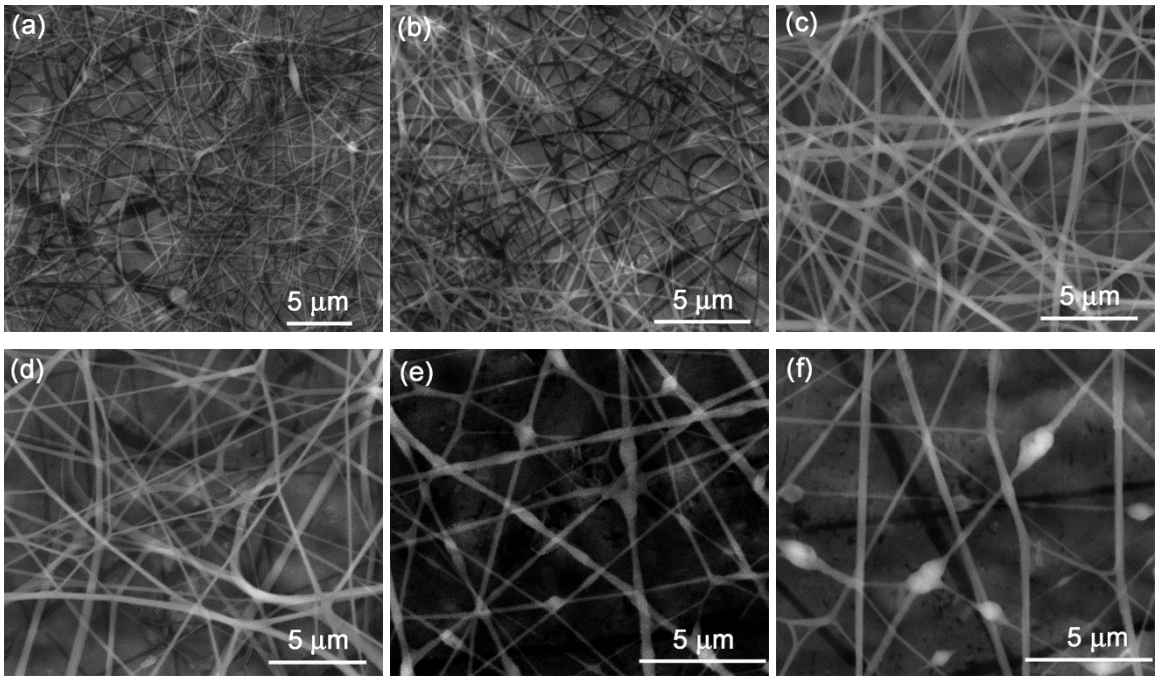

Figure 3.1 SEM micrographs of the electrospun 50/50 w/w PEO/SA blend electrospun aged for (a) 5, (b) 10, (c) 15, (d) 20, (e) 25, and (f) 30 days

This was proven by studying the influence of alginate degradation in the resulting nanofibres. An aliquot of aged alginate was removed from the alginate solution and mixed with freshly prepared PEO solution followed by electrospinning. The nanofibres of the blends, PEO and the alginate extracted after different periods of time, were successfully fabricated as shown in Figure 3.2. Beaded and wet nanofibres were obtained from 5 to 15 days (Figures 3.2(a) to 3.2(c)). After 15 days, only droplets were collected (Figure 3.2(d)). This is probably due to a drastic decrease in the viscosity of the alginate solution and a lack of strong interaction between the PEO and SA.

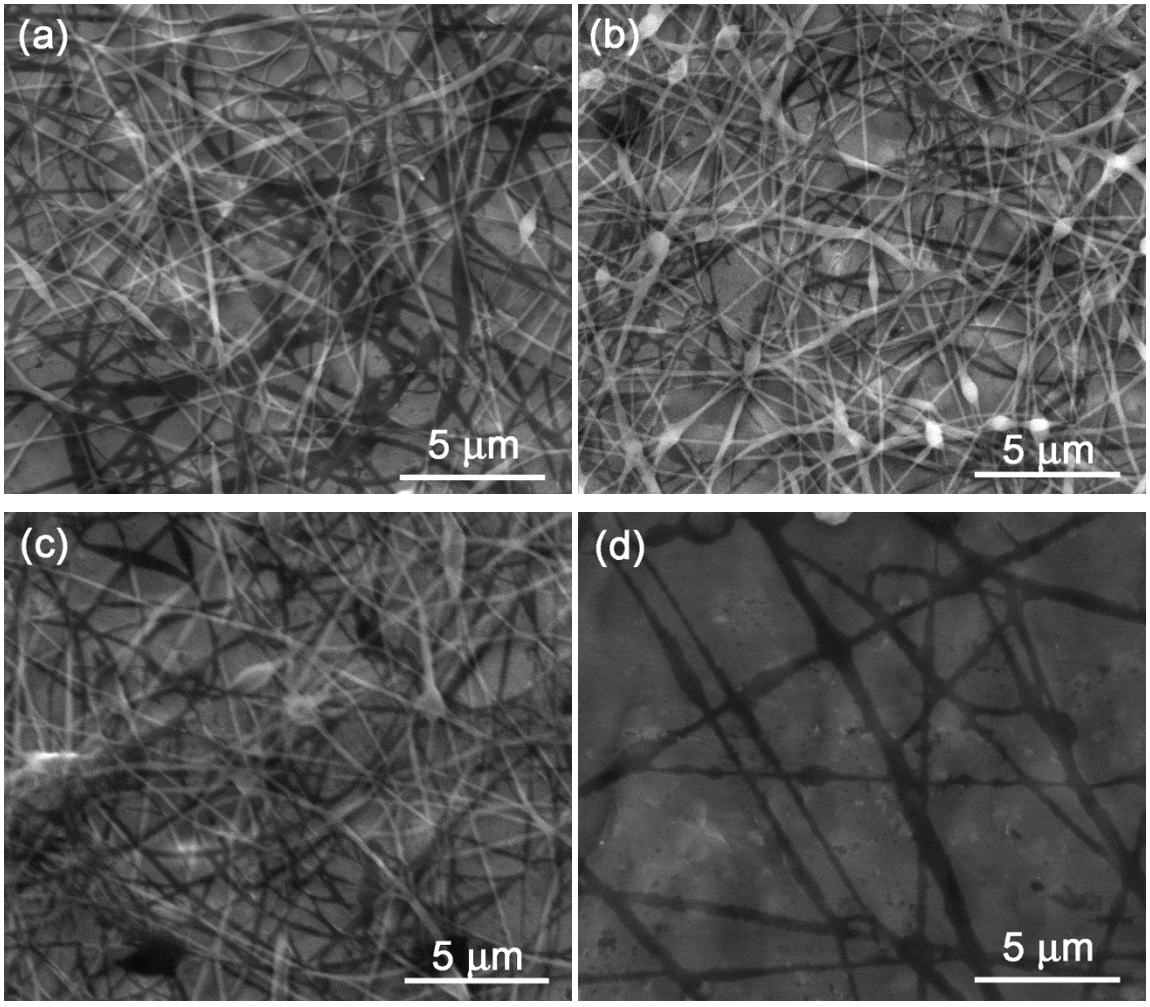

Figure 3.2 SEM micrographs of PEO/SA 50/50 w/w from SA aliquots extracted after (a) 5, (b) 10, (c) 15 and (d) 20 days

Figure 3.3(a) shows the FTIR spectra of electrospun PEO, 50/50 w/w PEO/SA and $CaCl_2$-treated nanofibres (CaA). The characteristic peaks of PEO were observed at 2881 cm^{-1} (CH stretching), 1456 cm^{-1} (CH_2 wagging), 1100 and 839 cm^{-1} (C-O-C stretching and bending), and 960 cm^{-1} corresponding to CH_2 rocking and twisting [19]. The addition of alginate to

PEO showed new peaks corresponding to alginate at 3358 cm^{-1} (OH stretching), 1602 cm^{-1} (COO^- asymmetric stretching), 1410 cm^{-1} (COO^- symmetric stretching) [18,20]. The OH and COO^- stretching peaks shifted from 3358 to 3256 cm^{-1} and 1602 to 1596 cm^{-1}, respectively. This is probably due to the interaction that occurred between the carboxyl and hydroxyl groups of alginate and the ether group of PEO through hydrogen bonding. After washing with aqueous calcium solution, all the peaks, associated with PEO, disappeared.

The TGA curves of PEO, PEO/SA blend and calcium alginate (CaA) are shown in Figure 3.3(b). PEO shows a single degradation step around 400°C, while the blend shows three degradation steps. The first mass loss below 100°C can be related to the evaporation of water. The second step can be associated with thermal degradation of alginate, while the third corresponds to the thermal degradation of PEO. After washing the blend and crosslinking with calcium chloride (CaA), the degradation step corresponding to PEO was not visible (Figure 3.3(b)). This is in agreement with the FTIR results which confirmed the complete removal of PEO from the blend.

The average pore size of in the fibres was determined as 215 nm, the surface area as 18.03 m^2 g^{-1}, and the average pore volume as 0.96 cm^3 g^{-1}, which indicate that the electrospun alginate membranes were macro-porous.

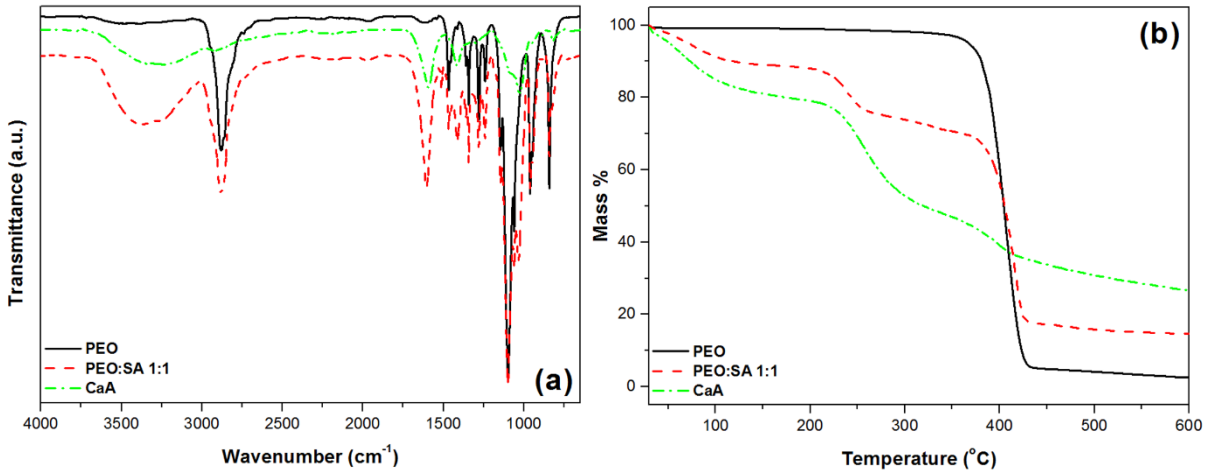

Figure 3.3 (a) FTIR spectra and (b) TGA curves for electrospun PEO, the blend and the CaA nanofibres

3.3.2 Biosorption studies

3.3.2.1 Effect of pH

In this study, Cu(II) was selected as a model heavy metal to evaluate the adsorption capacity of the electrospun alginate membranes (CaA). One of the most valuable factors in metal adsorption is the solution pH since it influences the surface charge of the adsorbent, as well as the degree of ionization [6]. For the effect of pH on the adsorption capacity of CaA, 0.05 g of membrane was immersed in an aqueous solution of Cu for 3 hours at 25°C. The pH values of the metal were kept below 7 in order to avoid the precipitation of the metal ions [21,22], and 0.1M NaOH and 0.1M HCl were used to adjust pH values. The adsorption of the electrospun alginate membrane was found to depend on the pH values as shown in Figure 3.4. At a pH value of 4 (when compared to a pH of 2) the Cu(II) uptake increased from 56 to 79% and from 49 to 64% for 100 and 600 mg L^{-1} concentrations, respectively. At low pH values, the binding sites are limited due to the competition between the metal ion (M^{2+}) and the high H^{+} ions concentration. As the pH increases, the H^{+} ions are released from the adsorbent which increases the number of the negatively charged active sites available to bind to the metal ion, hence the increase in adsorption at a pH value of 4. This can be associated with the ionization of carboxyl (–COOH) groups along the alginate chains [3]. The ionised carboxyl groups therefore improve the sorption capacity of the alginate. The pH of 4 displayed the maximum removal percentage of Cu ions from the Cu aqueous medium, regardless of the solution concentration (Figure 3.4). The difference between the metal uptake at low and high concentration maybe attributed to the availability of more Cu ions at higher concentrations, which compete for the available binding sites on the adsorbent. In addition, the adjustment of the solution pH using NaOH may have impeded the uptake of Cu(II). Sodium hydroxide has a tendency to react with copper ions to form a precipitate; in this case it is possible that the NaOH would rather react with the Cu ions to form $Cu(OH)_2$ instead of the ions being adsorbed by the alginate, especially at higher pH (>4) and higher Cu(II) concentrations (>600 mg L^{-1}) [21]. Consequently, an aqueous solution with a pH of 4 was used as the optimum medium throughout the study.

3.3.2.2 The effect of contact time

In order to study the effect of equilibration time for the electrospun alginate nanofibrous membranes, a solution with a concentration of 100 mg L^{-1} and a pH of 4, was utilized. For the first 30 minutes, the adsorption was approximately 37% and it gradually increased with increase in time until the 90^{th} minute (Figure 3.5), and then levelled off after 120 minutes. Similar behaviour was reported by Aliabadi *et al.* [10] for the removal of different metal ions using electrospun PEO/chitosan nanofibres. They found that the equilibration time was 120 minutes. In contrast, Pandey *et al*. [6] reported that the equilibration time for calcium alginate beads was 7 hours. This could be related to the size of the beads when compared to the electrospun alginate nanofibres that have large surface areas and high pore volumes. Therefore, 180 minutes (3 hours) was used through-out the study to ensure maximum adsorption.

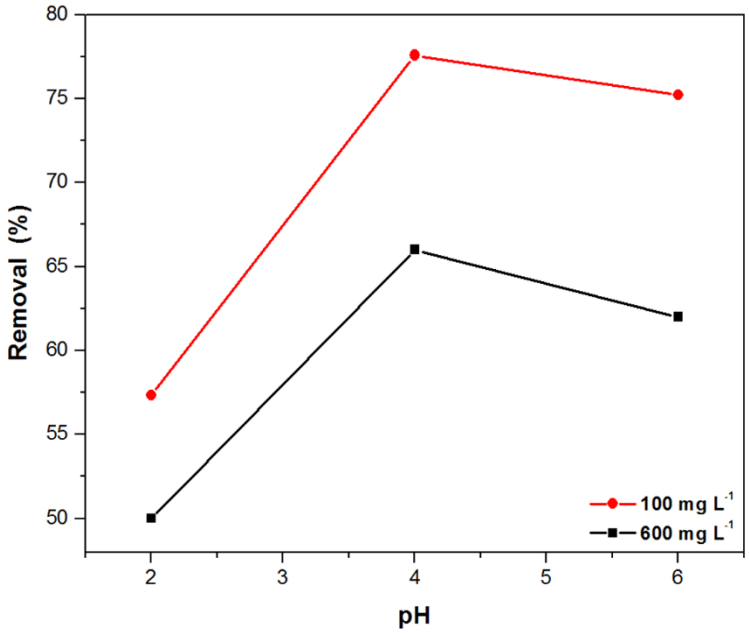

Figure 3.4 Effect of pH on the adsorption capacity of the electrospun alginate membrane

3.3.2.3 Adsorption isotherms

The Langmuir and Freundlich isotherms were used to predict the isotherm which best describes the mechanism occurring during the adsorption process. The Langmuir isotherm is often used to describe the adsorption of an adsorbate onto a homogeneous adsorbent, in which an adsorptive site can only be occupied once [23]. It is described by Equation 3.

$$Q_e = \frac{Q_0\ b\ C_e}{1+b\ C_e} \qquad (3)$$

where Q_e (mg g^{-1}) is the maximum amount of Cu adsorbed at equilibrium, Q_0 (mg g^{-1}) is related to the Cu monolayer capacity of the adsorbent, b (Lmg^{-1}) represents the energy adsorption, and C_e (mg g^{-1}) is the equilibrium Cu concentration. The linearized Langmuir method is mathematically expressed in Equation 4.

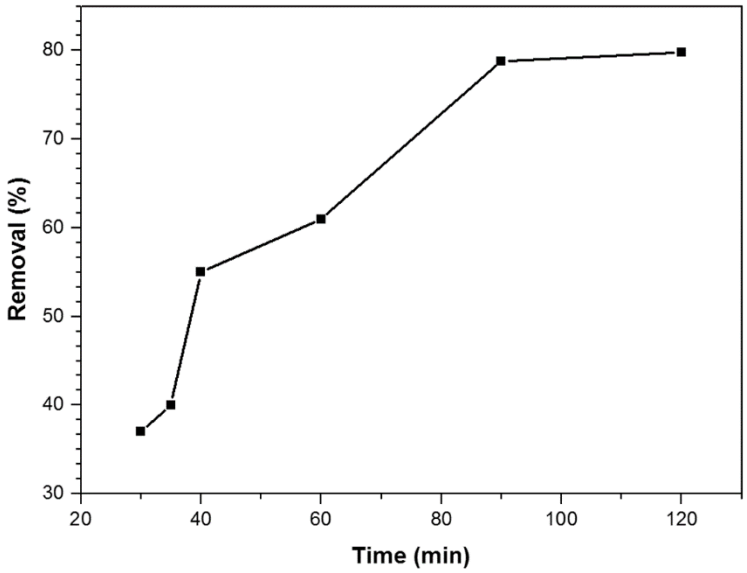

Figure 3.5 The effect of contact time on the adsorption of Cu(II) onto alginate nanofibrous membranes

$$\frac{C_e}{Q_e} = \frac{C_e}{Q_0} + \frac{1}{Q_0 b} \qquad (4)$$

The performance of the adsorption behaviour can be predicted by the R_L value, which is calculated from the following Equation 5 [24]:

$$R_L = \frac{1}{1+(b \times C_0)} \qquad (5)$$

where C_0 is the initial concentration and b is the Langmuir isotherm constant. If $R_L < 1$, it expresses the fact that the adsorption is favourable under the experimental conditions, $R_L = 0$ stipulates that the adsorption is irreversible, $R_L = 1$ indicates that the adsorption is linear and $R_L > 1$ shows that the adsorption process is unfavourable. In this study, the results indicate that

the R_L values were less than zero, indicating a favourable adsorption (Table 3.2), confirming that the equilibrium isotherms can be described by the Langmuir method. The adsorption of Cu onto the electrospun alginate membrane at 25, 40, and 60°C fitted the Langmuir isotherm quite well (Figure 3.6). All the plots of *Ce/Qe* versus *Ce* gave linear graphs for all the experimental conditions used in this study. The correlation coefficient (R^2) and Langmuir constants (Q_0 and *b*) were determined from the graphs and are listed in Table 2. The *b* value is related to the affinity of the adsorbate for the adsorbent [18]. At all the three temperatures, the *b* value was too small, which indicates that the Cu(II) had a weak affinity for electrospun alginate membranes. This may be due to the presence of the Ca(II), used to crosslink the electrospun alginate nanofibres, occupying most of the available binding sites. In addition, NaOH was used to adjust the pH during the solution preparation, leading to some reactions between Na and Cu and thereby impeding the adsorption of Cu(II). The maximum monolayer adsorption capacity (Q_0) value decreased with an increase in temperature. This could be due to the swelling of the alginate nanofibres which caused a blockage of the inner pores of the membranes and impeded the diffusion of the metal ions.

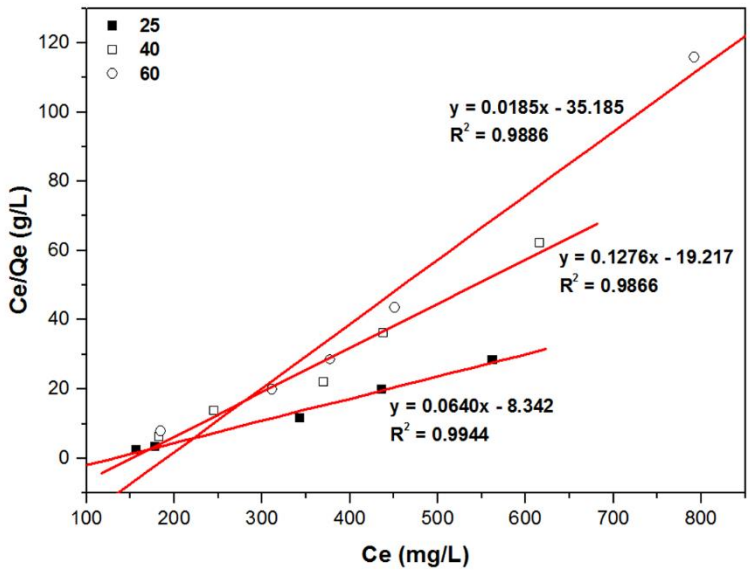

Figure 3.6 Linearized Langmuir isotherms for the adsorption of Cu ions onto electrospun alginate membranes

The Freundlich model is usually used to describe the adsorption of the adsorbate onto a heterogeneous surface of an adsorbent [23]. The Freundlich adsorption isotherm is given in Equation 5.

$$Q_e = K_f (C_e)^{\frac{1}{n}} \qquad (5)$$

where K_F ((mg g^{-1}) (mg L^{-1})) is a Freundlich constant for a particular adsorption isotherm and *n* is the dimensionless Freundlich constant related to the adsorption intensity. The linearized Freundlich model was used in this study to fit the adsorption data. Mathematically, the linearized Freundlich is expressed in Equation 6.

$$\ln Q_e = \ln K_F + \frac{1}{n} lnC_e \qquad (6)$$

In the case of Freundlich model, all the *R* coefficient values (R<0.92) were lower than the those displayed by the Langmuir model (R<0.98) (Figure 3.7, Table 2.2). This indicates that the Langmuir model better fitted the equilibrium data of Cu ions than the Freundlich model. The suitability of the Langmuir isotherm when compared to the Freundlich isotherm implies that monolayer adsorption was prevalent under the experimental conditions.

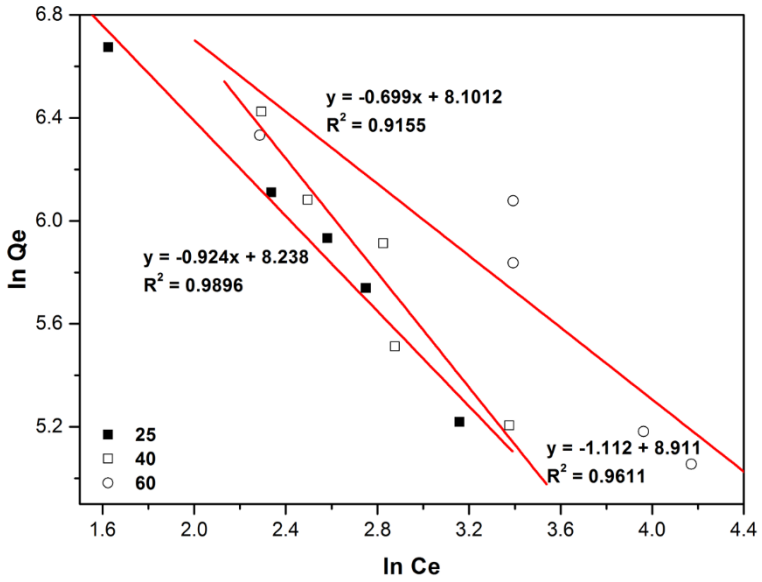

Figure 3.7 Linearized Freundlich isotherms for the adsorption of Cu ions onto electrospun alginate membranes

Table 3.2 Kinetic parameters of Cu adsorption onto electrospun alginate membranes

	Langmuir				Freundlich		
Temp (°C)	**Q_0 (mg g^{-1})**	**b (L mg^{-1})**	**R_L**	**R^2**	**K_F (mg g^{-1}) (mg L^{-1})**	**N**	**R^2**
25	15.6	-0.0076	-0.152to -1.92	0.994	3780	1.082	0.989
40	7.83	-0.0066	-0.178 to -3.125	0.987	7412	0.899	0.961
60	5.41	-0.0052	-0.238 to -25	0.989	3298	1.431	0.915

Table 3.3 shows the adsorption data of Cu(II) ions on various adsorbents. Based on these findings, the electrospun alginate membrane (CaA) showed a metal adsorption capacity comparable to or higher than some other types of adsorbents without any further functionalization or optimization, and therefore the CaA electrospun nanofibres have the potential to be used for wastewater treatment.

Table 3.3 Comparison on the sorption capacity of some adsorbents for Cu(II)

Adsorbent	**Q_0 (mg g^{-1})**
Calcium alginate (beads)[25]	15.80
Woolkeratose/silk fibroin nanofibres[9]	2.88×10^{-3}
Grafted thiol cellulose acetate nanofibres[11]	7.47
Chitosan flakes[26]	20.92
Humic acid-activated carbon[20]	5.98
Activated carbon[27]	38.00
CaA [in this study]	15.60

3.3.2.4 Regeneration of electrospun alginate (CaA) membranes

The regeneration of the adsorbent is of significance for the long-term use, especially for commercial applications. We regenerated the electrospun alginate nanofibres five times by using a 0.1M of EDTA. Adsorption/desorption cycles were performed using a Cu(II) solution with a concentration of 100 mg L^{-1}, a pH of 4 and a temperature of 25°C. There was a slight decrease in the adsorption capacity from the first to the fifth cycle (Figure 3.8). This could be related to the loss of the adsorbent shape/structure during washing and drying, which caused a deformation in the morphology and thereby reducing the porosity of the electrospun alginate membranes (Figure 3.9). Washing with EDTA caused the fibres to swell and fuse with each other, destroying the pores in the membrane (compare Figures 3.9a and 3.9b). This reduced the porosity of the membrane by blocking the interior pores, which resulted in a gradual decrease in the adsorption of the membrane, because of an increase in the number of desorptions. Electrospun alginate nanofibrous membranes from seaweeds can be reused without a significant loss in adsorption capacity.

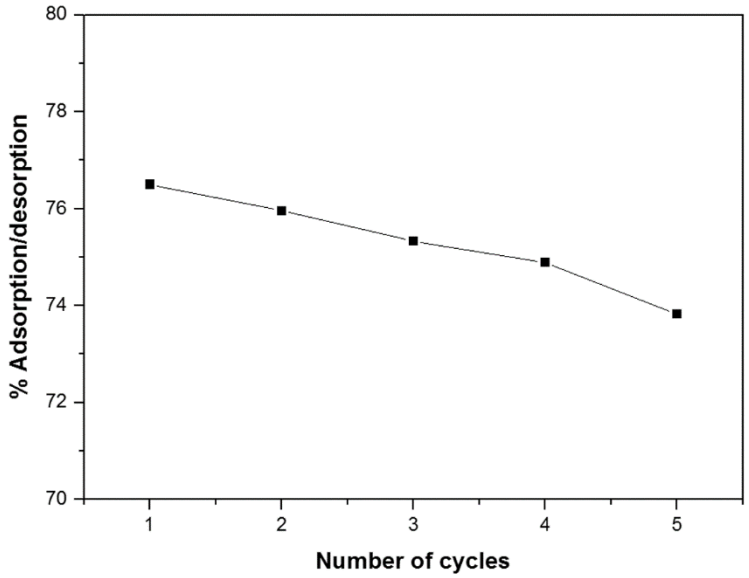

Figure 3.8 Percentage adsorption of Cu(II) by the electrospun nanofibres after regeneration for five desorption/adsorption cycles

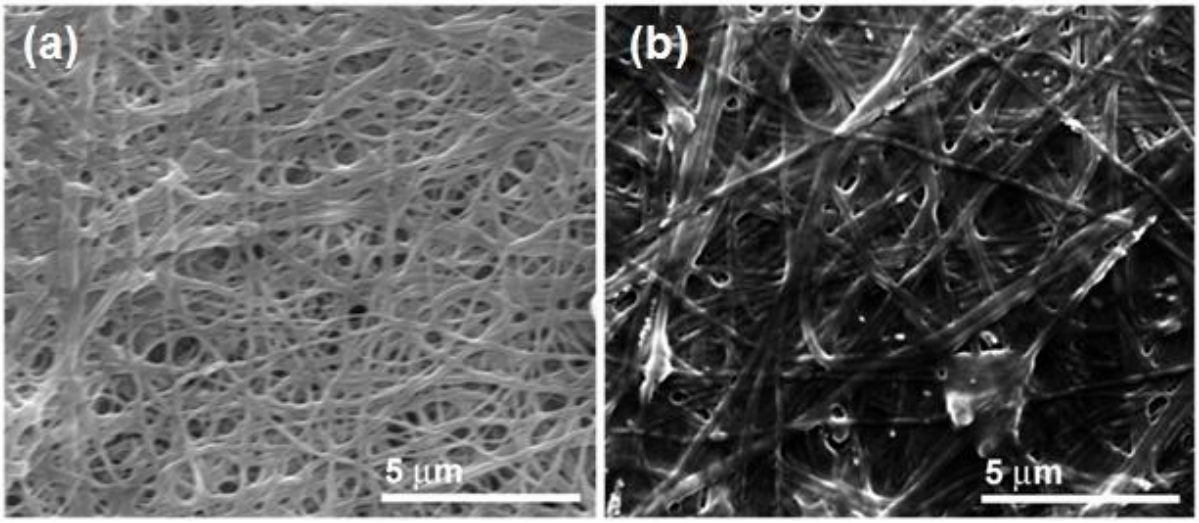

Figure 3.9 Micrographs of electrospun alginate nanofibres (CaA)(a) before adsorption and (b) after the first adsorption.

3.4 Conclusions

PEO/SA blends were successfully electrospun after their storage under controlled conditions. The storage conditions were found to play a significant role in the degradation of the alginate, which in turn influenced the electrospinnability of the nanofibre blends. Similar to previous reports, this study proved that environmental conditions are among the critical parameters that influence the electrospinning process. In this case, the optimal number of storage days ranged

between 10 and 20, and a reduction in viscosity and the formation of a large number of carboxylate groups contributed in facilitating the electrospinning process of the alginate nanofibre blends. It was further found that not only viscosity played a major role in the morphology of the resulting alginate nanofibres, but also the interactions between PEO and the alginate which further improved overtime.

The adsorption studies showed that the electrospun calcium alginate nanofibrous membranes, with large surface areas and the presence of carboxyl and hydroxyl groups, were efficient in the removal of copper ions from aqueous solutions. The membrane showed a maximum metal adsorption capacity of 15.6 mg g^{-1} at 25°C and a pH of 4, and it maintained a reasonable metal adsorption capacity over 5 recycling intervals. Therefore, the electrospun alginate nanofibrous membranes proved to be a suitable material for potential application in wastewater treatment.

3.5 References

[1] O.E.A. Salam, N.A. Reiad, M.M. ElShafei, A study of the removal characteristics of heavy metals from wastewater by low-cost adsorbents, Journal of Advanced Research, 2 (2011) 297-303.

[2] A.A. Taha, Y.-N. Wu, H. Wang, F. Li, Preparation and application of functionalized cellulose acetate/silica composite nanofibrous membrane via electrospinning for Cr (VI) ion removal from aqueous solution, Journal of Environmental Management, 112 (2012) 10-16.

[3] S.K. Papageorgiou, F.K. Katsaros, E.P. Kouvelos, J.W. Nolan, H. Le Deit, N.K. Kanellopoulos, Heavy metal sorption by calcium alginate beads from *Laminaria digitata*, Journal of Hazardous Materials, 137 (2006) 1765-1772.

[4] T.C. Mokhena, V. Jacobs, A.S. Luyt, A review on electrospun bio-based polymers for water treatment, eXPRESSPolymer Letters, 9 (2015) 839-880.

[5] S. Kamsonlian, S. Suresh, C. Majumder, S. Chand, Characterization of banana and orange peels: Biosorption mechanism, International Journal of Science Technology & Management, 2 (2011) 1-7.

[6] A. Pandey, D. Bera, A. Shukla, L. Ray, Studies on Cr (VI), Pb (II) and Cu(II) adsorption-desorption using calcium alginate as biopolymer, Chemical Speciation & Bioavailability, 19 (2007) 17-24.

[7] S. Haider, S.-Y. Park, Preparation of the electrospun chitosan nanofibers and their applications to the adsorption of Cu(II) and Pb(II) ions from an aqueous solution, Journal of Membrane Science, 328 (2009) 90-96.

[8] K. Saeed, S. Haider, T.-J. Oh, S.-Y. Park, Preparation of amidoxime-modified polyacrylonitrile (PAN-oxime) nanofibers and their applications to metal ions adsorption, Journal of Membrane Science, 322 (2008) 400-405.

[9] C. Ki, E. Gang, I. Um, Y. Park, Nanofibrous membrane of wool keratose/silk fibroin blend for heavy metal ion adsorption, Journal of Membrane Science, 302 (2007) 20-26.

[10] M. Aliabadi, M. Irani, J. Ismaeili, H. Piri, M.J. Parnian, Electrospun nanofiber membrane of PEO/chitosan for the adsorption of nickel, cadmium, lead and copper ions from aqueous solution, Chemical Engineering Journal, 220 (2013) 237-243.

[11] T. Xiang, Z. Zhang, H. Liu, Z. Yin, L. Li, X. Liu, Characterization of cellulose-based electrospun nanofiber membrane and its adsorptive behaviours using Cu(II), Cd(II), Pb(II) as models, Science China Chemistry, 56 (2013) 567-575.

[12] A. Patanaik, V. Jacobs, R. Anandjiwala, Performance evaluation of electrospun nanofibrous membrane. Journal of Membrane Science 352 (2010) 136-142.

[13] S. Haider, S.-Y. Park, Preparation of the electrospun chitosan nanofibers and their applications to the adsorption of Cu(II) and Pb(II) ions from an aqueous solution, Journal of Membrane Science, 328 (2009) 90-96.

[14] S. Babel, T.A. Kurniawan, Low-cost adsorbents for heavy metals uptake from contaminated water: Areview, Journal of Hazardous Materials, 97 (2003) 219-243.

[15] H. Zhu, Y. Fu, R. Jiang, J. Yao, L. Xiao, G. Zeng, Optimization of copper (II) adsorption onto novel magnetic calcium alginate/maghemite hydrogel beads using response surface methodology, Industrial & Engineering Chemistry Research, 53 (2014) 4059-4066.

[16] G. Ozdemir, N. Ceyhan, E. Manav, Utilization in alginate beads for Cu(II) and Ni(II) adsorption of an exopolysaccharide produced by *Chryseomonas luteola* TEM05, World Journal of Microbiology and Biotechnology, 21 (2005) 163-167.

[17] M.S. Islam, M. Ashaduzzaman, S.M. Masum, J.H. Yeum, Mechanical and electrical properties: Electrospun alginate/carbon nanotube composite nanofiber, Dhaka University Journal of Science, 60 (2012) 125-128.

[18] N. Bhattarai, Z. Li, D. Edmondson, M. Zhang, Alginate-based nanofibrous scaffolds: Structural, mechanical, and biological properties, Advanced Materials, 18 (2006) 1463-1467.

[19] I. Pucić, T. Jurkin, FTIR assessment of poly(ethylene oxide) irradiated in solid state, melt and aqeuous solution, Radiation Physics and Chemistry, 81 (2012) 1426-1429.

[20] N. Bhattarai, M. Zhang, Controlled synthesis and structural stability of alginate-based nanofibers, Nanotechnology, 18 (2007) 455601.

[21] H. Liu, S. Feng, N. Zhang, X. Du, Y. Liu, Removal of Cu(II) ions from aqueous solution by activated carbon impregnated with humic acid, Frontiers of Environmental Science & Engineering, 8 (2014) 329-336.

[22] M. Adeli, Y. Yamini, M. Faraji, Removal of copper, nickel and zinc by sodium dodecyl sulphate coated magnetite nanoparticles from water and wastewater samples, Arabian Journal of Chemistry, In press (2012) http://dx.doi.org/10.1016/j.arabjc.2012.10.012.

[23] X.-J. Hu, J.-S. Wang, Y.-G. Liu, X. Li, G.-M. Zeng, Z.-L. Bao, X.-X. Zeng, A.-W. Chen, F. Long, Adsorption of chromium (VI) by ethylenediamine-modified cross-linked magnetic chitosan resin: Isotherms, kinetics and thermodynamics, Journal of Hazardous Materials, 185 (2011) 306-314.

[24] Z. Aly, A. Graulet, N. Scales, T. Hanley, Removal of aluminium from aqueous solutions using PAN-based adsorbents: Characterisation, kinetics, equilibrium and thermodynamic studies, Environmental Science and Pollution Research, 21 (2014) 3972-3986.

[25] M.B. Desta, Batch sorption experiments: Langmuir and Freundlich isotherm studies for the adsorption of textile metal ions onto teff straw (*eragrostis tef*) agricultural waste, Journal of Thermodynamics, 2013 (2013)375830.

[26] C. Huang, Y.-C. Chung, M.-R. Liou, Adsorption of Cu(II) and Ni(II) by pelletized biopolymer, Journal of Hazardous Materials, 45 (1996) 265-277.

[27] R. Bassi, S.O. Prasher, B. Simpson, Removal of selected metal ions from aqueous solutions using chitosan flakes, Separation Science and Technology, 35 (2000) 547-560.

[28] L. Monser, N. Adhoum, Modified activated carbon for the removal of copper, zinc, chromium and cyanide from wastewater, Separation and Purification Technology, 26 (2002) 137-146.

Chapter 4

Nanofibrous alginate membrane reinforced with cellulose nanowhiskers for water purification

This chapter has been submitted for publication as:
T.C. Mokhena, N.V Jacobs, A.S. Luyt, Nanofibrous alginate membrane reinforced with cellulose nanowhiskers for water purification, Journal of Membrane Science.

Abstract

The aim of this study was to develop a filtration membrane based on two-layered nanoscale alginate nanofibres reinforced with maize cellulose nanowhiskers (diameter between 3 and 12 nm). Reinforcing of the membrane with cellulose nanowhiskers improved the mechanical properties of the membrane. The membrane was capable of completely removing water contaminants (10-100 nm nanoparticles) by size exclusion and the oil/water retention was higher than 99%. The rejection of chromium was found to increase with an increase in the feed solution pH. The rejection percentage for chromium (Cr(VI)) at a pH of 11 was found to be 80%, which shows that the membrane can be applied for short-term waste-water treatment and/or as a domestic water purification material.

Keywords: Electrospun Alginate nanofibres; Maize cellulose nanowhiskers; Oil/water retention; Chromium; Water purification

4.1 Introduction

Water scarcity spurred efforts to develop advanced technology to purify water at relatively low cost and energy [1-4]. More than one billion people do not have access to portable water and sanitation, and another more than a billion live in water-scarce areas [1,5]. The rapid growth of the global population and the socio-economic developments add to this burden, which demands effective and cost-efficient water purification methods [1,5,6]. Pressure driven membrane filtration processes such as microfiltration (MF), ultrafiltration (UF), nanofiltration (NF) and reverse osmosis (RO) are the most economic and energy efficient

water purification methods [5,7]. Most of the conventional polymeric filtration membranes are usually manufactured *via* phase immersion processes [5,8,9]. These membranes have some limitations such as low flux and high fouling, due to their asymmetric structure [8-10]. It is recognized that nanofibrous membranes prepared by electrospinning can overcome some of these limitations [8,10].

Electrospinning is capable of generating diverse nanofibrous materials from various polymers [11-13]. The operator has control over the morphology and structure of the electrospun nanofibres by varying the processing variables [1,14]. The ensuing fibres have diameters ranging from a few micrometers to a few nanometers with unique features such as large surface-to-area ratio (20-120 m^2 g^{-1} depending on the fibre diameter), interconnectivity and high porosity (>80) [1,10]. These unique features enticed researchers to explore the utilization of electrospun nanofibrous in various filtration applications [10,14-17]. Some contaminants (such as metal ions) are, however, too small to be filtered by size exclusion. Therefore, additional mechanisms to remove such contaminants are required to enhance water purification without hampering the membrane productivity [18]. This can be achieved by using different materials with unique properties (functional groups, stability and malleability) to remove various pollutants from waste-water streams [18-20]. Cellulose is such a material due to the presence of hydroxyl groups on its surface, which can further be functionalized to enhance its performance.

Cellulose is the most studied natural polymer because of its abundant availability and environmental benign. Recently, there has been a growing interest to apply cellulose nanowhiskers as barrier layer in thin film composite membranes based on electrospun nanofibrous membranes [4,8,21-23]. It has been applied as a selective layer for various filtration applications such as ultrafiltration (UF) [22,24], and microfiltration (MF) [4,23]. In these studies high flux and retention were achieved. Cao *et al*. [21] produced a robust electrospun polyacrylonitrile nanofibrous membrane coated with jute nanowhiskers, which displayed superior mechanical properties, a high filtration efficiency of 7-40 nm particles, and oil/water retention of 99.5%. Ma *et al*. [22] produced a three-tier membrane with cellulose nanowhiskers as barrier layer. The membrane displayed high flux (18 times higher than a commercial ultrafiltration (PAN10) membrane) and high oil/water retention (>99.6%).
Although these membranes used cellulose nanofibres as barrier layer, most of the second (middle) layers are manufactured from synthetic polymers. It is recognized that the end of life of the membrane is one of the most important aspects that has to be considered, especially

when a new membrane is produced. In reality, all membranes are prone to clogging over time, which spurs interest for the production of membranes from natural based in order to address environmental concerns regarding their disposal. Natural polymers are abundantly available, renewable and environmentally benign, which is very important from environmental and economic viewpoints. The main aim of this study was to produce a filtration membrane from natural polymers. Maize stalk cellulose nanowhiskers were used as a barrier layer and electrospun alginate as substrate. The electrospinnability of alginate was facilitated by using polyethylene oxide (PEO) as a copolymer, followed by washing with aqueous calcium solution for crosslinking. Through the use of these inherently hydrophilic polymers, the membrane should be less susceptible to fouling, which should increase the flux and selectivity, producing the ideal membrane for water purification.

4.2 Materials and methods

4.2.1 Preparation of nanofibrous membrane

PEO (M_w = 1000 kDa) and sodium alginate (M_w = 100 kDa) were purchased from Sigma Aldrich, South Africa. These chemicals were used without further purification and the electrospinning process was conducted at room temperature. 3 wt% each of PEO and alginate were dissolved separately in deionized water and mixed at different volume ratios (80/20, 50/50, 40/60, 20/80 and 10/90). The mixtures were stirred for 4 hours for homogeneity and electrospun after being stored in a controlled environmental chamber (Binder GmBH) set at 23 ± 2°C for 10 days. The electrospinning setup consisted of a high voltage supply (0-30 kV), controllable pump syringe, and grounded detachable flat metal screen adjustable to a desired height and inclination. A high voltage supply was used to generate a voltage of 17 kV, the distance was maintained at 17 cm, and the feeding rate was set at 0.8 ml hr^{-1}.

4.2.2 Preparation of nanofibrous composite membrane

The electrospun nanofibrous membrane from the polyethylene oxide (PEO) and sodium alginate (SA) blend was washed using a $CaCl_2$ solution in order to remove PEO. The membrane was soaked in 80% ethanol for 5 min and rinsed with 2 wt% of aqueous $CaCl_2$ solution in 80% ethanol. The membrane was then incubated in $CaCl_2$ solution for an hour, and then immersed in deionized water for another hour. The $CaCl_2$ treated membrane was rinsed

with deionized water followed by repeated washes with absolute ethanol, and dried at room temperature (this membrane is designated CaA throughout this paper). The nanofibrous composite membrane was prepared by coating extracted maize stalk nanowhiskers (CNs) onto the $CaCl_2$ treated electrospun alginate nanofibres (this membrane is designated CaA-CNs throughout this paper). The maize nanowhiskers were extracted *via* sulphuric acid hydrolysis according to [25,26]. The maize stalks were powdered with a Hamermeul mill and dried in a vacuum oven at 60°C for 24 hours. The powder was then treated with 1.5% NaOH, 1.5% $NaClO_2$, and 1.5% KOH, respectively. Each treatment was repeated four times with repeated washes by using deionized water until the pH was neutral. The fibres were then dried and ground to a finer powder with a Fritsch Pulverisette. Acid hydrolysis was carried out using 50% sulphuric acid at 40°C for 30 min under mechanical stirring. The acid/pulp ratio was kept at 20:1 (ml g^{-1}). The hydrolysis process was terminated with the addition of ice cubes and washing by successive centrifugations at 10°C and 8000 rpm for 10 minutes, followed by dialysis with deionized water for 3 days (until pH was neutral). A complete dispersion of the cellulose whiskers was obtained by sonication for 1 min. The dispersed suspension was filtered through a No.1 fritted glass filter in order to remove any residual aggregates and stored at 4°C after the addition of few drops of chloroform in order to avoid fungal growth. The cellulose nanowhiskers (0.1 g) suspension was then coated over the alginate nanofibres and dried in a vacuum oven at 40°C, as schematically shown in Figure 4.1.

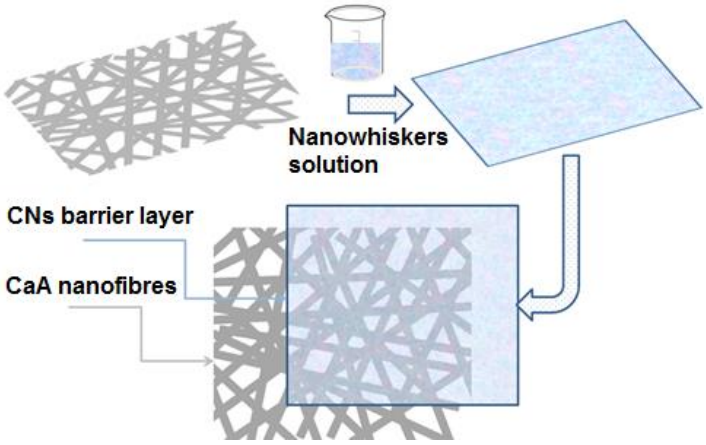

Figure 4.1 Preparation process of the CaA-CNs composite membrane

4.2.3 Characterization

The viscosity and conductivity of the electrospinning solutions were measured by a Crison CM 35 conductivity meter and a Brookfield DV-II viscometer. The structure and diameter of

the electrospun nanofibres were investigated by an FEI Quanta 200 scanning electron microscope (SEM). The fibres were gold-coated for 30 seconds in order to reduce the charging and about 40 different points were used to measure the average diameter of the fibres. A Philips CM 200 transmission electron microscope (TEM) was used to measure the dimensions of the cellulose nanowhiskers. A drop of the cellulose nanowhiskers suspension was deposited on a carbon grid, stained with 2 wt% uranyl acetate, and allowed to dry at room temperature. BET was used to evaluate the surface area and pore size of the electrospun alginate nanofibrous membrane by a nitrogen adsorption/desorption test method.

The tensile properties of the nanofibrous membranes were measured by using an Instron tensile tester equipped with a 0.5 kN load cell and 25 mm gauge length. The rectangular bar specimens with dimensions 50×10×~0.01 mm were cut from the electrospun nanofibrous membrane and the tensile measurements were performed at a cross head speed of 5 mm min^{-1}. At least ten specimens were tested per sample, and the mean values and standard deviations are reported.

4.2.4 Water purification test

The test of the nanoparticles removal from an aqueous solution was carried out by flow through dead end filtration, as shown in Figure 4.2. 0.15 wt% each of TiO_2 (100 nm) and Cu (10-35 nm) nanoparticles were dispersed in distilled water by ultrasonic dispersion for 15 minutes. These two types of nanoparticles were used because of their size difference, and because TiO_2 is widely used in different products although it can cause brain and nerve damage. In order to evaluate the oil/water separation ability of the membrane systems, oily wastewater was prepared by mixing vegetable oil with distilled water and surfactant for 20 minutes by using a homogenizer at 5000 rpm.

The transmittance of feed and filtrate solutions were measured from 300 to 900 nm by using a UV-vis spectrophotometer (Agilent 8453). The concentration of Cu, TiO_2 and oil were established by measuring the maximum absorbance of the feed and filtrate at wavelengths of 279, 540 and 230 nm. The oil concentration was established by a calibration curve ranging from 10 to 100 ppm and the relationship between the absorbance and oil concentration was found to be linear ($R^2 = 0.995$).

The removal percentage (R) of the particulates by the composite membrane was calculated by using Equation 1.

$$R(\%) = \left(\frac{C_f - C_i}{C_f}\right) \times 100 \qquad (1)$$

where C_f is the concentration of the feed solution and C_i is the concentration of the filtrate.

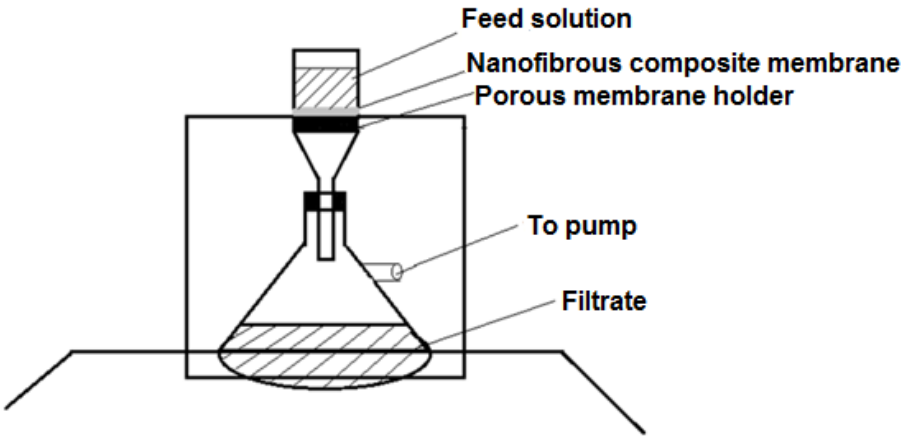

Figure 4.2 Flow through filtration setup

4.2.5 Metal ion retention

For the evaluation of the metal ion retention of the membranes, a 20 mg/L chromium (Cr(VI)) solution was filtered through a 50 mm diameter membrane at room temperature. The pH was varied in order to assess the maximum pH for the metal ion retention. The pH was adjusted with 0.1 M HNO_3 and 0.1 M NaOH solutions. The nanofibrous composite membranes were assembled in cross flow dead end filtration (Figure 4.2) and metal solution was filtered through the membrane disc. The Cr(VI) concentrations were measured by using atomic absorption spectroscopy (Varian Spectra AAS 220Z) and the rejection percentage was calculated by using Equation 1.

4.3 Results and discussion

4.3.1 Characterization and preparation of electrospun nanofibres

PEO was chosen as a copolymer due to its water-solubility and compatibility with alginate. The alginate could not be electrospun on its own due to its high viscosity and conductivity as a result of its inherent polyelectrolytic character and rigid structure (see Table 4.1). The SEM micrographs of the electrospun PEO and PEO/alginate blend produced at different alginate volume ratios are shown in Figure 4.3. The PEO electrospun nanofibrous membrane consisted of smooth bead-free nanofibres (Figure 4.3(a)), with an average diameter of 313 ± 86 nm (Table 4.1). For the blend of PEO/sodium alginate (SA), uniform nanofibres were obtained when the volume ratio of sodium alginate was between 20 and 60% (v/v) (Figure 4.3(b-d)). At high sodium alginate contents, no fibrous structures were formed and only droplets were generated (electro-spraying) (Figure 4.3(e-f)). This can be due to the lack of chain entanglements in the alginate polymer. In comparison with neat PEO, the diameters of the electrospun nanofibres decreased with an increase in the alginate volume ratio in the composition (Table 4.1). This can be attributed to the increase in conductivity (Table 4.1), which led to an increase in charge density on the surface of the jet, resulting in enhanced solution stretching under the electric field which reduced the diameter of the fibres. Furthermore, the increase in solution conductivity (when the alginate content was increased) resulted in larger electrostatic forces which caused the jet to split into smaller and more beaded fibres. PEO/SA 60/40 v/v was therefore selected for the preparation of composite membranes for subsequent experiments.

Table 4.1 The solution properties of PEO, sodium alginate and the PEO/alginate blend

Sample	Conductivity (mS/cm)	Viscosity (Pas)	Morphology	Diameter (nm)
Sodium Alginate (SA)	5.60 ± 0.01	12.40 ± 0.16	Electrospray	-
PEO	4.91 ± 0.09	0.10 ± 0.00	Smooth	313 ± 86
SA/PEO 20/80	1.24 ± 0.05	0.87 ± 0.00	Smooth	209 ± 58
SA/PEO 50/50	2.74 ± 0.04	2.52 ± 0.02	Smooth	112 ± 47
SA/PEO 60/40	3.06 ± 0.04	3.02 ± 0.01	Smooth	109 ± 56
SA/PEO 80/20	4.77 ± 0.16	4.20 ± 0.30	Beaded	53 ± 17
SA/PEO 90/10	4.96 ± 0.01	6.23 ± 0.01	Electrospray	-

4.3.2 Preparation and characterization of cellulose nanowhiskers

The TEM micrographs of the maize biomass extracted cellulose nanowhiskers (CNs) are shown in Figure 4.4. The acid hydrolysis treatment was able to cleave the amorphous regions of the cellulosic fibres, which resulted in intact crystalline domains. The pretreatment of the fibres with NaOH, bleach and KOH solutions removed the other constituents of the fibre, which improved the acid hydrolysis efficiency. The CNs displayed diameters ranging between 3 and 12 nm, and lengths ranging between 120 and 180 nm. These findings correlate with those obtained by Mtibe *et al*. [26]. They reported diameters of 3-7 nm and the lengths of 150-450 nm for the CNs obtained from maize stalk.

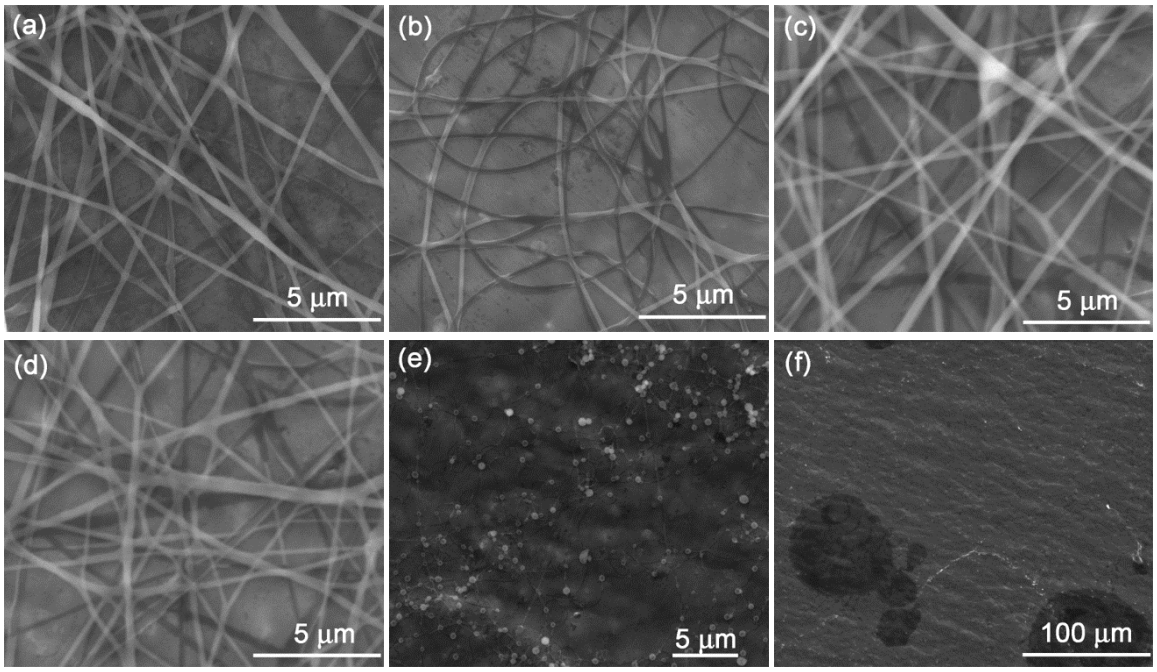

Figure 4.3 SEM micrographs of PEO/SA ((a) 100/0, (b) 80/20, (c) 50/50, (d) 60/40, (e) 20/80, (f) 90/10

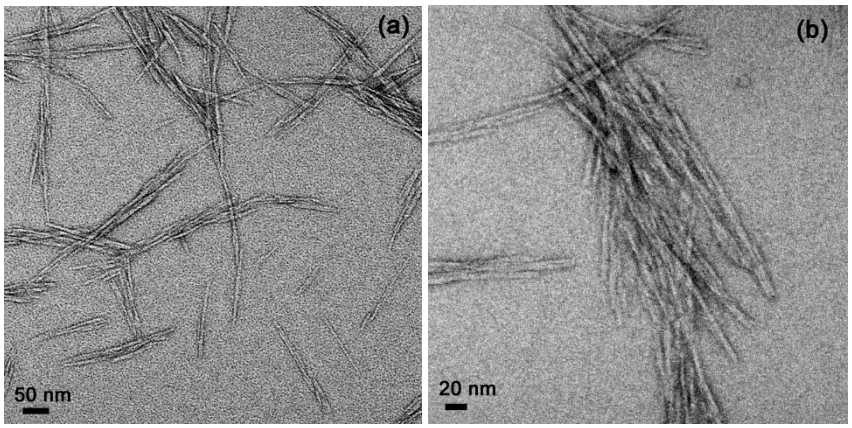

Figure 4.4 TEM micrographs of cellulose nanowhiskers

4.3.3 Characterization of the CaA-CNs composite membrane

The SEM images of the surface morphology of the CaA and CaA-CNs membranes are shown in Figure 4.5. It can be seen that the CaA membrane was highly porous (Figure 4.5(a)) which can provide high permeation, while the CaA-CNs surface was smooth and dense with evenly distributed tiny pores on the surface (Figure 4.5(b)).

The BET specific surface area of the CaA membrane was 23.34 m^2 g^{-1}, and it decreased to 3.82 m^2 g^{-1} for the CaA-CNs composite membrane. This was due to the compactness of the cellulose nanowhiskers on the surface of the electrospun nanofibres. The pore size for the CaA membrane ranged from 222 to 263 nm, whilst that for the CaA-CNs membrane ranged from 63 to 243 nm.

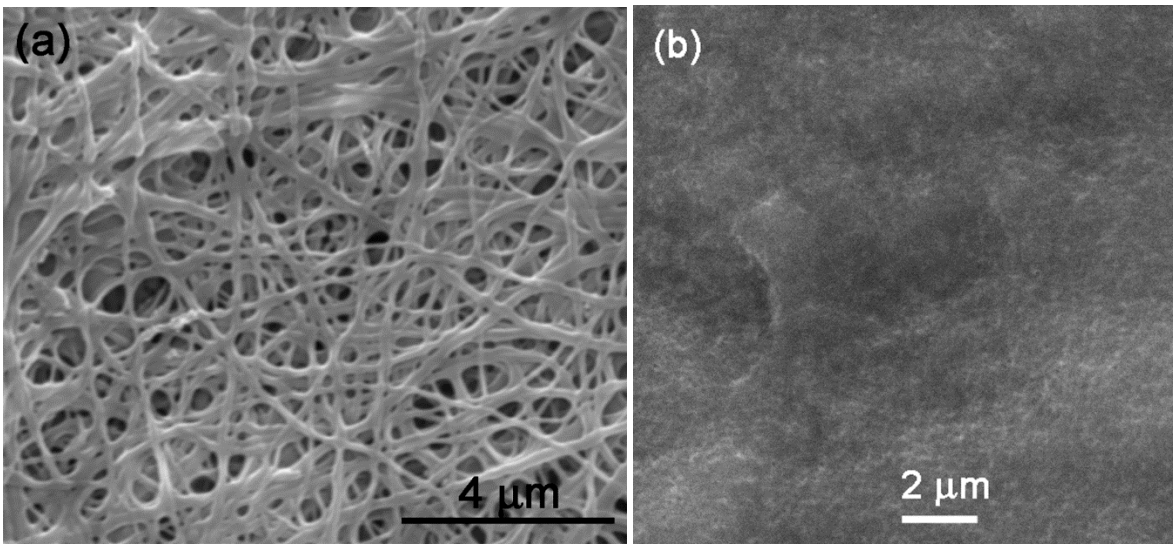

Figure 4.5 SEM images of (a) alginate nanofibrous membrane and (b) TFC membrane

4.3.4 Tensile properties

There are several factors that influence the mechanical properties of electrospun mats such as composition, interfacial interaction between the two components, and the fibre structure, diameter and density [27,28]. The tensile properties of the electrospun PEO, PEO/SA blend, CaA and CaA-CNs are presented in Table 4.3. When compared to pure PEO, the tensile strength of the electrospun PEO/SA increased by 14%, but the elongation at break significantly decreased by 72%. This is probably due to the rigid structure of alginate and the interaction between the alginate and PEO [27,29]. After crosslinking with calcium chloride

(CaA), the tensile strength showed a further two-fold increase, while the elongation at break showed a five-fold decrease. The crosslinking of the alginate chains contributed to the stiffness of the electrospun mats, restricting their mobility and reducing the extent of their elongation. The coating of the cellulose nanowhiskers onto the CaA nanofibrous membrane increased the tensile strength of CaA, while reducing the elongation at break by ~29%, when compared to CaA. This can be ascribed to the stiff cellulose nanowhiskers on the surface of the electrospun CaA, and the strong hydrogen bonding network between them [21]. There is also a probability that the cellulose nanowhiskers have entered some pores of the electrospun alginate and formed hydrogen bonds with the alginate.

Table 4.2 Tensile properties of the investigated samples

Sample	Tensile strength (MPa)	Elongation at break (%)
PEO	5.2 ± 0.1	45.1 ± 5.3
PEO/SA blend	5.9 ± 0.2	12.5 ± 3.0
CaA	11.2 ± 1.0	9.2 ± 1.2
CaA-CNs	16.2 ± 2.1	6.5 ± 1.4

4.3.5 Filtration efficiency evaluation

4.3.5.1 Nanoparticles removal

The CaA-CNs composite membrane showed very high retention of the Cu and TiO_2 nanoparticles, although the membrane was not yet totally optimized. The CaA membrane also showed very promising results with retentions of 70 and 86% for Cu and TiO_2, respectively. The pore sizes in the CaA-CNs membrane were considerably smaller than the size of the TiO_2 nanoparticles, which provides the removal of TiO_2 essentially by size exclusion. This implies that the CaA-CNs membrane acts as a screen filter. The sizes of the Cu nanoparticles were smaller than the pore sizes of both the CaA-CNs and CaA membranes. The retention in this case can be explained by the two modes involved in filtration. Firstly, the filter may act as a screening filter due to small pore sizes, rejecting the suspended contaminants, and the second mechanism involves depth filtration [30,31]. In the depth filtration, the suspended particles enter the membrane and end up residing in the membrane due to the interconnected pore structure of the membrane. This assists in the rejection of the suspended particles regardless of the membrane pore size. The tortuous path within the nanofibres, created by their

interconnected pore structure, increased the contact time and improved the interaction between the nanoparticles and the membrane components, which assisted in filtration efficiency. TiO_2 probably had a stronger interaction with the membrane fibre surfaces than Cu because of the attraction between its oxygen and the -OH groups on the surfaces of the membrane fibres [32]. It was also visually observed that the nanoparticles formed a cake-like layer on top of the membrane, which in turn assisted in rejecting more particles due to the blockage of the pores during filtration, as confirmed by the UV-vis spectra in Figure 4.6. The spectrum of the filtrate was relatively close to that of pure water, which is supported by the inserted images that show that the filtrates were clear. The formation of the cake-like layer could, however, lead to a high transmembrane pressure which would limit the productivity of the membrane.

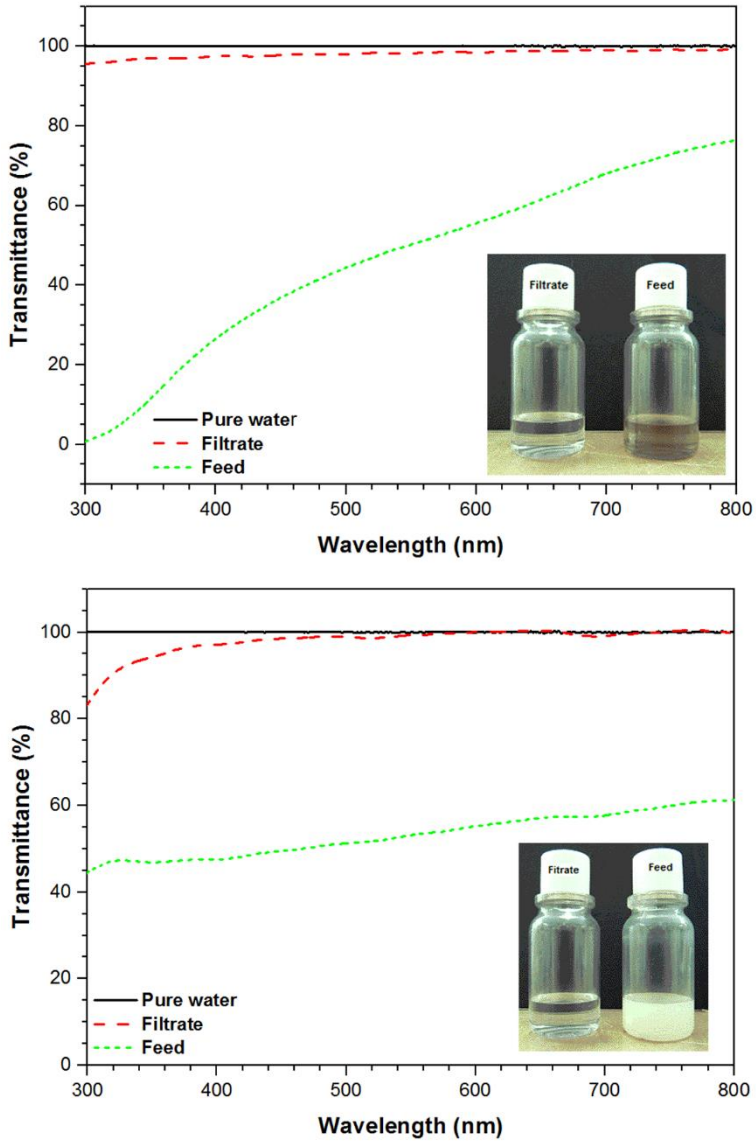

Figure 4.6 UV-vis spectra of the nanoparticles feed suspension (Cu (a) and TiO_2 (b)), filtrate and pure water for CaA-CNs composite membrane

Table 4.3 Retention of copper and titanium oxide suspensions for CaA and CaA-CNs membranes

Sample	Copper NPs (10-35 nm)	Titanium oxide NPs (>100 nm)
CaA-CNs	100.0	100.0
CaA	70.0	85.6

4.3.6 Oil/water retention

Oily waste-water affects water sources, crop production, endangers aquatic species and human health [33]. The objective of the oil/water treatment was to be within the limit of maximum allowable emission of oily waste-water into the environment. The CaA-CNs composite membrane showed 98.4% removal of oil from water (Figure 4.7); the CaA membrane displayed 96.6% retention and the resulting oil concentration in the filtrate was ~6 and 18 mg L^{-1}. The oil concentration for the CaA-CNs membrane was well below the required maximum discharge (>10 mg L^{-1}), which may be attributed to the membrane surface hydrophilicity and the tight pores that prevented the oil droplets from penetrating the membrane pores and resulted in the formation of a water layer on the surface of the membrane [34,35]. The thickness of the water layer depends on the hydrophilicity of the membrane surface [35]. The higher the hydrophilicity of the membrane, the thicker the water layer blocking the larger pores and increasing the oil retention. As can be clearly seen in the inserted image in Figure 4.7, the filtrate was clear while the feed solution was cloudy. This shows that the CaA-CNs membrane is effective in removing oil from polluted water. The reason for the incomplete removal of the oil is that, although the CaA was hydrophilic, some oil droplets may have entered the pores by deformation due to the filtration pressure exerted by the pump or due to the swelling of the alginate.

4.3.7 Chromium retention

Heavy metal ions are recognized as the primary source of different respiratory, neural and intestinal diseases, hence their removal from waste-water streams are of significant importance. Chromium (Cr(VI)) was used to evaluate the retention of these ions by the nanofibrous composite membranes. One of the most important variables in the heavy metal ion adsorption process is the pH, as can be seen in Figure 4.8. Contrary to most reports on the adsorption of Cr(VI) stating that the optimal pH value was below 7 [23,36,37], in our case,

the metal retention increased with an increase in pH over the whole pH range investigated for the CaA-CNs membrane, but at higher pH values it remained the same as that at a pH of 7 for the CaA membrane.

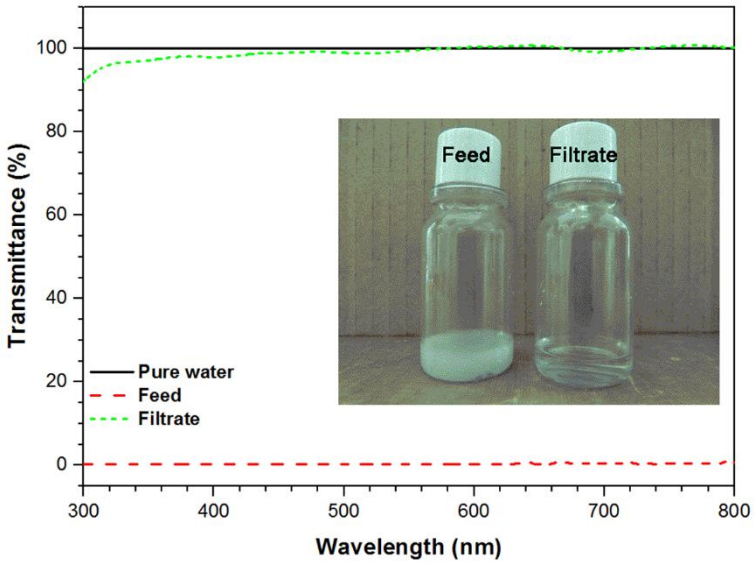

Figure 4.7 UV-vis spectra of oil/water feed, filtrate and pure water for CaA-CNs composite membrane

Wang *et al*. [23] used a two-layered membrane based on polyacrylonitrile (PAN) and polyethylene terephthalate (PET) infused with ultrafine amino-modified cellulose nanofibres. They reported the maximum Cr(VI) adsorption at a pH value of 4, and stated that the pH influenced the protonation of amino groups and changed the Cr(VI) into its negatively charged form ($HCrO_4^-$), which was attracted to the positively charged amino groups (NH_3^+). Taha *et al*. [37] found a Cr(VI) maximum adsorption at a pH value of 1 due to the protonated amino groups (NH_3^+) and the availability of negatively charged Cr(VI) complex ions which improved the interaction between them. They used an NH_2 functionalized cellulose acetate/silica nanofibrous composite membrane. Pradhan *et al*. [36] recorded the maximum Cr(VI) adsorption of red mud at a pH value of 5.2. This was ascribed to the net positive centres on the surface of the red mud and the charge form of Cr (IV), which were directly dependent on the pH value.

Cellulose nanowhiskers with sulphates and hydroxyl groups on its surface, and alginate with carboxyl and hydroxyl groups, were used in our study. These functional groups dissociate in an alkaline solution to give a highly negative charge on membrane surface which rejects the negatively charged Cr(IV). At low pH, the chromium ions exist mostly as acid chromates

(H_2CrO_4), and with an increase in pH the chromium ions change to acid chromates ($HCrO_4^-$) at well below a pH of 7. At pH values above 7, chromate ions (CrO_4^{2-}) become more dominant, while the presence of dichromate ($Cr_2O_7^{2-}$) depends on the feed concentration [38,39]. Due to their high charge density, the chromate ions are easily retained. Muthukrishnan and Guha [39] also reported that the retention of Cr(VI) at low concentrations was higher at high pH values, but that the opposite trend was observed for higher Cr(VI) concentrations. They stated that at higher feed concentrations the dissociation to bi- and multivalent ions was more extensive in an acidic medium, which explained the higher rejection at high feed concentration in the acidic medium. A reverse scenario was observed for low feed concentration, which had extensive dissociation in an alkaline medium The higher rejection percentages for the CaA-CNs membrane, and the lack of increase in the rejection percentage for the CaA membrane at pH values above 7, can be linked to the presence of sulphates and additional hydroxyl groups on the surfaces of the cellulose nanowhiskers that were present in the CaA-CNs membrane, but not in the CaA membrane.

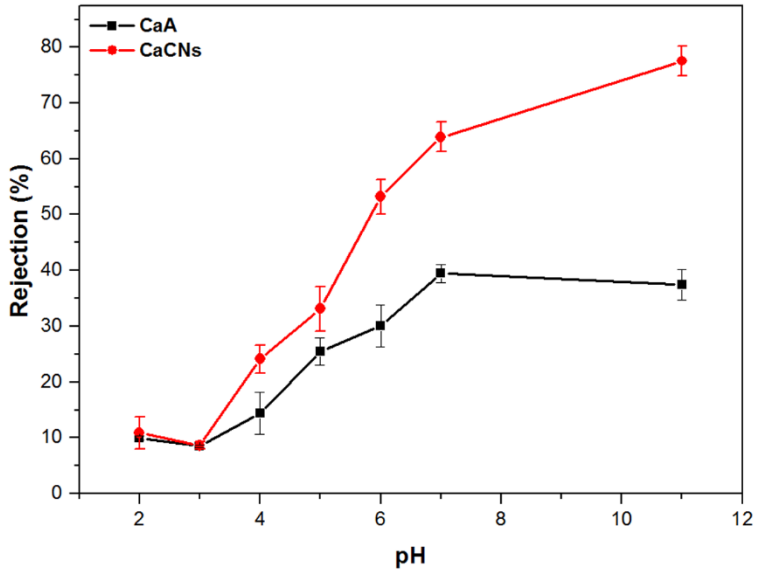

Figure 4.8 Effect of pH on the rejection of Cr(IV) for CaA and CaA-CNs membranes

4.4 Conclusions

Alginate-based nanofibrous membranes were successfully electrospun with the aid of PEO as copolymer. An increase in alginate content in the blend increased the conductivity of the electrospinning solution, which reduced the diameter of the fibres in the resulting nanofibrous membrane. Nanofibres were only obtained at low alginate content in the blend (20-60 v/v%), while at higher contents (80 and 90 v/v%) only beaded fibres and droplets were generated.

The nanofibrous membrane that contained nanowhiskers extracted from maize stalk was found to have a high filtration efficiency, although the membrane prepared without cellulose nanowhiskers was also performing well, but not as good as the nanowhiskers-containing membrane. This efficiency was demonstrated in terms of the retention of Cu and TiO_2 nanoparticles, the separation of oil from an oil/water emulsion, and the removal of chromium ions from an aqueous solution.

The mechanical properties of the membrane were improved after coating with CNs, but can be further improved with additional modifications of the top layer and crosslinking of the middle layer. This will also enhance antifouling and membrane productivity. It can be concluded that the membrane can be used for short-term domestic water treatment applications.

4.5 References

[1] T.C. Mokhena, V. Jacobs, A.S. Luyt, A review on electrospun bio-based polymers for water treatment, eXPRESS Polymer Letters, 9 (2015) 839-880.

[2] Y. Tian, M. Wu, R. Liu, Y. Li, D. Wang, J. Tan, R. Wu, Y. Huang, Electrospun membrane of cellulose acetate for heavy metal ion adsorption in water treatment, Carbohydrate Polymers, 83 (2011) 743-748.

[3] K. Desai, K. Kit, J. Li, P.M. Davidson, S. Zivanovic, H. Meyer, Nanofibrous chitosan non-wovens for filtration applications, Polymer, 50 (2009) 3661-3669.

[4] H. Ma, C. Burger, B.S. Hsiao, B. Chu, Nanofibrous microfiltration membrane based on cellulose nanowhiskers, Biomacromolecules, 13 (2011) 180-186.

[5] R. Wang, Y. Liu, B. Li, B.S. Hsiao, B. Chu, Electrospun nanofibrous membranes for high flux microfiltration, Journal of Membrane Science, 392-393 (2012) 167-174.

[6] X. Wang, X. Chen, K. Yoon, D. Fang, B.S. Hsiao, B. Chu, High flux filtration medium based on nanofibrous substrate with hydrophilic nanocomposite coating, Environmental Science & Technology, 39 (2005) 7684-7691.

[7] S. Kaur, S. Sundarrajan, D. Rana, T. Matsuura, S. Ramakrishna, Influence of electrospun fiber size on the separation efficiency of thin film nanofiltration composite membrane, Journal of Membrane Science, 392-393 (2012) 101-111.

[8] K. Yoon, K. Kim, X. Wang, D. Fang, B.S. Hsiao, B. Chu, High flux ultrafiltration membranes based on electrospun nanofibrous PAN scaffolds and chitosan coating, Polymer, 47 (2006) 2434-2441.

[9] X. Wang, D. Fang, K. Yoon, B.S. Hsiao, B. Chu, High performance ultrafiltration composite membranes based on poly(vinyl alcohol) hydrogel coating on crosslinked nanofibrous poly(vinyl alcohol) scaffold, Journal of Membrane Science, 278 (2006) 261-268.

[10] R. Barhate, S. Ramakrishna, Nanofibrous filtering media: Filtration problems and solutions from tiny materials, Journal of Membrane Science, 296 (2007) 1-8.

[11] C.A. Bonino, K. Efimenko, S.I. Jeong, M.D. Krebs, E. Alsberg, S.A. Khan, Three-dimensional electrospun alginate nanofiber mats via tailored charge repulsions, Small, 8 (2012) 1928-1936.

[12] R. Konwarh, N. Karak, M. Misra, Electrospun cellulose acetate nanofibers: The present status and gamut of biotechnological applications, Biotechnology Advances, 31 (2013) 421-437.

[13] N. Bhardwaj, S.C. Kundu, Electrospinning: A fascinating fiber fabrication technique, Biotechnology Advances, 28 (2010) 325-347.

[14] A. Patanaik, V. Jacobs, R.D. Anandjiwala, Performance evaluation of electrospun nanofibrous membrane, Journal of Membrane Science, 352 (2010) 136-142.

[15] D. Bjorge, N. Daels, S. De Vrieze, P. Dejans, T. Van Camp, W. Audenaert, J. Hogie, P. Westbroek, K. De Clerck, S.W. Van Hulle, Performance assessment of electrospun nanofibers for filter applications, Desalination, 249 (2009) 942-948.

[16] R. Gopal, S. Kaur, Z. Ma, C. Chan, S. Ramakrishna, T. Matsuura, Electrospun nanofibrous filtration membrane, Journal of Membrane Science, 281 (2006) 581-586.

[17] S. Kaur, D. Rana, T. Matsuura, S. Sundarrajan, S. Ramakrishna, Preparation and characterization of surface modified electrospun membranes for higher filtration flux, Journal of Membrane Science, 390-391 (2012) 235-242.

[18] S. Haider, S.-Y. Park, Preparation of the electrospun chitosan nanofibers and their applications to the adsorption of Cu(II) and Pb(II) ions from an aqueous solution, Journal of Membrane Science, 328 (2009) 90-96.

[19] K. Saeed, S. Haider, T.-J. Oh, S.-Y. Park, Preparation of amidoxime-modified polyacrylonitrile (PAN-oxime) nanofibers and their applications to metal ions adsorption, Journal of Membrane Science, 322 (2008) 400-405.

[20] J. Wang, C. Chen, Biosorbents for heavy metals removal and their future, Biotechnology Advances, 27 (2009) 195-226.

[21] X. Cao, M. Huang, B. Ding, J. Yu, G. Sun, Robust polyacrylonitrile nanofibrous membrane reinforced with jute cellulose nanowhiskers for water purification, Desalination, 316 (2013) 120-126.

[22] H. Ma, C. Burger, B.S. Hsiao, B. Chu, Ultrafine polysaccharide nanofibrous membranes for water purification, Biomacromolecules, 12 (2011) 970-976.

[23] R. Wang, S. Guan, A. Sato, X. Wang, Z. Wang, R. Yang, B.S. Hsiao, B. Chu, Nanofibrous microfiltration membranes capable of removing bacteria, viruses and heavy metal ions, Journal of Membrane Science, 446 (2013) 376-382.

[24] Z. Wang, H. Ma, B.S. Hsiao, B. Chu, Nanofibrous ultrafiltration membranes containing cross-linked poly (ethylene glycol) and cellulose nanofiber composite barrier layer, Polymer, 55 (2014) 366-372.

[25] T.C. Mokhena, A.S. Luyt, Investigation of polyethylene/sisal whiskers nanocomposites prepared under different conditions, Polymer Composites, 35 (2014) 2221-2233.

[26] A. Mtibe, L.Z. Linganiso, A.P. Mathew, K. Oksman, M.J. John, R.D. Anandjiwala, A comparative study on properties of micro and nanopapers produced from cellulose and cellulose nanofibres, Carbohydrate Polymers, 118 (2015) 1-8.

[27] S. Moon, B.-Y. Ryu, J. Choi, B. Jo, R.J. Farris, The morphology and mechanical properties of sodium alginate based electrospun poly (ethylene oxide) nanofibers, Polymer Engineering & Science, 49 (2009) 52-59.

[28] J.-W. Lu, Y.-L. Zhu, Z.-X. Guo, P. Hu, J. Yu, Electrospinning of sodium alginate with poly (ethylene oxide), Polymer, 47 (2006) 8026-8031.

[29] H. Nie, A. He, J. Zheng, S. Xu, J. Li, C.C. Han, Effects of chain conformation and entanglement on the electrospinning of pure alginate, Biomacromolecules, 9 (2008) 1362-1365.

[30] R. Gopal, S. Kaur, C.Y. Feng, C. Chan, S. Ramakrishna, S. Tabe, T. Matsuura, Electrospun nanofibrous polysulfone membranes as pre-filters: Particulate removal, Journal of Membrane Science 289 (2007) 210-219.

[31] V. Thavasi, G. Singh, S. Ramakrishna, Electrospun nanofibers in energy and enviromental applications, Energy & Enviromental Science 1 (2008) 205-221.

[32] X. Li, X. Wu, G. He, J. Sun, W. Xiao, Y. Tan, Microspheroidization treatment of macroporous TiO2 to enhance its recycling and prevent membrane fouling of photocatalysis-membrane system, Chemical Engineering Journal 251 (2014) 58-68.

[33] L. Yu, M. Han, F. He, A review of treating oily wastewater, Arabian Journal of Chemistry, In press (2013).
http://doi:10.1016/j.arabjc.2013.07.020

[34] Y. Zhang, P. Cui, T. Du, L. Shan, Y. Wang, Development of a sulfated Y-doped nonstoichiometric zirconia/polysulfone composite membrane for treatment of wastewater containing oil, Separation and Purification Technology, 70 (2009) 153-159.

[35] L. Wang, K. Pan, L. Li, B. Cao, Surface hydrophilicity and structure of hydrophilic modified PVDF membrane by nonsolvent induced phase separation and their effect on oil/water separation perfomance, Industrial & Engineering Chemistry Research, 53 (2014) 6401-6408.

[36] J. Pradhan, S.N. Das, R.S. Thakur, Adsorption of hexavalent chromium from aqueous solution by using activated red mud, Journal of Colloid and Interface Science, 217 (1999) 137-141.

[37] A.A. Taha, Y.-N. Wu, H. Wang, F. Li, Preparation and application of functionalized cellulose acetate/silica composite nanofibrous membrane via electrospinning for Cr (VI) ion removal from aqueous solution, Journal of Environmental Management, 112 (2012) 10-16.

[38] A. Hafiane, D. Lemordant, M. Dhahbi, Removal of hexavalent chromium by nanofiltration, Desalination, 130 (2000) 305-312.

[39] M. Muthukrishnan, B.K. Guha, Effect of pH on rejection of hexavalent chromium by nanofiltration, Desalination, 219 (2008) 171-178.

Chapter 5

Electrospun alginate nanofibres impregnated with silver nanoparticles: Fabrication and the analysis of property

This chapter has been submitted for publication as:
T.C. Mokhena, A.S. Luyt, Electrospun alginate nanofibres impregnated with silver nanoparticles: Fabrication and the analysis of property, Carbohydrate Polymers.

Abstract

Silver nanoparticles are amongst the most valuable nanoparticles with interesting properties, such as a non-toxic nature and high antibacterial efficiency, making them applicable for tissue scaffold, protective clothing and wound dressing. In this study, silver nanoparticles (AgNPs) have been synthesized using chitosan as reducing and stabilizing agent. The formation of silver nanoparticles was confirmed by UV-vis, and TEM showed that different shapes were obtained depending on the heating duration. The chitosan/AgNPs was coated onto an electrospun alginate membrane to produce stable polyelectrolyte complex (PEC) nanofibrous composites with high antibacterial efficiency. These composites were characterized by scanning electron microscopy (SEM), Fourier transform infrared spectroscopy (FTIR) and X-ray diffraction (XRD). AgNPs were successfully impregnated into the PEC nanofibrous composite, while there was complexation between the electrospun alginate and the chitosan/AgNPs composite. PEC demonstrated a good antibacterial activity against gram negative and gram positive bacteria.

Keywords: Chitosan; Silver nanoparticles; Electrospun alginate; Polyelectrolyte complex; Antibacterial activity

5.1 Introduction

Electrospinning has attracted a lot of attention during the past two decades because of its capability to produce flexible nanofibrous membranes with micro- or nanoscale diameters from synthetic and natural polymers [1-3]. A processor can control the processing variables

such as solution properties (conductivity, concentration and surface tension), setup parameters (tip-to-collector distance, flow rate, and needle geometry) and environmental conditions (humidity and temperature) in order to produce a desired morphology and/or structure of the resulting nanofibres [3,4]. These nanofibres have unique features such as large surface-to-volume ratio, interconnective structure and high porosity [4]. These open doors for a wide variety of applications such as antimicrobial mats, protective clothing, tissue engineering and sensors [3,4].

A wide variety of nanoparticles (NPs), such as carbon nanotubes (CNT) [5], silica (SiO_2) [6], hydroxyapatite (HAp) [7], zinc [8] and silver nanoparticles (AgNPs) [9-11], have been incorporated into polymeric nanofibres in order to produce hybrid multifunctional materials for different applications. Amongst these nanoparticles, silver nanoparticles (AgNPs) have received significant interest due to their good antibacterial activity and plasma response property [9-11]. They are widely used in various fields such as sensors, biotechnology, filtration and detectors [9,11-13]. These hybrid materials are usually prepared by either *in-situ* or *ex-situ* blending, because they are easily controllable, simple and less costly [9,10,12]. The incorporated nanoparticles, however, end up being buried inside the host material which is unfavourable for their release and/or contact with the target [12]. In order to overcome this challenge, coating of the polymer nanofibres with NPs has been widely used to prepare different hybrid materials in order to improve the activity of these particles. One of the coating technologies involves the formation of a polyelectrolyte complex for effective activity, and transportation of active substances from the host by coating it with an active substance or an additional polymer combined with an active substance [14].

Over the past years, there has been growing interest in the preparation of polyelectrolyte complexes (PEC) to encapsulate different substances and active components for a wide variety of applications (e.g. drug delivery and tissue engineering) because of its ability to precisely control the release of these substances [14,15]. PEC results from electrostatic interaction between two counter-ions. Several studies demonstrated that various opposite charged materials can be combined alone or with other components to target a specific application [16-22]. Chitosan and its derivative have been widely studied due to the presence of the amino functional groups and their biocompatibility [14,15,23]. For example, Tapia *et al*. [15] prepared a PEC from chitosan-alginate and chitosan-carrageenan to encapsulate diltiazem clorhydrate. The results pointed out that both systems can be used for prolonged drug release with different drug realese mechanisms. The swelling behaviour of the chitosan-

alginate controlled the drug release from the matrix. In the case of the chitosan-carrageenan sytem, the disintergration of the system plays a major role in the drug release mechanism.

One of the most interesting properties of chitosan and its derivatives is their capability to stabilize and reduce different metal oxides [24-26]. The latter has been explored to synthesize different metal nanoparticles such as silver and gold nanoparticles [24-27]. Wei *et al*. [26] synthesized silver nanoparticles by using chitosan as a stabilising and reducing agent. They obtained spherical nanoparticles with diameters of about 6-8 nm after 12 hours of thermal treatment. The AgNPs/chitosan showed highly potent antibacterial activity towards gram negative and gram positive bacteria. Shih *et al*. [28] synthesized gold nanoparticles with diameters ranging between 50 and 200 nm by using chitosan as both a capping and a reducing agent. Laudenslager *et al*. [29] used both carboxymethyl chitosan and chitosan as the template for the growth of platinum, gold and silver nanoparticles. They reported that chitosan and carboxymethyl chitosan produced nanoparticles of similar size and shape for gold and platinum, while silver nanoparticles from chitosan were slightly smaller. Quaternized carboxymethyl chitosan was also used by Huang *et al*. [30] as a stabilizer and a reductant for the synthesis of AgNPs. They obtained spherical nanoparticles with an average diameter of 24.7 ± 2.8 nm.

In this study, we first report on the synthesis of AgNPs by a simple and environmentally benign method by using a natural polymer, chitosan, as a stabilizing and at the same time as a reducing agent with the aid of heat. Secondly, we report on the preparation of the polyelectrolyte complex (PEC) from chitosan and an electrospun nanofibrous alginate membrane to improve the stability of the silver nanoparticles (AgNPs) on the surface of the nanofibres as well as to control their distribution and release. To the best of our knowledge, this is the first time that an antibacterial substrate composed of three different components *viz* electrospun alginate nanofibres, chitosan and AgNPs, has been developed.

5.2 Experimental

5.2.1 Materials

Chitosan (310 kDa), poly(ethylene oxide) (PEO, 1000 kDa), sodium alginate (SA, 100 kDa), dimethylsulfoxide (DMSO, 99%), and Triton^{TM} X-100 were obtained from Sigma Aldrich,

South Africa. Silver nitrate ($AgNO_3$, 99.8%), calcium chloride ($CaCl_2$, 96%), acetic acid (99.7%) and ethanol (99%) were purchased from Ibhayi Laboratory Supplies, South Africa.

5.2.2 Synthesis of silver nanoparticles (AgNPs)

Chitosan (0.5 wt%) was dissolved in 2% acetic acid and centrifuged for 30 minutes at 4000 rpm in order to remove the undissolved particles. The obtained chitosan supernatant (20 ml) was mixed with 5 ml aqueous solution of freshly prepared 10 mM silver nitrate ($AgNO_3$) and stirred for 3 hours. In order to synthesize the AgNPs, the mixture was heated at 90°C for 3, 6, 12, 24 and 48 hours, under vigorous stirring. The colour change of the reaction mixture was visually observed.

5.2.3 Preparation of the composite nanofibrous membrane

PEO/SA nanofibres were prepared by dissolving PEO (3 wt%) and SA (3 wt%) separately in deionized water. A 50/50 v/v% mixture of the PEO and SA solutions was stirred for 4 hours and stored in an environmental chamber (Binder GmBH) set at ~25 °C for 10 days. 0.5 wt% Triton X-100 and 5 wt% DMSO were added to the mixture in order to improve the nanofibrous structure of the resulting fibres. The blend solution was added into a 20 ml syringe mounted onto a syringe pump. The solution feeding rate was 0.8 ml hr^{-1}, the voltage was 17 kV and the tip-to-collector distance was 17 cm. The nanofibres were then crosslinked with calcium chloride by soaking it in 80% ethanol for 5 min and rinsing with a 2 wt% $CaCl_2$ in ethanol solution for 10 min. The nanofibres were incubated in an aqueous solution of $CaCl_2$ for an hour, and then immersed in deionized water for another hour. The $CaCl_2$ treated membranes were then rinsed with deionized water, followed by washing with absolute ethanol, and dried at room temperature. Finally, the nanofibres were coated with a mixture of chitosan and silver nanoparticles (AgNPs). The nanofibres were immersed in the chitosan-AgNPs solution containing 1 wt% AgNPs for 5 minutes (denoted PEC_5min), followed by drying in a desiccator. The dried nanofibrous composites were then washed with ethanol and distilled water, then dried and stored in a desiccator at room temperature until used. The samples designated as PEC_10min and PEC_15min were also prepared by immersion of the electrospun alginate in the chitosan-AgNPs (1 wt% AgNPs) solution for 10 and 15 minutes, and used only for the antibacterial activity study by disk diffusion method.

5.2.4 Structural characterization

The UV-Vis spectrum of the synthesized silver nanoparticles was obtained with a Shimadzu UV-3100 (190-1100 nm) UV-Vis-NIR recording spectrophotometer at a resolution of 0.5 nm. In order to evaluate the content of the AgNPs in the chitosan solution, the chitosan solutions with (and without) silver nanoparticles were dried overnight in a vacuum oven at 40°C. Three pieces were then cut at different locations and thermogravimetric analyses were performed by using a Perkin Elmer TGA7 from 35 to 600°C under nitrogen flow of 20 ml min^{-1}. The morphology of the silver nanoparticles was determined by depositing a drop of suspension onto the carbon grid and allowed to dry at room temperature. The grids were observed with a Philips CM 200 transmission electron microscope operated at an accelerating voltage of 80 kV.

The morphology and composition of the electrospun nanofibres and composite membranes were examined with a field emission scanning electron microscope (FESEM) (FEI Quanta 200) equipped with an energy dispersive X-ray analyser (EDX) for elemental analysis.

The IR spectra were acquired by using a Perkin Elmer Spectrum 100 FTIR spectrometer equipped with an attenuated total reflection (ATR) accessory with a diamond/ZnSe crystal (16 scans, 4 cm^{-1} resolution, wavenumber range 500-4000 cm^{-1}).

X-ray diffraction spectra were measured by using a Bruker AXS X-ray diffractometer D8 Advanced with a position sensitive detector (PSD) Vantec-1 and Cu-K_α radiation ($\lambda = 1.5406$ Å).

5.2.5 Antibacterial studies

In order to examine the antibacterial activity of the PEC nanofibrous composites (PEC_5min, PEC_10min and PEC_15min), the gram positive (*Staphylococcus aureus (ATCC 6538)* and *Bacillus pumilus (ATCC 14884)*) and gram negative (*Escherichia coli (ATCC 8739)* and *Klebisiella pneumoniae (ATTC 13047)*) susceptibility were investigated by an agar well diffusion method. Mueller-Hinton broth was used at 37°C for 12-20 hours to revive the bacterial cultures obtained from the Department of Zoology and Entomology, University of the Free State. The Mueller-Hinton agar medium was prepared and sterilized at 120°C for 15

minutes. The agar medium was transferred into sterile petri dishes and allowed to solidify under laminar airflow. About 100 µl of the revived bacterial cultures were then cultured on the surface of the medium. The coated nanofibrous membranes were placed on a plate and incubated at 37°C for 24 hours. The electrospun alginate nanofibres were used as a control. The inhibition zone formed around the coated nanofibrous membrane was measured and recorded as the antibacterial efficacy.

5.2.6 Silver release from the composite membrane

The silver leaching from the nanofibrous composite was determined by placing 0.02 g (1 cm × 1 cm) of the specimen in distilled water and extracting a small portion of the solution at different intervals and measuring the conductivity by using a Crison CM 35 conductivity metre.

5.2.7 Kinetic antibacterial test

For the kinetic antibacterial test, *S. aureus* and *E. coli* were grown in a Mueller-Hinton broth. PEC nanofibrous composites of 1 cm × 1 cm (0.02 g) were immersed in a glass tube containing a bacterial suspension (9.9 ml broth solution and 0.1 ml of microbial inoculation). The mixture was vortexed for 20 s and kept in an incubated shaker at 37°C. 0.1 ml aliquots were removed at set time intervals and added to 9.9 ml saline solution (8.5 wt% NaCl), and then vortexed for 20 seconds. From the vortexed dilution, 100 µl was plated on agar plates and incubated for 12-24 hours at 37°C. Colonies formed after incubation were counted, and the corresponding number of colonies represented viable bacteria in each suspension at the time of withdrawal.

5.3 Results and discussion

5.3.1 Synthesis and characterization of AgNPs

5.3.1.1 UV-Vis spectroscopy analysis

Figure 5.1 shows the UV-Vis spectra of the solutions and silver nanoparticles synthesized by using chitosan solution at different times. The silver nanoparticles were simply synthesized by heating a mixture of silver nitrate and chitosan without external agents at 90°C. $AgNO_3$ showed a band at ~300 nm which disappeared when it was mixed with the chitosan solution

(Figure 5.1a). This is probably due to the chelation of Ag^+ by the surface functional (amine and hydroxyl) groups of chitosan, and there was no colour change from this reaction mixture (inserted image in Figure 5.1a). After heating for 3 hours at 90°C, the colour changed to pale yellow, indicating the formation of silver nanoparticles (inserted image in Figure 5.1a). All the spectra show a surface plasmon peak at 428 nm in the extinction spectra arising from the excitation of the surface plasmon vibrations of Ag atoms (Figure 5.1b), except for the 24 and 48 hours of heating (not shown). The intensity of the surface plasmon peak was directly dependent on the heating duration. The colour became more intense with an increase in heating duration with the intensity of the peak increasing up to 12 hours of heating (Figure 5.1b). The long heating periods slowly increased the reduction process and the consumption of the reactants resulting in the formation of, and/or increase in the number of, silver nanoparticles produced. Heating over 24 hours resulted in a black coloured solution with a very broad peak from 300 nm to 842 nm (not shown). This is probably due to the AgNPs agglomeration resulting from the degradation of chitosan at longer heating periods and high temperatures in an acidic medium [31]. Sun *et al*. [31] studied the degradation behaviour of chitosan during the synthesis of gold nanoparticles. They reported that the intrinsic viscosity [η] of chitosan gradually decreased during the reduction process, and levelled-off after 10 hours of heating at 55 °C due to chain breakage. Thus, the degradation of chitosan during the reduction process may result in a shortage of polymer chains to stabilize the nanoparticles and hence leading to aggregation. According to other reports, the preparation for silver nanoparticles with chitosan as capping and reducing agent normally took between 3 to 12 hours [26,27]. Wei *et al*. [26] sythesized spherical silver nanoparticles (6-10 nm) by heating a mixture of silver nitrate and chitosan at 95°C for 12 hours. They obtained a yellowish brown coloured solution and the AgNPs' characteristic surface plasmon resonance band centred at ~420 nm. Kumar-Krishnan *et al*. [27] also synthesized silver nanoparticles using chitosan solution in 1% acetic acid and silver nitrate. They reported a dark yellow colour after 8 hours of heating at 95°C with the absorption peak centrered between 412 and 416 nm.

5.3.1.2 Morphology analysis

Figure 5.2 represents the TEM images of the synthesized silver nanoparticles. It can be seen that spherical AgNPs were obtained after 3 hours of heating at 90°C with diameters ranging between 8 and 28 nm (Figure 5.2a). After 6 and 12 hours of heating there were spherical and a few irregular shaped AgNPs, and their sizes ranged from 8 to 30 nm (Figure 5.2b). After the 12 hours of heating, about 80% of these nanoparticles had sizes ranging between 5 and 20 nm with very few being above 50 nm. Heating for 24 hours resulted in spherical nanoparticles (5-

80 nm) with some clusters (80-180 nm), whereas heating for 48 hours resulted in a mixture of rod-like (76-121 nm) and a few spherical (28-50 nm) nanoparticles. This explains the black colour and broadness of the plasmon peak (not shown). Therefore, the optimum preparation time for silver nanoparticles (AgNPs) was fixed to 12 hours in our experiments.

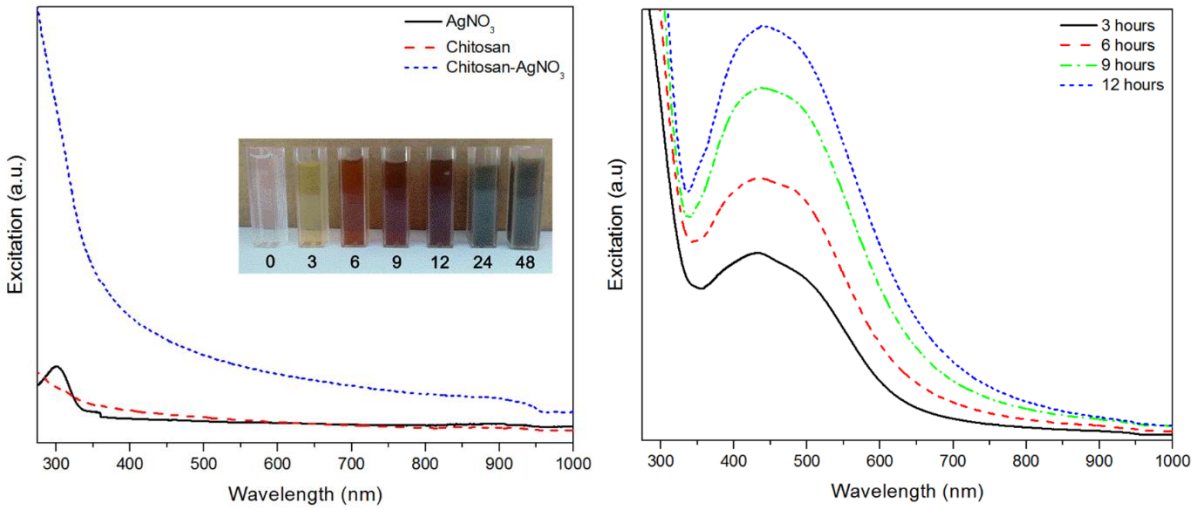

Figure 5.1 UV-Vis spectra of (a) $AgNO_3$, chitosan and a mixture of $AgNO_3$ and chitosan solutions, (b) AgNPs synthesized for different times using chitosan solution

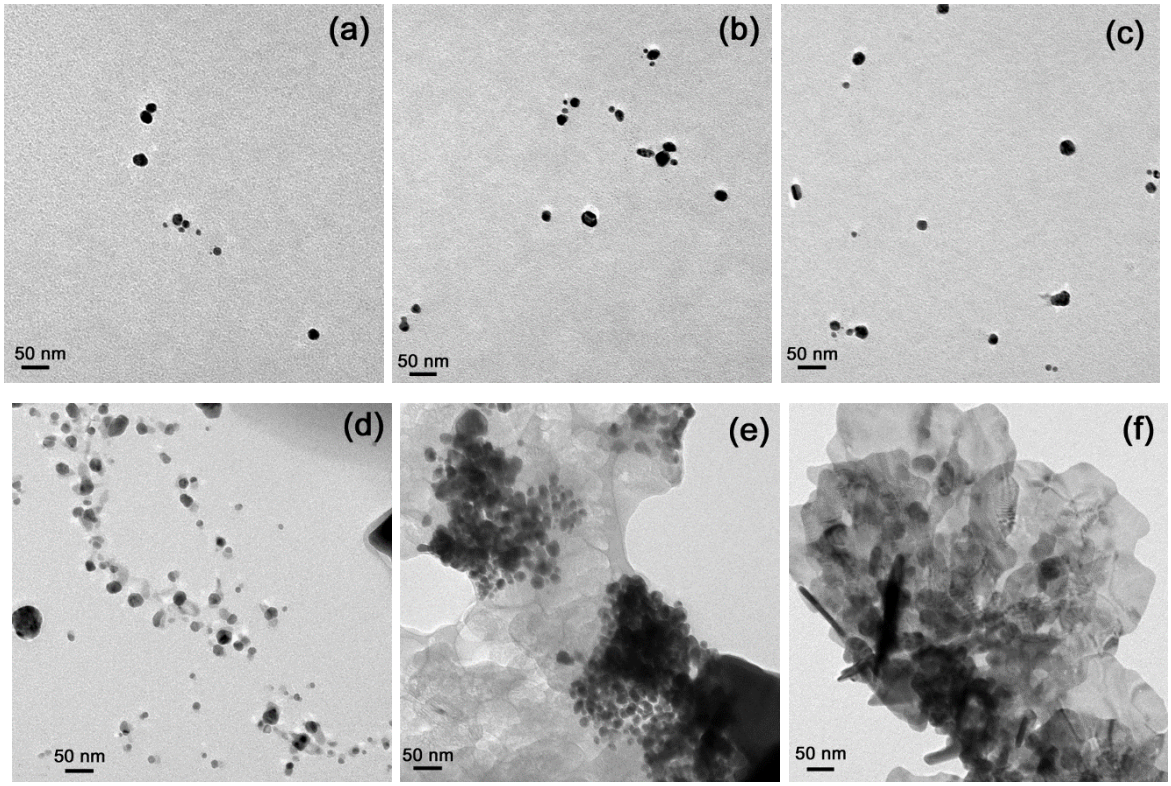

Figure 5.2 TEM images of silver nanoparticles: (a) 3, (b) 6, (c) 9, (d) 12, (e) 24 and (f) 48 hours

5.3.1.3 Thermogravimetric analysis (TGA)

Figure 5.3 shows the TGA curves of pure chitosan and the chitosan-AgNPs composite films (12 hours thermally treated). Both chitosan and the composite material show two degradation steps. The first mass loss in the range 50-120°C is attributed to the evaporation of water loosely bound to the samples; the second degradation step in the range of 140 to 400°C is related to the dehydration, deacetylation and depolymerisation processes, followed by the formation of char residue at temperatures above 400°C. The intermediate thermal degradation of the chitosan is usually associated with the formation of crosslinked structures from the radical products, which leads to the formation of thermally stable products that are included in the char residue [32]. The temperatures associated with 50% mass loss of chitosan and chitosan/AgNPs composite were ~292°C and ~307°C, respectively. This can be attributed to the presence of silver nanoparticles, which enhanced the thermal stability of the composite material [33]. The silver nanoparticles reduced the mobility of the polymer chains which supressed the transfer of free radicals thus inhibiting the inter-chain reaction so that the decomposition of the composite material occurred at higher temperatures [33,34]. It is also possible that the AgNPs interacted with the degradation volatiles and delayed their diffusion from the sample. The char residue content at 550°C for chitosan was ~28%, and 34% for the composite material, meaning that the AgNPs content in composite material was ~6%. The high yield of AgNPs implies that this process is feasible for the fabrication of nanoparticles with a good possibility for large scale production, considering the abundant availability of chitosan and the non-toxic solvents used.

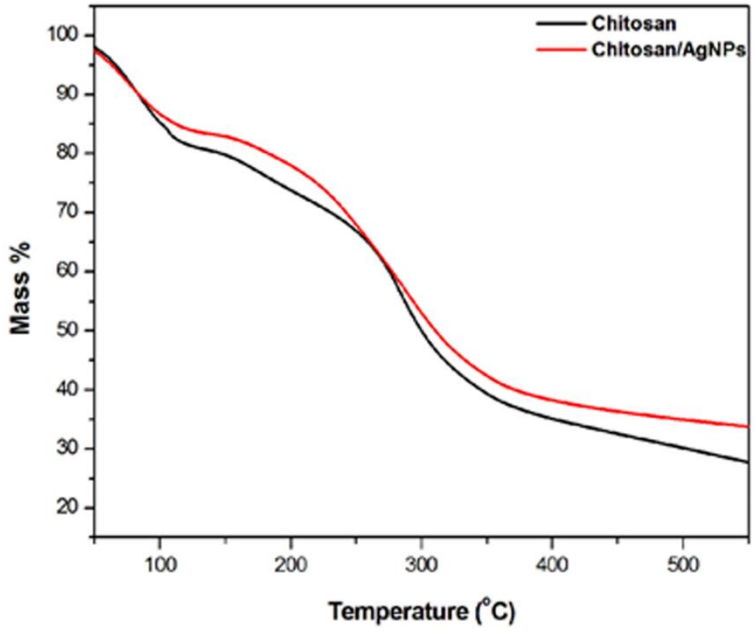

Figure 5.3 TGA curves of chitosan and chitosan-AgNPs films

5.3.2 Nanofibrous composite membrane

5.3.2.1 Morphology and chemical analysis

The SEM images, at different magnifications, of polyelectrolyte complex (PEC) composed of the electrospun alginate nanofibres immersed in a chitosan-AgNPs solution for 5 minutes are shown in Figure 5.4. The SEM images show many bright spherical particles on the surfaces of the nanofibres (indicated by arrows) and some were covered by a thin layer of polymer. These particles are probably AgNPs, because silver can scatter electrons more than polymers. It can, therefore, be deduced that the AgNPs were well impregnated in between the chitosan layer and the electrospun alginate nanofibres, and were well dispersed on the surfaces of the electrospun nanofibres without any observable agglomerations or clusters. The nanofibrous structure of the mats was also maintained.

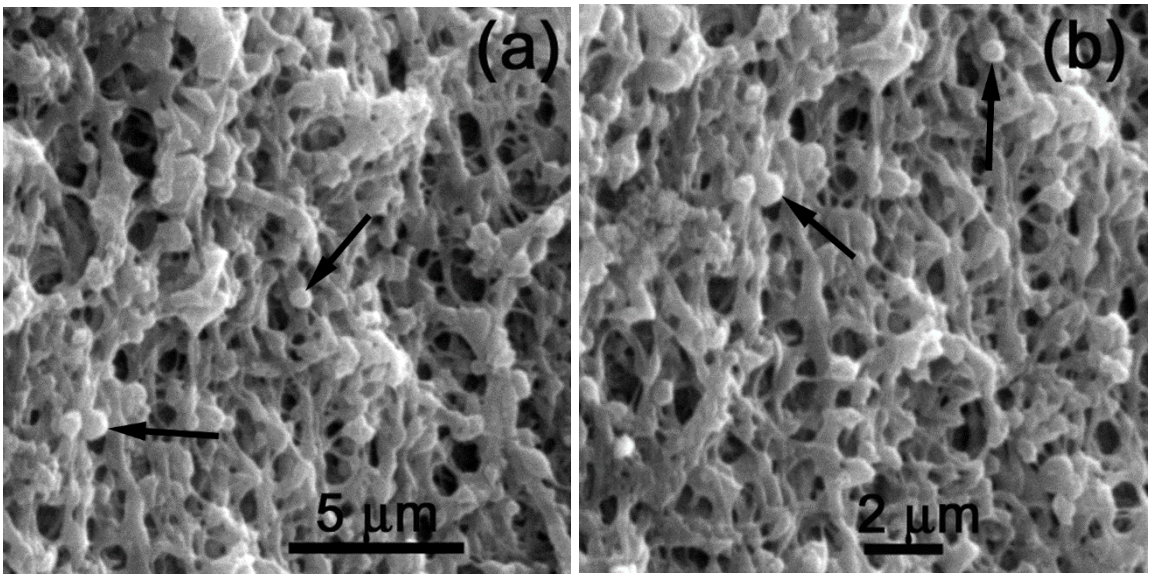

Figure 5.4 SEM images of polyelectrolyte complex (PEC_5min)

The SEM was equipped with energy dispersive X-ray spectroscopy (EDX) for elemental analysis as shown in Figure 5.5. As expected, the EDX analysis confirmed that all the characterized samples composed mainly of oxygen, calcium and carbon which resulted from the chitosan and alginate crosslinked with calcium. Small amounts of other elements such as chlorine, silicone, copper, iron, bromine, titanium and silver were also observed. It is not clear what the sources of the other particles were, but the silver is probably from the Ag-NPs. Interestingly, different immersion times led to different contents of silver ions in the PEC composites. Long immersion periods resulted in high silver ions contents. The most probable

explanation for this is that during the immersion process the chitosan/AgNPs solution adhered onto the nanofibrous alginate mat *via* complexation resulting in the AgNPs attaching to the surfaces of the fibres. Therefore, long immersion periods led to large numbers of AgNPs attached to the surfaces of the fibres with some penetrating into the porous nanofibrous structure.

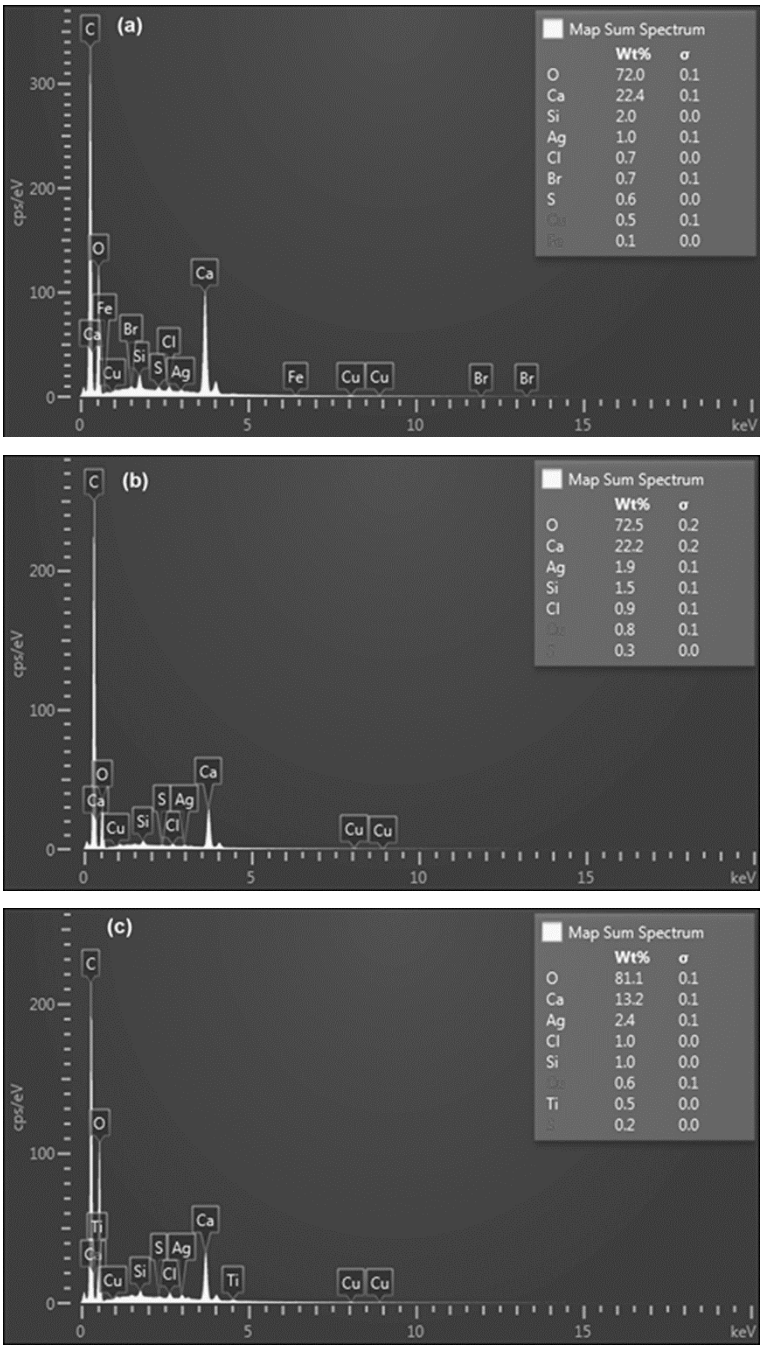

Figure 5.5 EDX spectra of (a) PEC_5 min, (b) PEC_10min and (c) PEC_15min

Figure 5.6 shows the ATR-FTIR spectra of PEC_5min, chitosan with AgNPs film (chitosan-AgNPs), chitosan film and electrospun alginate nanofibres (Alg). Chitosan displayed the

characteristic peaks in the infrared spectrum at 1648, 1543 and 1376 cm^{-1}, respectively representing amide I, amide II and amide III bands. The vibration band at 3255 cm^{-1}, assigned to the overlapped N-H and O-H stretching [27], shifted to higher wavenumbers due to the interaction of the silver with the N and O atoms in these groups [27,33,35]. The absorption peak at 1648 cm^{-1} shifted to 1639 cm^{-1}, the one at 1543 cm^{-1} to 1558 cm^{-1}, and the one at 1376 cm^{-1} to 1379 cm^{-1} after the synthesis of silver nanoparticles using chitosan. This is probably due to the attachment of synthesized silver nanoparticles to the chitosan through the lone pair interaction between the electron-rich nitrogen in the amino groups and the vacant orbitals in the silver [33]. Similar observations were reported by An *et al*. [33] in their study of the synthesis of silver nanoparticles using chitosan as stabilizing agent and sodium borohydride as reducing agent. They stated that the stretching peak of the NH_2 group at 1598 cm^{-1} shifted to 1567 cm^{-1} due to the formation of a chemical bond between the chitosan molecules and the Ag nanoparticles. Kumar-Krishna *et al*. [27] found that the bands at 3370 cm^{-1} (amine and hydroxyl groups) and 1556 cm^{-1} decreased in intensity and slightly shifted to lower wavenumbers as a result of the interaction of the primary amino groups in chitosan with the AgNPs surfaces. The crosslinked electrospun alginate nanofibres with Ca^{2+} displayed absorption peaks at 1422 and 1592 cm^{-1} due to the asymmetric and antisymmetric vibrations respectively of the carboxylate groups [36]. The IR spectrum of PEC_5min showed all the peaks that were observed in the alginate and chitosan-AgNPs absorption spectra. The absorption peak at 1592 cm^{-1} shifted to 1598 cm^{-1} which is probably due to the interaction between the carboxyl anions and the $-NH^{3+}$ groups of chitosan. Ribeiro *et al*. [37] studied alginate microspheres coated with chitosan and observed that the antisymmetric stretching at 1560 cm^{-1} shifted to 1573 cm^{-1} upon coating the alginate microspheres with chitosan due to complexation. Sharma *et al*. [35] studied an alginate-AgNPs-chitosan blend and observed a broad band from 1566 to 1647 cm^{-1} arising from the amide group of chitosan and the carboxyl anions of alginate resulting from complexation between the alginate and chitosan. These changes are similar to our findings, which confirms the complexation between chitosan and alginate.

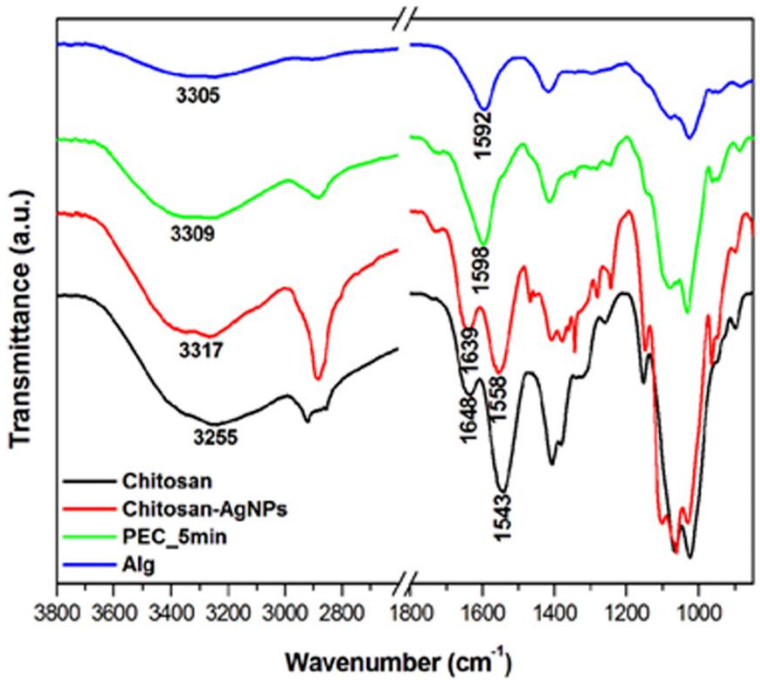

Figure 5.6 FTIR spectra of electrospun alginate nanofibres, chitosan, chitosan-AgNPs and PEC

5.3.2.3 X-ray diffraction (XRD) analysis

The XRD patterns of chitosan, chitosan-AgNPs and the PEC_5min nanofibrous composite are shown in Figure 5.7. The electrospun alginate shows a peak at 2θ = 13.35° and a broad halo from 22.67 to 39.06° corresponding to the (110) lattice plane from guluronate and an amorphous halo from the amorphous region [38,39]. Pure chitosan shows the characteristic peaks at 2θ = 11.66° and 19.49° associated with anhydrous crystals, whereas the amorphous part of the chitosan is represented by a broad peak that ranges from 20.30 to 37.56° [34]. The chitosan-AgNPs film shows well-defined peaks at 2θ = 38.28, 44.61, 64.50 and 77.62° assigned to the (111), (200), (220), and (311) lattice planes of the face centred cubic (fcc) structure of silver [33,35]. The sharp absorption peaks at 19.02° and 23.19° may be attributed to the organic compounds from chitosan that were responsible for the reduction and stabilization of the silver nanoparticles. The PEC nanofibrous composite shows well-defined peaks between 13.35 to 30.05° and very weak peaks at 2θ = 39.82° which were similar to those of the chitosan-AgNPs. Since the amount of AgNPs components in PEC was too small, with some of these nanoparticles impregnated in between the composite' components, the intensities of these peaks were weak in the pattern of the PEC nanofibrous composite. The results suggest the presence of silver nanoparticles that were mostly embedded between the alginate and chitosan ionic complex.

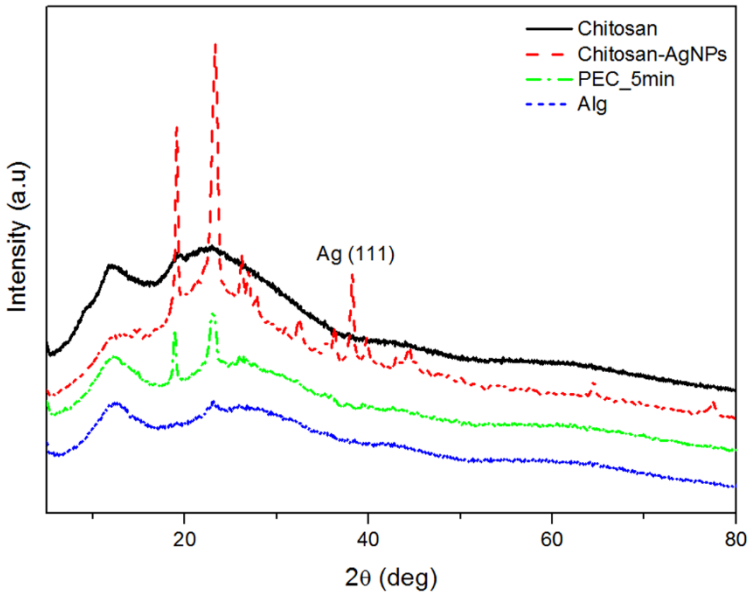

Figure 5.7 X-ray spectra of electrospun alginate nanofibres, chitosan, chitosan AgNPs and PEC nanofibrous composite

5.3.2.2 Antibacterial studies

For the antibacterial activity, the nanofibrous composite was immersed in chitosan-AgNPs for different time periods (5, 10 and 15 minutes, respectively denoted as PEC_5min, PEC_10min and PEC_15min) followed by washing and drying. The antibacterial activity was investigated through the agar well diffusion method (Figure 5.8 with results presented in Table 5.1).

Electrospun alginate nanofibres were used as a control to investigate the possibility of antibacterial efficiency without any additives. No inhibition zone against all strains was observed around the electrospun alginate nanofibres. The PEC exhibited a different antibacterial activity against four bacteria (two gram negative and two gram positive bacteria), regardless of the time of immersion of the electrospun mats in the chitosan-AgNPs solution. The inhibition zone increased with increasing immersion time of the electrospun alginate nanofibres in the chitosan-AgNPs solution. This could be due to a large number of the nanoparticles that were not captured into the porous nanofibrous structure and released during the incubation as confirmed by EDS (Figure 5.1). Silver nanoparticles are capable of inhibiting the bacterial growth due to their high surface area providing a good contact with the microbes. The proposed mechanism for the antibacterial effect of silver nanoparticles involves i) the attachment of AgNPs to the cell wall which disturbs the cell membrane permeability or disrupt the cell membrane, ii) the penetration of the AgNPs through the cell wall and their reaction with the thiol and phosphorus containing compounds which disturbs

the respiration and replication processes, and iii) the release of silver ions by the nanoparticles [40]. All these mechanisms contribute to the bacteriostatic and bactericidal effects of AgNPs.

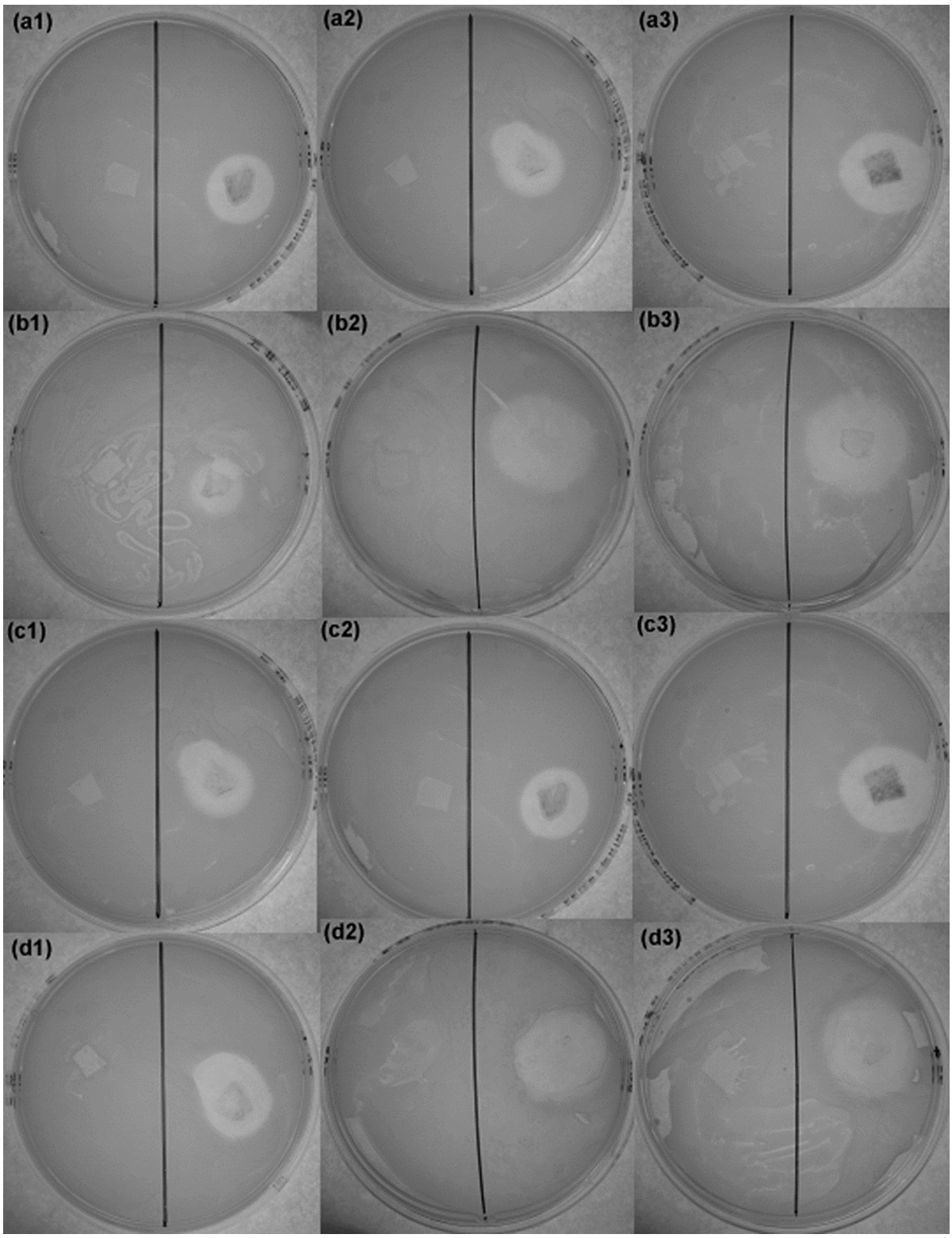

Figure 5.8 Antibacterial zone of inhibition against (a) K. pneumoniae, (b) E. coli, (c) B. pumilus, and (d) S. aureus; the left and right hand side of the plates are alginate (negative control) and PEC (1, 2 and 3 represents PEC_5min, PEC_10min and PEC_15 min)

Table 5.1 Comparison of the inhibition zones towards gram negative and gram positive

Sample	**Inhibition zone (cm)**	
	Gram negative	
	K. pneumoniae	**E. coli**
Alginate nanofibres	0	0
PEC_5 min	1.63 ± 0.14	1.42 ± 0.06
PEC_10 min	2.07 ± 0.18	1.77 ± 0.06
PEC_15 min	2.35 ± 0.13	3.04 ± 0.16
	Gram positive	
	B. pumilus	**S. aureus**
Alginate nanofibres	0	0
PEC_5min	1.91 ± 0.20	1.63 ± 0.19
PEC_10 min	2.12 ± 0.12	2.04 ± 0.16
PEC_15 min	2.40 ± 0.15	2.53 ± 0.26

5.3.2.3 Silver nanoparticles release

One of the important variables contributing to the antibacterial efficiency of a membrane is the rate at which it releases the silver atoms into the media. In order to measure the silver nanoparticle release from PEC, a certain quantity of the water containing PEC was extracted at varying time intervals followed by conductivity measurements (Figure 5.9a). For the first hour, the conductivity significantly increased for all the investigated samples and then levelled-off. PEC_15min, however, displayed higher conductivities than its counterparts, especially between 200 to 1400 minutes. This could be due to a large number of silver nanoparticles situated on top of the electrospun nanofibres. It is of interest to note that although the conductivity increased significantly for the first hour, there was only a slow increase after this before it levelled off, which implies that some of AgNPs were impregnated in between the alginate and chitosan ionic complex. There is thus a possibility that the AgNPs could be released over longer periods.

In order to understand the release mechanism of the PEC nanofibrous composite, the antibacterial kinetics using *E. coli* and *S. aureus* as model bacteria was investigated. Rectangular-shaped pieces of membrane from PEC_5min was placed inside glass tubes

containing the bacterial solutions (*E. coli* and *S. aureus*) of known colony forming units per ml (10^{-7} cfu ml^{-1}). A quantity of 1 ml of the bacterial solution was extracted at different time intervals, plated on agar plates, and incubated in order to calculate the number of colonies formed. A plot of colony forming units (cfu ml^{-1}) against time is shown in Figure 5.9b. The sample was able to eradicate more than 72% of gram negative and 98% of gram positive bacteria within an hour, which justifies the significant increase in the conductivity curves (Figure 5.9a). No growth was observed for gram negative and gram positive bacteria after 24 hours. This can be explained through the release of the silver ions into the solution due to the porous structure of the PEC nanofibrous composite. The porous structure assists in absorbing water which in turn helps in releasing the silver nanoparticles into the media. It is interesting to note that the impregnation of silver nanoparticles using complex formation between chitosan and alginate electrospun nanofibres could improve both fast and long antibacterial efficiency.

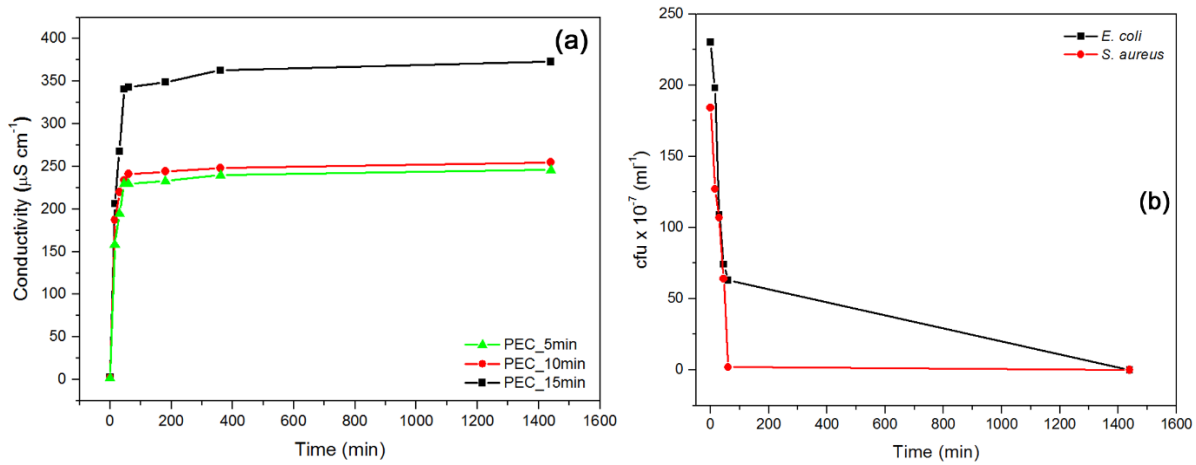

Figure 5.9 (a) Silver nanoparticles release and (b) antibacterial activity for PEC_5min nanofibrous composite membrane toward *E. coli* and *S. aureus*

5.4 Conclusions

AgNPs were successfully synthesized by thermal treatment using a biodegradable polymer, chitosan, as a stabilizing and reducing agent. The AgNPs synthesized were successfully impregnated into electrospun nanofibrous alginate by complexation with chitosan. The nanoparticles were well dispersed on the surfaces of the electrospun nanofibres, with some covered with polymer, which influenced their release into the medium. The PEC nanofibrous composite obtained, showed high antibacterial activity towards gram negative and gram positive bacteria for short and long periods of time. Our results demonstrated that it is

possible to generate a nanofibrous composite with sustained release of silver nanoparticles which can be utilized for biomedical or wastewater treatment.

5.5 References

[1] N. Bhardwaj, S.C. Kundu, Electrospinning: a fascinating fiber fabrication technique, Biotechnology Advances, 28 (2010) 325-347.

[2] A. Greiner, J.H. Wendorff, Electrospinning: a fascinating method for the preparation of ultrathin fibers, Angewandte Chemie International Edition, 46 (2007) 5670-5703.

[3] Z.-M. Huang, Y.-Z. Zhang, M. Kotaki, S. Ramakrishna, A review on polymer nanofibers by electrospinning and their applications in nanocomposites, Composites Science and Technology, 63 (2003) 2223-2253.

[4] S. Ramakrishna, K. Fujihara, W.-E. Teo, T. Yong, Z. Ma, R. Ramaseshan, Electrospun nanofibers: solving global issues, Materials Today, 9 (2006) 40-50.

[5] F. Miao, C. Shao, X. Li, K. Wang, N. Lu, Y. Liu, Electrospun carbon nanofibers/carbon nanotubes/polyaniline ternary composites with enhanced electrochemical performance for flexible solid-state supercapacitors, ACS Sustainable Chemistry & Engineering, 4 (2016) 1689-1696.

[6] A.A. Taha, Y.-N. Wu, H. Wang, F. Li, Preparation and application of functionalized cellulose acetate/silica composite nanofibrous membrane via electrospinning for Cr (VI) ion removal from aqueous solution, Journal of Environmental Management, 112 (2012) 10-16.

[7] M. Aliabadi, M. Irani, J. Ismaeili, S. Najafzadeh, Design and evaluation of chitosan/hydroxyapatite composite nanofiber membrane for the removal of heavy metal ions from aqueous solution, Journal of the Taiwan Institute of Chemical Engineers, 45 (2014) 518-526.

[8] S. Lee, Multifunctionality of layered fabric systems based on electrospun polyurethane/zinc oxide nanocomposite fibers, Journal of Applied Polymer Science, 114 (2009) 3652-3658.

[9] J. Ning, X. Zhang, H. Yang, Z.-L. Xu, Y.-M. Wei, Preparation of porous PVDF nanofiber coated with Ag NPs for photocatalysis application, Fibers and Polymers, 17 (2016) 21-29.

[10] J. Dolina, T. Jiříček, T. Lederer, Membrane modification with nanofiber structures containing silver, Industrial & Engineering Chemistry Research, 52 (2013) 13971-13978.

[11] X. Zhuang, B. Cheng, W. Kang, X. Xu, Electrospun chitosan/gelatin nanofibers containing silver nanoparticles, Carbohydrate Polymers, 82 (2010) 524-527.

[12] N.A.M. Barakat, M.F. Abadir, F.A. Sheikh, M.A. Kanjwal, S.J. Park, H.Y. Kim, Polymeric nanofibers containing solid nanoparticles prepared by electrospinning and their applications, Chemical Engineering Journal, 156 (2010) 487-495.

[13] M. Venkatesham, D. Ayodhya, A. Madhusudhan, N.V. Babu, G. Veerabhadram, A novel green one-step synthesis of silver nanoparticles using chitosan: catalytic activity and antimicrobial studies, Applied Nanoscience, 4 (2014) 113-119.

[14] S. Lankalapalli, V.M. Kolapalli, Polyelectrolyte complexes: a review of their applicability in drug delivery technology, Indian Journal of Pharmaceutical Sciences, 71 (2009) 481.

[15] C. Tapia, Z. Escobar, E. Costa, J. Sapag-Hagar, F. Valenzuela, C. Basualto, M.N. Gai, M. Yazdani-Pedram, Comparative studies on polyelectrolyte complexes and mixtures of chitosan-alginate and chitosan-carrageenan as prolonged diltiazem clorhydrate release systems, European Journal of Pharmaceutics and Biopharmaceutics, 57 (2004) 65-75.

[16] J.-P. Chen, G.-Y. Chang, J.-K. Chen, Electrospun collagen/chitosan nanofibrous membrane as wound dressing, Colloids and Surfaces A: Physicochemical and Engineering Aspects, 313 (2008) 183-188.

[17] Z. Chen, B. Wei, X. Mo, C.T. Lim, S. Ramakrishna, F. Cui, Mechanical properties of electrospun collagen-chitosan complex single fibers and membrane, Materials Science and Engineering: C, 29 (2009) 2428-2435.

[18] M. Yadollahi, S. Farhoudian, H. Namazi, One-pot synthesis of antibacterial chitosan/silver bio-nanocomposite hydrogel beads as drug delivery systems, International Journal of Biological Macromolecules, 79 (2015) 37-43.

[19] K. Sugiura, K. Ohkawa, T. Hirai, T. Fujii, ATPase-coupled release control from polyion complex capsules encapsulating muscle proteins, Macromolecular Bioscience, 7 (2007) 508-516.

[20] A.C. Wan, E.K. Yim, I. Liao, C. Le Visage, K.W. Leong, Encapsulation of biologics in self-assembled fibers as biostructural units for tissue engineering, Journal of Biomedical Materials Research Part A, 71 (2004) 586-595.

[21] H. Yamamoto, C. Horita, Y. Senoo, A. Nishida, K. Ohkawa, Polyion complex fiber and capsule formed by self-assembly of poly-L-lysine and gellan at solution interfaces, Journal of Applied Polymer Science, 79 (2001) 437-446.

[22] M.V.R. Rigo, D.A. Allemandi, R.H. Manzo, Swellable drug–polyelectrolyte matrices (SDPM) of alginic acid: Characterization and delivery properties, International Journal of Pharmaceutics, 322 (2006) 36-43.

[23] S.I. Jeong, M.D. Krebs, C.A. Bonino, J.E. Samorezov, S.A. Khan, E. Alsberg, Electrospun chitosan-alginate nanofibers with in situ polyelectrolyte complexation for use as tissue engineering scaffolds, Tissue Engineering Part A, 17 (2010) 59-70.

[24] H. Huang, X. Yang, Synthesis of chitosan-stabilized gold nanoparticles in the absence/presence of tripolyphosphate, Biomacromolecules, 5 (2004) 2340-2346.

[25] N. Yang, W.-H. Li, Preparation of gold nanoparticles using chitosan oligosaccharide as a reducing and capping reagent and their in vitro cytotoxic effect on Human fibroblasts cells, Materials Letters, 138 (2015) 154-157.

[26] D. Wei, W. Sun, W. Qian, Y. Ye, X. Ma, The synthesis of chitosan-based silver nanoparticles and their antibacterial activity, Carbohydrate Research, 344 (2009) 2375-2382.

[27] S. Kumar-Krishnan, E. Prokhorov, M. Hernández-Iturriaga, J.D. Mota-Morales, M. Vázquez-Lepe, Y. Kovalenko, I.C. Sanchez, G. Luna-Bárcenas, Chitosan/silver nanocomposites: Synergistic antibacterial action of silver nanoparticles and silver ions, European Polymer Journal, 67 (2015) 242-251.

[28] C.-M. Shih, Y.-T. Shieh, Y.-K. Twu, Preparation of gold nanopowders and nanoparticles using chitosan suspensions, Carbohydrate Polymers, 78 (2009) 309-315.

[29] M.J. Laudenslager, J.D. Schiffman, C.L. Schauer, Carboxymethyl chitosan as a matrix material for platinum, gold, and silver nanoparticles, Biomacromolecules, 9 (2008) 2682-2685.

[30] S. Huang, J. Wang, Y. Zhang, Z. Yu, C. Qi, Quaternized carboxymethyl chitosan-based silver nanoparticles hybrid: Microwave-assisted synthesis, characterization and antibacterial activity, Nanomaterials, 6 (2016) 1-13.

[31] C. Sun, R. Qu, H. Chen, C. Ji, C. Wang, Y. Sun, B. Wang, Degradation behavior of chitosan chains in the ‘green’synthesis of gold nanoparticles, Carbohydrate Research, 343 (2008) 2595-2599.

[32] D. de Britto, S.P. Campana-Filho, Kinetics of the thermal degradation of chitosan, Thermochimica Acta, 465 (2007) 73-82.

[33] J. An, Q. Luo, X. Yuan, D. Wang, X. Li, Preparation and characterization of silver-chitosan nanocomposite particles with antimicrobial activity, Journal of Applied Polymer Science, 120 (2011) 3180-3189.

[34] Z.H Mbhele, M.G. Salemane, C.G.C.E. van Sittert, J.M. Nedeljković, V. Djokovic, A.S. Luyt, Fabrication and characterization of silver-polyvinyl alcohol nanocomposites, Chemistry of Materials, 15 (2003) 5019-5024

[35] S. Sharma, P. Sanpui, A. Chattopadhyay, S.S. Ghosh, Fabrication of antibacterial silver nanoparticle-sodium alginate-chitosan composite films, RSC Advances, 2 (2012) 5837-5843.

[36] G. Lawrie, I. Keen, B. Drew, A. Chandler-Temple, L. Rintoul, P. Fredericks, L. Grøndahl, Interactions between alginate and chitosan biopolymers characterized using FTIR and XPS, Biomacromolecules, 8 (2007) 2533-2541.

[37] A.J. Ribeiro, C. Silva, D. Ferreira, F. Veiga, Chitosan-reinforced alginate microspheres obtained through the emulsification/internal gelation technique, European Journal of Pharmaceutical Sciences, 25 (2005) 31-40.

[38] S. Hua, H. Ma, X. Li, H. Yang, A. Wang, pH-sensitive sodium alginate/poly (vinyl alcohol) hydrogel beads prepared by combined Ca^{2+} crosslinking and freeze-thawing cycles for controlled release of diclofenac sodium, International Journal of Biological Macromolecules, 46 (2010) 517-523.

[39] J. Fabia, Cz. Ślusarczyk, A. Gawlowski, Supermolecular structure of alginate fibres for medical aplications studied by means of WAXS and SAXS methods, Fibres & Textiles in Eastern Europe, 13 (2005) 114-117.

[40] P. Kanmani, J.-W. Rhim, Physicochemical properties of gelatin/silver nanoparticle antimicrobial composite films, Food Chemistry, 148 (2014) 162-169.

Chapter 6

Development of multifunctional nano/ultrafiltration membrane based on a chitosan thin film on alginate electrospun nanofibres

This chapter has been submitted for publication as:
T.C. Mokhena, A.S. Luyt, Development of multifunctional nano/ultrafiltration membrane based on a chitosan thin film on alginate electrospun nanofibers, Journal of Environmental Management.

Abstract

The aim of this study was to develop a high flux three-tier composite membrane composed of a coating layer based on chitosan and chitosan with silver nanoparticles, electrospun alginate nanofibres as a midlayer and nonwoven as a mechanical support substrate. The nanofibres were prepared by electrospinning of alginate with the aid of synthetic electrospinnable polyethylene oxide (PEO), and ionically crosslinked with calcium chloride followed by chemical crosslinking by using glutaraldehyde. The silver nanoparticles were synthesized using a chitosan solution and thermal treatment. The silver nanoparticles were found to be well dispersed on the coating layer, which improved the antibacterial activity of the membrane against gram negative and gram positive bacteria. The chitosan and silver nanoparticles containing chitosan-coated membrane displayed similar flux and rejection ratios. Both membranes showed a high flux rate and a high rejection of nanoparticles (> 98%) and oil emulsions (> 93%) when compared to a commercial membrane. These observations show that the incorporation of silver nanoparticles can enhance the antibacterial activity of the membrane without hampering the membrane productivity.

Keywords: Electrospun alginate; Chitosan; Silver nanoparticles; Filtration membrane; Water purification

6.1 Introduction

An ideal filtration membrane must have high selectivity and flux, long service life and low energy consumption [1]. Efforts for achieving this goal are leading to the replacement of the traditional filtration membranes with new advanced thin-film composite (TFC) membranes [2,3]. TFC membranes are composed of two or more different layers, i) a top thin selective barrier, ii) a porous mid-layer, and iii) a bottom mechanical support layer. These conventional TFC membranes are typically made from synthetic polymers such as polyethersulphone, polyacrylonitrile, polyimide, aliphatic polyamide, poly(vinyl fluoride) and polyetherether ketone *via* a phase immersion process [1]. This process leads to some limitations such as low flux and high fouling due to an asymmetrical pore structure and a relatively broad pore size distribution [4,5]. Nowadays, a lot of research is being devoted to the production of nanofibre-based TFC membranes, especially from electrospinning [2,4]. It was demonstrated that these membranes exhibit high flux with the same filtration efficiency, because of the inherent properties of electrospun nanofibres. They have high porosity, interconnected pores and tuneable pore sizes, which can overcome the limitations of conventional TFC membranes [1,2,4].

Despite the good properties and productivity of nanofibrous-based TFC membranes, most of these membranes are usually made from synthetic polymers and they contribute to environmental pollution when disposed [2,6]. In this study, we demonstrate the production and use of high flux TFC membranes made of natural polymers, which are chitosan as coating layer and electrospun alginate as mid-layer. Chitosan is a biodegradable polysaccharide polymer derived from the second most available natural polymer on earth, chitin [5,7,8]. Chitin is found on the exoskeleton of crustaceans, crabs and shrimp shells, insects and fungal mycelia [5,8]. It can also be obtained from the wastes of mushrooms such as *Agaricus bisporus*. More than 1000 metric tons/year of chitin is generated from mushroom wastes [5]. Chitosan is generated from the deacetylation of chitin. It is composed of N-acetyl-D-glucosamine and D-glucosamine monomeric units [5,9]. The D-glucosamine content is directly dependent on the degree of chitin deacetylation. A high degree of deacetylation would lead to a large number of positively charged groups on the chitosan backbone, which mainly contribute to its unique properties such as chelation of metal ions and inhibition for the growth of a variety of fungi, yeasts and microorganisms [5,7]. Desai *et al*. [5] fabricated nanofibrous filter media by electrospinning PEO/chitosan blend solutions onto a spunbonded

non-woven propylene substrate. They reported a 2-3 log reduction in the *E. coli* cfu with only 6 hours contact time due to the presence of protonated amine groups. Chitosan has also been used as barrier layer to improve the antifouling and selectivity of the filtration membrane [4,5,10]. Yoon *et al*. [4] prepared a high flux nanofiltration (NF) medium based on electrospun polyacrylonitrile (PAN) coated with chitosan. The membrane exhibited an order of magnitude higher flux rate than a commercial NF filter, while maintaining high filtration efficiency with a rejection ratio greater than 99.9% when compared to commercial NF.

Alginate has been selected due to its strong interaction with chitosan *via* complexation. It is a linear polysaccharide copolymer composed of two monomeric units, β-D-mannuronic acid and α-L-guluronic acid [8,11]. It is extracted from brown seaweeds (algae) [11]. Recently, alginate has been studied as a part of the membranes employed to enhance antifouling [12-14]. Guo *et al*. [14] prepared a three-tier membrane composed of calcium alginate/carbon nanotubes as selective layer, electrospun polyhydroxybutyrate (PHB)-calcium alginate as midlayer, and PHB nanofibrous substrate. The membrane displayed a flux of 36.72 L m^{-2} h^{-1} for pure water and 30.85 L m^{-2} h^{-1} for oil emulsions after 60 minutes of filtration, and the rejection of oil emulsions was 98% due to its hydrophilic nature and good antifouling property. The flux for Brilliant Blue was 32.95 L m^{-2} h^{-1} with a rejection rate of 98.20%.

In this study, we attempted to develop a water filtration membrane composed mostly of natural polymers. Three-tier composite membranes composed of alginate nanofibres, electrospun onto a mechanical support layer of non-woven polyethylene terephthalate (PET) fabric as a midlayer, and coated with either chitosan (CaA-CS) or silver nanoparticles containing chitosan (CaA-AgNPs) as selective barrier layer, were fabricated. The silver nanoparticles were synthesized by using chitosan as reducing and at the same time, a capping agent *via* thermal treatment. Dual crosslinking (calcium and glutaraldehyde) was utilized to improve the stability of electrospun alginate nanofibres in water. The membranes were characterized in order to evaluate their performance when compared to the commercially available membranes. This work opens up a new dimension that explores a combination of, and the use of, abundant available natural polymers for filtration applications.

6.2. Materials and methods

6.2.1 Materials

Poly(ethylene oxide) (PEO), sodium alginate (SA), chitosan (CS), dimethylsulphoxide (DMSO), Triton^{TM} 100 and glutaraldehyde (GA) were purchased from Sigma Aldrich, South Africa. Silver nitrate ($AgNO_3$) was obtained from Ibhayi Laboratory Supplies, South Africa. Congo Red was purchased from Fluka Chemical Cooperation, South Africa. Commercial membrane (PLAC07610) (PLA) regenerated cellulose-based with a molecular weight cut-off (MWCO) of 1 kDa was purchased from Millipore, South Africa.

6.2.2 Fabrication of composite membrane

The PEO/SA nanofibres were prepared by dissolving PEO (3 wt%) and SA (3 wt%) separately in deionized water. A 50/50 v/v% mixture of the PEO and SA solutions was stirred for 4 hours and stored in an environmental chamber (Binder GmBH) set at ~25 °C for 10 days. 0.5 wt% Triton X-100 and 5 wt% DMSO were added to the mixture in order to improve the nanofibrous structure of the resulting fibres. The blend solution was added into a 20 ml syringe mounted onto a syringe pump. The solution feeding rate was 0.7 ml hr^{-1}, the voltage was 25 kV and the tip-to-collector distance was 18 cm. The nanofibres were then ionically crosslinked with calcium chloride by soaking it in 80% ethanol for 5 min and rinsing it with a 2 wt% $CaCl_2$ in ethanol solution for 10 min. The nanofibres were incubated in an aqueous solution of $CaCl_2$ for an hour, and then immersed in deionized water for another hour. The $CaCl_2$ treated membranes were then rinsed with deionized water, followed by washing with absolute ethanol, and dried at room temperature. For filtration analysis, the alginate was electrospun onto a PET nonwoven fabric that was provided by the Council for Scientific and Industrial Research (CSIR), Port Elizabeth. The membrane was further crosslinked with glutaraldehyde vapour in a desiccator at room temperature for 24 hours. The pH value of the glutaraldehyde solution was adjusted to 3 by using hydrochloric acid, and the glutaraldehyde concentrations were varied from 0.01 M to 0.1 M in order to obtain the optimal concentration. Finally, the chitosan-containing-silver nanoparticles solutions were coated onto the nanofibrous membrane. The chitosan-containing-silver nanoparticles (AgNPs) was obtained by mixing 0.07 wt% chitosan and 10 mM silver nitrate, and heated at 90 °C for 12 hours. 2 wt% of chitosan was mixed with 0.07 wt% of chitosan-containing AgNPs at 50/50 v/v to increase the viscosity of the solution in order to control the infusion of the solutions into the

mats. A similar procedure was followed in the case of the non-silver containing chitosan solutions. The membranes' acronyms and descriptions are given in Table 6.1.

Table 6.1 Abbreviations and their descriptions for the membranes used in this study

Abbreviations	Description
CaA	Ionically crosslinked alginate
Ga-CaA	Glutaraldehyde crosslinked electrospun alginate
CaA-CS	Glutaraldehyde crosslinked electrospun alginate coated with chitosan
CaA-AgNPs	Glutaraldehyde crosslinked electrospun alginate coated with chitosan-containing AgNPs
PLA	Commercial ultrafiltration membrane (PLAC07610)

6.2.3 Structural characterization

The IR spectra were obtained using a Perkin Elmer Spectrum 100 FTIR spectrometer equipped with an attenuated total reflection (ATR) accessory with a diamond/ZnSe crystal (16 scans, 4 cm^{-1} resolution, and wavenumber range of 500-4000 cm^{-1}).

The morphology and composition of the electrospun nanofibres and nanofibrous composite materials were examined by a TESCAN VEGA-II scanning electron microscope (SEM) equipped with an energy dispersive X-ray analyser (EDX) for elemental analysis.

BET analyses of the composite membranes, before and after coating with chitosan solutions, were carried out in order to evaluate their specific surface areas and average pore sizes.

6.2.4 Antibacterial studies

The antibacterial activity of the nanofibrous composites towards gram negative (*Escherichia coli (ATCC 8739)* and gram positive (*Staphylococcus aureus (ATCC 6538)* was investigated by an agar well diffusion method. The bacteria were spread on the surface of the nutrient agar medium and the nanofibrous membranes were placed on the agar plate surface. The samples were incubated overnight at 37°C, and the resulting inhibition zones were measured.

6.2.5 Water permeability and nanoparticles separation test

Water permeability was determined using an Amicon® stirred ultrafiltration cell model 8400 which was able to withstand a maximum pressure of 75 psi, with a feed capacity of 400 ml. The pressure was applied by using nitrogen gas to the feed solution, and the time required to pass equal volumes of solution through the membranes was measured. This test was performed using pressures ranging from 3 to 36 psi and the flux (J) was calculated using Equation 1.

$$J = \frac{Q}{A \times T} \qquad (1)$$

where Q is the permeation volume of water, A is the effective membrane area, and T is the testing time.

For the removal of contaminants from water streams, silica nanoparticles were used as model contaminants. 0.05 g of SiO_2 (10-35 nm) were dispersed in water by sonication for 15 minutes and allowed to pass through the membranes by using the Amicon® stirred ultrafiltration cell model 8400 at ambient temperature, and the pressure was kept at 3 psi. The transmittance of both the feed and filtrate solutions were measured from 300 to 900 nm with a Shimadzu UV-3100 (190-1100 nm) UV-Vis-NIR recording spectrophotometer at a resolution of 0.5 nm. The concentrations of the mixtures were determined by the UV-vis method.

The rejection percentage (R) of the particulates by the composite membrane was calculated by using Equation 2.

$$R(\%) = \left(\frac{C_f - C_i}{C_f}\right) \times 100 \qquad (2)$$

where C_f is the concentration of the feed solution and C_i is the concentration of the filtrate.

6.2.6 Oil/water separation

In order to evaluate the oil/water separation ability of the membrane systems, oily wastewater was prepared by mixing vegetable oil with distilled water and surfactant for 20 minutes using

a homogenizer at 5000 rpm. A circular membrane with a diameter of 76 mm and an effective area of 41.8 cm^2 was fixed into the Amicon® ultrafiltration stirred cell and 20 ml of the oil solution was filtered through the membrane at ambient conditions and pressure of 3 psi. The transmittance of the feed and permeates were measured with a Shimadzu UV-3100 (190-1100 nm) UV-Vis-NIR recording spectrophotometer and the rejection percentage was calculated by using Equation 2.

6.2.7 Dye removal

For the evaluation of the dye removal efficiency of the membranes, Congo Red (CR) was used as a model dye. A circular membrane with 76 mm diameter and effective area of 41.8 cm^2 was fixed into the Amicon® ultrafiltration stirred cell and 50 ml of CR solution was filtered through the membrane at ambient conditions and a pressure of 0.3 psi. The filtration process was repeated 5 times and the membranes were flushed with pure water after each filtration cycle. The concentration of the dye was then measured with a Shimadzu UV-3100 (190-1100 nm) UV-Vis-NIR recording spectrophotometer. The amount of dye removed was calculated from the concentration change before and after filtration, as determined by optical absorption at 498 nm using Equation 2.

6.3. Results and discussion

6.3.1 Electrospun alginate nanofibres

To find the optimum concentration of glutaraldehyde, the swelling properties of the chemically crosslinked fibres were studied by immersion in water for 24 hours to ascertain the optimum glutaraldehyde concentration for crosslinking the alginate fibres (Figure A.1). It was found that chemical crosslinking reduced the swelling of the fibres from ~160% to less than 50% by using 0.1 M of glutaraldehyde for 24 hours. Concentrations higher than 0.1 M led to considerable shrinkage and a colour change of the mats to yellowish (Figure A.2 in the Appendix). Thus, fibres treated with 0.1 M glutaraldehyde for 24 hours were used throughout the study. The SEM images of the electrospun nanofibre membranes of the PEO/sodium alginate blend (PEO/SA), as well as calcium crosslinked (CaA) and the dual crosslinked (calcium and glutaraldehyde crosslinked (GA-CaA)) alginate nanofibres, are shown in Figure 6.1. In the case of the PEO/SA blends solution, well defined nanofibres without any structural

defects were obtained (Figure 6.1(a)). The mean diameter of the fibres was approximately 97.4 ± 20.3 nm. After the ionic crosslinking using calcium chloride (CaA), the fibres interfused into an interlocked network structure (Figure 6.1(b)). Some of these fibres adhered to each other at different bonding sites to form a film-like structural integrity, while the fibres maintained their nanofibrous structure. However, the average diameter of the fibres slightly increased to 144 ± 48 nm, which could be due to the swelling of the fibres during dissolution of PEO. The dual crosslinking (Ga-CaA) led to a significant binding of the fibres and the diameter (152 ± 45 nm) of the fibres was not significantly influenced when compared to that of the ionically crosslinked fibres (Figure 6.1(c)).

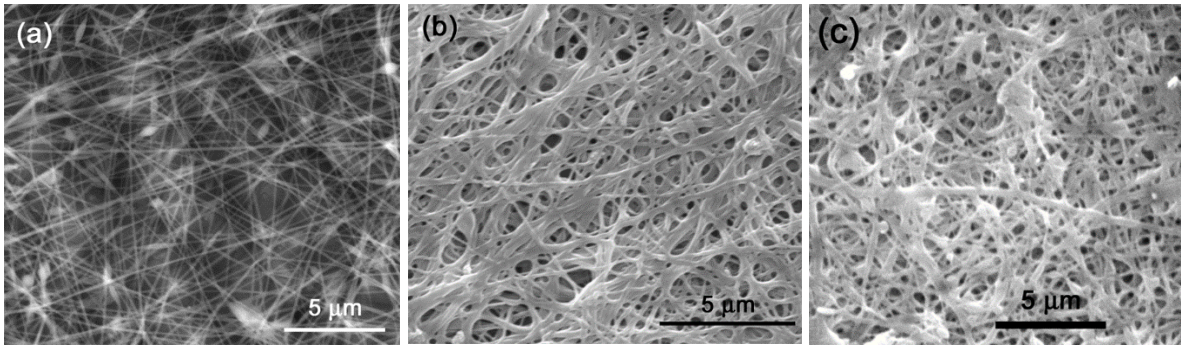

Figure 6.1 SEM images of (a) PEO/SA, (b) ionically crosslinked alginate (CaA), and (c) glutaraldehyde crosslinked nanofibres (Ga-CaA)

The IR spectra for the different electrospun nanofibre membranes are shown in Figure 6.2. The CaA nanofibres displayed absorption bands at 3268, 1589, 1414, and 1026 cm^{-1} corresponding to –OH stretching, COO^- asymmetric stretching, COO^- symmetric stretching and C-O-C stretching, respectively. All these vibrations correspond to those of the pure alginate [8,15]. The electrospun PEO/SA blend fibres showed similar peaks to those of the CaA nanofibres, with additional peaks at 2881 cm^{-1} (CH stretching), 1456 cm^{-1} (CH_2 wagging), 1100 and 839 cm^{-1} (C-O-C stretching and bending), and 960 cm^{-1} corresponding to CH_2 rocking and twisting. These peaks are related to the presence of PEO, and they disappeared after ionic crosslinking because of the washing of the fibres in water during which the PEO was removed through dissolution. After chemical crosslinking with glutaraldehyde, the -OH stretching peak at 3268 cm^{-1} shifted to 3338 cm^{-1} because the -OH groups would have taken part in the formation of acetyl bridges between the alcohol groups in the alginate and the aldehydes in glutaraldehyde [16,17]. Leung *et al*. [17] observed a similar shift in the -OH stretching after crosslinking with glutaraldehyde because of the reaction between the alginate and glutaraldehyde. The new absorption peaks at 1345 cm^{-1}, 839 cm^{-1}

and 959 cm^{-1} correspond to the C-O-C vibrations from the acetyl rings and ether linkages. The presence of these peaks, the shift in the -OH peak, and the presence of a new peak at 1345 cm^{-1} confirmed the crosslinking of the alginate with glutaraldehyde through the formation of acetyl and ethyl linkages [16]. The absorption bands at 2860 (C-H stretching) and 1606 cm^{-1} (C=O stretching) became better resolved are ascribed to the aldehyde groups [17]. In the crosslinking of the alginate with glutaraldehyde, only one aldehyde group is often used for two carboxyl groups from the alginate [16]. Therefore, the increase in intensity and sharpening of these absorption bands is probably due to the unreacted aldehydes on the surfaces of the alginate polymer chains. This is confirmed by an increase in the intensity of these peaks with increasing in concentration (see Figure A.3 in the Appendix).

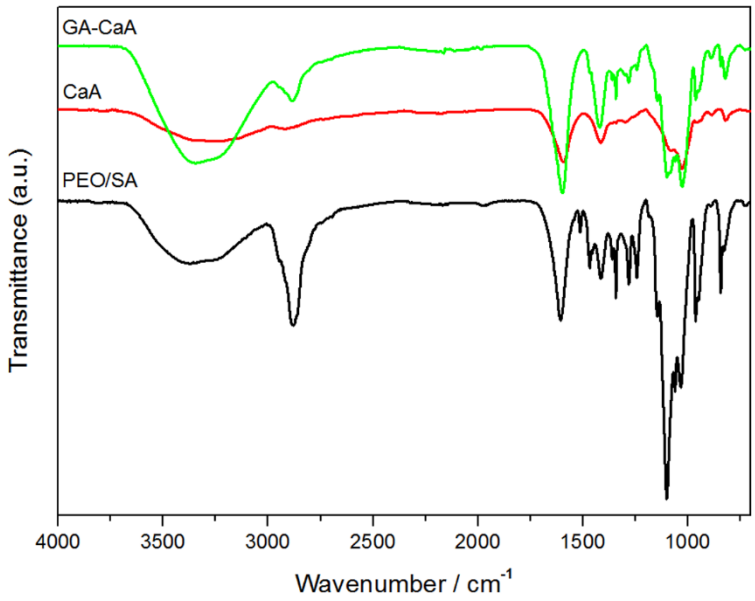

Figure 6.2 FTIR spectra of uncrosslinked and crosslinked alginate nanofibres

6.3.2 Nanofibrous composite membrane

Figure 6.3 shows the surface morphology of CaA-CS and CaA-AgNPs. The chitosan-coated membrane shows a smooth and flat surface (Figure 6.3(a)), while in the chitosan/AgNPs-coated membrane the layer was rough with white spots well dispersed throughout the micrograph (Figure 6.3(b)). These spots can be attributed to silver nanoparticles, since they can scatter electrons more than the polymer.

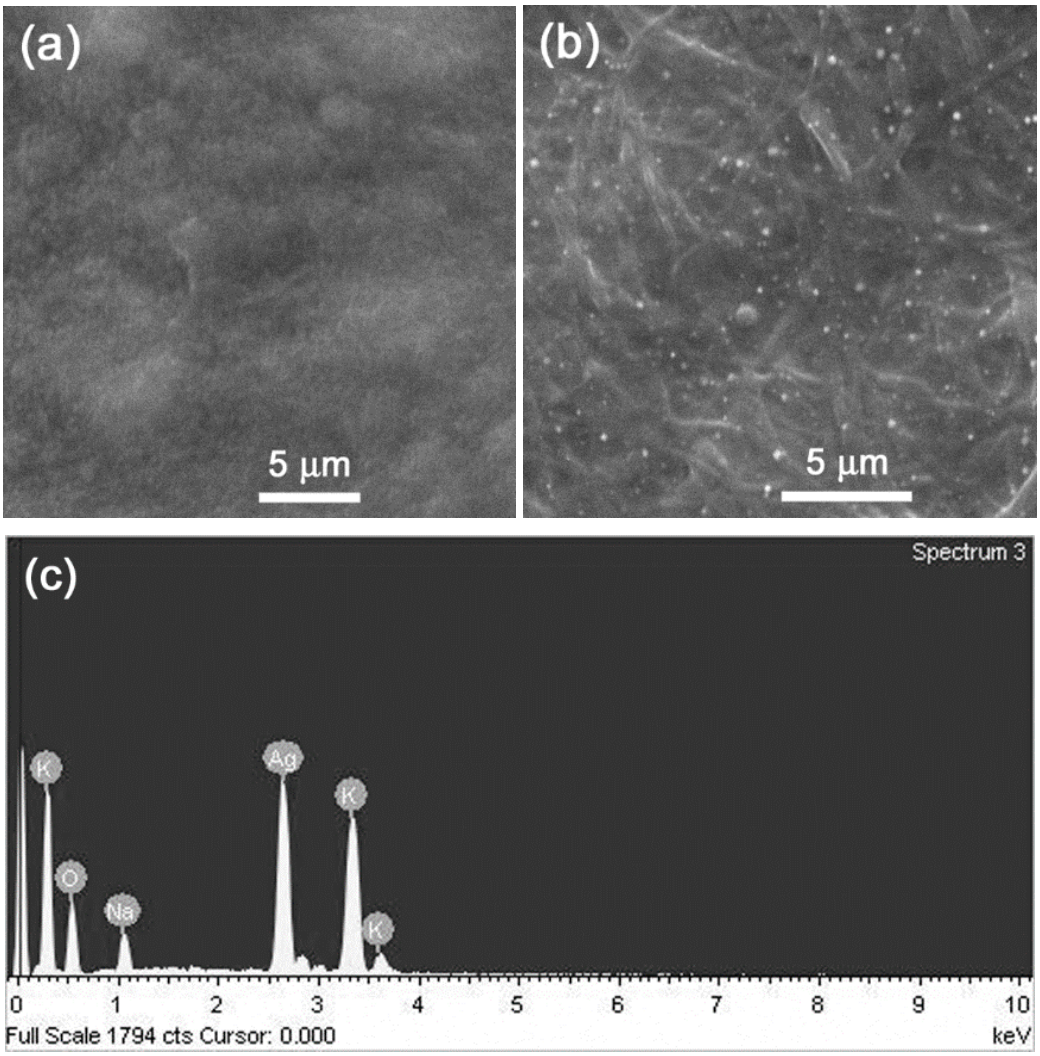

Figure 6.3 SEM micrographs of (a) CaA-CS, (b) CaA-AgNPs and (c) EDX spectra of CaA-AgNPs

The presence of silver nanoparticles was confirmed by EDX as shown in Figure 6.3(c). There is a strong signal for silver at approximately 2.7 keV. This is the result of the surface plasmon of silver which confirms the reduction of the silver ions to elemental silver. Guzman *et al*. [18] and Kaviya *et al*. [19] reported emission peaks for silver nanoparticles at approximately 3 keV. There are also signals for other elements such as oxygen, sodium, and potassium. The presence of oxygen is probably originates from chitosan. Sodium and potassium were contaminants in the silver nitrate, that were mentioned in the manufacturer' specification data sheet.

The antibacterial efficiency of the composite membranes was evaluated by the zone inhibition method (Figure 6.4 and the results are tabulated in Table 6.2). Glutaraldehyde crosslinked

electrospun alginate nanofibres were used as a control, and no inhibition zone against all strains was observed around its mats (area 1 in Figures 6.4(a) and 6.4(b)). The CaA-CS membrane showed a bacteriostatic effect towards *E. coli* (area 2 in Figure 6.4(a)). This is due to the positive charges on the surface of chitosan which can easily react with the negatively charged bacteria and inhibit the bacterial growth on the mat when compared to the positively charged bacteria [9]. The CaA-AgNPs membrane showed high potency towards *E. coli* and *S. aureus* (area 3 in Figures 6.4(a) and 6.4b)). This is due to the presence of silver nanoparticles. The *E. coli* showed more susceptibility than the *S. aureus*, probably because of the synergistic effect between the chitosan and silver nanoparticles acting towards the gram negative bacteria. The *S. aureus* has a thicker peptidoglycan in the cell wall than the *E. coli*, which acts against the invasion of the AgNPs [20,21]. Silver nanoparticles are well-known for their high potency towards gram negative and gram positive bacteria [21]. However, the exact mechanism of their antibacterial activity is not fully understood and three mechanisms were proposed [18,20,22]. Firstly, the silver nanoparticles (AgNPs) attach to the cell membrane and compromise permeability and respiration. Secondly, AgNPs can penetrate the bacteria and interact with the sulphur and phosphorus containing compounds such as DNA, hence affecting the cell viability. Thirdly, AgNPs release silver ions which contribute to its antibacterial effect [20]. The results demonstrate that the AgNPs coated membrane can eradicate gram negative and gram positive bacteria, therefore it can be used for anti-biofouling in filtration applications.

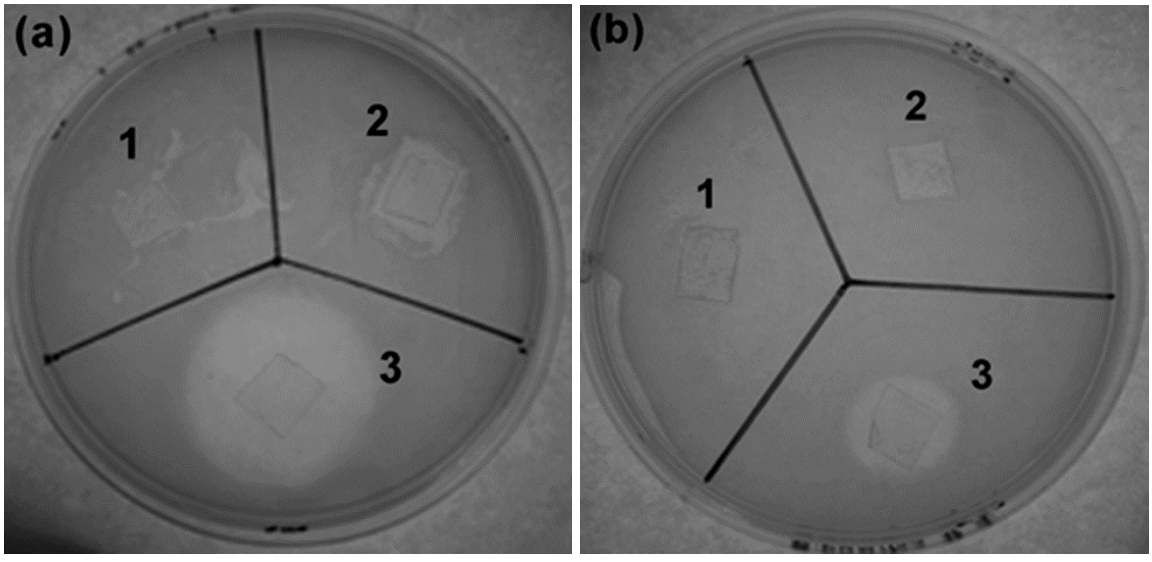

Figure 6.4 Antibacterial inhibition zones against (a) E. coli and (b) S. aureus

Table 6.2 Comparison of the inhibition zones towards gram negative and gram positive bacteria

Bacteria	Inhibition zone /cm		
	Ga-CaA	CaA-CS	CaA-AgNPs
E. coli	0	0_b	3.32 ± 0.20
S. aureus	0	0	2.31 ± 0.17

b = bacteriostatic

The pure water flux through the composite membranes is shown in Figure 6.5. All the tested membranes showed an increase with increasing in pressure, except for the commercial PLA membrane where the flux remained fairly constant independent of the applied pressure. This can be ascribed to the low surface porosity and broad pore size distribution [4]. These properties are often exhibited by membranes that are produced mainly by phase immersion. The effect of coating with chitosan (CaA-CS) and chitosan-containing AgNPs (CaA-AgNPs) can be seen from the difference in flux when compared to that of the uncoated dual crosslinked membrane (GA-CaA). The superiority displayed by the uncoated GA-CaA membrane throughout the applied pressure can be attributed to the porous structure of the electrospun nanofibres which formed an interconnected network structure (see Figure 6.1(c)) resulting in a high filtration flux. CaA-CS, CaA-AgNPs and commercial PLA displayed similar flux, especially at low pressures. At high pressures, there was a clear difference between these membranes. The CaA-CS membrane shows a slightly higher flux than the CaA-AgNPs membrane, which is due to the presence of AgNPs in the selective barrier which reduced the pore size of the membrane.

The results for BET analysis and the nanoparticles removal efficiency of the membranes are summarized in Table 6.3. The BET surface area of the GA-CaA membrane was 8.06 m^2 g^{-1}, and it decreased to 3.08 and 2.32 m^2 g^{-1} respectively for the CaA-CS and CaA-AgNPs membranes. Similarly, the average pore size decreased from 199.0 to 50.2 and 37.6 nm after coating. It is clear that the coatings decreased the pore size and surface area, which is due to the formation of a thin film/layer on top of the electrospun nanofibres, resulted in smaller pores. This confirms the water permeation results, where the coated membranes showed lower water flux than the GA-CaA membrane.

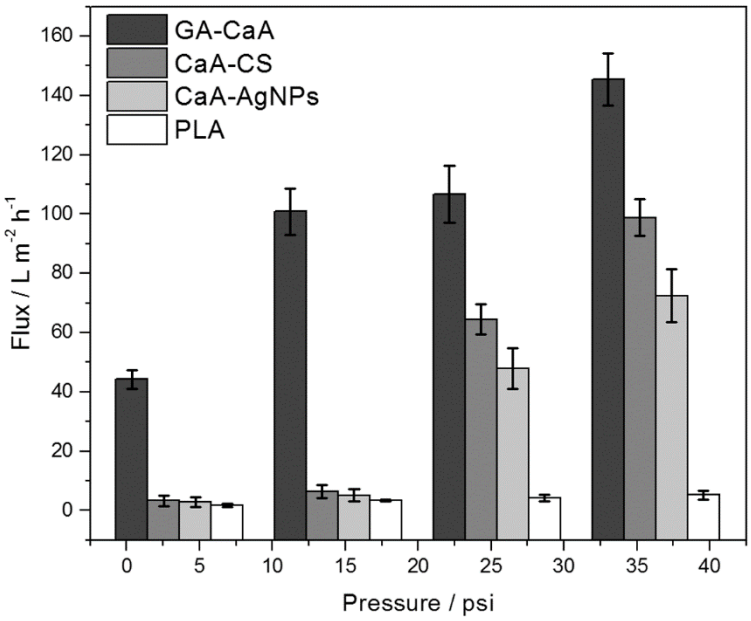

Figure 6.5 Water permeation of GA-CaA, CaA-CS, and CaA-AgNPs composite membranes

Table 6.3 BET results of the nanofibrous composite membranes

Type	BET surface area / $m^2 g^{-1}$	Average pore size / nm	Rejection of 10-35 nm particles / %
GA-CaA	8.06	199	79.1 ± 0.9
CaA-CS	3.08	50.2	98.3 ± 1.5
CaA-AgNPs	2.32	37.6	99.5 ± 0.4
Commercial PLA	-	-	85.8 ± 1.5

The evaluation of the separation capacity and confirmation of the membrane pore size were carried out by filtering SiO_2 (10-35 nm) nanoparticles as model contaminants (Figure 6.6). The UV spectra of the permeates from the CaA-CS and CaA-AgNPs membranes were relatively similar to that of pure water. Visually, the permeates were more transparent than the feed solution (Figure A.4 in Appendix). The filtrates for GA-CaA and PLA, on the other hand, showed very similar UV spectra. The recorded absorbance at 320 nm was used to confirm the filtration capacity of the membranes (Table 6.3). It can be seen that for CaA-CS and CaA-AgNPs the particle rejection was greater than 98%, while that for the commercial PLA membrane and the GA-CaA membrane were respectively ~86% and ~79%. The high rejection capacity of the CaA-CS and CaA-AgNPs membranes is due to their smaller pore sizes. However, the average pore size of the membranes was bigger than the sizes of the

nanoparticles. In this case, the nanoparticles entered the mesoporous thin layer on the surface of the membranes and were attracted to the surfaces of the inner pores as they passed through the membrane. This reduced the pore sizes and contributed to the high rejection. Also, the nanoparticles are believed to have been attracted to the outer surfaces of the membranes, thereby forming a dense 'cake-like' film which contributed to the separation efficiency of the membranes [23]. It was visually observed at the end of the filtration test that the membrane surface was covered by a thin layer of the nanoparticles.

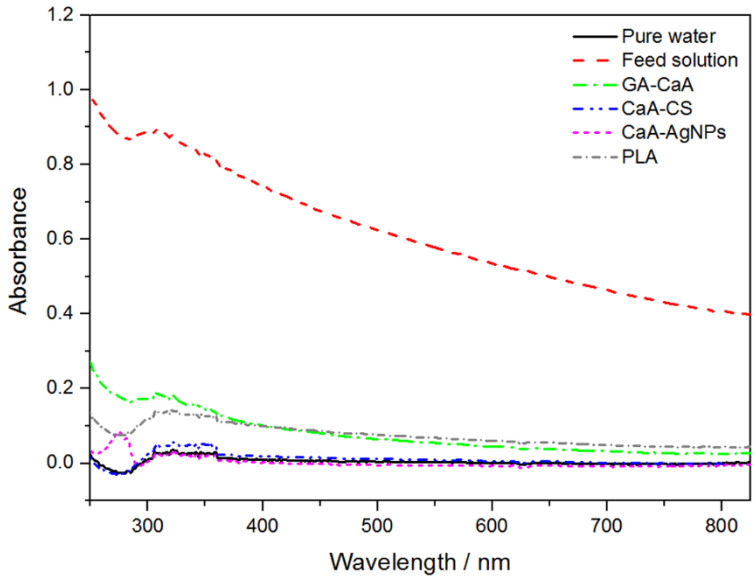

Figure 6.6 Filtration performance for the TFC membranes to silicon dioxide (SiO_2) rejection

Separation of oil/water emulsions was evaluated for the TFC membranes as shown in Figure 6.7. The UV spectra of the filtrate for the CaA-AgNPs, CaA-CS and commercial PLA membranes are very similar, showing that an acceptable amount of oil was rejected. The Ga-CaA spectrum showed that almost no oil was rejected, which is ascribed to the large pore size of the porous GA-CaA membrane. The oil separation efficiency is summarized in Table 6.4. The CaA-CS and CaA-AgNPs membranes showed the highest removal efficiency, closely followed by the commercial PLA membrane. The rejection percentage for the Ga-CaA membrane was significantly lower than those of the others. Although the rejection of oil by the membranes is due to their hydrophilic character, the smaller pore size of the coated membranes significantly contributed to their very effective oil rejection. The presence of the silver nanoparticles in the chitosan coating layer obviously had no additional influence on the separation behaviour of the membrane, which was to be expected. The visual observations of the solutions are shown in Figure A.5 in the Appendix.

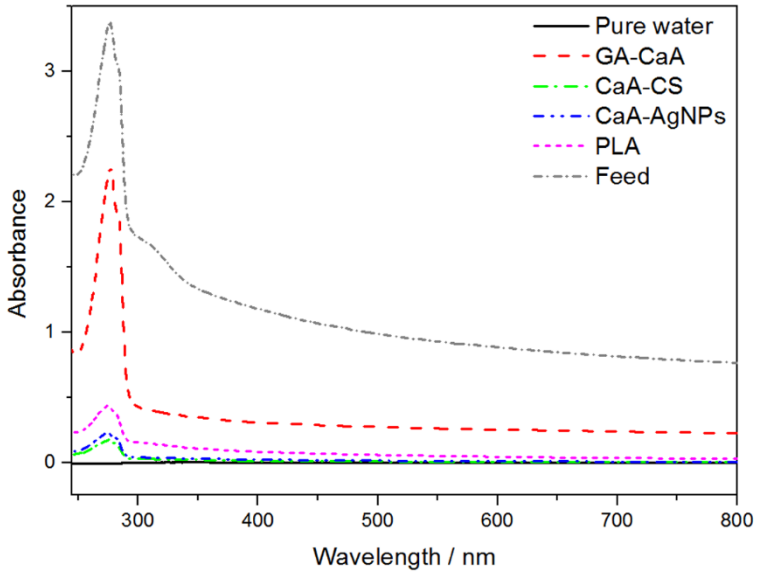

Figure 6.7 UV-visible spectra of oil concentration after passing through TFC membranes

Table 6.4 Oil/water emulsion separation efficiency by TFC membranes

Sample	% Rejection
Ga-CaA	33.0 ± 8.9
CaA-CS	94.9 ± 2.0
CaA-AgNPs	93.5 ± 2.6
PLA	87.3 ± 1.0

The dye removal efficiency of the TFC membranes was evaluated by passing the CR dye through all the membranes investigated, and the UV spectra of the respective filtrates are shown in Figure 6.8. The intensity of the peak at 498 nm increased with the number of filtration cycles for GA-CaA and CaA-CS. For the porous GA-CaA, the high rejection during the first filtration cycle was the result of the adsorption of the dye by the membrane due to its large surface area. The adsorption was the result of the ionic interaction between the carboxyl groups on the surface of the fibres and the amino groups in the CR dye. However, the membrane performance decreased with an increase in the number of filtration cycles (Figure 6.9). The reason for this is that the dye was initially adsorbed onto the fibre surfaces, but after all the active binding sites were occupied, the remainder of the dye penetrated through the pores of the membrane. The performance of the CaA-CS membrane also decreased with an increase in the number of filtration cycles. The CaA-AgNPs membrane, however, maintained a fairly high rejection until the third cycle, after which it slightly decreased, while the

commercial PLA maintained a high rejection throughout the test. The CaA-CS and CaA-AgNPs membranes have similar functional groups, and therefore the difference between these membranes' performance depended more on the sizes of the pores and on the presence of the silver nanoparticles. It is possible that during the filtration, the crosslinked alginate nanofibres (midlayer) swelled to a certain extent (Figure A.1 in the Appendix). If this is the case, the surface coating layer could have been damaged, allowing the dye to pass more freely. The presence of the AgNPs in the barrier layer, however, reinforced the coated layer and delayed its damage during the washing and filtration cycles. Even though the CaA-CS and CaA-AgNPs membranes were not yet fully optimized, they displayed comparable rejection percentages to the commercial membrane in the first 2 to 3 filtration cycles. Crosslinking of the barrier layer can improve its stability, as well as the overall strength performance of these membranes.

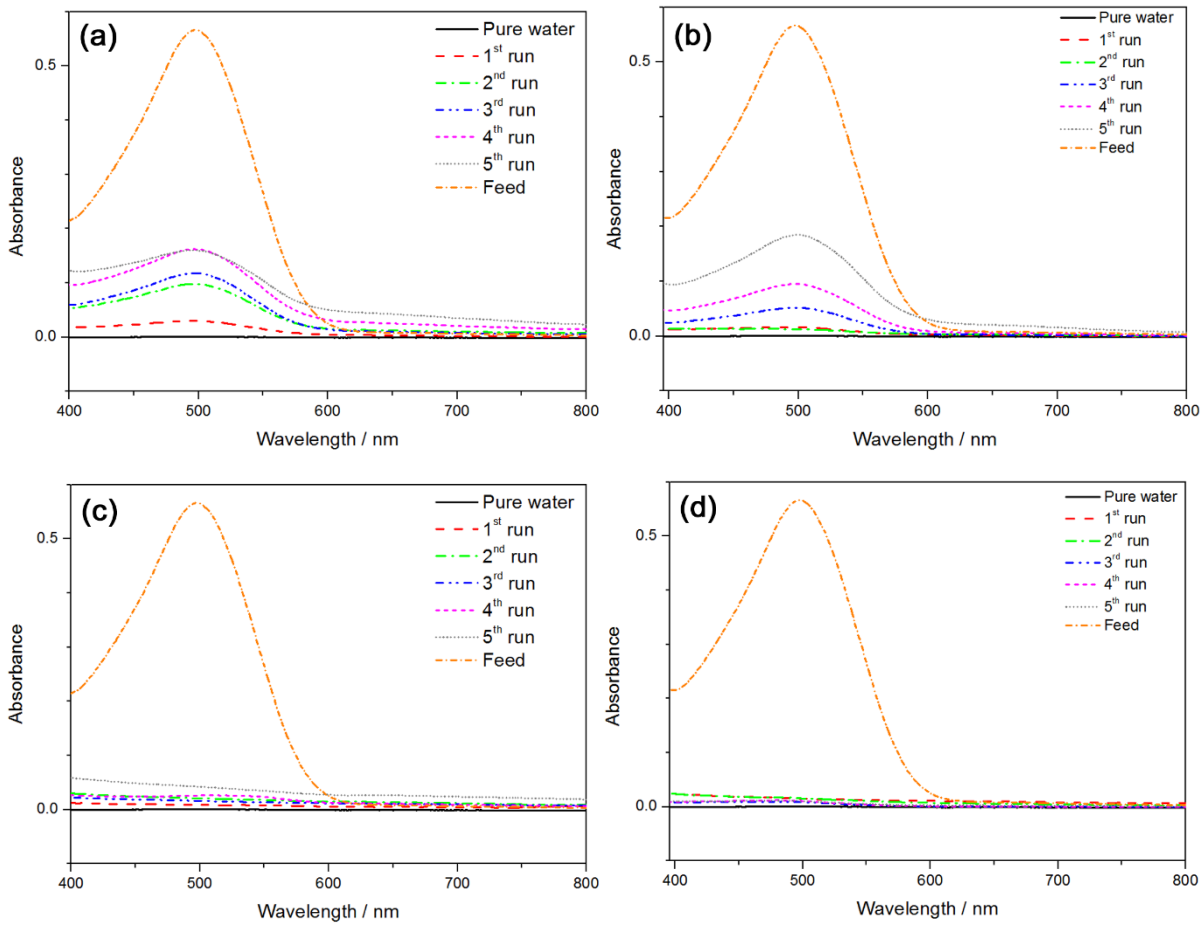

Figure 6.8 UV-visible spectra of dye after passing through membrane (a) GA-CaA, (b) CaA-CS, (c) CaA-AgNPs, and (d) PLA at 0.3 psi for 5 times

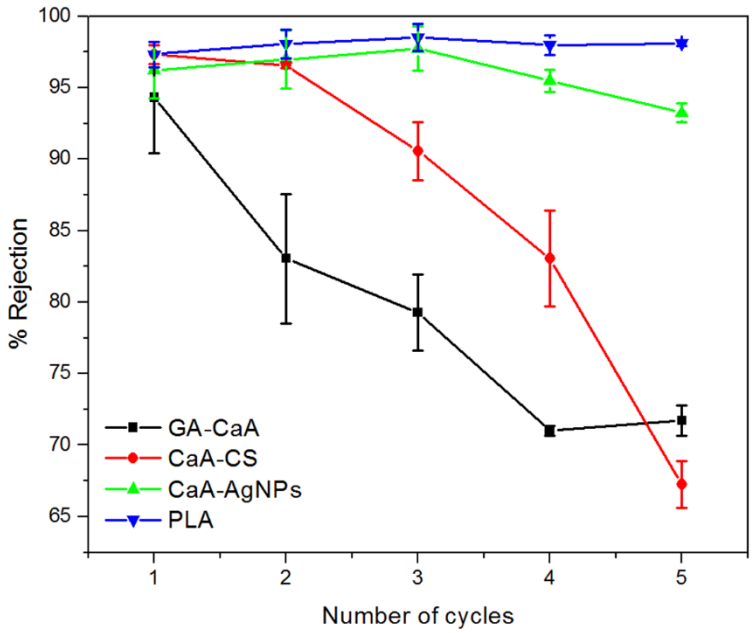

Figure 6.9 The dye rejection percentage of the composite membranes

6.4 Conclusions

A TFC membrane coated with chitosan and silver nanoparticles for water purification was developed. AgNPs were well dispersed on the surface of the membrane and showed good antibacterial activity against gram negative and gram positive bacteria. The results presented suggest that the presence of AgNPs in the selective barrier layer improved the stability and the antibacterial activity of the membrane without affecting the membrane productivity. Both the chitosan and chitosan-containing coated membranes exhibited a higher flux than the commercially available membrane (PLAC07610), while maintaining a good rejection of the nanoparticles (10-35 nm) and oil emulsions. The work in progress currently focusses on the crosslinking of the barrier layer in order to improve the stability under applied pressures during filtration.

6.5 References

[1] S. Subramanian, R. Seeram, New directions in nanofiltration applications – Are nanofibers the right materials as membranes in desalination?, Desalination, 308 (2013) 198-208.

[2] H. Ma, C. Burger, B.S. Hsiao, B. Chu, Ultrafine polysaccharide nanofibrous membranes for water purification, Biomacromolecules, 12 (2011) 970-976.

[3] S.-J. Park, R.K. Cheedrala, M.S. Diallo, C. Kim, I.S. Kim, W.A. Goddard III, Nanofiltration membranes based on polyvinylidene fluoride nanofibrous scaffolds and crosslinked polyethyleneimine networks, Journal of Nanoparticle Research, 14 (2012) 1-14.

[4] K. Yoon, K. Kim, X. Wang, D. Fang, B.S. Hsiao, B. Chu, High flux ultrafiltration membranes based on electrospun nanofibrous PAN scaffolds and chitosan coating, Polymer, 47 (2006) 2434-2441.

[5] K. Desai, K. Kit, J. Li, P. Michael Davidson, S. Zivanovic, H. Meyer, Nanofibrous chitosan non-wovens for filtration applications, Polymer, 50 (2009) 3661-3669.

[6] X. Wang, D. Fang, K. Yoon, B.S. Hsiao, B. Chu, High performance ultrafiltration composite membranes based on poly(vinyl alcohol) hydrogel coating on crosslinked nanofibrous poly(vinyl alcohol) scaffold, Journal of Membrane Science, 278 (2006) 261-268.

[7] K. Sun, Z. Li, Preparations, properties and applications of chitosan based nanofibers fabricated by electrospinning, eXPRESS Polymer Letters, 5 (2011) 342-361.

[8] S.I. Jeong, M.D. Krebs, C.A. Bonino, J.E. Samorezov, S.A. Khan, E. Alsberg, Electrospun chitosan–alginate nanofibers with in situ polyelectrolyte complexation for use as tissue engineering scaffolds, Tissue Engineering Part A, 17 (2010) 59-70.

[9] Y.-C. Chung, H.-L. Wang, Y.-M. Chen, S.-L. Li, Effect of abiotic factors on the antibacterial activity of chitosan against waterborne pathogens, Bioresource Technology, 88 (2003) 179-184.

[10] Z. Zhao, J. Zheng, M. Wang, H. Zhang, C.C. Han, High performance ultrafiltration membrane based on modified chitosan coating and electrospun nanofibrous PVDF scaffolds, Journal of Membrane Science, 394 (2012) 209-217.

[11] J.-W. Lu, Y.-L. Zhu, Z.-X. Guo, P. Hu, J. Yu, Electrospinning of sodium alginate with poly(ethylene oxide), Polymer, 47 (2006) 8026-8031.

[12] X. Zhang, B. Lin, K. Zhao, J. Wei, J. Guo, W. Cui, S. Jiang, D. Liu, J. Li, A free-standing calcium alginate/polyacrylamide hydrogel nanofiltration membrane with high anti-fouling performance: Preparation and characterization, Desalination, 365 (2015) 234-241.

[13] K. Zhao, X. Zhang, J. Wei, J. Li, X. Zhou, D. Liu, Z. Liu, J. Li, Calcium alginate hydrogel filtration membrane with excellent anti-fouling property and controlled separation performance, Journal of Membrane Science, 492 (2015) 536-546.

[14] J. Guo, Q. Zhang, Z. Cai, K. Zhao, Preparation and dye filtration property of electrospun polyhydroxybutyrate–calcium alginate/carbon nanotubes composite nanofibrous filtration membrane, Separation and Purification Technology, 161 (2016) 69-79.

[15] N. Bhattarai, M. Zhang, Controlled synthesis and structural stability of alginate-based nanofibers, Nanotechnology, 18 (2007) 455601.

[16] C. Yeom, K.H. Lee, Characterization of sodium alginate membrane crosslinked with glutaraldehyde in pervaporation separation, Journal of Applied Polymer Science, 67 (1998) 209-219.

[17] V. Leung, R. Hartwell, S.S. Elizei, H. Yang, A. Ghahary, F. Ko, Post electrospinning modifications for alginate nanofiber-based wound dressings, Journal of Biomedical Materials Research Part B: Applied Biomaterials, 102 (2014) 508-515.

[18] M. Guzman, J. Dille, S. Godet, Synthesis and antibacterial activity of silver nanoparticles against gram-positive and gram-negative bacteria, Nanomedicine: Nanotechnology, Biology and Medicine, 8 (2012) 37-45.

[19] S. Kaviya, J. Santhanalakshmi, B. Viswanathan, J. Muthumary, K. Srinivasan, Biosynthesis of silver nanoparticles using Citrus sinensis peel extract and its antibacterial activity, Spectrochimica Acta Part A: Molecular and Biomolecular Spectroscopy, 79 (2011) 594-598.

[20] Q. Feng, J. Wu, G. Chen, F. Cui, T. Kim, J. Kim, A mechanistic study of the antibacterial effect of silver ions on Escherichia coli and Staphylococcus aureus, Journal of Biomedical Materials Research, 52 (2000) 662-668.

[21] T. Maneerung, S. Tokura, R. Rujiravanit, Impregnation of silver nanoparticles into bacterial cellulose for antimicrobial wound dressing, Carbohydrate Polymers, 72 (2008) 43-51.

[22] M. Rai, A. Yadav, A. Gade, Silver nanoparticles as a new generation of antimicrobials, Biotechnology Advances, 27 (2009) 76-83.

[23] R. Gopal, S. Kaur, Z. Ma, C. Chan, S. Ramakrishna, T. Matsuura, Electrospun nanofibrous filtration membrane, Journal of Membrane Science, 281 (2006) 581-586.

Chapter 7

Conclusions

This study investigated the electrospinnability of alginate polymer and its application as the main component in filtration membranes used for wastewater treatment. Other natural polymers and silver nanoparticles were also used to enhance the filtration performance of the electrospun alginate under different filtration conditions.

Storage of the alginate/PEO blends before electrospinning had a significant influence on their electrospinnability because of the interaction between the blend components. It was also found that the addition of surfactant (Triton X-100) and co-solvent (dimethylsulfoxide (DMSO)) to the blend solution, enhanced the nanofibrous structure of the resulting nanofibres. The electrospun alginate nanofibers, without any additional functionalization, showed a high adsorption capacity for the heavy metal ions in wastewater due to their large surface areas and the presence of the hydroxyl and carboxyl groups on the alginate polymer. The porous structure of the electrospun nanofibres made them unfeasible for the retention of micro and/or nanosized materials found in water streams. The coating of the electrospun alginate nanofibres with cellulose nanowhiskers as barrier/selective layer was then investigated. The coated cellulose nanowhiskers barrier layer reduced the sizes of the pores, and improved the retention of the nanoparticles, chromium and oil emulsions, as well as the overall mechanical properties of the membrane.

The exposure and release of nanoparticles from the electrospun nanofibres was investigated by coating the electrospun alginate nanofibres with silver nanoparticles (AgNPs) containing chitosan *via* immersion process. The results showed that complexation between the chitosan and alginate nanofibres induced the dispersion of the AgNPs on the surface of the porous structure, which helped with the nanoparticles' release into the medium, and thus enhanced the antibacterial activity towards gram positive and gram negative bacteria. We further investigated how the addition of AgNPs into the barrier layer and dual crosslinking (ionic and chemical crosslinking) of the midlayer can influence the filtration behaviour of the membrane. It was found that the AgNPs reduced the pore sizes of the membrane, while dual crosslinking reduced the swelling of the fibres. All these phenomena improved the membrane rejection of

oil emulsion and nanoparticles with a good antibacterial activity. The AgNPs also improved the stability of the barrier layer.

Recommendations for future work:

- Crosslinking of the alginate by using other techniques in order to control and/or improve its stability in the medium.
- Crosslinking of the coating layer in order to improve its stability to withstand high pressure and washings.
- Improving the interaction between the substrate and the electrospun nanofibres and studying the effect of the thickness of the barrier.

Acknowledgements

I would to thank the God Almighty for giving me constant strength, courage and endless blessings throughout this work and in my life, without which the preparation and assembling of this work would have been impossible.

I would like to express my sincere gratitude to my supervisors, Prof. Adriaan S. Luyt and Dr. Valencia Jacobs for their patient guidance, enthusiastic encouragement and useful critique of this research work. The help and guidance given by them throughout this work shall carry me a long way in the journey of life on which I am about to embark.

I would also like to extend my thanks to the CSIR, Port Elizabeth and the University of the Free State, Qwaqwa Campus for the opportunity to study under their umbrella.

Special thanks to my late parents, Letsatsi Ramateka Mokhena and Maboteng Agnes Nondlala and the entire Mokhena family, Mmipi, Malaka and Nondlala. I am grateful for their guidance, unconditional love and constant support.

I would also like to thank:

- My fellow research group members and colleagues (Dr Makgaotsa Jonas Mochane, Mr Teboho Motsoeneng, Dr Essa Ahmad, Mr Modise Serero, Mr Jacob Mabena, Dr Mfiso Mngomezulu, Dr Tshwafo Motaung, Dr Thabang Mokhutho, Dr Asanda Mtibe, Mr Osei Ofosu, Dr B. Hlangothi, Dr SP Hlangothi, Dr Doice Moyo, Dr Linda Linganiso, Dr Dusco Dudic, Mr Mzwamadoda Notayi, Mr Cyrus Tshifuralo, Mr Tladi Mofokeng, Dr Jeremiah Sefadi, Mr Tsietsi Tsotetsi, Mr Neo Moji, Mrs Nomampondomise Molefe, Mrs Moipone Malimabe, Dr Julia Mofokeng, Dr Motshabi Sibeko, Ms Zanele Clarke, Dr Sunshine Blouw, Dr Rajesh Anandijwala, Prof Lawrence Hunter, Ntsike Dumakude, Enn Fortuin, Dr Maya John, Steve Chapel, Kelly-Anne Mathews, Dr Neil Trollip, Jacques Nel, Musikwa Mufeba, Lebo Maduna, Mlando Mvubu, Sandisiwe Bala, Bosi Thandiwe, Andiswa Sulo, Basset Bredan, Tshepiso Molaba, Patricia Gumede, Charlie Sunnyboy, Mpho Lefatle, Abongile Gada, Sakiwo Silingo, Darren Naidu, Princeton Pillay, Yusuf M Dalhat, Dr Anton Botha, Haydon Whitebooi, Dr Asis Patnaik, Dr Sudhakar Muniyasamy, Dr Mamoeletsi

Mosia, Puleng Moleko, Sunday Niyi, and Prof Tshentu) for their support and valuable inputs. I am grateful for their cooperation during the period of this assignment.

- My siblings: Hlouwe Malaka, Lesuping Mokhina and Madikotsi Mokhina.
- My teachers: Ntate Samora Selometsi, Thabo Mpiti, Letuka Tshupane, Keta Tobalete, Sechaba Motloung, Adries Mokoena, Mr Moloi, Jimmy Selometsi, Mr Mokoena, Rashokoe Mpiti , Mpesi Mokhotla, Mrs Tselane Mbhele, Mrs Mokhatla, Mrs Moshoadiba, Mrs Ncanga, Mr Sekhonyane , Mr Rabiki, and Mrs Jane Sethabela for their constant support and exemplary guidance.
- My friends: Thabo Molefi, Mpedi Mosia, Mantsi Lesia, Tumelo Taemane, Dr Essa Ahmad, Dr Asanda Mtibe, Mzwa Notayi, Tshepo Mokoena, Benny Mokomatsili, Motlatsi Sethabela, Dominic Tomeng, Lotha Lungisa, Setjhaba Mohlakoana, Moeti Taioe, Bongane Salemane, Teboho Motsoeneng, Dr Jonas Mochane, Modise Serero, and Cyrus Tshifularo for being there for me through hard times and constant encouragement without which this work would not be possible.
- Last but not least, the Postgraduate Football Club (PGSV, NMMU) for the opportunity to know new faces and share ideas with each other.

I would like to extend special thanks to Modise Serero for accommodating and assisting me with the antibacterial bioassays and may God bless him through his PhD studies.

All thanks go to the Zoology Department (UFS Qwaqwa Campus), especially Dr Lisa Komoreng, Jacob Mabena and Valeria Makhosazana for sharing with me their laboratory and advice during the antibacterial studies.

I would like to thank Ms Nthabiseng W. Salamane for her endurance and understanding during this demanding assignment.

Appendix

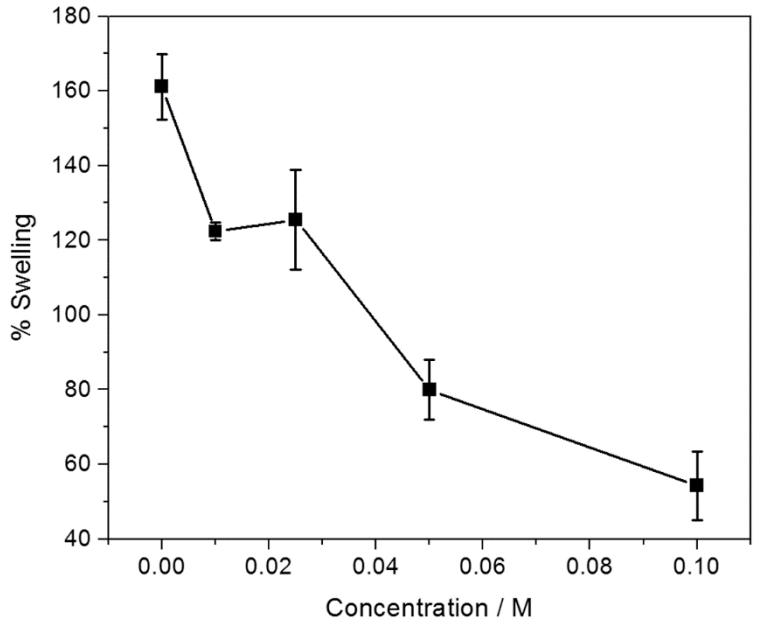

Figure A.1 Swelling behaviour of crosslinked alginate nanofibres

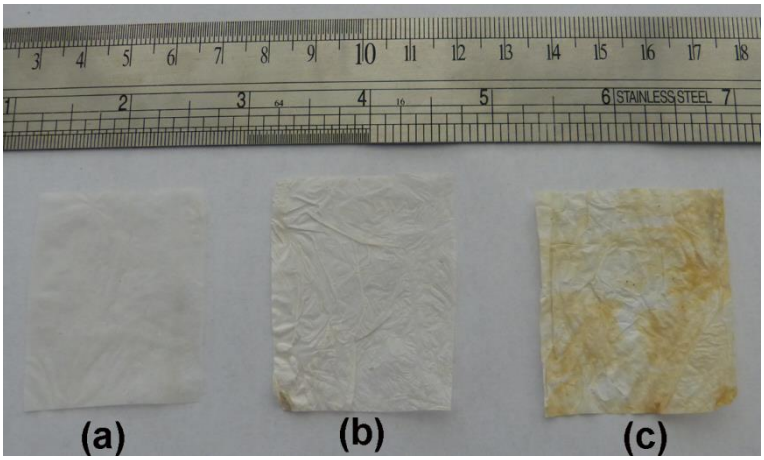

Figure A.2 Images of electrospun nanofibres: (a) uncrosslinked, and crosslinked with (b) 0.1 M and (c) 0.2M glutaraldehyde for 24 hours

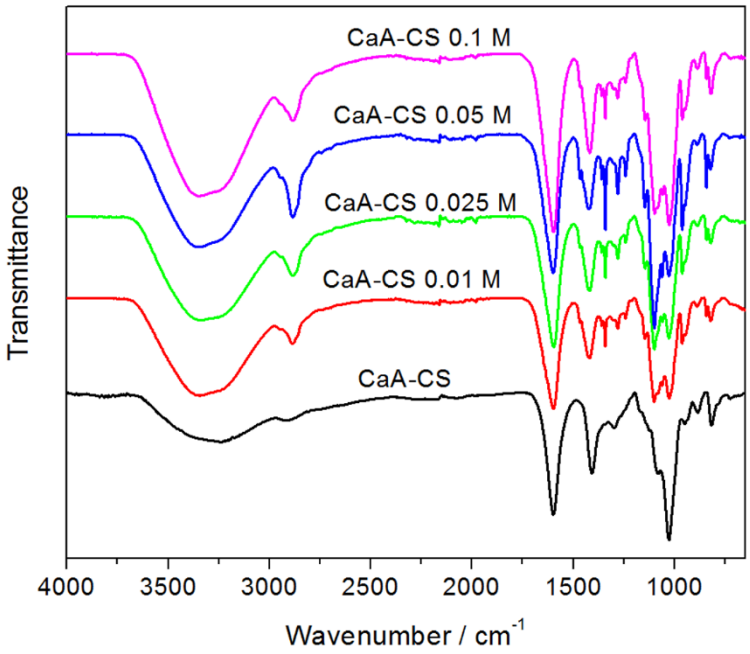

Figure A.3 FTIR spectra of alginate crosslinked with different glutaraldehyde concentrations for 24 hours

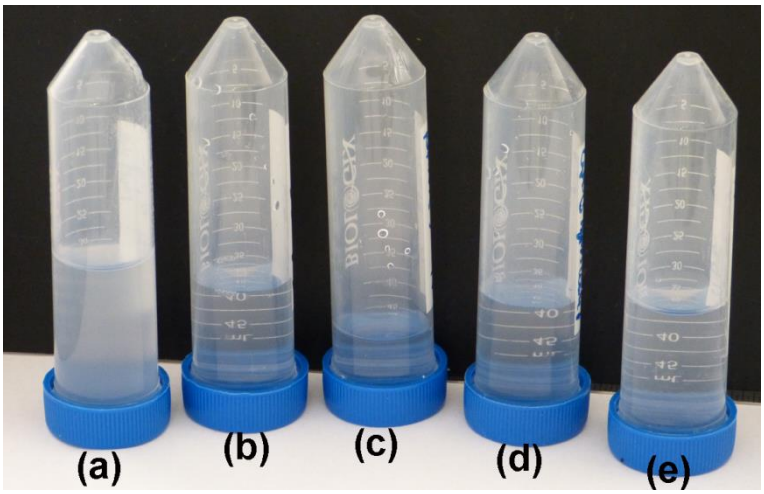

Figure A.4 The permeates from SiO_2 filtration with TFC membranes: (a) feed, (b) GA-CaA, (c) CaA-CS, (d) CaA-AgNPs, and (e) PLA

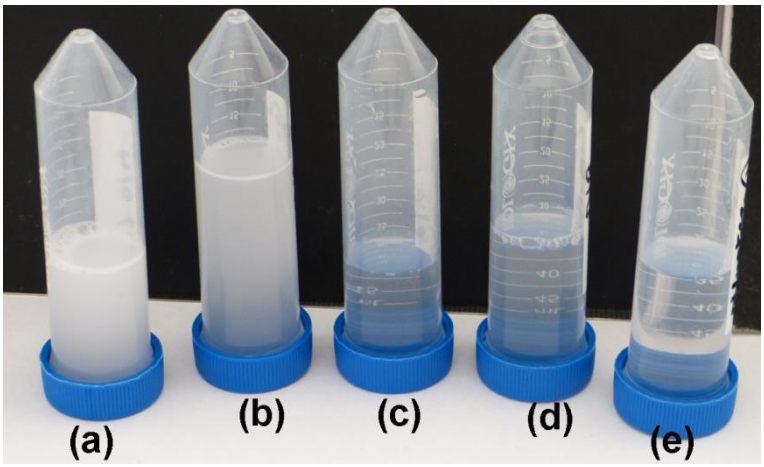

Figure A.5 The filtrates from oil separation for TFC membranes: (a) feed, (b) GA-CaA, (c) CaA-CS, (d) CaA-AgNPs, and (e) PLA